THE HYDROLOGIC BEHAVIOUR OF WASTE ROCK PILES IN THE CANADIAN ARCTIC:

SNOWMELT INFILTRATION AND THE ONSET OF LONG TERM FREEZING IN TEST PILES

by

ANDREW KRENTZ

B.ASc., Queen's University, 2011

A THESIS SUBMITTED IN PARTIAL FULFILLMENT OF THE REQUIREMENTS FOR THE DEGREE OF

MASTER OF APPLIED SCIENCE

in

THE FACULTY OF GRADUATE AND POSTDOCTORAL STUDIES

(Geological Engineering)

The University of British Columbia

(Vancouver)

November 2014

Abstract

This thesis examines the hydrology of three experimental waste rock piles located in the Canadian Arctic at Diavik Diamond Mine (DDMI). Seven years of hydrology data is presented, including measurements of moisture contents, outflow volumes and soil tensions, along with an estimate of annual rainfall infiltration. The hydrology of each pile is influenced by freezing and thawing, and pore water flow is restricted to the time periods when the pile is thawed. The base of each pile contains drain pipes used to collect pore water from the piles, and these pipes are lined with internal heat traces. This research shows that the heat traces significantly influence the thermal behaviour and hydrology of the waste rock. A flooding event in the winter of 2012 interrupted power to the heat trace in two of the waste rock piles, and led to altered outflow volumes and patterns in 2013. A heat trace in the base of the third pile was intentionally turned off in 2011, and led to a significant decrease in the volume of outflow collected from the pile in 2012 and 2013.

A bromide tracer was applied to the crest of one of the piles in 2007, and the recovery of the tracer is analysed until 2013. The results of this analysis are used to quantify the average residence time and flow velocity of pore water within the pile. The concentration of stable isotopes is analysed in outflow from the same pile, and is used to estimate the contribution of snowmelt to the total recharge received by the pile. The infiltration of snowmelt into another waste rock pile is estimated using the results of four snow surveys, a snowmelt ablation model, and an infiltration model suitable for use on frozen porous media.

The research contained in this thesis provides information that will be incorporated into the final closure plan for DDMI, and will be used to help prevent the formation and release of low quality effluent from the full scale waste rock pile located at the mine site.

Preface

The original research conducted for this thesis is presented in four chapters (Ch. 2, 3, 4, 5). Chapters 3, 4 and 5 are formatted as papers intended for publication in peer reviewed journals.

The Diavik Waste Rock Research Group is a collaborative effort involving students and professors at the University of Alberta, the University of British Columbia and the University of Waterloo. Unless stated otherwise, I was responsible for all of the research and data presented in this thesis. My direct field responsibilities included the collection, analysis and interpretation of hydrology data (TDR, ECH_2O, tensiometer, outflow and rainfall) collected at the test piles during 2012 and 2013. The hydrology dataset between 2007 and 2011 (including estimates of infiltration) was summarized by Nathan Fretz (2013), and this data is contained within my thesis. The infiltration of rainfall in 2012 and 2013 was estimated for this thesis using a template that was provided by Fretz. Additionally, the mass loading of bromide and chloride from the base of the type III pile was determined by Sean Sinclair (2014) until the end of 2012. I estimated the mass recovery of bromide and chloride in 2013, and was responsible for the interpretation of the data in the context of the tracer test. I analysed the isotope data contained in this thesis, and am also responsible for the snowmelt and infiltration model used on the covered pile.

My research supervisor, Leslie Smith, provided feedback on the scientific interpretation found in this thesis.

Table of Contents

List of Tables

List of Figures

Acknowledgements

To…

…Leslie Smith. Thank you for your excellent guidance, support and supervision.

…David Blowes, Richard Amos and Dave Sego. Thank you for the leadership and advice

…The test piles crew past and present. Thank you to Nate Fretz for answering all of my hydrology questions, even late in the project. Thank you also to Sean Sinclair for his expertise on all things test piles related. To Jordan Zak, my successor and brotégé, best of luck with the project.

..My fellow grad students. Your friendship, energy and support have been an amazing bonus to my time spent at UBC. I wish you all my very best.

…Lysa. Thank you for joining me on this adventure, and I cannot wait to embark on another.

Dedication

This thesis is dedicated to my parents, Val and Dan Krentz. Thank you for always believing in me and for supporting me in all of my endeavours.

Chapter 1: Introduction

1.1 The Diavik Waste Rock Project

The Diavik waste rock project is an ongoing research endeavor with the goal of understanding the thermal, hydrological and geochemical behavior of an 80m high waste rock pile located at Diavik Diamond Mine ($64^{o}29'$N, $100^{o}18'$W) (Figure 1-1). The project consists of laboratory scale experiments conducted at the University of Waterloo, along with 2m and 15m scale experiments located at the mine site. The findings from these experiments will be used to develop up-scaling relationships for the prediction of solute releasefrom the full scale waste rock pile. Data from the project has been collected continuously since 2007, and the findings of the project will be incorporated into the closure plan for the mine.

1.2 Importance of the Project

The weathering of sulfide bearing waste rock can produce low quality effluent known as acid rock drainage (ARD). ARD is a common problem in mining, and there is an abundance of literature regarding the generation and mitigation of ARD in mine sites throughout the world (ex. Johnson and Hallberg (2005)). The Diavik project is unique because it is located in a region of continuous permafrost, with fluid flow restricted to areas that thaw in the summer (the active zone). This affects flow and reaction rates within the waste rock, and has important implications regarding effluent volumes and the mass loading of solutes from the pile. Understanding the evolution of waste rock located in Arctic environments is increasingly important as mining activities continue to progress in northern Canada. The findings of the Diavik project will also be useful for guiding future research conducted on experimental waste rock piles, regardless of location.

1.3 Scope

This thesis is focused on the hydrology of two heavily instrumented, 15m high waste rock piles constructed by the Waste Rock Research Group(WRRG), and known as the test piles. The first pile is uncovered, constructed of acid generating rock, and is referred to as the type III pile. The second pile has an acid generating core overlain with an engineered dry cover of till and non-acid generating rock, and is referred to as the covered pile.Previous research on the hydrology of the waste rock piles was conducted by Matthew Neuner (2009), Nathan Fretz (2013) and Steve Momeyer (2014). Neuner (2009) focused on the initial hydrological response of the piles and physically characterized the waste rock. Research on the hydrology of the piles was continued by Fretz (2013), who quantified infiltration into the crests of the piles and examined the wet-up, storage and outflow from each pile between 2007 and 2011. Momeyer (2014) studied infiltration and solute transport in the piles between 2008 and 2009. This thesis contains the ongoing data analysis for both piles until 2013, and is also intended to address two primary goals:

1. Quantify an average flow velocity and residence time for pore water in the core of thetype III waste rock pile.
2. Quantify the component of recharge that the type III and covered piles receive through the infiltration of snowmelt each spring.

These goals have been identified by the waste rock group as two of the largest missing components required for a comprehensive understanding of the hydrology of the waste rock piles.

1.4 Organization

This thesis contains a total of four research based chapters plus an introductory chapter and a conclusions chapter. The introductory chapter (Chapter 1) is intended to introduce the reader to the study site and to the experiments being conducted. Background information on each experiment is

provided, and references are given where additional information can be found in previously published work.

Chapter 2 focuses on the ongoing analysis of hydrologic data from the two experimental piles examined in this thesis. It is intended to demonstrate the importance of the stated research goals, and to maintain the continuity of data collected from each experiment.

Chapter 3 contains the analysis for a tracer released in 2007, and is intended to quantify the velocity and residence time of pore water in the type III experimental waste rock pile. This has important implications regarding the rate of solute loading from the pile, and providesnecessary information for any future work conducted on the hydrology and geochemistry of the piles.

Chapters 4 and 5 are focused on quantifying the infiltration of snowmelt into the waste rock piles. The infiltration of melted snow is an important component of recharge to the piles, and is a function of total snowfall amounts, wind transport, sublimation, and melting. In Chapter 4 the relative infiltration of snowmelt and rainfall through the batters of the type III pile is quantifiedusing stable isotopes measured in outflow from the pile. In Chapter 5 the infiltration of snowmelt into the covered pile is modeled based on the results of four snow surveys conducted in 2010, 2011, 2013 and 2014. Quantifying the infiltration ofsnowmelt into thetest pilesis required to evaluate the water balance of the individual piles, and will be beneficial when developing up-scaling relationships to the full scale waste rock pile.

Chapters 3, 4 and 5 in this thesis are written as articles intended for publication. Each article contains all of the background information required for the research being conducted, and as such there is some necessary repetition of information between chapters.

Chapter 6 presents conclusions and recommendations for future work. The recommendations are intended to guide future research both at Diavik and for other projects studying experimental waste rock piles.

1.5 Background

This section contains background information regarding the mine site, the waste rock that was created during mining, and the experiments conducted by the WRRG. The construction of two 15m scale experimental piles is summarized, along with a brief description of the hydrological instrumentation installed within each pile. An aerial photograph of the field site is shown in Figure 1-2 for reference. Note that the type I pile and active zone lysimeters (AZLs) shown in Figure 1-2 are not directly discussed in this thesis. The full suite of data collected from these experiments is summarized in Appendix A. For a complete description of the type I pile and the AZLs the reader is directed to (L. J. Smith 2009).

1.5.1 Site Description

The climate at Diavik is characterized by long, cold winters and short, warm summers. The mine is located in a semi-arid region and had 280mm of annual average precipitation between 1997 and 2007, with 65% falling as snow (Environment Canada 2010). Since the piles were constructed in 2006 and 2007 the annual precipitation has averaged 250mm (to 2013), with approximately 60% falling as snow (Figure 1-3).

1.5.2 Waste Rock at Diavik

Waste rock is created when the excavation of non-economical rock (country rock) is required during mining operations. At Diavik the removal and stockpiling of 200 MT of country rock was required to access three diamond bearing kimberlite pipes. This rock is primarily Archean age granite and pegmatite granite, with xenoliths of metasedimentary biotite-schist. The schist contains pyrrhotite, which is the only significant source of sulphur in the country rock. Following excavation, the rock is sorted by sulfur content into type 1 (<0.04 wt. % S), type II (0.04-0.08 wt. % S) and type III (>0.08 wt. % S) material, and is

stored in an 80m tall stockpile. Carbonate concentrations are low in the country rock, and both the type II and type III material produce ARD when stockpiled (Sinclair 2014), (Langman, et al. 2014).

The WRRG conceptually divides the waste rock as a function of grain size. Material that is less than 5mm in size is referred to as the matrix, while everything that is greater than 5mm in size is referred to as non-matrix material.

1.6 The Experimental Waste Rock Piles

The 15m high experimental waste rock piles are the largest experiments built by the WRRG. The piles are heavily instrumented, and the rate and volume of outflow from the piles is measured. Samples of outflow collected from the piles are taken every 2-3 days for geochemical analysis. The research conducted for this thesis is focused on the type III and covered piles shown in Figure 1-2, and background information regarding the construction and instrumentation of these piles is presented below. Only information that is relevant to this thesis is included; however, for a complete description of each pile the reader is referred to L. J. Smith (2009).

1.6.1 The Type III (Uncovered) Waste Rock Pile

The type III waste rock pile was constructed in 2006 using end-dumping and push-dumping techniques. The pile is constructed of rock with an average sulfur content of 0.053%. This material is actually classified as type II rock; however, the pile is referred to as the 'Type III Pile' to reflect its acidic outflow.

The batters of the type III pile are sloped at the angle of repose (38^{o}), and the pile has a basal footprint of just over 50m x 60m. The type III waste rock pile is considered to be a batter dominated system, as the batters overlay 55% of the total basal area of the pile. The crest of the type III pile is a matrix and non-matrix supported surface used by haul trucks during construction (Figure 1-4). A significant

portionof the batters is non-matrix supported (Figure 1-5) and the average grain size increases non-linearly from top to bottom (Chi 2010).

1.6.2 The Covered Waste Rock Pile

The covered waste rock pile has a basal footprint of 100 x 125m and is differentiated from the type III pile by its unique construction. The core of the covered pile consists of type III rock with an average sulfur content of 0.083 wt. % S. This core was created using end and push dumping techniques, and was then re-graded to a 3:1 (18^{o}) slope. A cover consisting of 1.5m of till was placed on top of the re-graded type III core using bulldozers. Following placement of the till cover, 3m of type I waste rock was placed onto the pile using both free dumping and bulldozers. The batters of the pile were left at a 3:1 slope to allow walking access. The covered waste rock pile is more batter dominated than the type III pile, as the batters slope at a much shallower angle than the batters of the type III pile. The construction of the covered pile resulted in batter surfaces that have a grain size distribution more similar to the crests of the piles than to the batters on the type III pile (Figure1-6). A schematic cross section of the covered pile is shown in Figure 1-7.

The engineered cover is designed to restrict the ingress of water and oxygen into the reactive type III core of the pile in order to minimize the formation and release of low quality effluent from the pile. The type I layer is designed to freeze and thaw annually while the till layer and core of the pile remain frozen.The frozen layer of till is intended to act as a permeability barrier to both water and air.A similar cover system is proposed in the mine closure plan for Diavik, and the covered pile is therefore an important analogue for gauging the success of this type of cover.

1.6.3 Drainage from the Piles

Both of the piles are constructed atop of an HDPE liner that directs flow to a perforated, heat traced PVC pipe referred to as a basal drain. The liner under the type III pile is 50 x 60m, and underlies the majority

of the pile. The liner at the base of the covered pile is 84 x 59m, and underlies only 40% of the total footprint of the pile. The drains were placed prior to construction, and are located in a protective 40cm thick layer of crush material. Basal pore water is conducted out of the pile by the drains, and the rate and volume of outflow is recorded by tipping buckets. The type III pile has two basal drains, referred to as the north and south drains, while the drain for the covered pile is referred to as the covered pile basal drain.

Both piles also contain basal collection lysimeters (BCLs) designed to study spatial variability in flow and geochemistry within the pile. The BCLs are plywood boxes lined with HDPE. They are located at the base of the piles, and each pile contains six 2 x 2m BCLs and six 4 x 4m BCLs (Figure 1-8). Pore water that flows into the BCLs is collected by a zero tension drain and conducted through a heat traced PVC pipe to Young Model 2202 tipping buckets, which record flow volumes. The BCLs in the covered pile have never conducted flow. It is assumed that they are broken, and as such they are not discussed further in this thesis. The BCLs in the type III pile are functioning as anticipated, and have provided valuable information regarding the variability in the flow and geochemistry of pore waterconducted through the batters and the core of the pile. A schematic of the drainage system used in each pile, including the locations of the HDPE liner, the BCLs, and the basal drain(s) is shown in Figures 1-9 a-band 1-10.

Differences in Drainage Systems Between Piles

The drainage pattern in the type III pile is different from that of the covered pile. Basal flow in the type III pile is directed from the centre of the pile outwards, while basal flow in the covered pile is directed to a diagonal pipe passing through the centre of the pile. This difference is important because under natural conditions each pile thaws inward from the batters each year. Flow only occurs in areas that are thawed, and therefore water reaching the basal liner in the covered pile will not report to the basal

drain until a thawed pathway becomes available. In comparison, all of the water arriving at the HDPE liner of the type III pile each spring has a thawed pathway to the drainage pipes.

In addition to the different drainage schemes, different crush materials were used to protect the drain pipes in the piles. 2" inch minus material was used in the covered pile, while 1.25 inch minus material with no fines was used in the type III pile (L. Smith 2006). The absence of fines in the crush used in the type III pile means that water will not be retained through capillarity in this layer. Conversely, the fines in the crush of the covered pile will retain water and act as a storage reservoir for pore-water prior to reaching the basal liner. This has two main effects:

1. The crush in the covered pile will require wetting up prior to pore water reaching the basal liner and drain. Assuming a field capacity of 0.1 to 0.15 for the crush (Fretz 2013), this is anticipated to require around 200-300m^3 of water.
2. The water held in the crush may act as a thermal sink and promote multi-year freezing in the core of the pile. This will restrict flow to the covered pile drainage pipe.

The extent of the basal liner is also different between the two waste rock piles. The liner in the type III pile extends almost to the very edge of the batters, while the liner in the covered pile does not (Figures 1-9 and 1-10). This means that infiltration through the outer edges of the type III pile will be collected by the drain pipes, while infiltration around the outer edges of the covered pile will not. The development of a permanently frozen core in the covered pile will therefore lead to a significant decrease in outflow collected by the basal drain. Conversely, the extent of the liner and the location of the drain pipes in the type III pile dictate that significant outflow will continue to be collected even if a frozen core develops.

1.6.4 Internal Flow and Storage in the Waste Rock Piles

The experimental rock piles are unsaturated, and pore water is located primarily in the <5mm fraction of the waste rock known as the matrix. Material that is greater than 5mm does not have capillarity, and

does not retain water under unsaturated conditions (Yazdani et al., 2000). One dimensional flow through the matrix of the pile is controlled by capillarity and infiltration, and is described using the one dimensional Richards equation (Equation 1)

$$\frac{\partial \theta}{\partial t} = \frac{\partial}{\partial z}\left[K_{(\Psi)}\left(\frac{\partial \Psi}{\partial z} + 1\right)\right] \quad (1)$$

Where θ is moisture content, z is elevation above a datum, and $K_{(\Psi\ )}$ is the hydraulic conductivity as a function of pressure head (Ψ).

The porosity contained within the non-matrix (>5mm) portion of the pile only conducts water during intense infiltration events, and flow through this domain is referred to as preferential flow. Preferential flow mechanisms include macropore flow through interconnected void spaces, and film flow along the surface of boulders. Both of these mechanisms channelize flow within the pile and lead to rapid flow velocities, relatively short residence times, and low solute loading compared to matrix flow. The relationship between preferential and matrix flow in waste rock is difficult to quantify (Stockwell, et al. 2006), but has important implications for the modeling of flow and geochemistry in the pile.

Fluid flow within the type III pile is seasonal due to an annual freeze-thaw cycle. Initial outflow from the pile each spring is derived from the batters (where thawing is initiated), with an increasing proportion of the pile contributing to outflow as thawing progresses. Freezing begins in October, and advances from the outside and base of the pile inwards. Flow from the basal drains and BCLs terminates by November each year.

Fluid flow within the covered pile is also controlled by freezing and thawing; however, the internal temperature of the pile was influenced by a heat trace that was turned on between 2007 and 2011. The heat trace maintained an artificially thawed state in the base of the pile, and significant outflow from the pilewas observed in the winter months each year. After the heat trace was turned off the core of

the pile cooled and froze during 2012 and 2013. The effect this had on the hydrology of the covered pile is discussed in Chapter 2.

1.7 Instrumentation in the Type III and Covered Piles

The meteorological and hydrological instrumentation used for this research are summarized in Table 1-1. Meteorological data is collected at a MET station located approximately 1km from the waste rock piles, and through 4 rain gauges located on the crests of the piles. The hydrological instrumentation contained within the piles consists of tensiometers, EHC_2O probes, and time domain reflectometry (TDR) sensors. These instruments were selected to allow for the quantification of infiltration, internal flow and storage in each pile. The tensiometers, TDRs and ECH_2O probes all rely on unfrozen conditions to record accurate measurements, and the data obtained is therefore only considered reliable during times when the pile is thawed.

Table 1-1: Instrumentation in the waste rock piles

Instrument	Model	# in TIII Pile (Depth in pile)	# in Covered Pile (Depth in Pile)	Measurement
Rain Gauge	Young Model 2202	1 (Crest)	2 (Crest)	Rainfall
Weather Station[1]	-	-	-	Temperature, wind speed and direction, relative humidity, solar radiation
Tensiometer	Soil Moisture Model 2725	4 (0.6 & 1.2m)	4 (0.6 & 1.2m)	Matric Tension
ECH$_2$O Probe	Decagon Devices TE and 5TE	0	7 (In TI and till)	Volumetric moisture content
TDR	Custom Built[2]	12 (1-9m)	10 (6-10m)	Volumetric moisture content
Tipping Bucket (Drain)	Custom Built[3]	2 (Basal)	1 (Basal)	Flow volumes through basal drains
Tipping Bucket (BCL)	Young Model 2202	12 (Basal)	0	Flow volumes through BCLs

[1] The weather station is run by the Diavik Health Safety and Environment team

[2] Following the design of (Nichol 2002)

[3] Blueprint for tipping bucket found in (Fretz 2013)

1.8 Key Parameter Estimates from Previous Work

Previous research has focused on physically characterizing the waste rock piles. The main hydrologic properties determined by Neuner (2009) and Fretz (2013) are summarized in Table 2. Information regarding how each parameter was calculated can be found in the references provided.

Table 1-2: Key parameter estimates from previous work

Parameter (units)	Value	Reference
Bulk Porosity (-)	0.25	(Neuner 2009)
Porosity attrib. to macropores (-)	0.2	(Neuner 2009), (Fretz 2013)
Porosity attrib. to matrix(-)	0.05	(Fretz 2013)
Porosity of matrix (-)	0.25	(Fretz 2013)
Bulk K_{sat} (m/s)	6×10^{-3}	(Fretz 2013)
Matrix K_{sat} (m/s)	9×10^{-6}	(Neuner 2009)
Bulk field capacity (m^3/m^3)	0.06	(Neuner 2009)
Infiltration Capacity(m/s)	5×10^{-6}	(Neuner 2009)

1.9 Comparison of the Test Piles to the Full Scale Pile

The full scale pile is a volumetrically core dominated system; however, the majority of the core of the covered pile is currently frozen year round. Fluid flow is restricted to the active zone that forms on the outer edges of the pile each summer, and infiltration into the pile is anticipated to occur through the crest and batters of the pile. The closure plan for the full scale pile utilizes an engineered cover similar to that found on the covered test pile. The performance of the experimental covered pile will be used to modify the mine closure plan in order to ensure that the active zone of the full scale pile does not contain acid generating rock.

1.10 Figures for Chapter 1

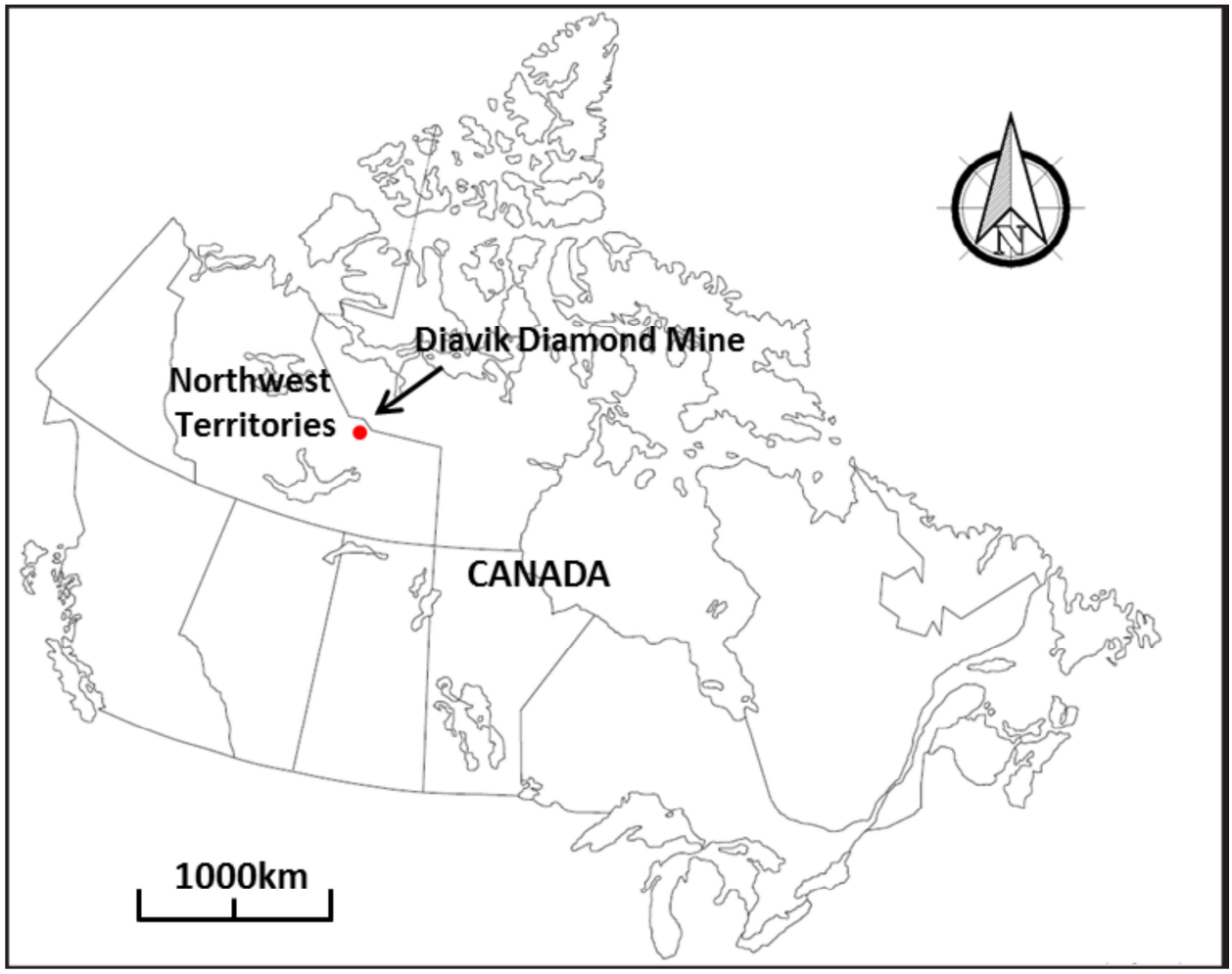

Figure 1-1: Location of Diavik Diamond Mine. Figure from Fretz (2013)

Figure 1-2: Aerial photograph of the test piles research area. Photo from Fretz (2013)

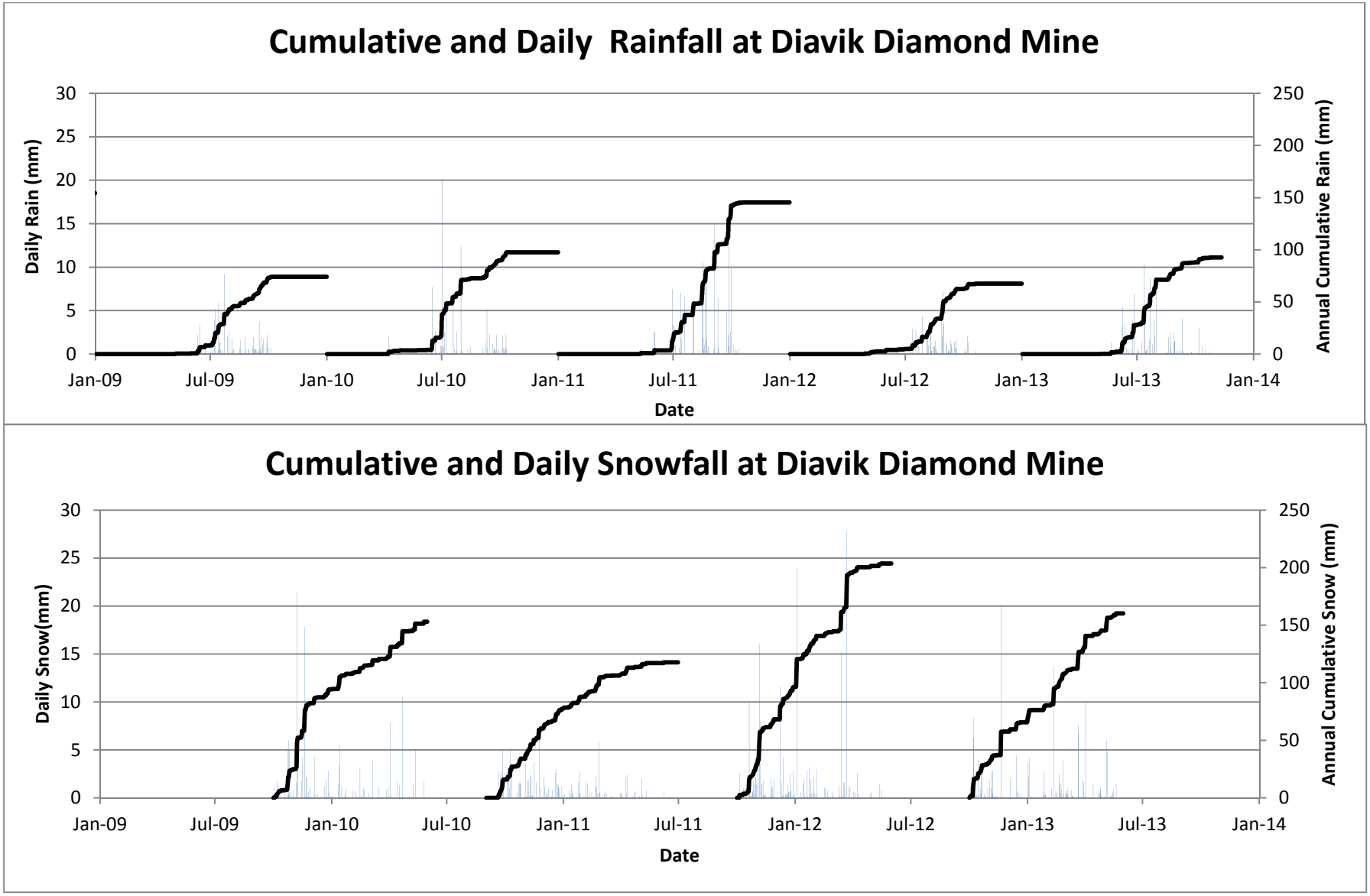

Figure 1-3: Daily and cumulative annual precipitation at Diavik

Figure 1-4: Representative surface textures on the crest of the waste rock piles. 1 x1m scale. Images from (Fretz, 2013)

Figure 1-5: Representative surface texture of the batters of the uncovered piles. 1m x 1m rectangle in bottom left of image for scale and comparison to Figures 1-4 and 1-6.

Figure 1-6: Representative surface textures on the batters of the covered pile. 1m x 1m rectangle in bottom centre of image for scale and comparison to Figures 1-4 and 1-5.

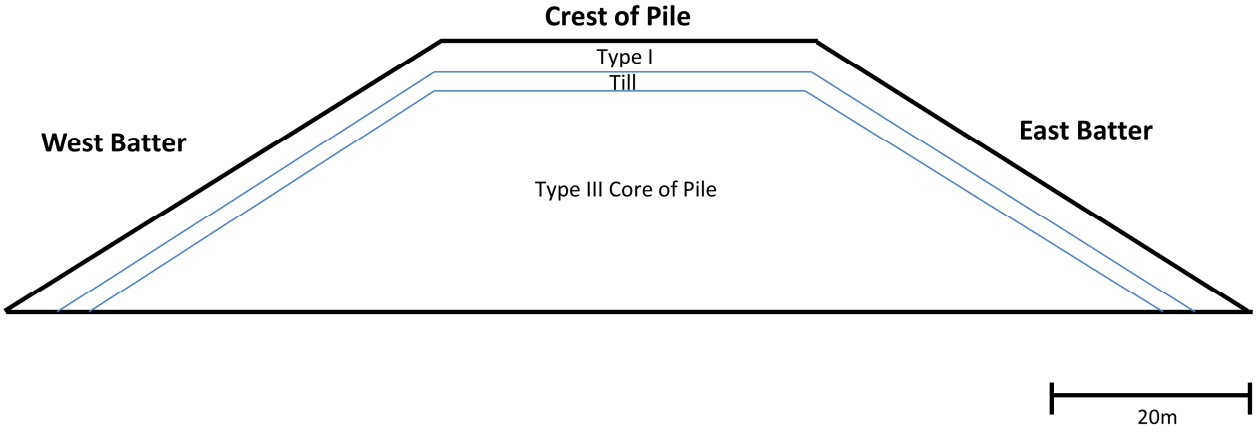

Figure 1-7: Schematic cross section of the covered pile.

Figure 1-8: Construction of the BCL cluster in the type III pile. Image from Smith (2006)

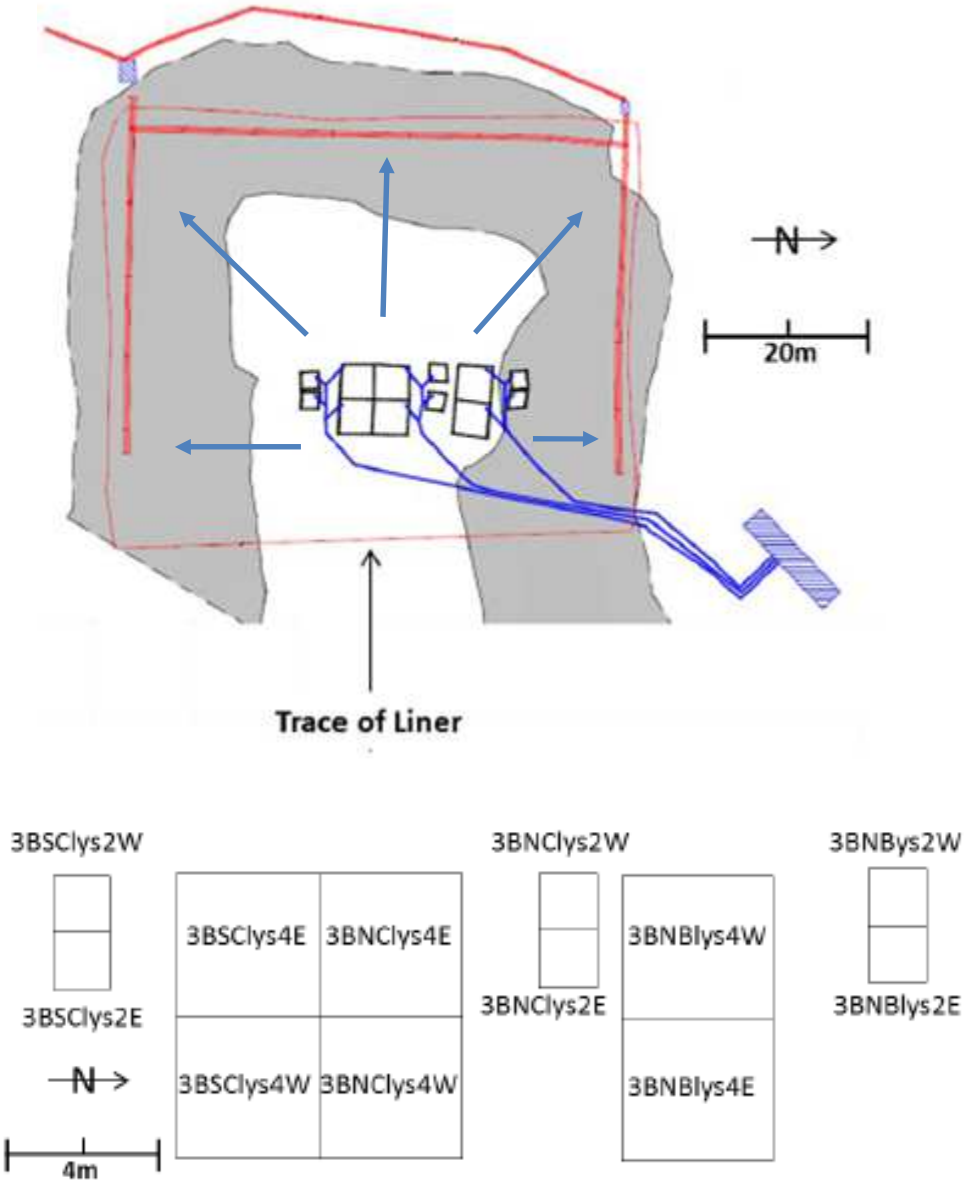

Figure 1-9 a-b: Drainage within the type III pile

a. As built drawing of the pile. White represents the crown of the pile, grey represents the batters. The thick red lines show the location of the basal drain, and the thin red line shows the extent of the HDPE liner. The BCLs are shown as black rectangles under the crown of the pile. The blue arrows show intended flow directions. Image modified from Fretz (2013)

b. Schematic showing the name of each BCL in the type III pile

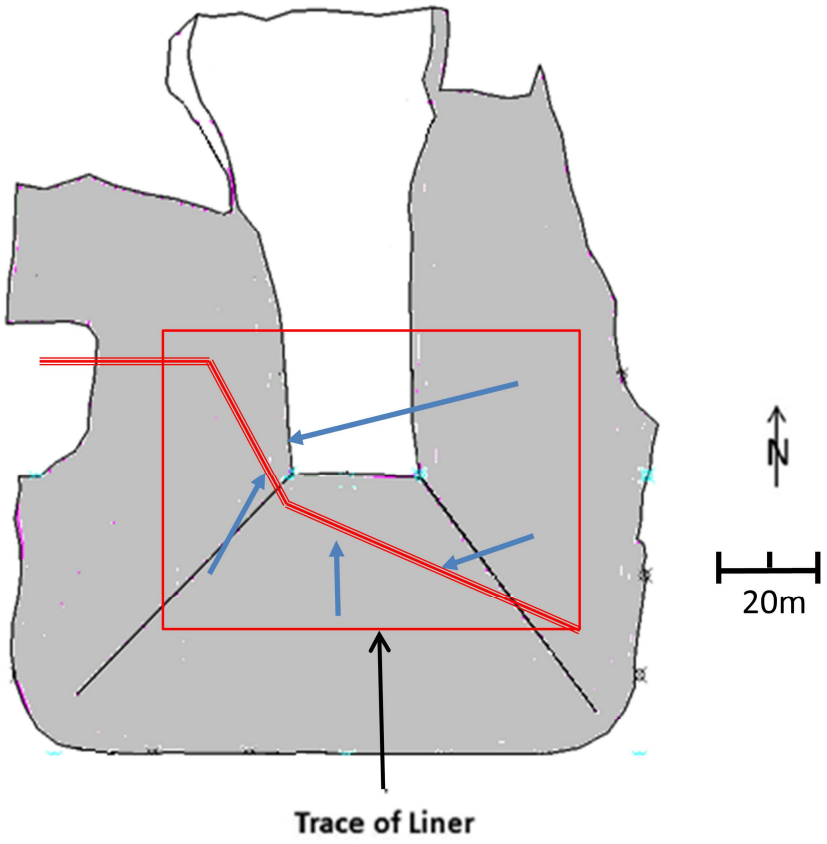

Figure 1-10: Drainage within the covered test pile.

White represents the crown of the pile, grey represents the batters. The thick diagonal red line shows the basal drain location, and the thin red line shows the extent of the HDPE liner. The blue arrows show intended flow directions. The BCLs in the covered pile are not shown, since they have never conducted flow.

Chapter 2: Ongoing Data Analysis

The hydrology of the waste rock piles has been continuously monitored since 2007, and the dataset from 2007-2013 is presented in this chapter. Infiltration into the crest of each pile is discussed in terms of the Penman Monteith formulation utilized by Fretz (2013). Following this, the hydrology of the type III and covered piles is discussed in terms of initial wet up, storage and outflow. Some of the information and figures contained in this chapter are also used in Chapters 3, 4 and 5 in order to provide the necessary background information to make each chapter a standalone article.

The full suite of hydrological data collected by the WRRG between 2007 and 2013 is compiled in Appendix A.

2.1 Infiltration into the Waste Rock Piles

2.1.1 Infiltration of Rainfall into the Crest of the Piles

Infiltration through the surface of the waste rock piles is divided between snowmelt and rainfall. The annual infiltration of rainfall into the crest of the uncovered rock piles was estimated by Fretz (2013) using the Penman Monteith formulation and results from the four 2m scale active zone lysimeters shown in Figure 1-2. The work conducted by Fretz was extended to estimate infiltration into the crest of the type III pile in 2012 and 2013. Additionally, the infiltration of rainfall into the crest of the covered pile was estimated for each year between 2007 and 2013 using the same formulation. A summary of the total rainfall and infiltration into the crest of each pile is presented in Table 2-1.Note that the difference in rainfall and infiltration between the piles in 2006 and 2007 is a result of artificial rainfall events that were applied to the crest of the type III pile.

Table 2-1: Estimates of rainfall infiltration into the crest of the waste rock piles. The type III pile received artificial and natural rainfall events in 2006 and 2007

	Type III Pile		Covered Pile	
Year	Rainfall (mm)	Estimated Net Infiltration (mm)	Rainfall (mm)	Estimated Net Infiltration (mm)
2006	58	51	-	-
2007	153	92	92	40
2008	154	88	154	88
2009	74	11	74	11
2010	98	40	98	40
2011	146	84	146	84
2012	68	9	68	9
2013	91	26	91	26

2.1.2 Infiltration of Snowmelt into the Experimental Waste Rock Piles

The infiltration of snowmelt into the waste rock piles has not been quantified prior to this research. Snowmelt infiltration represents a significant portion of the total recharge received by the piles each year, and Chapters 4 and 5 in this thesis are devoted to understanding the relative contributions of snowmelt to the total recharge received by the piles.

2.2 Dataset for the Type III Pile

The dataset for the type III pile consists of volumetric moisture contents measured by TDR probes, and outflow recorded at both basal drains and the BCLs. This data is also presented in Chapter 3, although less detail is provided regarding the daily outflow from the pile.

2.2.1 Flooding in December, 2012

In December of 2012 the trailer that houses the instrumentation for the type III pile was flooded and the electrical systems in the trailer were destroyed. Power to the trailer was not restored until September, 2013. This event influenced the thermal regime of the type III pile by temporarily cutting power to the heat trace in the drainage pipes for the basal drains and BCLs. The disruption of the heat trace is

believed to have induced or enhanced long-term (multi-year) freezing in the core of the pile (discussed further in Chapter 3).

2.2.2 Pore Water Storage in the Type III Pile

Within the pile, the volumetric moisture content of the matrix is determined using 12 time domain reflectometry probes. TDR probes measure the dielectric permittivity of a material, and the VMC of that material can be calculated from this measurement. The dielectric permittivity of ice is very similar to that of air and the TDRs therefore show a rapid decrease in apparent moisture content during freezing each year. This is not reflective of the actual water content in the pile, and for this reason the TDR measurements are only considered accurate during times when the pile is thawed.

The TDRs were placed along tipping faces during construction, and are located in two lines, one that is 2m south of centre and one that is 2m north of centre. The location of each probe is shown in Figure 2-1, and the VMC measured by each TDR from 2007-2013 is shown in Figure 2-2. Note that the onset of melting and freezing can be clearly seen each year. The collection of data from the TDRs was interrupted by the flood in late 2012 and early 2013; however, data was collected continuously during the 2013 flow season. The type III pile wet up to a depth of at least 9m in 2008, and in general the moisture content of the pile reaches a maximum each year of between 20-25% (80-100% matrix saturation). Most seasonal drying occurs in the upper two to three metres of the pile; although a very dry year in 2012 (9mm infiltration) caused drying to a depth of at least 5 metres. Although the upper portions of the pile were drier than average in 2012 and 2013, it is assumed that the pile has attained a pseudo steady state of matrix storage over a multi-year period. This means that infiltration into the pile over this time period will either be matched by outflow, or may result in the formation of multi-year ice in macropores at the base of the pile.

2.2.3 Outflow from the Type III Pile

Outflow from the type III pile is collected through the north drain, the south drain and the basal collection lysimeters.

Outflow from the Basal Drains

The daily and cumulative annual flow recorded at both basal drains between 2007 and 2013 is shown in Figure 2-3. Following the flooding event in 2012, the volume of outflow from the south basal drain was the lowest ever recorded. Conversely, the volume of outflow observed from the north basal drain following the flooding event was higher than average. These observations are interpreted to be the result of ice formation in the core of the pile, and are discussed further in Chapter 3.

Outflow from the Basal Collection Lysimeters

Outflow from the BCLs is sporadic and unpredictable (Figure 2-4). Flow collected by the BCLs is most likely a function of freezing and thawing within the pile, which is expected to vary from year to year at the local scale. After the flooding event flow was not observed from the BCLs until power was restored to the heat trace in the base of each BCL in September of 2013.

Total Outflow from the Type III Pile

Figure 2-5 is a summary of the total annual flow volumes collected from the type III pile. Since 2007, 85% of the total volume of outflow has been collected by the south drain, 13% by the north drain, and 2% by the BCL's. Outflow from the pile peaked in 2010 and has decreased steadily since. This decrease is likely due to the formation of multiyear ice in the centre of the pile, which increases the amount of water retained in storage, and therefore decreases total outflow. The potential formation of multi-year ice in the core of the type III pile is discussed further in Chapter 3.

2.2.4 Summary of the Type III Pile Dataset

The type III pile is the most comprehensively studied of the experimental waste rock piles. The wet up period of the pile was described by Neuner (2009) and Fretz (2013), and the geochemistry of pore water from the pile was described by Bailey (2013) and Sinclair (2014). The largest unresolved issues

concerning the hydrology of the type III pile are: the difference in flow volumes conducted by the north and south drains, the velocity and residence time of pore water in the pile, the potential formation of multi-year ice at the base of the pile, and the quantification of snowmelt and rainfall infiltration through the batters of the pile. The research contained within this thesis addresses these issues.

2.3 The Covered Pile

In this section the hydrology of the covered pile is discussed. The hydrologic dataset for the covered pile consists of volumetric moisture contents measured by TDR and ECH2O probes, matric suction measured by tensiometers, and outflow recorded at the basal drain. The data presented in this section is also found in Chapter 5, although less detail is provided regarding the daily outflow from the pile and storage immediately below the till layer.

2.3.1 The Effect of Turning Off a Heat Trace

The thermal regime of the pile was significantly altered when a basal heat trace was turned off in June, 2011. Prior to 2011 the heat trace maintained a thawed state in the base of the pile and significant outflow was observed in the winter months each year. After the heat trace was turned off the core of the pile cooled and froze during 2012 and 2013 (Figure 2-6). As previously mentioned, the basal liner in the covered pile only drains 40% of the piles total surface area, and is centred underneath the core of the pile (Figure 1-10). In comparison, the basal liner in the type III pile underlies both the core and the batters of the pile. This means that the onset of freezing conditions in the core of the covered pile will have a much greater impact on outflow than freezing in the core of the type III pile.

The instrumentation located in the covered pile is powered independently of the trailer that was damaged by flooding; because of this there was no loss of data collected from the covered pile due to the flood.

2.3.2 Pore Water Storage in the Covered Waste Rock Pile

The storage of pore water in the covered pile is measured in the type III and till material using TDR and ECH_2O probes respectively. The VMC of the type I material in the covered layer is estimated using measurements of matric tension and a water retention curve developed by Neuner (2009).

Type III Material

The VMC of the type III matrix material is measured using 10 TDR probes that range in depth from 6 to 10m below the crest of the pile. The TDR probes were placed along tipping faces during construction, and are located in two lines, one that is 2m east of centre and one that is 2m west of centre. The location of each TDR probe is shown in Figure 2-7, and the VMC measured by each TDR from 2007-2013 is shown in Figure 2-8. The type III rock was placed below residual saturation, and wet up over a two year period following construction. By the end of 2009 all but one of the TDRs was recording VMCs between 15 and 25% (60-100% saturation). From 2009 until 2012 the pile had an average peak moisture content of between 20 and 25% each year. From August 2012 to August 2013 the data from each of the TDR probes showed a strong drying trend and some of the TDRs froze. The drying trend may be due to low infiltration in 2012 and 2013 (Table 2-1) or may reflect the gradual onset of freezing conditions in the matrix surrounding the TDRs. Ongoing thermal modelling by Pham (2014) shows that the portion of the pile surrounding the TDR probes was consistently around 0^oC during this time period. Experiments conducted by Neuner demonstrated that some moisture in the pile remains liquid at temperatures just below 0^oCdue to capillary forces imparted from the small particles in the matrix (Figure 2-9).

Till

The gravimetric moisture content (GMC) of the till was measured during construction, and averaged 8%. It was measured again during an excavation conducted on the east batter of the pile in July, 2011, and was relatively unchanged with an average GMC of 9% (L. Smith 2014).

The VMC of the till is measured by ECH_2O probes that were installed in shallow boreholes during the summer of 2008. Like the TDRs, the ECH_2O probes only produce accurate data when the pile is thawed. The VMC at the top and in the middle of the till peaks to around 40% each year in July and August respectively, likely due to the arrival of snowmelt (Figure 2-10). Following this the VMC of the till decreases to around 10% at both locations prior to freezing. Most infiltration into the type I material in the pile occurs in the autumn each year (Fretz, 2013); however, this is not reflected in the moisture contents measured in the till. This suggests that the infiltration which occurs each fall does not reach the till layer until the following spring.

The VMC measured by the deepest ECH_2O probe peaks at around 25%. This is equal to the matrix porosity of the type III material, and suggests that the probe is actually located at the very top of the type III material, rather than in the till where it was intended to be. The peak in VMC seen at this depth each year is interpreted to be a result of result of thawing and the infiltration of snowmelt.

The temperature of the covered pile is monitored using thermistors, and ongoing thermal modelling conducted by Pham (2014) shows that the till layer freezes and thaws annually (Figure 2-6). The type I cover placed on top of the till was intended to keep the till frozen year round to prevent infiltration into the core of the pile. Since permanently frozen conditions have not been established in the till, it is anticipated that infiltration into the core of the pile will continue during the summer months each year.

Type I Material

The matric tension of the type I material is measured using tensiometers installed on the crest of the pile at depths of 0.6 and 1.2m. The measurements recorded by the tensiometers in 2013 are shown in Figure 2-11. Note that measurements are only taken during the summer months, as the tensiometers are removed each winter. The suction measured by the tensiometers can be correlated to a volumetric moisture content using a water retention curve developed by Neuner (2009) (Figure 2-12). In general,

the VMC of the TI material decreases between infiltration events, sometimes to as low as 5%. Following an infiltration event the tensiometers at 0.6m depth show a rapid increase in VMC, while the tensiometers at 1.2m do not fluctuate as quickly. Vertical upward and downward gradients are seen throughout the flow season, and are a function of infiltration. In general, upward gradients are observed during infiltration periods in the spring, and autumn. Periods with no infiltration in the summer can induce downward gradients, as shown in Figure 2-11.

2.3.3 Outflow from the Covered Pile

Outflow from the covered pile is collected exclusively through the basal drain, and the volume of outflow observed each year was strongly altered by turning off the heat trace in 2011. The daily and cumulative outflow observed from the covered pile basal drain is shown in Figure 2-13. From 2008 to 2011 the basal drain tipping bucket recorded outflow volumes of 27 to 105 m^3 per year, with most outflow recorded during the winter. After the heat trace was turned off flow continued until the end of 2012 as the pile slowly cooled and froze. By 2013 the total annual outflow from the pile decreased to only 6m^3.

2.3.4 Summary of the Covered Pile Dataset

The dataset for the covered pile between 2007 and 2011 was presented by Fretz (2013). Since this time the hydrology of the covered pile has been strongly altered due to turning off a basal heat trace in June of 2011. As of 2013 flow through the basal drain has essentially stopped, and it is anticipated that water that infiltrates through the till each summer will now result in the formation of multiyear ice in the frozen portions of the pile. This ice will not be measured by any of the existing instrumentation in the pile, and for this reason, it is important to quantify the amount of infiltration through the surface of the covered pile, and the proportion of this infiltration that passes through the till layer. The amount of snowmelt and rainfall infiltrating the surface of the covered pile each year is examined in this thesis. A tracer test conducted on the east batter of the pile in the summer of 2013 is intended to determine the

amount of infiltration occurring through the till layer. The data from this experiment is currently being analysed by Jordan Zak (Ongoing).

2.4 Figures for Chapter 2

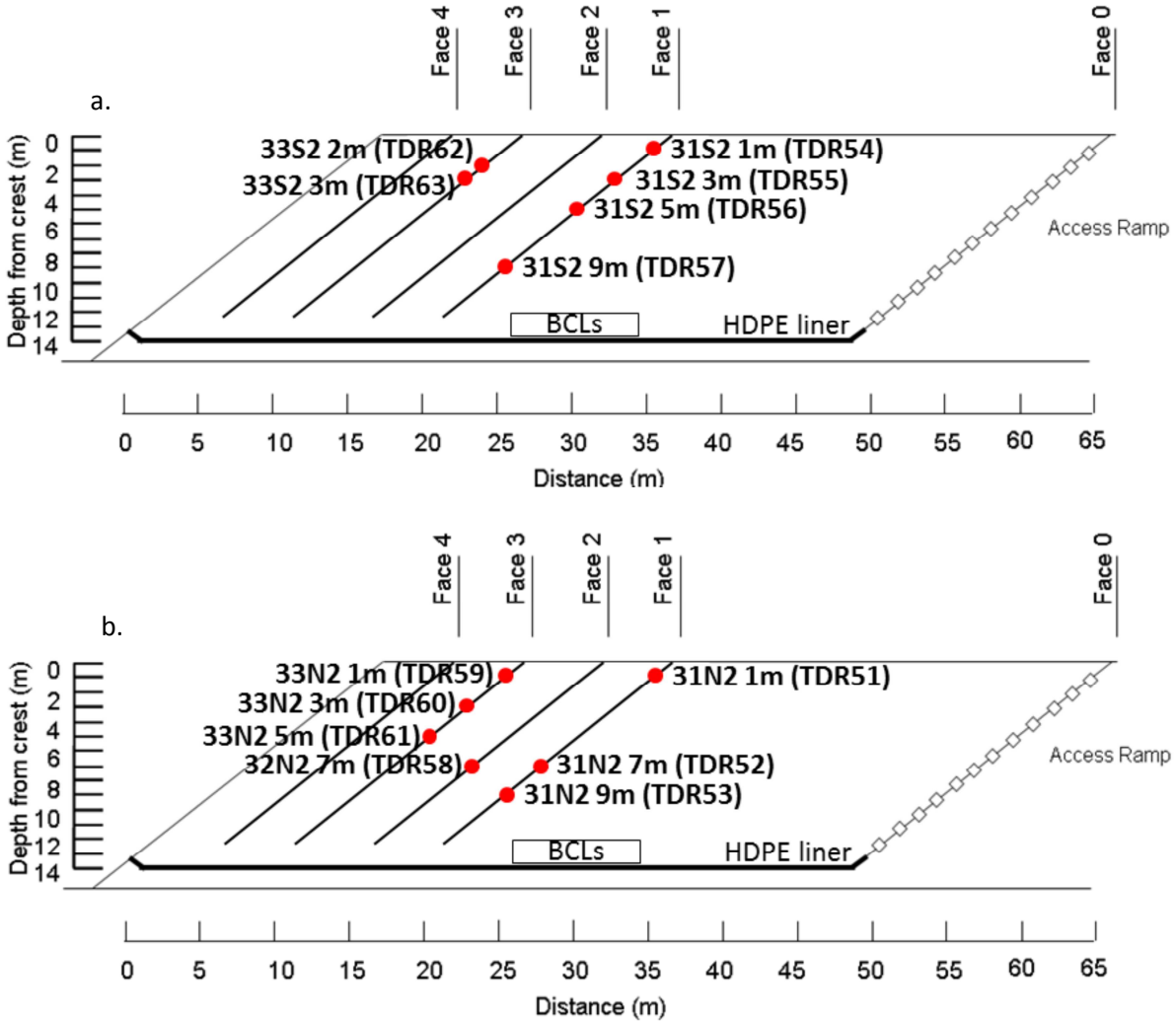

Figure 2- 1: Location of the TDR probes in the type III pile. Image from Fretz (2013)

a. Probes located 2m south of the centre line

b. Probes located 2m north of the centre line.

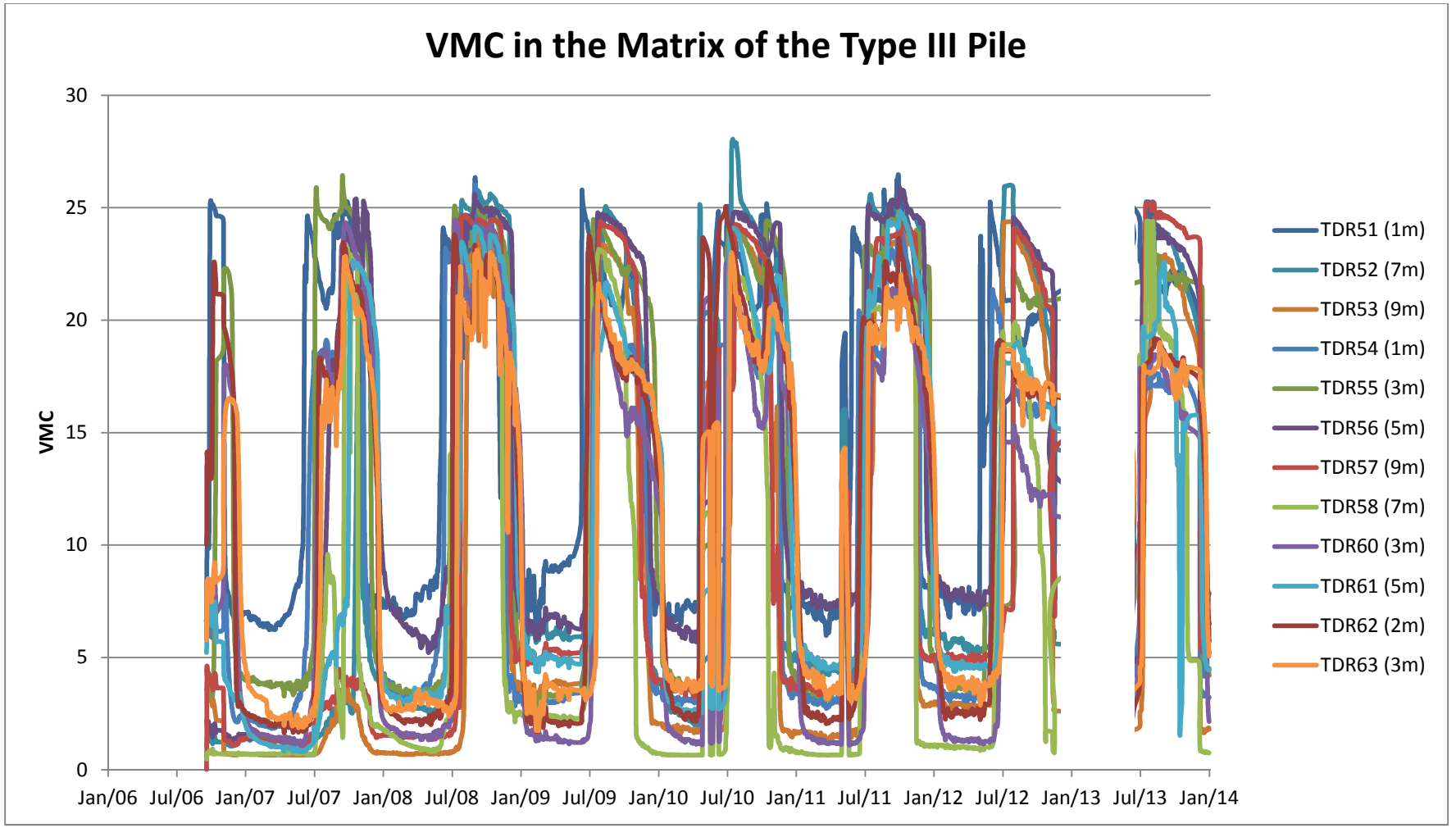

Figure 2-2: Volumetric moisture contents measured by TDR probes in the type III pile

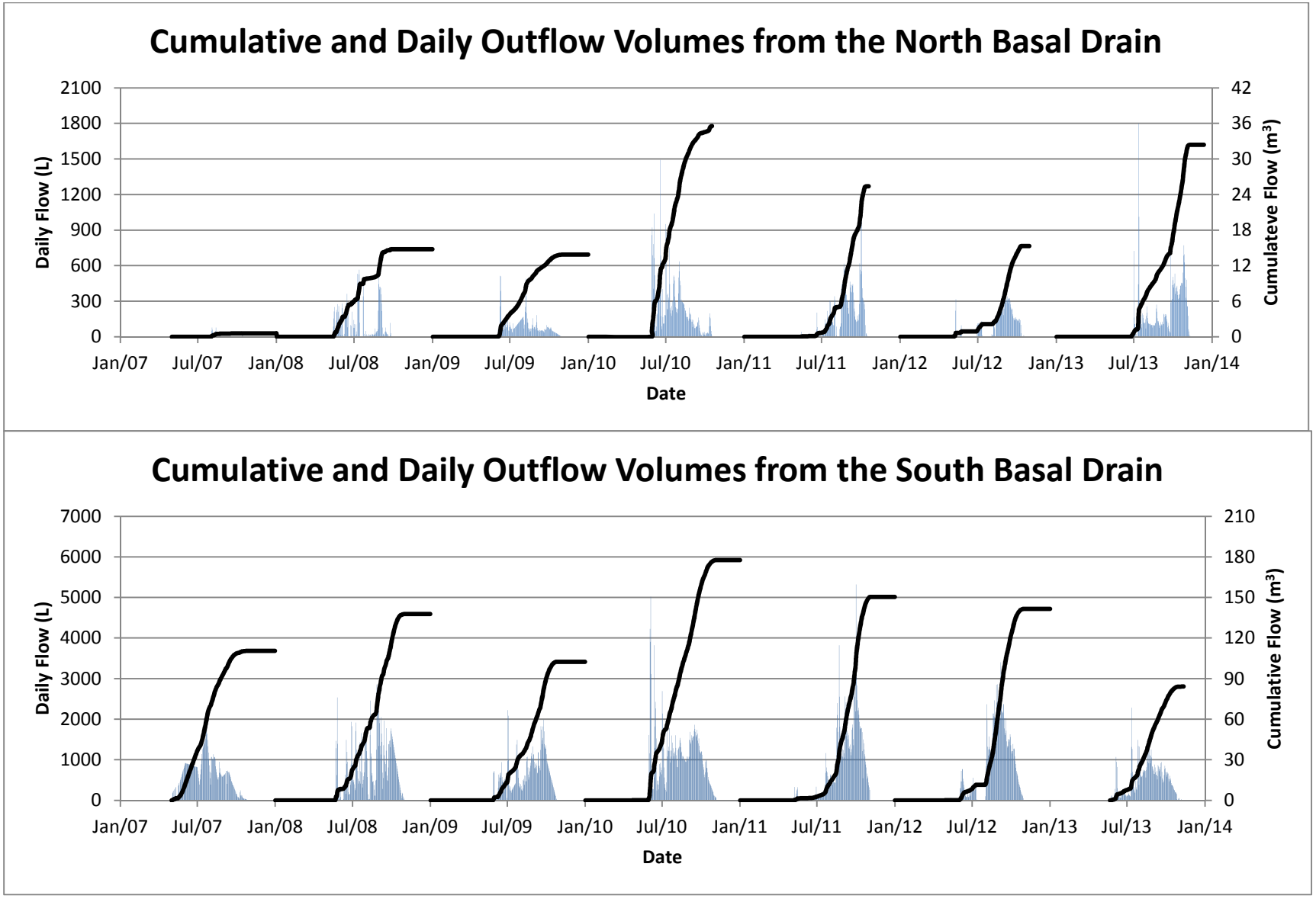

Figure 2-3: Daily and cumulative outflow volumes measured at the north and south drains

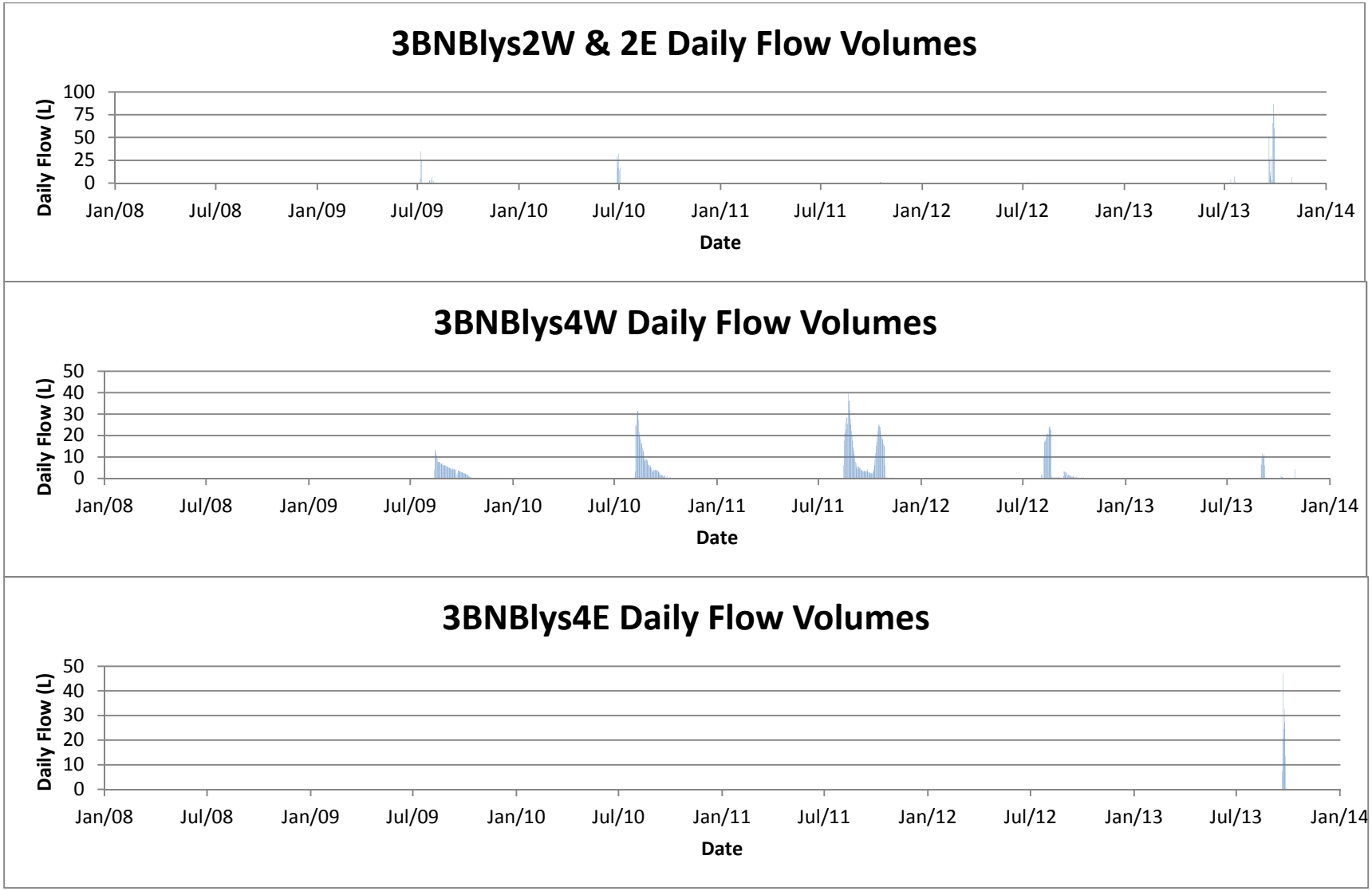

Figure 2-4: Flow through the basal collection lysimeters in the type III pile.

Figure continued on next page

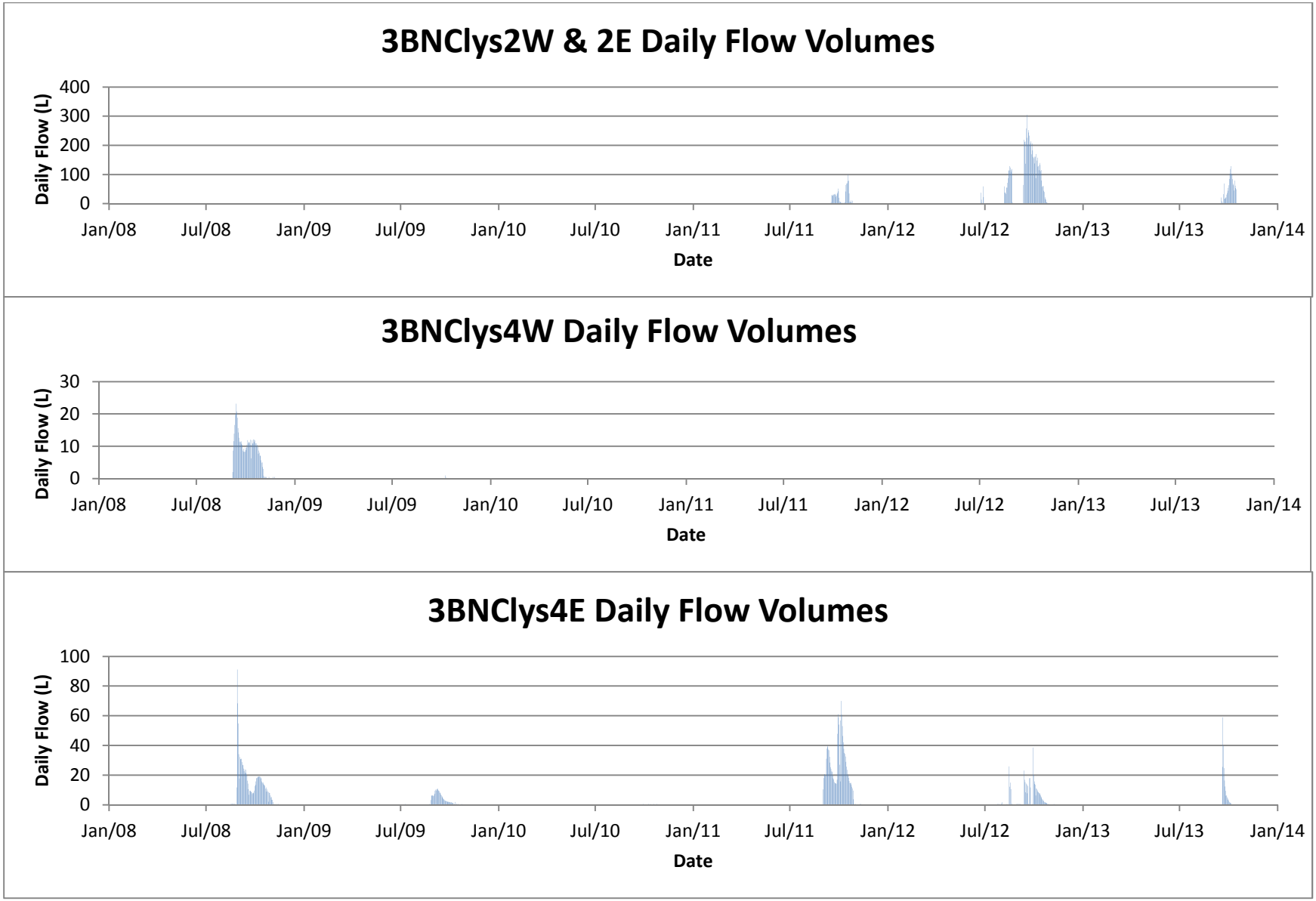

Figure2-4: Flow through the basal collection lysimeters in the type III pile. Figure continued on next page

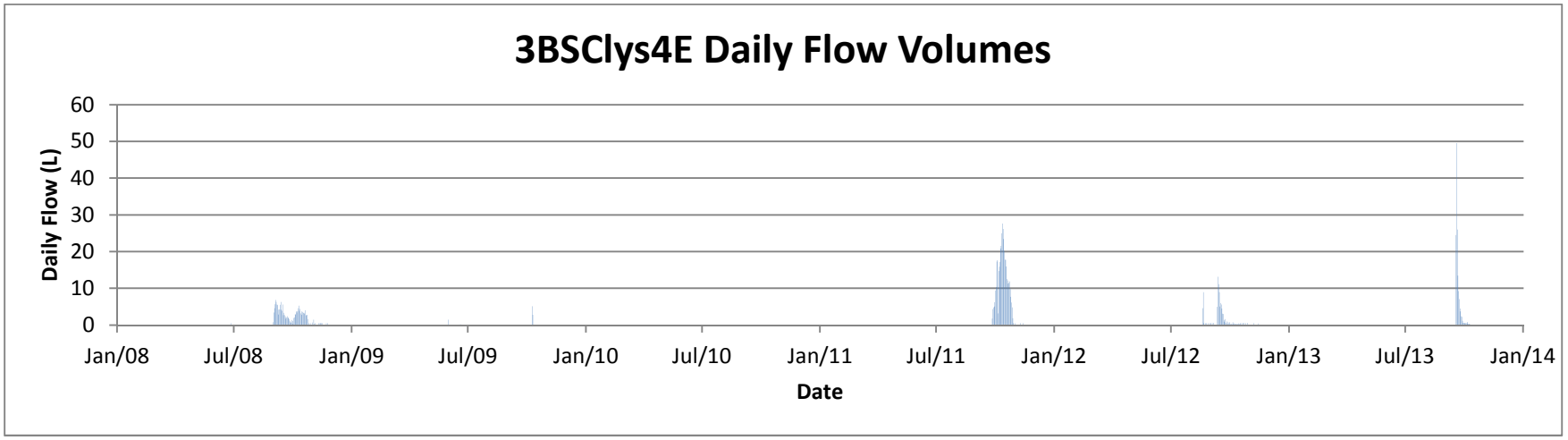

Figure 2-4: Flow through the basal collection lysimeters in the type III pile.

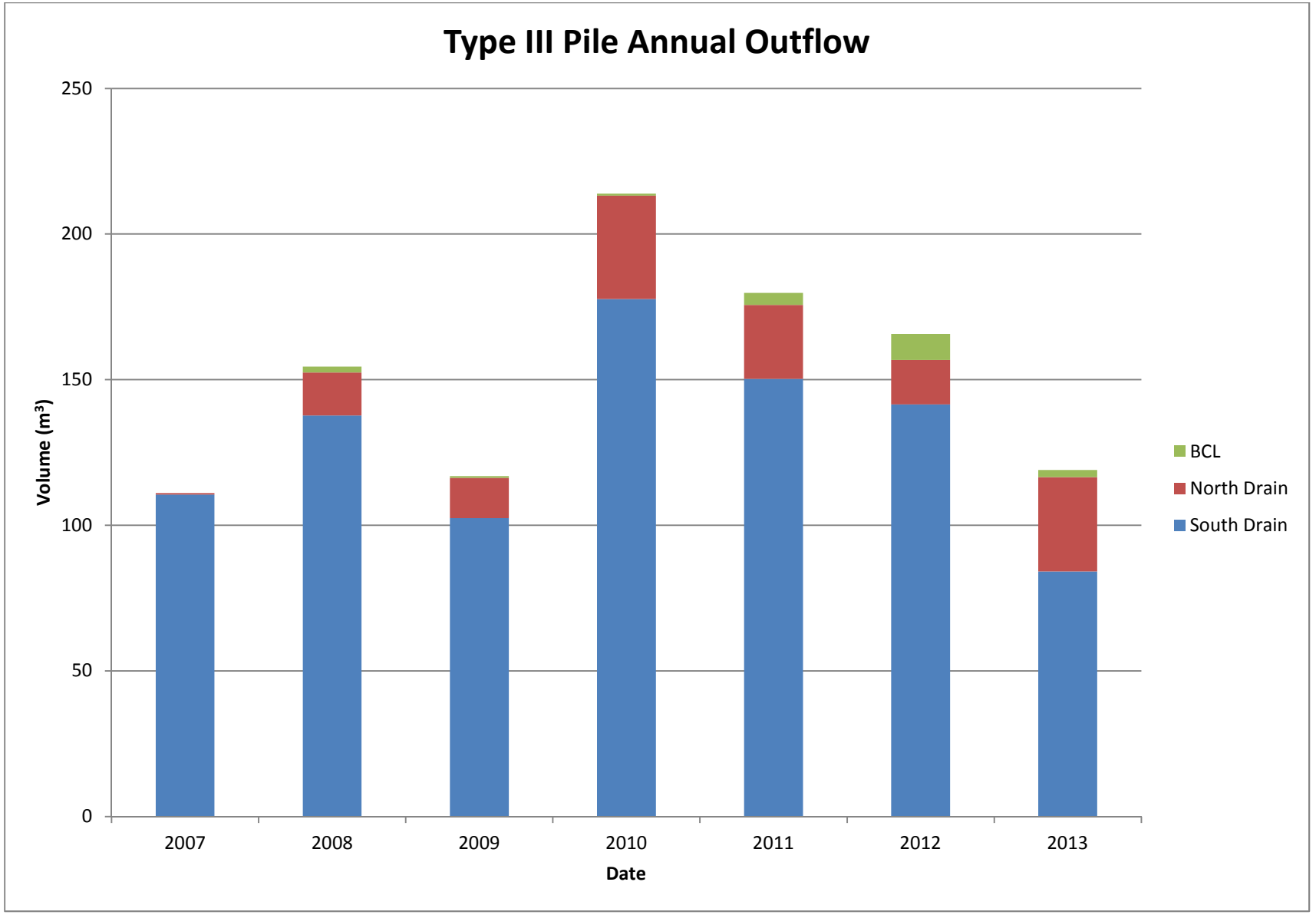

Figure 2-5: Total annual outflow from the type III pile

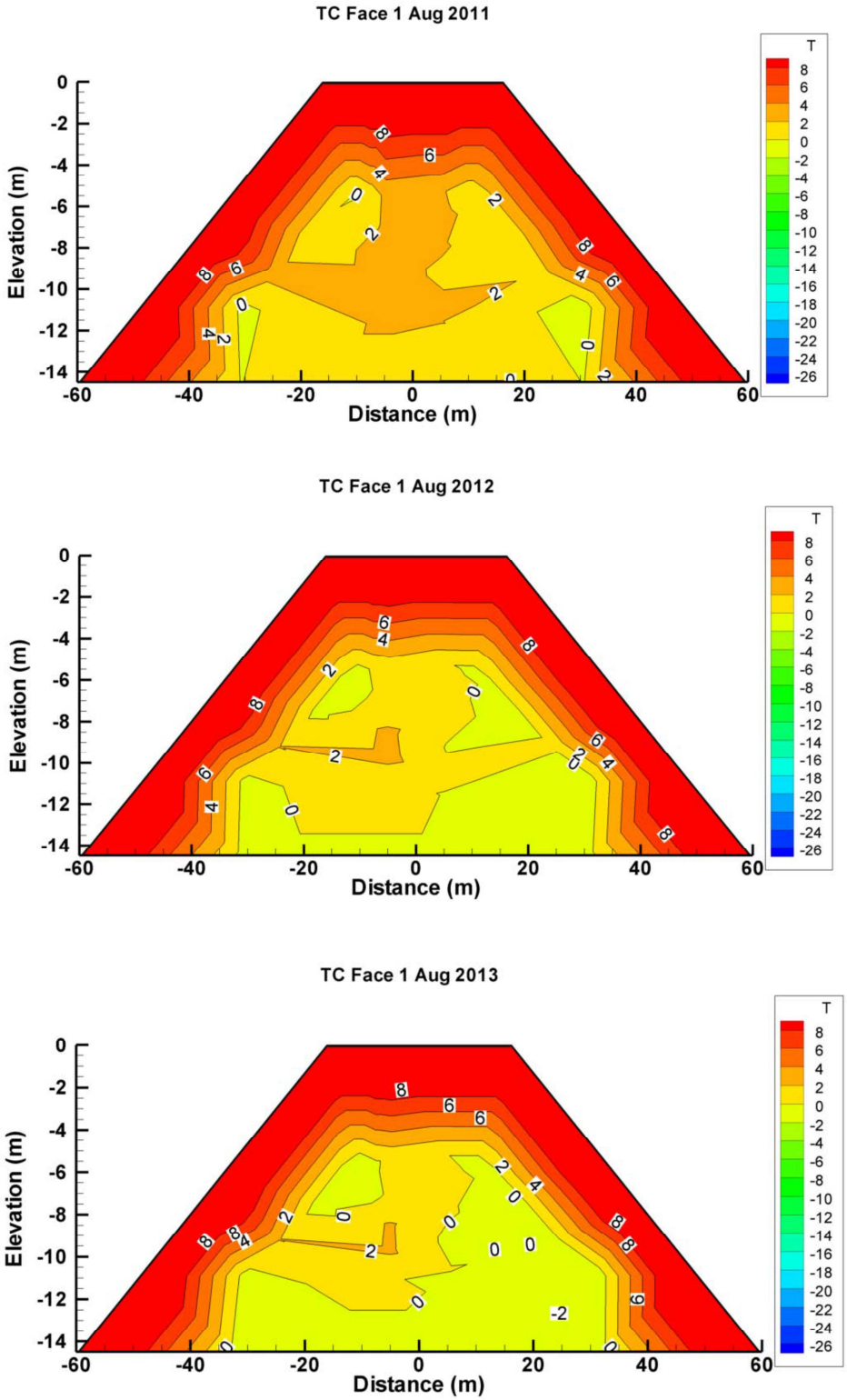

Figure 2-6: Ongoing thermal modelling of the covered pile. Image from Pham (2014)

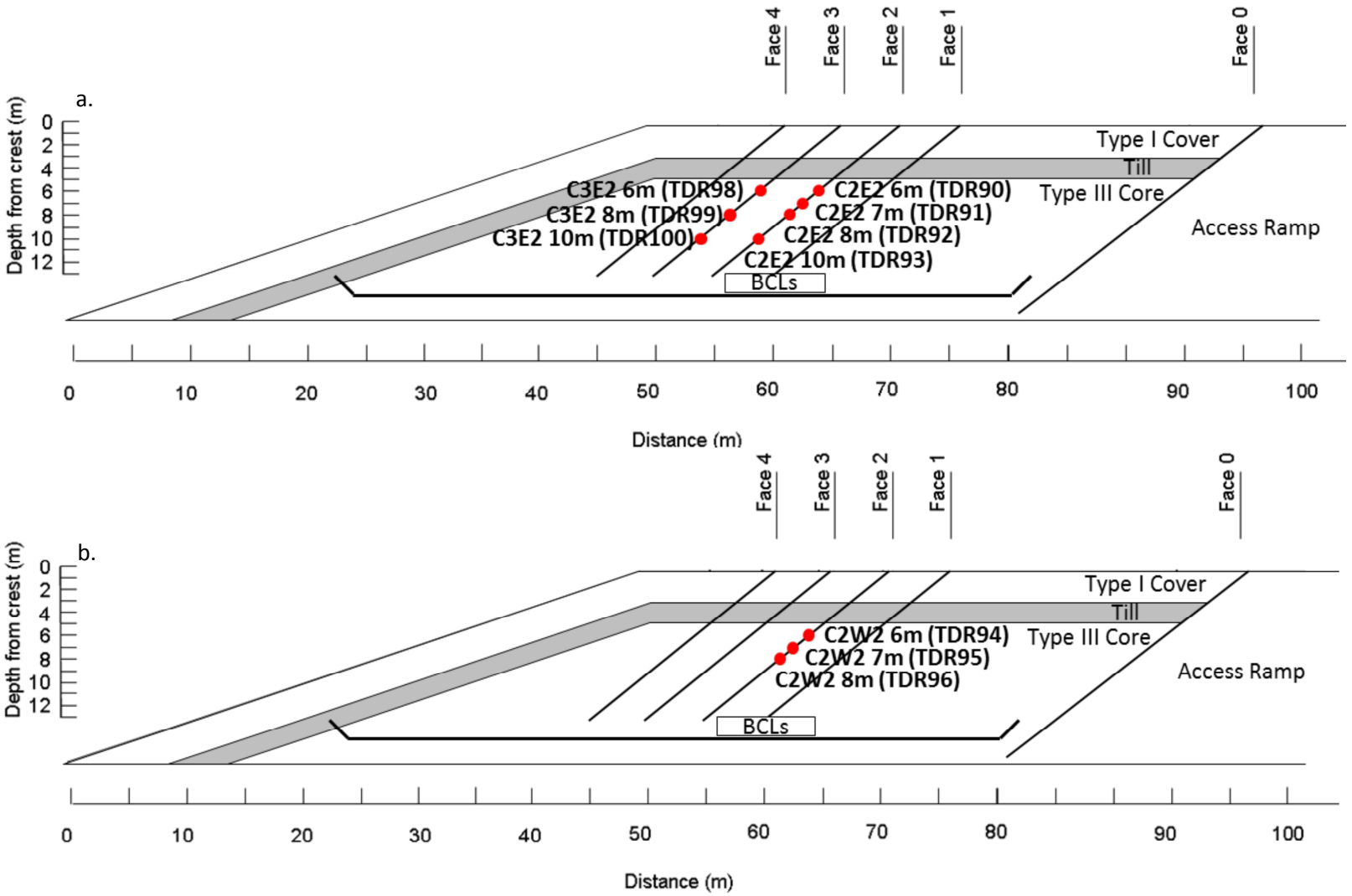

Figure 2-7a-b: Location of the TDR probes in the covered pile. Image from Fretz (2013)

a. Probes located 2m east of centre

b. Probes located 2m west of centre.

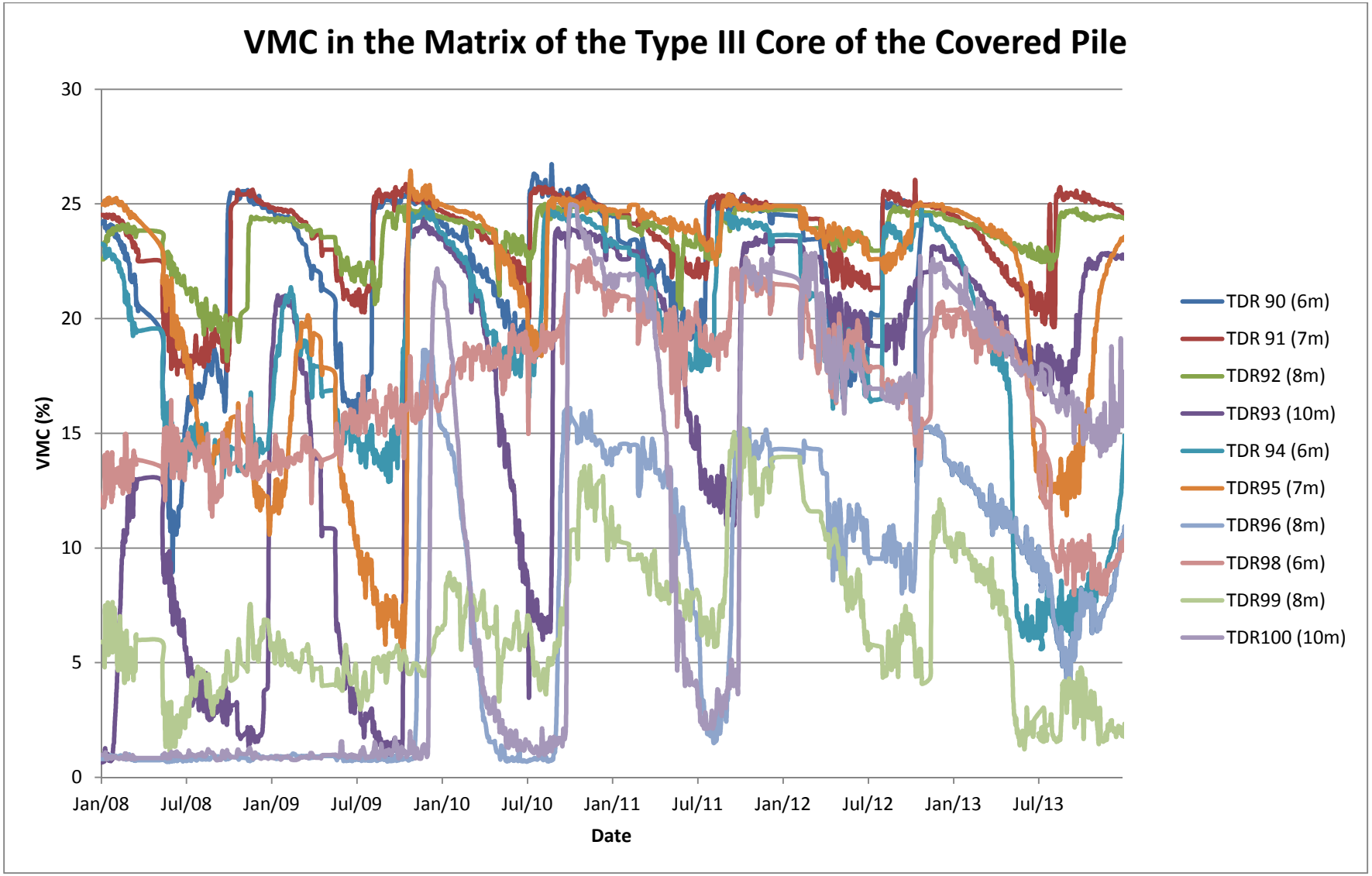

Figure 2-8: Volumetric moisture contents measured by TDR probes in the covered pile.

The depth of each probe is shown in brackets, and the location of each probe is shown in Figure 2-7.

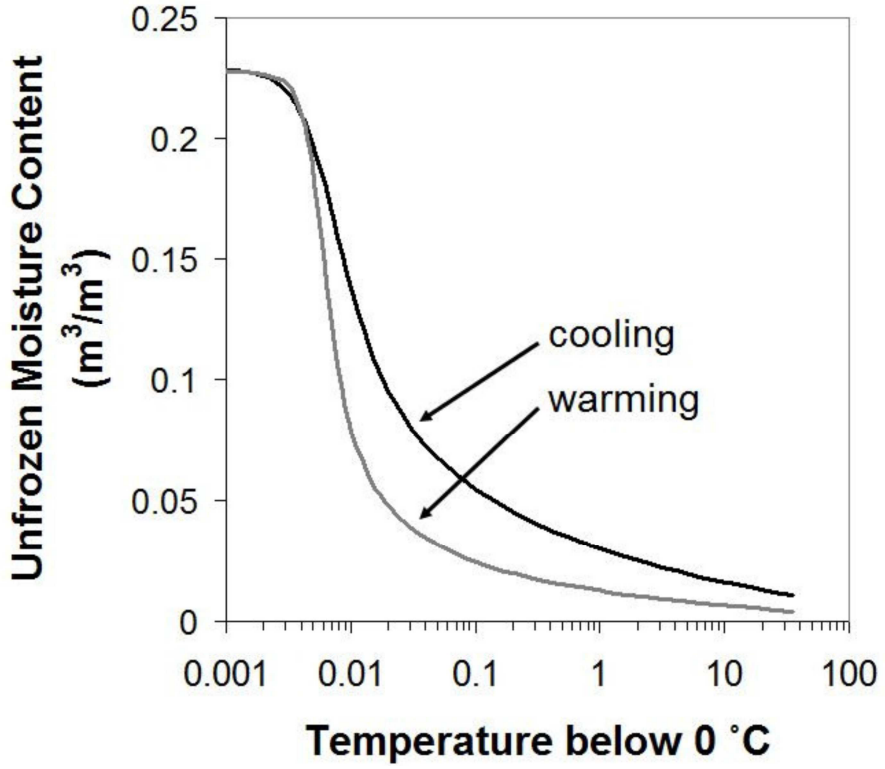

Figure 2-9: The estimated portion of moisture in the matrix material that remains liquid at below freezing temperatures due to capillary forces.

Image from Neuner (2009)

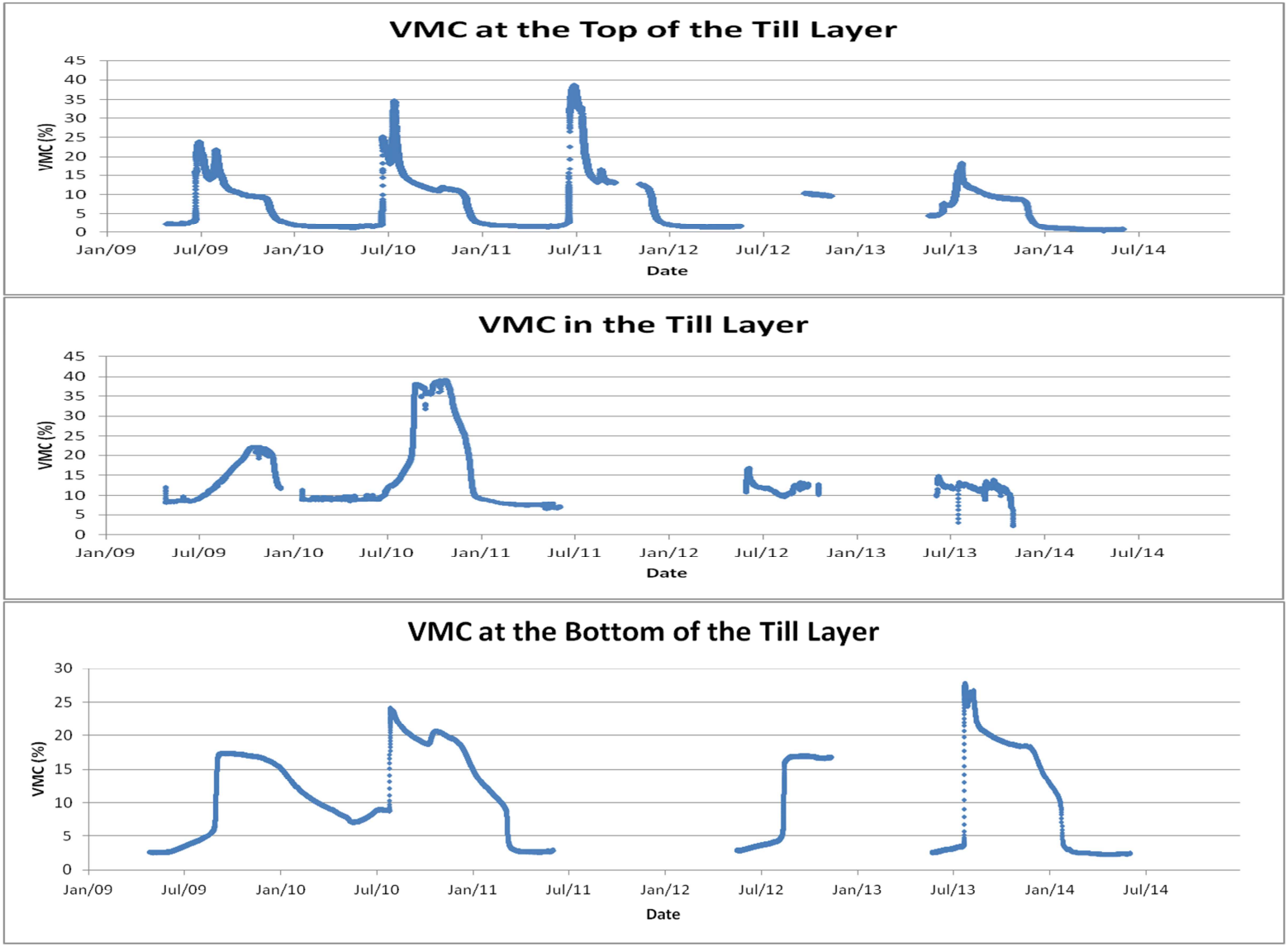

Figure 2-10: Volumetric moisture contents measured by ECH$_2$O probes in the till

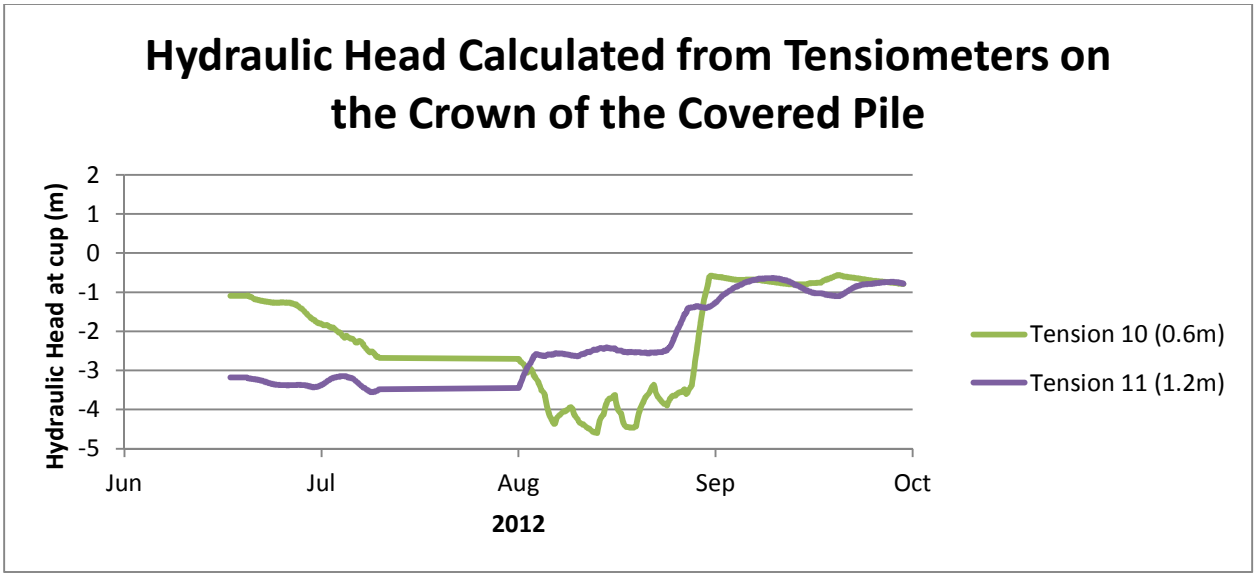

Figure 2-11: Matric tension measured by tensiometers in the TI material.

The tensiometers are removed each year during freezing conditions

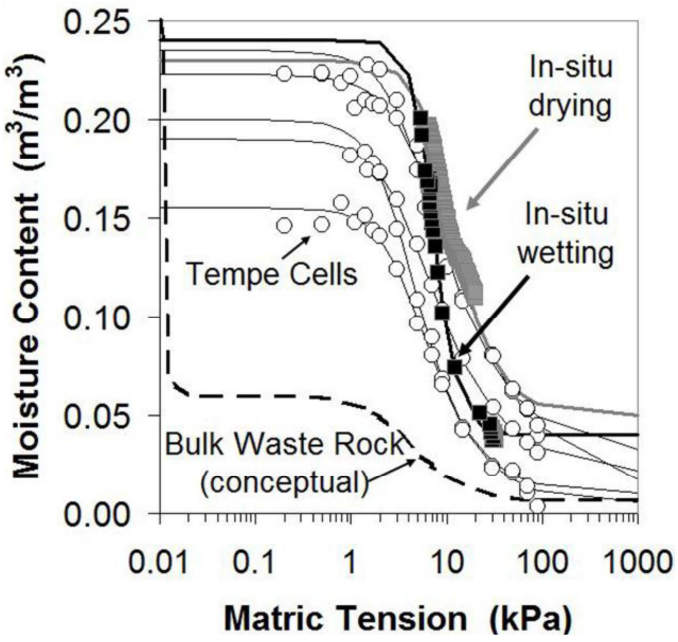

Figure 2-12: Water retention curve for the matrix material developed by Neuner (2009).

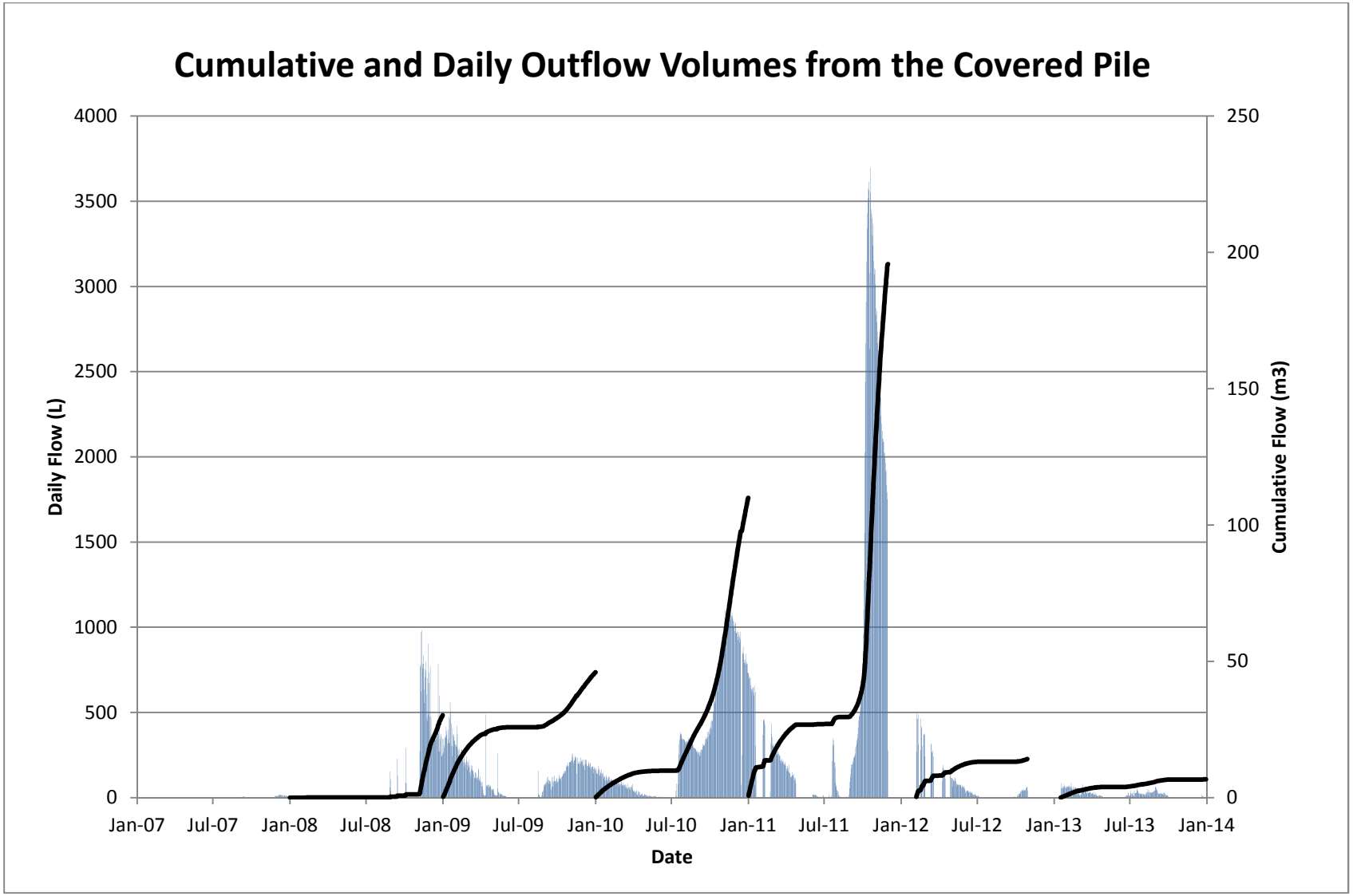

Figure 2-13: Daily and cumulative outflow volumes measured at the covered pile basal drain

Chapter 3: Quantifying the Flow Velocity and Residence Time of Pore Water in an Uncovered Waste Rock Pile in the Canadian Arctic

This chapter is written as a self contained article formatted for publication in a journal. It is intended to quantify the average flow velocity and residence time of pore water in the type III waste rock pile. Quantifying these parameters will facilitate a greater understanding of reaction rates within the waste rock, and will assist in future efforts to model the combined hydrology and geochemistry of the pile.

3.1 Summary of Chapter

A bromide and chloride tracer was applied to the crest of an uncovered experimental waste rock pile at Diavik Diamond Mine on September 13, 2007. The tracer was applied as an artificial rainfall event at a rate intended to induce preferential and matrix flow within the pile. Soil water solution samplers (SWSS) were used to observe the plume in the upper portions of the pile, and preferential flow velocities as high as 0.7m/day were seen to a depth of 9m. The presence of a low conductivity zone was inferred using a SWSS located at a depth of 2m, as samples from this SWSS yielded high concentrations of bromide for the duration of the study period (until 2013). Tracer that reached the base of the pile (14m below the crest) was recovered through a basal drain and 12 basal collection lysimeters. A second basal drain did not recover any tracer, and it was concluded that this drain only collects flow from the batters of the pile. The recovery and outflow concentrations of the tracer peaked in 2012, and as of November 2013 only 38% of the total mass of tracer has been recovered. A very low recovery of tracer in 2013 was likely caused by the formation of ice within the pile being enhanced by a non-functioning heat trace. The analysis for the tracer test therefore involves an extrapolation from the 2007-2012 data until 50% of the original tracer was recovered. The peak observed recovery occurred in 2012, and the extrapolated time to a 50% recovery occurred in 2013. The average flow velocity during times when the pile is thawed was determined to be 0.3 to 0.5 m/month, and the average residence time of pore water in the pile is estimated to be 6 years, provided that the heat trace is functioning.

3.2 Introduction

Sulfide bearing rock that has been mined and stored can produce low quality effluent known as acid rock drainage (ARD). ARD has the potential to negatively impact surrounding watersheds, and thus a comprehensive understanding of the flow and geochemistry within waste rock piles is necessary when developing a mine closure plan.

Diavik Diamond Mine (DDMI) is located in the continuous permafrost region of the Canadian Arctic ($64^{o}29'N$, $100^{o}18'W$) (Figure 3-1). Production at the mine began with open pit mining in 2003, and has since progressed into an underground operation. It is estimated that the complete mining of the kimberlite pipes at Diavik will require the removal and stockpiling of 200MT of country rock. The rock is currently sorted by its sulfur content, and is placed in a segregated 80m tall pile.

The Diavik waste rock project has the goal of developing a comprehensive understanding of the thermal, hydrological and geochemical evolution of waste rock piles at DDMI. The field portion of the project contains 2m and 15m scale waste rock experiments located at the mine site. Lab based research, including a multiyear humidity cell experiment, is based out of the University of Waterloo. This paper focuses on quantifying the flow velocity and residence time for pore water in one of the three experimental waste rock piles built for the project. An understanding of these two parameters is important because they both influence the rate of contaminant loading observed at the base of the pile.

3.3 Study Site

3.3.1 Diavik Diamond Mine

The climate at Diavik is semi-arid, and is characterized by cold, lengthy winters and warm, short summers. Historical precipitation at the mine averaged 280mm per year between 1998 and 2007, with 65% falling as snow (Environment Canada 2010). Since the piles were completed in the autumn of 2006 annual precipitation has averaged 250mm per year, with 60% falling as snow. Figure 3-2 is a plot showing the daily and cumulative snow and rainfall at DDMI from the end of 2006 until 2013.

The country rock at Diavik consists of Archean age granite and pegmatite granite. The only significant sulfur in the rock is in pyrrhotite located within xenoliths of metasedimentary biotite schist. Waste rock at the site is sorted by its sulfur content into type I (<0.04 wt. % S), type II (0.04-0.08 wt. % S) and type III (>0.08 wt. % S) rock. Each of the three rock types are also characterized by very low concentrations of carbonates, and both the type II and the type III material are acid generating.

3.3.2 Experimental Waste Rock Piles

Three 15m high rock piles were constructed for the waste rock project. Two of these piles (known as the type I and type III piles) are identified by their rock type, while the third (known as the covered pile) is identified by its unique structure. This paper is focused on the type III pile, however, for a complete description of the piles the reader is directed to Neuner (2009), Smith (2009) and Fretz (2013).

The type III pile was created using end-dump and push-dump techniques, with instrumentation installed along tipping faces during construction. The pile is underlain by a 50m x 60m HDPE liner located 14m below the crest of the pile. The crest of the pile is 1350m^2, and the batters of the pile are at the angle of repose (38^o). The construction techniques created a vertical gradation in the average grain size of material in the pile. The largest rocks are typically located at the base of the pile, while smaller rocks are more likely to be located near the crest of the pile (Smith 2009). An average grain size distribution for the entire pile is shown in Figure 3-3.

Effluent from the type III pile is captured through two basal drains and 12 basal collection lysimeters (BCLs). The BCLs are plywood boxes lined with HDPE and drained through a heat traced pipe into Young Model T2202 tipping buckets. There are six 2x2m BCLs and six 4x4m BCLs, which occupy a total area of 120m^2 under the crest of the pile. Water that does not enter the BCLs is captured by the basal HDPE liner and is directed through heat traced pipes into one of two custom built tipping buckets, referred to as the north and south drains. The slope of the basal liner was designed to divide flow between each

drain. Figure 3-4 is a schematic of the intended outflow system in the base of the pile, and Figure 3-5 is a schematic showing the intended infiltration and internal flow regime of the entire pile.

3.3.3 Hydrology of the Type III Pile (Background)

The hydrology of the type III waste rock pile has been continuously monitored since 2007. A description of the hydrology of the pile is presented below in terms of infiltration, internal flow, storage and outflow.

Infiltration

Infiltration into the type III pile is divided between infiltration into the crest of the pile and infiltration into the batters. Fretz (2013) quantified the infiltration of rainfall into the crest using four 2m scale lysimeters and the Penman Monteith formulation. The results of this work were extended to 2013, and are shown in Table 3-1. Rainfall is the only significant natural source of infiltration into the crest of the pile, as strong winds scour snow from the upper surfaces of the pile and onto the batters prior to melting.

The total infiltration of water into the batters of the pile has not been quantified; however, it is anticipated to be greater than infiltration into the crest due to the infiltration of snowmelt through the batters. Although the exact amount of infiltration through the batters has not been determined, an isotope analysis conducted for this thesis (Chapter 4) demonstrates that approximately 40% of the total recharge through the batters is derived from melted snow.

Table 3-1:Estimates of rainfall infiltration into the crest of the type III pile. All rainfall from 2008-2013 was naturally occurring. Table updated from (Fretz 2013)

Year	Rainfall (mm)	Estimated Net Infiltration (mm)	Percent Net Infiltration (%)
2006	58 (applied)	51	88* (applied)
2007	153 (61mm applied and 92mm natural)	92	60* (applied and natural)
2008	154	88	57
2009	74	11	15
2010	98	40	41
2011	146	84	58
2012	68	9	13
2013	91	26	29

*high infiltration in 2006 and 2007 is due to the nature of the applied rainfalls

Internal Flow

The type III waste rock pile is unsaturated and water is located preferentially in the matrix of the material (<5mm fraction). The matrix occupies 18% of the piles volume and has a porosity of 25%, accounting for 5% of the pile's total porosity (Fretz 2013). Flow through the matrix is controlled by both capillarity and the propagation of pressure waves during infiltration, and matrix flow is the dominant transport mechanism in the pile (Neuner 2009), (Fretz 2013), (Sinclair 2014). Flow in unsaturated media that exhibits capillarity can be described using the one dimensional Richards equation:

$$\frac{\partial \theta}{\partial t} = \frac{\partial}{\partial z}\left[K_{(\Psi)}\left(\frac{\partial \Psi}{\partial z} + 1\right)\right] \quad (1)$$

Where θ is moisture content, z is elevation above a datum, and $K_{(\Psi\ )}$ is the hydraulic conductivity as a function of pressure head (Ψ).

Non-matrix (non-capillary) flow also occurs in the pile, and is referred to as preferential flow. This is a non-specific term used to describe flow through interconnected macropores or along the surface of large boulders. Preferential flow is faster than matrix flow and interacts with larger grains containing less reactive surface area per unit volume than the matrix. Preferential flow therefore results in water

with lower solute concentrations than matrix flow (Fretz 2013). Although matrix flow is dominant in the type III pile it is anticipated that some degree of preferential flow occurs, particularly in the coarse grained lower batters.

Internal flow in the type III pile is seasonal, with flow occurring only in areas that are thawed. Thawing is initiated from the exterior of the pile each year in late May, while freezing begins in October each year, and advances from the outside and the base of the pile inwards (Sinclair 2014).

Storage of Pore Water

Capillarity is only significant in the matrix of the pile, and this is the principal location where the storage of liquid water is anticipated. The volumetric moisture content (VMC) of the matrix is measured using 12 time domain reflectometry probes (TDRs) located at depths between 1-9m (Figure 3-6). The interpretation of the data produced by the TDR's relies on the pore water being in a liquid state, and the TDR data is therefore only accurate when the pile is thawed. The freezing and thawing of the pile are shown by a rapid decrease and increase respectively in the VMC measured by the TDRs.

The pile wet up to a depth of 9m in 2008, and in general the moisture content of the pile reaches a maximum each year of between 20-25% (80-100% saturation). Most seasonal drying occurs in the upper two to three metres of the pile; although a very dry year in 2012 (9mm infiltration) caused drying to a depth of at least 5 metres. Although the upper portions of the pile were drier than average in 2012 and 2013, it is assumed that the matrix of the pile has attained a pseudo steady state of storage over a multi-year period. This means that infiltration into the pile will either be matched by outflow, or may result in the formation of multi-year ice in macropores at the base of the pile.

Outflow

Initial outflow each spring is derived from the batters, with an increasing proportion of the pile contributing as thawing progresses. In autumn a freezing front advances through the batters and the base of the pile and terminates flow through the drains by November of each year.

Outflow from the pile is collected through the north drain, the south drain and the basal collection lysimeters. Figure 3-7 is a plot of the flow volume collected at each location between 2007 and 2013. Since the initiation of flow, 85% of the total volume has been collected by the south drain, 13% by the north drain, and 2% by the BCL's. Outflow from the pile peaked in 2010 and has decreased each year since.

Disruption of the Type III Heat Trace

A flood during the winter of 2012/2013 cut power to the heat trace located in the drainage pipes of the BCLs and basal drains. Power was not restored until September 2013, and this may have contributed to long-term (multi-year) freezing in the core of the pile. The influence of the damaged heat trace on the internal flow regime of the pile is discussed in Section 3.5 below.

3.4 Application of the Tracer

A lithium bromide and lithium chloride tracer was applied to the type III pile on September 13, 2007 under the direction of M. Gupton. Six oscillating lawn sprinklers were used to apply the tracer to a 600m^2 (20 x 30m) area on the crest of the pile. The 29mm application occurred over 3.75 hours at an average rate of 7.8mm/hr (Neuner 2009). It is the second largest daily rainfall event to have occurred at the test piles since their completion in 2006 (Figure 3-2). Ponding was deliberately created in order to induce preferential flow, and occurred as a result of localized low infiltration capacity areas (Neuner 2009), (Fretz 2013). An aerial photo of the pile following the application of tracer is shown in Figure 3-8.

Bromide and chloride were selected as tracers because they are chemically stable, minimally-sorbing, and are transported at a rate equal to that of the groundwater flow velocity (Davis et al., 1980), (Mackay et al., 1986). The chloride and bromide were applied at concentrations of 2171 and 2576mg/L respectively, with a total of 38 kg of chloride and 45 kg of bromide used. Recovery of the tracer was intended to occur through the north drain, south drain and the BCLs, while 23 soil water solution samplers were used to track the movement of the tracer in the upper 9m of the pile.

3.4.1 Background Concentrations

The internal release of chloride in the pile is complicated by the presence of blasting residuals (Bailey et al., 2013),(Sinclair 2013b). For this reason, the analysis of the tracer test is focused on the observation and recovery of bromide.

The background concentration of bromide in outflow from the pile is 0.5mg/L. This value was calculated as the median concentration of all of the samples collected by the north and south drains prior to the tracer application. A separate background concentration for the BCLs was not calculated because they did not conduct any flow before September 13, 2007, when the tracer was applied. The background concentration of bromide is assumed to remain constant with time during the test, and has been removed from the calculations involving total mass recovery.

Pore water samples taken from the other two experimental piles have occasionally contained concentrations of naturally derived (non-tracer) bromide that are significantly above the background concentration of 0.5mg/L. In these cases, the ratio of chloride to bromide can be used to differentiate between naturally occurring bromide and bromide from the tracer test. The background concentrations observed in the north and south drains of the type III pile had a median chloride to bromide ratio of 12:1, with no samples having a ratio of less than 5:1. This ratio was also observed in water samples from the type 1 pile (99% of samples >5:1, no tracer tests) and the covered pile (100% of samples > 5:1, no Cl

or Br tracer tests prior to 2013). In comparison, the Cl:Br ratio of the tracer is 1:1, and samples with a Cl:Br ratio of 5:1 or less are therefore assumed to contain tracer from the experiment.

3.5 Results

3.5.1 Mass Recovery

Figure 3-9a-b is a plot of the average bromide concentrations and Cl:Br ratios in outflow collected from the type III drains and the BCLs. Significant tracer concentrations were observed in both the south drain and the BCLs, but not in the north drain. Additionally, the average Cl:Br ratio in the north drain never went below 9:1, while in the south drain and BCLs it went as low as 2:1 and 1:1 respectively. This dictates that the north drain did not recover any tracer; instead it collected flow from outside of the tracer area, most likely from the north batter (where no tracer was applied). This is a significant deviation from the intended design of the drains, and explains why the north drain has conducted so little effluent compared to the south drain (Figure 3-7).

Time to Peak Concentrations and Recovery

The annual mass of bromide recovered from the pile, along with the cumulative mass recovered (as a percentage of the total bromide released) is shown in Figure 3-10. The mass recovery was calculated by Sinclair (2014) until 2012, but was not analysed in the context of this tracer test. The mass recovery in 2013 was calculated for this paper using the same interpolation scheme as that used by Sinclair (2014). As of 2013, 38% of the total bromide applied to the pile has been recovered, with 83% of the total mass collected by south drain, and 17% collected through the BCLs. This is roughly proportional to the area under the tracer test that is occupied by the BCLs (20%). Mass recovery through the south drain was primarily influenced by the concentration of bromide in the effluent, while mass recovery in the BCL's was influenced both by the concentration of bromide and by large flow volumes (for the BCLs) in 2012 (Figures 3-7, 3-9 and 3-10).

Time to 50% Recovery

This section is based on the assumption that the internal flow regime of the TIII pile was significantly altered in 2013 due to the non-functioning heat trace. Disruption of the previously existing flow regime is most likely to have occurred due to the formation of ice in the basal region underlying the core of pile. This assumption is supported by the fact that outflow was not observed from the BCLs until after the heat trace was restored in September, 2013. The volume of outflow collected from the south basal drain was lower than in any other year since flow began, while outflow from the north drain, which drains only from the batters (where long term freezing is not anticipated), was unaffected. The heat trace in the TI pile (located adjacent to the TIII pile) was also disrupted by the flood, and basal outflow from the TI pile decreased significantly in 2013. A subsequent excavation of the TI pile has demonstrated that the base of the pile contained large volumes of pore water stored as ice. Finally, the very sharp break in slope observed in the plot shown in Figure 3-10 is not what is expected from a tracer test in a heterogeneous waste rock pile under unaltered flow conditions (Marcoline 2008), and is instead indicative of a disruption to the regular flow regime within the pile.

If it is assumed that the flow regime of the pile was significantly altered in 2013, then the mass recovery observed between 2007 and 2012 can be extrapolated forward until a mass recovery of 50% is reached (Figure 3-11). Based on this extrapolation, it is anticipated that 50% of the tracer would have been recovered by 2013 if the heat trace had not been damaged. This correlates to the tracer moving an average of 2.3m per year between 2007 and 2013. This value does not account for the fact that flow is seasonally transient due to freezing and thawing. The velocity of the tracer during times that the pile is thawed is discussed in Section 3.5.4 below. Based on the projected recovery shown in Figure 3-11, water located in the matrix material of the TIII pile has an average residence time of 6 years.

3.5.2 Travel Time Along the Basal Liner

The flow velocity given above does not account for transport along the HDPE liner to the drainage pipes of the south drain. Instead, it is assumed that this time is negligible in relation to the six year time span of the experiment. This assumption is supported by the fact that tracer recovery peaked in the small scale BCLs one year later than in the south drain. If travel time along the HDPE liner to the drain was significant over a six year period the opposite relationship would be expected, with the maximum recovery occurring later in the south drain than in the BCLs.

3.5.3 Tracking the Tracer

The movement of the tracer through the upper 9m of the pile was observed using a network of 23 soil water solution samplers (SWSS). The SWSS collect water in a porous cup located within matrix material. In order to obtain a sample, suction is applied to the interior of the cup. The pressure gradient between the cup and the matrix induces a flux of pore water into the cup, and this water can then be driven to the surface of the pile using compressed gas.

In total, 455 SWSS samples have been collected from 23 locations located at depths of 1-9m in the pile. Sampling occurs each year between June and November. Each round of sampling does not contain samples from every SWSS, as it is not always possible to acquire samples from certain locations (for example if they are frozen). Mass fluxes can be calculated from SWSS samples if the volumetric flux of water past the SWSS is known; however, this is not the case at the type III pile. Instead the concentrations of bromide measured in the SWSS samples are used to comment on preferential and matrix flow velocities.

The SWSS samples contained higher background concentrations of bromide and chloride than the drains. This is due to the fact that the SWSS sample preferentially from the matrix in the core of the pile, while the drains collect both preferential and matrix flow from the core and the batters. The ratio of chloride to bromide in each sample was used to determine if the bromide in the sample was derived

from tracer or background sources. Background ratios as high as 50:1 (Cl:Br) were found in the SWSS samples, and samples with ratios of greater than 5:1 are not included in this analysis. In total, 208 samples contained Cl:Br ratios indicative of the tracer; plots of the bromide concentrations measured in these samples are shown in Figure 3-12.

Variability in Flow Velocities

A high variability in flow velocities was seen over short horizontal distances in the SWSS (Figure 3-12). For example, tracer arrived at the 32N2sws07 sampler in 2007 but was not observed in 32S2sws07 until late 2008, despite both samplers being located only 4m apart from each other and at the same depth (7m). Another example can be seen by comparing the 5m SWSS plot to the3m SWSS plot. Tracer arrived at 33S2sws05 in 2007, but was not seen in any of the 3m depth SWSS until 2008. A high variability in flow velocities was also observed during tracer tests on similar unsaturated waste rock piles located at Cluff Lake (Nichol, Smith and Beckie 2005).

Preferential Transport Velocities

Preferential transport was seen in SWSS samples taken from depths of five, seven, and nine metres. Fingering of flow was observed at each of these depths. The fastest preferential flow was observed in samples taken from 33S2sws09, and had a velocity of 0.7 m/day (Figure 3-12). This is a good match to previous work, which determined that pore water can travel at velocities of up to 0.7m/day in response to large rainfall events (Neuner 2009)(Fretz 2013).

Matrix Transport Velocities

Quantifying the velocity of matrix transport using the SWSS is difficult due to the variability in velocities described above; however, the wetting front travelling through the matrix is spatially uniform compared to the fingering induced by preferential flow. The arrival of tracer at multiple SWSS of the same depth is therefore indicative of matrix transport. Using this criterion, the tracer moved an average of 2.9m per

year in the upper nine metres of the pile. This velocity does not account for the fact that flow is seasonally transient due to freezing and thawing, which is discussed in Section 3.5.4 below. Bromide concentrations returned to near background values in the 3 and 5m SWSS by the start of sampling in 2010, and Cl:Br ratios returned to >5:1 in 2013. Bromide concentrations returned to near background values in the 7m SWSS by the start of sampling in 2012, and Cl:Br ratios returned to >5:1 in 2013. Bromide concentrations in the 9m SWSS remained above background until 2013, with Cl:Br ratios staying below 5:1.

Evidence of Low Conductivity Zones

There is only one SWSS located at a depth of 2m. Samples from this SWSS contained elevated bromide concentrations from 2008-2013, and maintained a chloride to bromide ratio of less than 2:1 for the duration of this study. No significant preferential flow to the two metre SWSS was seen. This suggests that this SWSS is located in and sampling from a localized low mobility domain. A similar situation was observed in tracer tests conducted on experimental waste rock piles at Cluff Lake (Marcoline 2008).

3.5.4 Correcting for Seasonally Transient Flow

The mass recovery and SWSS datasets have shown that pore water in the matrix of the pile travels between 2.3 and 2.9m over a one year period; however, flow within the pile is limited to time periods when the pile is thawed (May-November). The location of the freezing and thawing front in the pile is tracked in two ways:

1. Using readings from the TDR probes, which show a large, rapid increase in volumetric moisture content during thawing and a similar decrease during freezing (Figure 3-6)
2. Using thermal modelling and temperature data from thermistors in the pile (Figure 3-13) (Pham 2012)

The average velocity of pore water when the pile is thawed was calculated to be 0.5m/month in the upper 9m of the waste rock pile. This was determined using the TDR data, thermal measurements, and the SWSS samples. Quantifying the velocity of pore water at depths below this is difficult, as there is no temperature data at depths between 11-14m. However, it is known that outflow from the pile is limited to the months between May and November each year. Using this information, the average velocity of flow during times when the pile is thawed is estimated to be 0.3m/month.

3.5.5 Location of the Unrecovered Bromide

In total only 38% of the total mass of bromide released was recorded by 2013. The bromide remaining in the type III pile at Diavik is anticipated to be segregated between two locations:

1. Low velocity flow paths: Tracer experiments in unsaturated, heterogeneous waste rock piles generally have long tails (Marcoline 2008), and it is anticipated that small amounts of bromide will continue to be recovered in subsequent years. This is supported by samples from the 9m depth SWSS that still contain tracer as of 2013. Samples taken from the 2m SWSS are indicative of a localized low conductivity domain, and it is anticipated that recovery from this domain will take a very long time.
2. Entrapment by Multi-Year Ice: Preliminary results from the excavation of the nearby type I pile indicate that a large amount of water can be retained as ice within the uncovered piles. Ice formation in both piles may have been enhanced by the disruption of heat trace during the 2012 flow season, leading to the low recovery of tracer from the TIII pile in 2013. Freezing will result in a decrease in flow volume collected from the core of the pile, and will block flow paths that would have otherwise been utilized by the tracer, even if the tracer itself has been segregated from the ice. A schematic of this process is shown in Figure 3-14.

3.6 Conclusions

In this paper 7 years of data was analysed to quantify the average flow velocity and residence time for pore water in the type III experimental waste rock pile. Recovery of the tracer appears to have been significantly altered by a heat trace that was damaged in the winter of 2012-2013, and because of this the data from 2007-2012 was extrapolated until a 50% recovery was achieved. The average velocity of pore water in the pile was determined to be 0.3 to 0.5m per month when the pile was thawed.This velocity is a time integrated average that reflects the six year precipitation, evaporation and infiltration history of the type III waste rock pile. Preferential velocities of 0.7 m/day were observed in the upper 9m of the pile in the days following the application of the tracer. This matches well with previous work, in which a maximum flow velocity of 0.7m/day was observed (Neuner 2009). Pore water in the matrix of the pile was determined to have an average residence time of 6 years.

The results of the tracer test also indicate that the north basal drain in the type III pile is not collecting water from the entire northern half of the pile, as was intended. Instead, flow collected by the north drain is primarily derived from pore water in the batters. This has important implications regarding hydrology, geochemical modelling and loading calculations.

The age and volume of ice in the core of the type I pile (located adjacent to the type III pile) is currently being investigated by Jordan Zak (Ongoing), and this will provide further information about the potential formation and evolution of multi-year ice in the type III pile.

3.7 Figures For Chapter 3

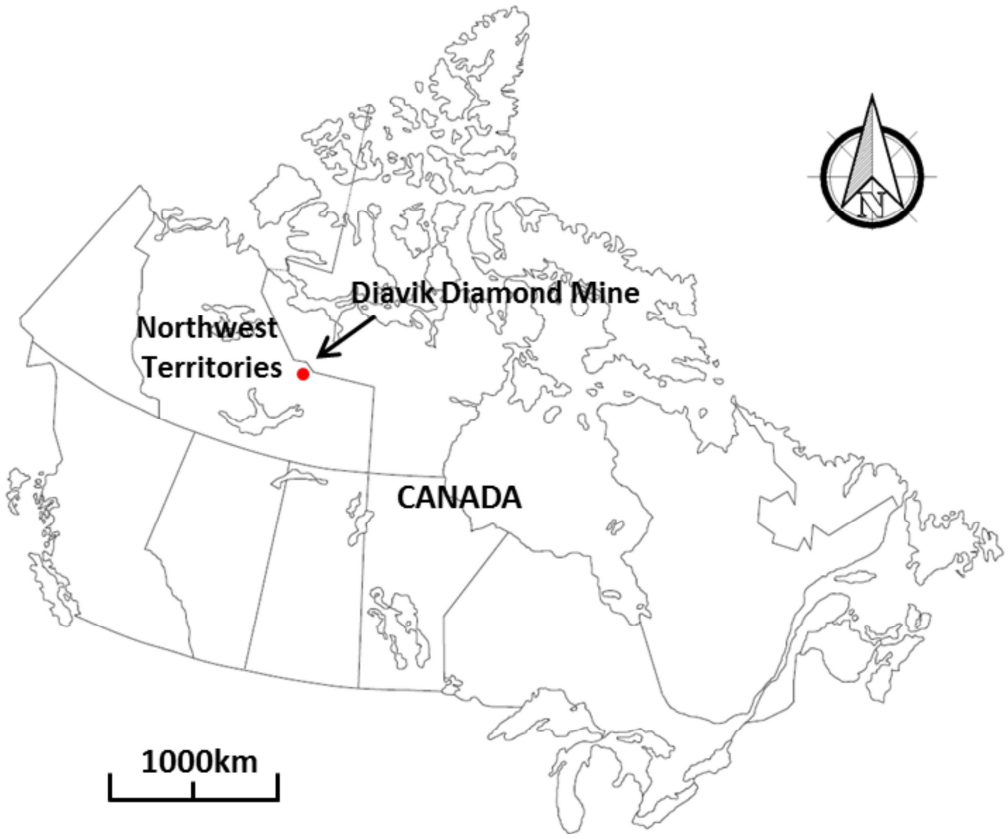

Figure 3-1: Location of Diavik Diamond Mine. Image from Fretz (2013)

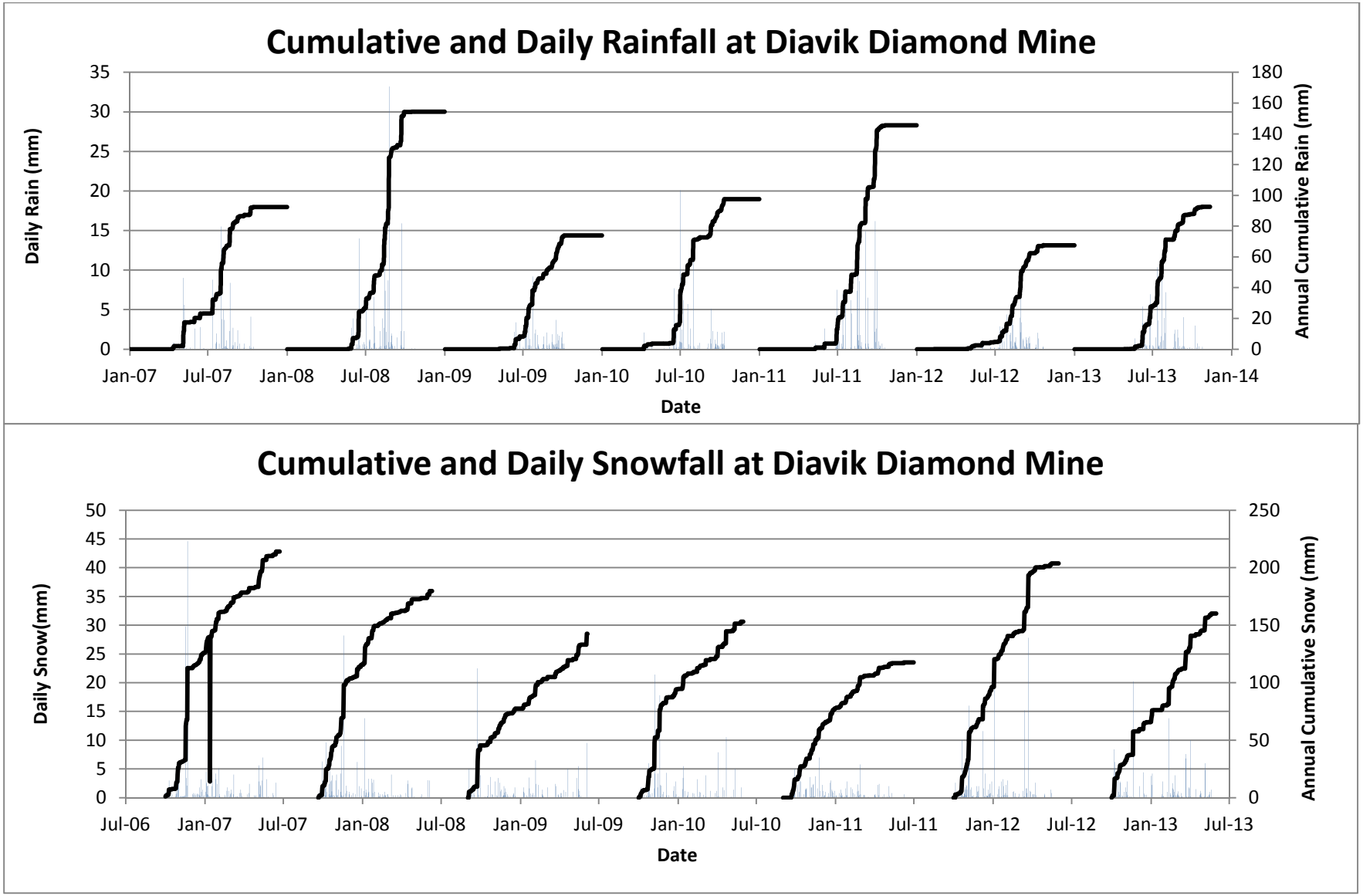

Figure 3-2: Daily and cumulative annual precipitation at Diavik

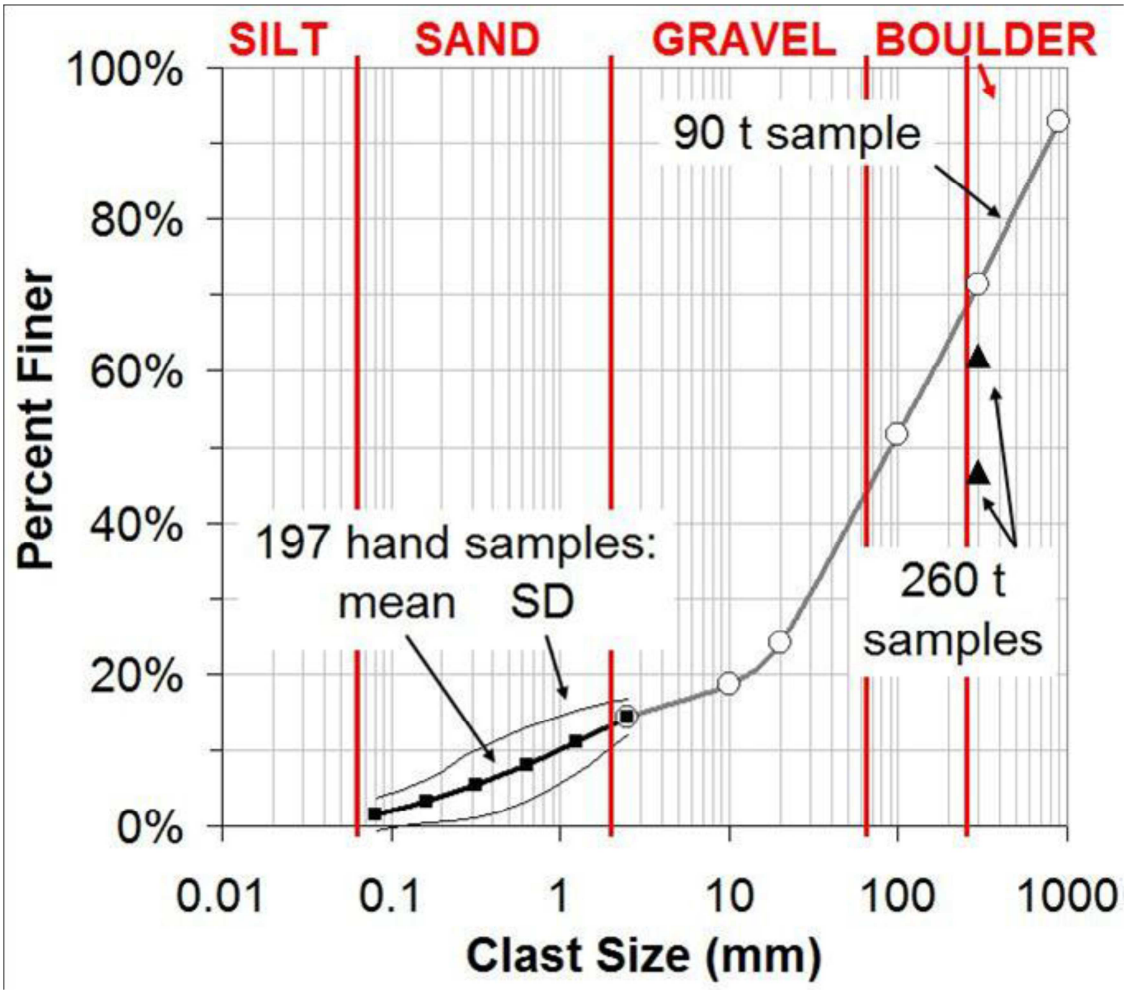

Figure 3-3: Grain size distribution of the type III pile. Image from Neuner (2009).

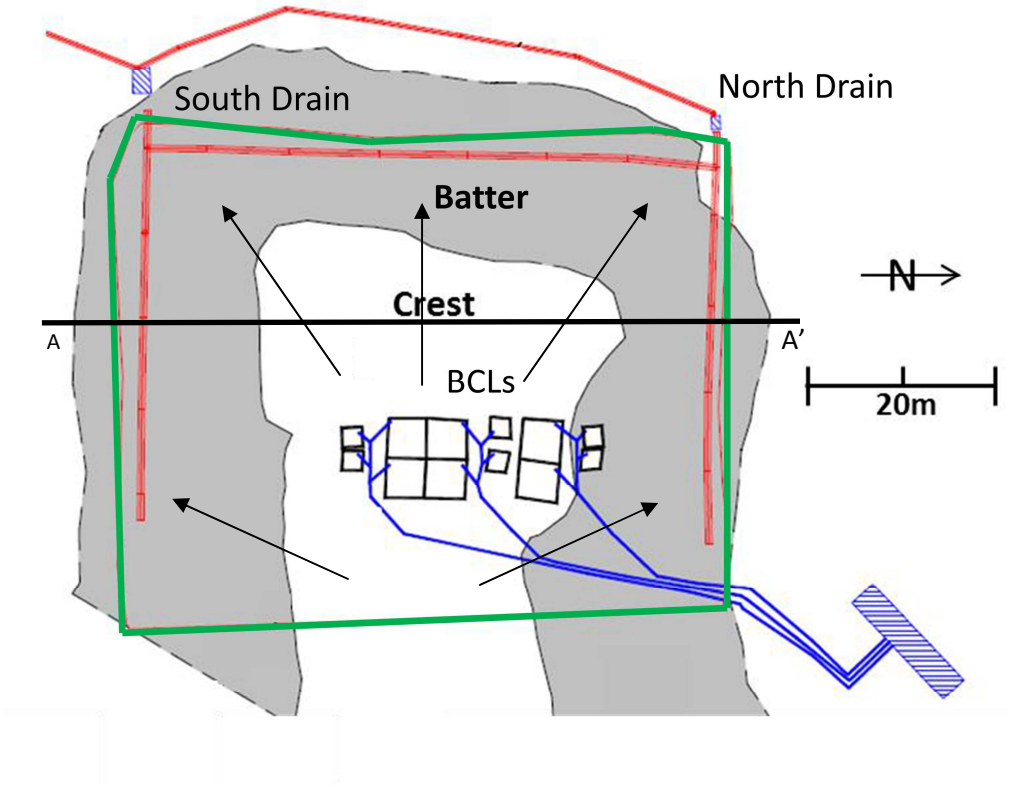

Figure 3-4: The location of the drains and BCLs in the type III pile.

The gray areas show the batters of the pile, the green lines show the extent of the basal liner, the red lines show the basal drainage pipes, the arrows show intended flow directions along the basal liner, and the blue lines show the BCL drainage pipes. Figure 3-5 is taken along line A-A' Image modified from Fretz (2013).

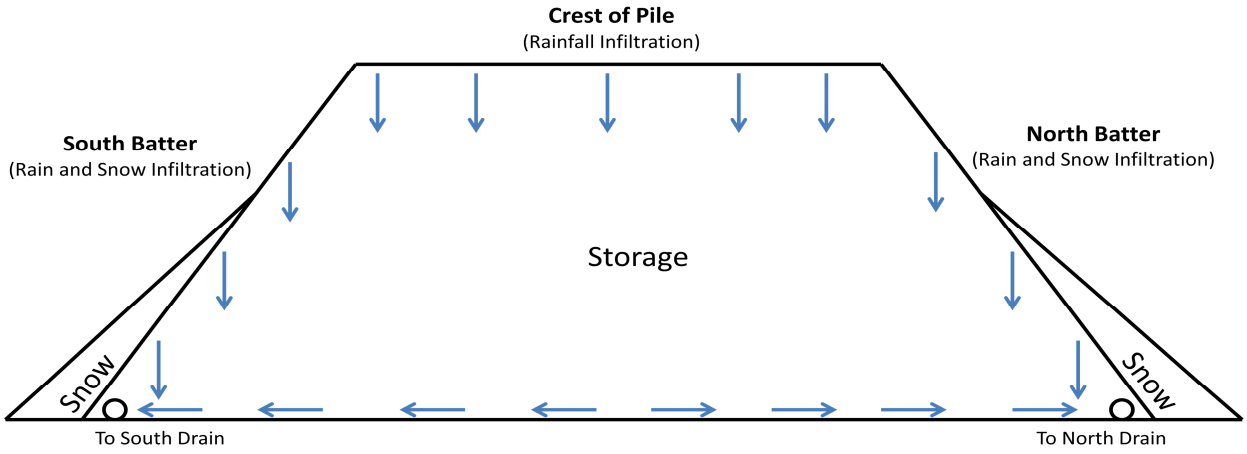

Figure 3-5: Schematic of the infiltration and internal flow regime of the type III pile along line A-A'.

Sources of infiltration are identified, and the arrows show the direction of internal flow.

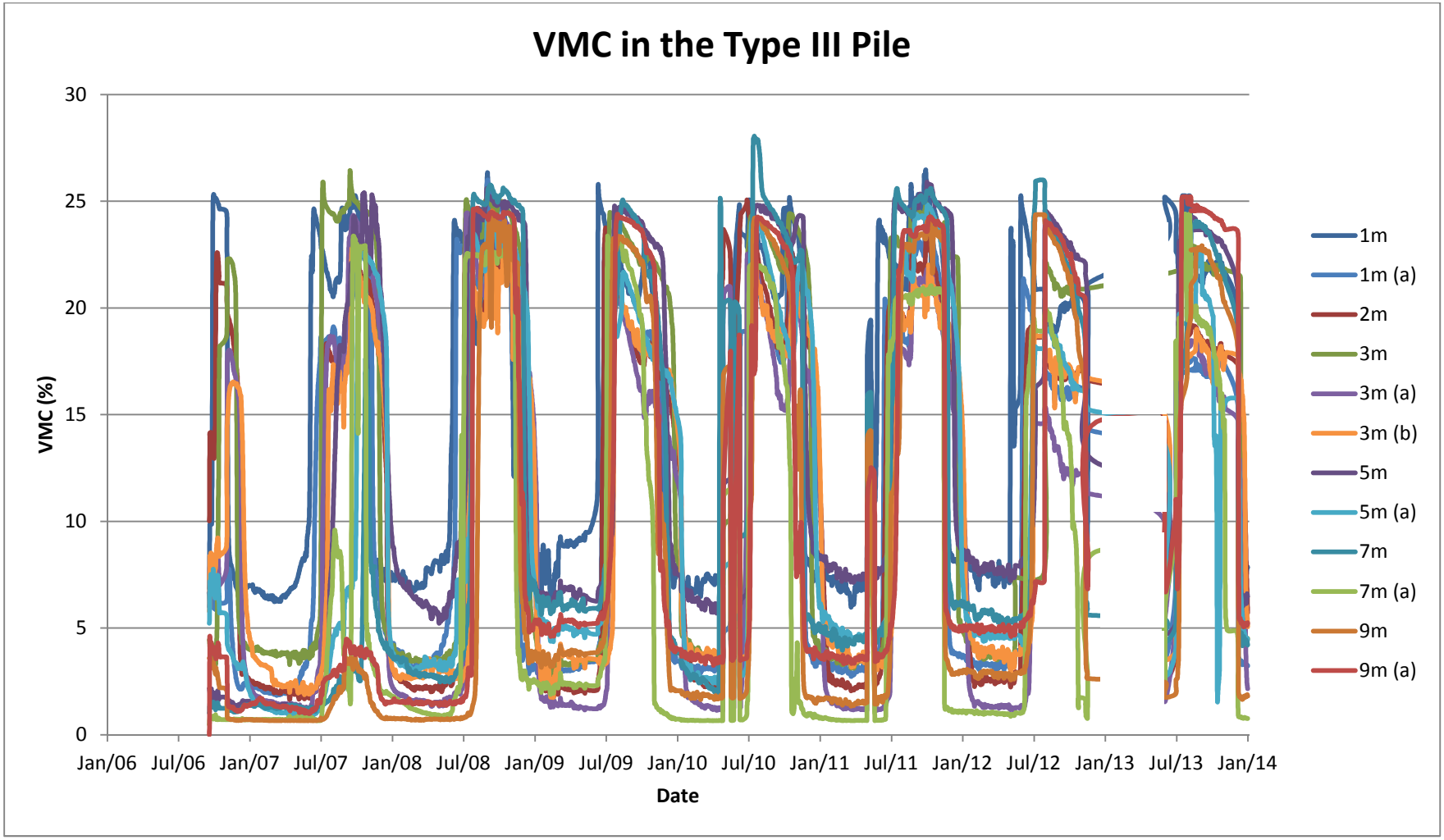

Figure 3-6: Volumetric moisture contents measured by TDR probes in the type III pile.

The depth of each probe is shown in the legend. In early 2013 data was not collected due to flooding, and the winter freeze was not recorded.

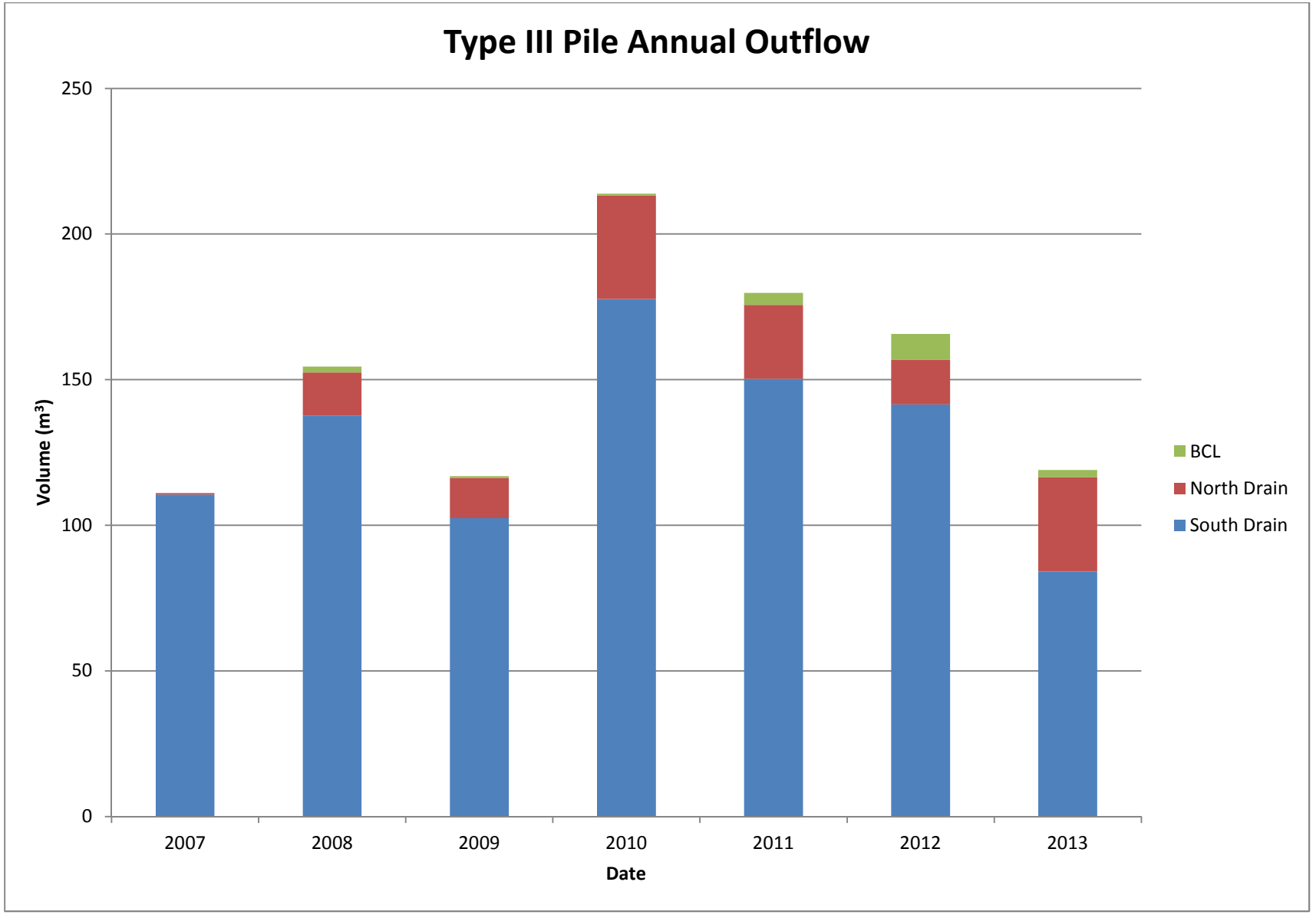

Figure 3-7: Annual outflow from the type III pile

Figure 3-8: The 20m x 30m footprint of the tracer test.

Photo taken from a man-lift 100ft above the surface. Image from Neuner (2009)

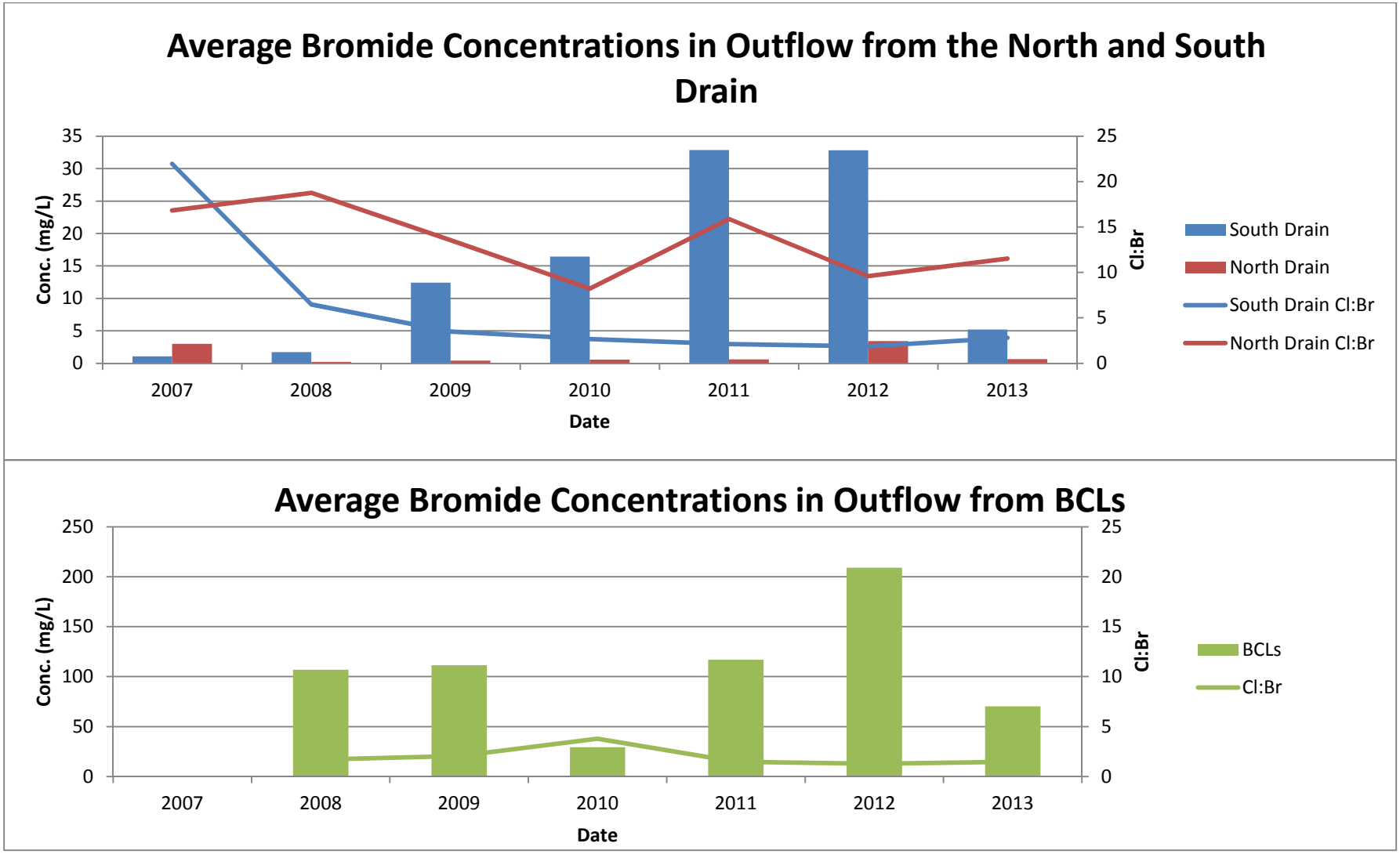

Figure 3-9: Average flow weighted concentrations of bromide in outflow from the type III pile.

The BCL's are plotted separately due to the fact that outflow from the BCLs was significantly more concentrated than outflow from either drain. The Cl:Br ratio in each location is overlain, and shown on the secondary vertical axis.

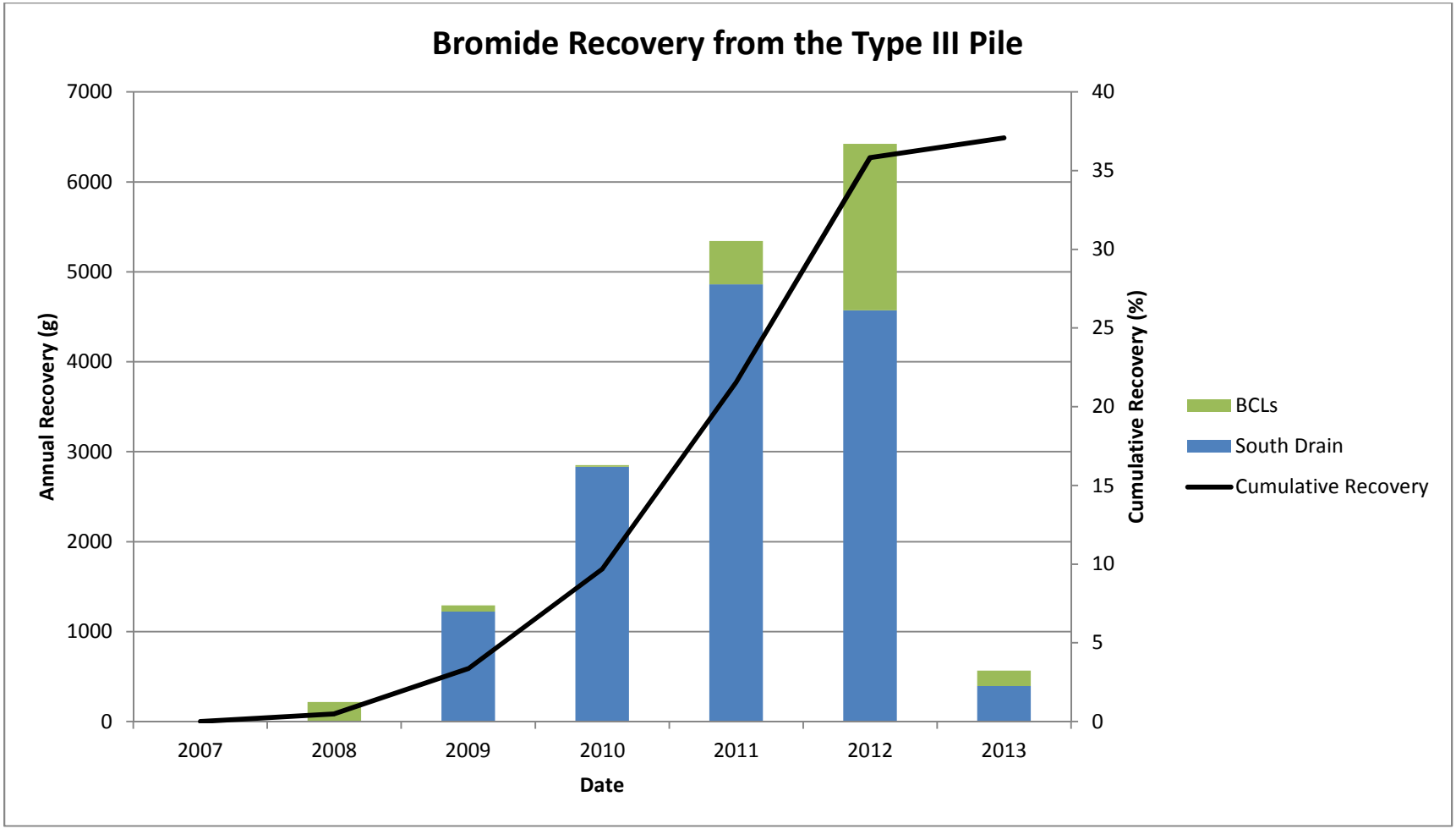

Figure 3-10: Annual and cumulative bromide recovery from the type III pile

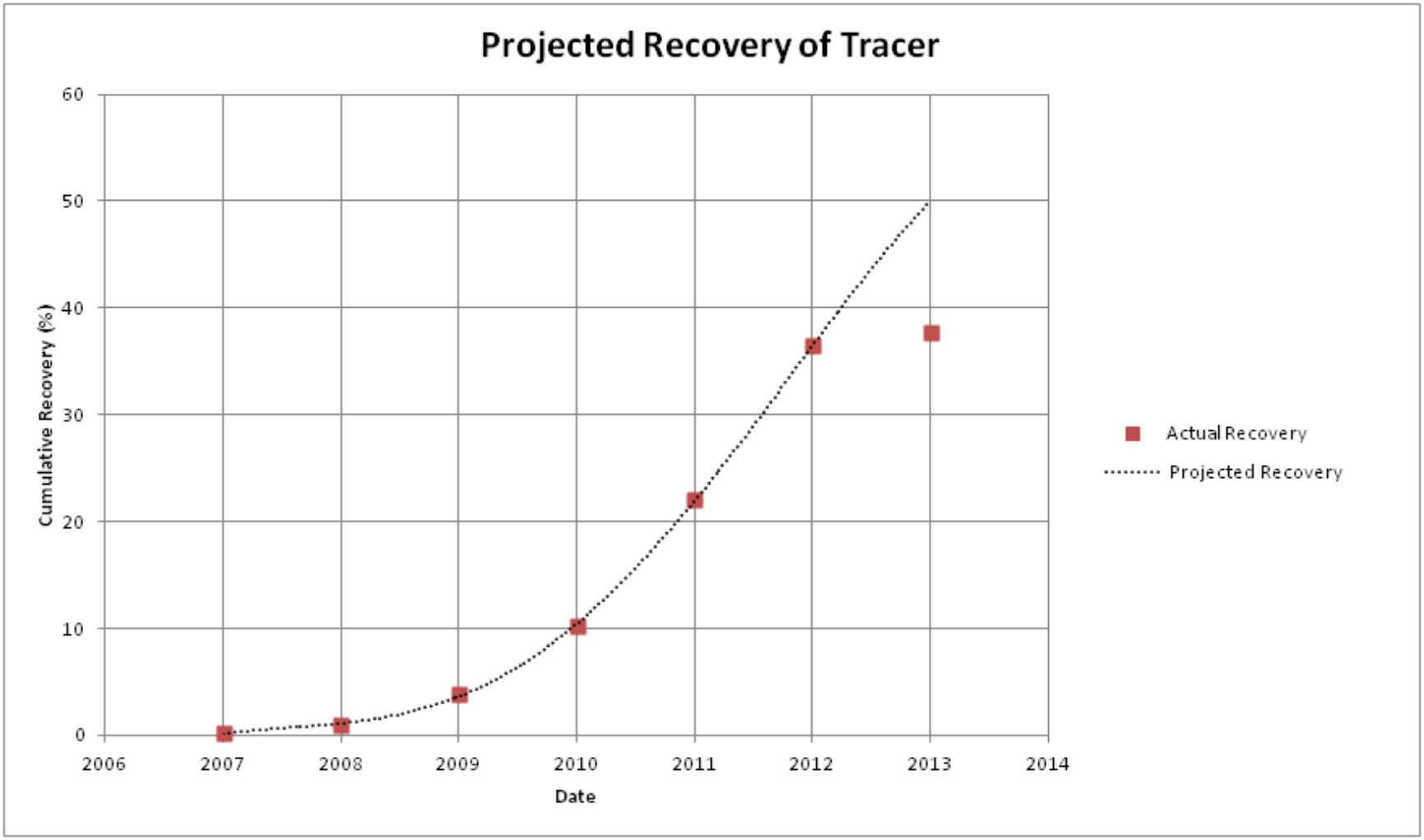

Figure 3-11: Projected recovery of the tracer.

In 2013 the recovery of the tracer was significantly lower than anticipated. This is interpreted to be the result of ice forming in the base of the pile while the heat trace was not functioning.

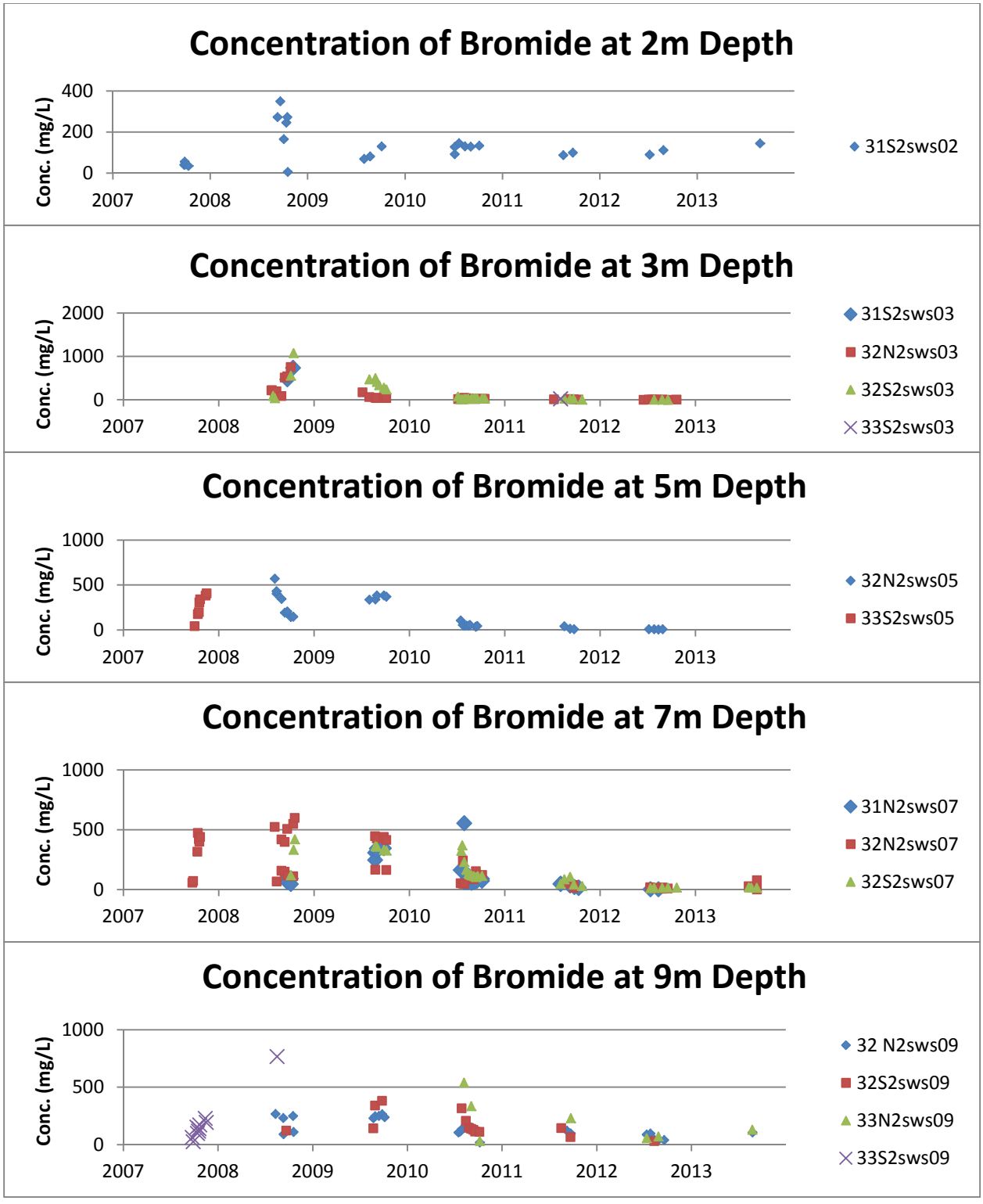

Figure 3-12: Bromide concentrations in the SWSS. Only samples with a Cl:Br ratio that indicates the presence of tracer are included

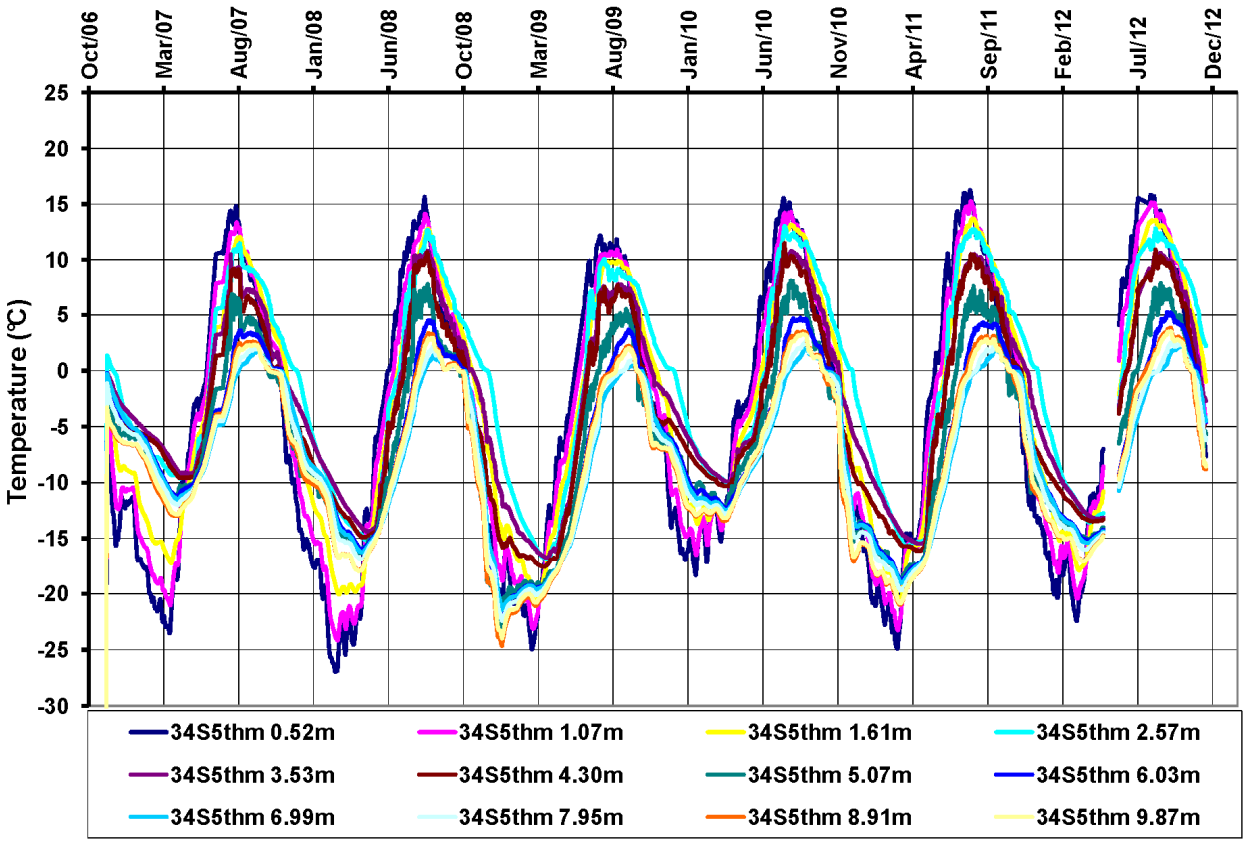

Figure 3-13: Thermal data from the type III test pile. Image from Pham (2014)

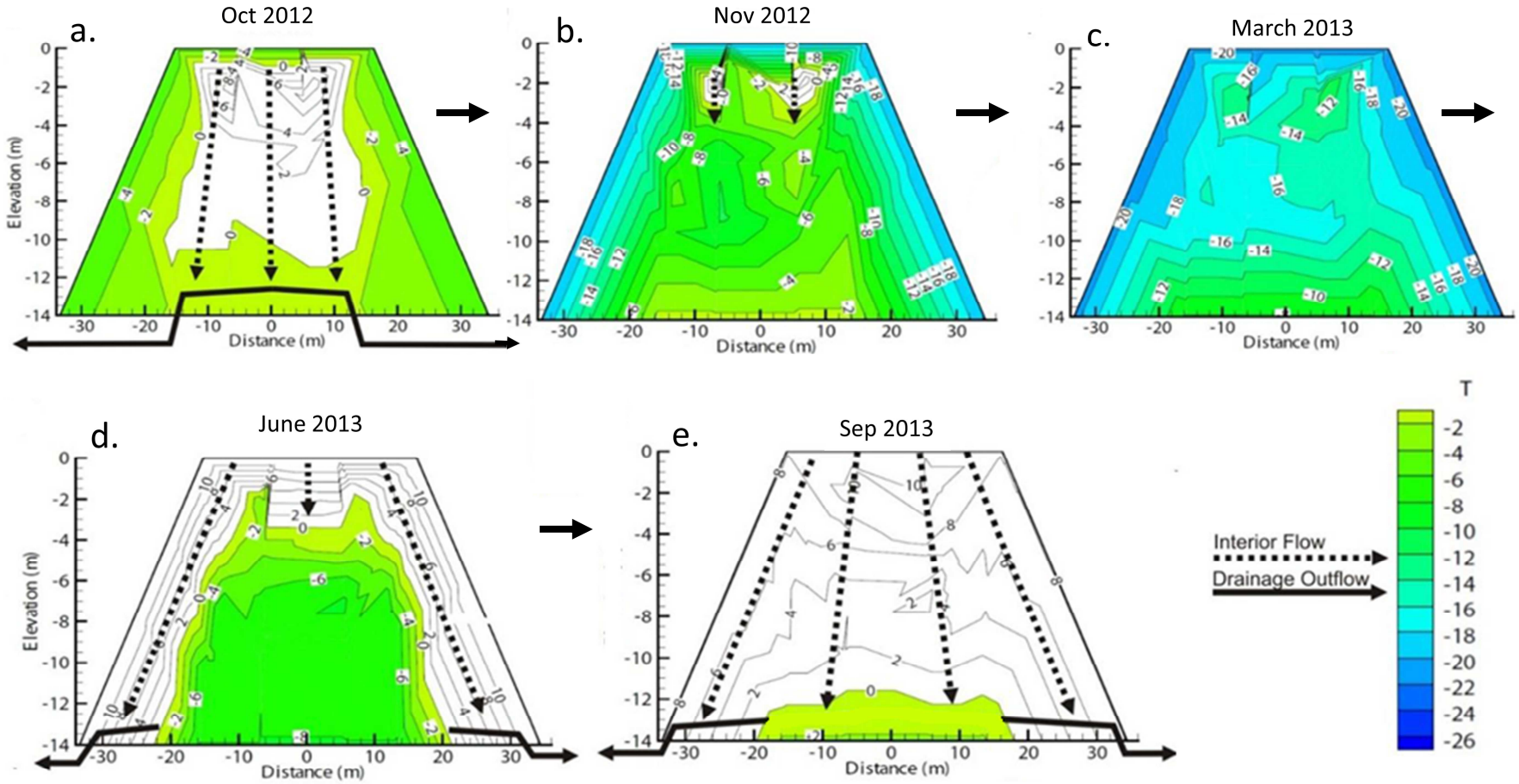

Figure 3-14: Schematic of tracer getting trapped by multiyear ice.

a) A freezing front advances from the outside and base of the pile inwards. Tracer may be preferentially excluded from the ice formation and be left in the centre of the pile b) The pile freezes in November c) Freezing conditions continue until March d) thawing begins from the outside of the pile inwards in June e) A frozen core remains. The tracer is trapped within or on top of this frozen core. Image modified from Sinclair (2014)

Chapter 4: Using Stable Isotopes to Quantify Snowmelt Infiltration into an Uncovered Waste Rock Pile in the Canadian Arctic

This chapter is written as a self contained article formatted for publication in a journal. It is intended to quantify the relative contributions of snowmelt and rainfall to the total recharge received through the batters of the type III test pile. The ability to differentiate between recharge derived from these two sources is important when explaining the chemistry of outflow from the pile, and when developing up-scaling relationships between the type III and full scale piles.

4.1 Summary of Chapter

In this paper the depletion of ^{18}O and ^{2}H in outflow from the batters of an experimental waste rock pile is compared to samples of snow and rain in order to determine the relative contributions of snowmelt and rainfall to infiltration. The results of this analysis demonstrate a clear correlation between the pH of the outflow and the proportion of the outflow water derived from the infiltration of snowmelt, based on the isotopic ratios. Circumneutral outflow observed each spring is determined to be the result of snowmelt infiltrating through the batters and travelling though preferential flow pathways to the base of the pile. Conversely, acidic outflow collected in the summer and autumn of each year containsa mixture of rain and snowmelt water thattravelled primarily through matrix material. In total, approximately 40% of the outflow from the batters of the pile is derived from the infiltration of snowmelt, while the remaining 60% is derived from the infiltration of rain water. On average, the proportion of snowmelt in the outflow reaches a maximum of 65% each spring, and a minimum of 30% by late autumn each year. Additionally, the analysis conducted for this research suggests that almost no evaporation occurs following the infiltration of rain or snow melt into the batters of the pile.

4.2 Introduction

Waste rock piles produced by mining can have significant environmental impacts due to the oxidation of sulfide minerals in the rock, leading to the generation of low quality acidic effluent. Predicting and

mitigating the release of acid rock drainage (ARD) into the environment is a necessary component of any mine closure plan, and requires a comprehensive understanding of the thermal, hydrological, geochemical and microbiological evolution of the waste rock. The Diavik waste rock project was created to develop a comprehensive understanding of these factors in low sulfide waste rock piles in the Canadian Arctic. The project is based at the Diavik Diamond Mine (DDMI), located 300km northeast of Yellowknife, NT, Canada (64°29' N, 110°18' W), (Figure 4-1). Production at the mine began with open pit mining in 2003 and has since progressed into an exclusively underground operation. Mining of the kimberlite pipes is anticipated to require the removal of 200MT of country rock. This material is sorted by its sulfur (pyrrhotite) content, and is stockpiled in an 80 m tall pile.

The waste rock project consists of laboratory, 2m and 15m scale experiments, with the intention of developing up scaling relationships from these experiments to the full-scale (80m) waste rock pile. The results from the project will be incorporated into the final plan for preventing ARD release from the mine site. This paper utilizes an analysis of stable isotopes to examine the importance of snowmelt infiltration into the batters of a large-scale (15m) experimental waste rock pile located at DDMI. The ability to differentiate between rainfall and snowmelt infiltration is required to understand the hydrologic systems that exist within the waste rock, and can also be used to explain annual patterns observed in the geochemistry of outflow from the pile.

4.3 Study Site

4.3.1 Diavik Diamond Mine

Climate

Since 2007 the annual precipitation at DDMI has averaged 250mm, with approximately 60% falling as snow. This paper is focused on the time period between 2011 and 2013, and the total rain and snowfall recorded at Diavik during this time is shown in Figure 4-2. The mine is located in a continuous

permafrost region with a mean annual temperature of -8.5^{0}C (Environment Canada 2010). Winters at DDMI are long, cold and dark, while summers are short and warm.

Country Rock

The country rock at Diavik consists of Archean granite and pegmatite granite. Within the granite there are metasedimentary biotite-schist xenoliths, and these contain the bulk of the sulfide found in the waste rock. Waste rock at Diavik is sorted from type I to type III by increasing sulfur content (acid generating potential). Type I waste rock has an average sulfur content of <0.04 wt. % S, type II rock has 0.04-0.08 wt. % S and type III rock has >0.08 wt. % S. Each of the rock types has a low neutralization potential, and the type II and type III rock are acid generating (Langman, et al. 2014), (Sinclair 2014).

4.3.2 Experimental Waste Rock Piles

Three large scale (15m tall) experimental rock piles were constructed for the waste rock project. For a full description of each pile the reader is directed to (Neuner 2009), (L. Smith 2009), (Fretz 2013) and (Sinclair 2014). This paper focuses on the effluent from a single pile, known within the project as the type III pile, and named after the rock it was constructed from.

The type III pile is underlain by a 50m by 60m HDPE liner. The crest of the pile has a surface area of 1350m^2, and the batters of the pile slope downwards at the angle of repose (38^0) to the basal liner. The pile was created using end-dumping and push-dumping techniques, with instrumentation placed between four different tipping faces. These construction techniques created a gradient in grain sizes between the crest and the batters of the pile. The crest and upper batters contain finer material, while coarser material is preferentially located at the base.

The type III pile is unsaturated, and internal flow within the pile occurs primarily within the <5mm fraction of the waste rock, referred to as the matrix. Preferential flow through the non-matrix (>5mm)

material is induced during rapid infiltration events, and occurs through interconnected macropore pathways or as film flow along the surface of boulders.

Effluent from the pile is collected through two basal drains and several basal collection lysimeters (BCLs). The BCLs are plywood boxes with an HDPE liner and a drain that directs flow into heat traced pipes. Effluent from these pipes passes through Young model T2202 tipping buckets, which record the rate and volume of effluent. The BCLs are divided into three clusters, each of which contain two 2x2m BCLs and two 4x4m BCLs. Water that does not enter the BCLs is collected by the basal HDPE liner, and is directed into perforated, heat traced drain lines. This effluent then passes through one of two custom built tipping buckets, known as the north and south drains. The tipping buckets record the volume and rate of discharge through each drain pipe. The drainage and flow system of the type III pile, including the location of both drains and the BCLs, is shown schematically in Figures 4-3 and 4-4.

4.3.3 Snowpack on the Type III Test Pile

The spatial distribution of snow on the type III pile is driven by wind and total snowfall amounts, and results in a unique snowpack each winter (Figure 4-5 a-b). By the time melting begins the snowpack has a relatively consistent distribution each year, with most of the remaining snow overlying the lower batters (as in Figure 4-5 b). Although an average of 60% of the total precipitation at Diavik occurs as snowfall, it is not anticipated that 60% of the total infiltration into the pile will be derived from snowmelt. This is due to sublimation and wind transport away from the pile. It is estimated that 30% of the total snowfall at Diavik is sublimated each winter (L. Smith 2014), and modelling work conducted in Chapter 5 of this thesis shows that significant sublimation occurs each spring.

4.3.4 Flow Paths and Residence Times in the Type III Pile

The lower batters of the pile are characterized by short flow paths to the basal liner, large grain sizes, and abundant void spaces between boulders. Snowmelt occurs rapidly each year, and it is anticipated that some of the snowmelt will utilize preferential flow pathways and travel quickly to the basal liner.

In general, pore water with a long residence time in the pile is characterized by a low pH and high solute concentrations, while water with a short residence time is characterized by a higher pH, and a lower concentration of solutes. This effect is magnified in pore water that has travelled primarily through preferential flow pathways, which contain a smaller reactive surface area than the matrix material, and result in very short residence times for the water. Sinclair (2014) used this relationship to propose that the initial outflow collected from the basal drains each year is primarily a result of snow melt infiltrating through the batters and being preferentially transported to the base of the pile. This initial outflow is characterized by a circum-neutral pH and low solute concentrations, while flow later in the year is characterized by a lower pH (~4.5) and high solute concentrations. Figure 4-6 shows the pH measured in outflow from the pile between 2011 and 2013, and highlights the divide between the initial circum-neutral outflow and later, more acidic outflow.

4.3.5 Importance of the North Drain in this Analysis

The north drain primarily collects outflow derived from the batters of the pile (Figures 4-3 and 4-4). As previously mentioned, this is where the majority of snowmelt infiltration occurs. This paper therefore focuses exclusively on effluentcollected from the north drain in order to highlight the importance of snowmelt to the total recharge received through the batters of the pile.

4.4 Background for Stable Isotope Analysis

4.4.1 Isotopic Mass Balance

The ratios of hydrogen ($^{2}H/^{1}H$) and oxygen ($^{18}O/^{16}O$) isotopes are used to define the isotopic composition of water. Rather than using absolute values, the composition of water is expressed as a deviation from Standard Mean Ocean Water (SMOW) (Gibson, Edwards and Bursey 1993):

$$\delta_{sample} = \frac{R_{sample}}{R_{SMOW}} * 1000 \quad (1)$$

where R equals $^{2}H/^{1}H$ or $^{18}O/^{16}O$.

Controls on the isotopic composition of precipitation include: altitude, latitude, a continental effect, seasonal variation and amount effects (larger rainfalls are more depleted in both heavy isotopes) (Coplen, Herczeg and Barnes 2000). For a given location, the influence of altitude, latitude, and the continental effect remain constant. This leaves seasonal variation and amount effects as the controls on the isotopic composition of precipitation for a given area. Of these, seasonal variation is dominant, with snow being significantly more depleted in both heavy isotopes than rain (Coplen et al., 2000). Water comprised from multiple sources retains its isotopic mass balance and can therefore be used to estimate the relative contributions of snow and rainfall to recharge within the waste rock piles (Equations 2 and 3). A schematic of this process is shown in Figure 4-7.

$$\%\text{Rainfall} = \frac{(\delta_{\text{snow}} - \delta_{\text{sample}})}{(\delta_{\text{snow}} - \delta_{\text{rain}})} \quad (2)$$

$$\%Snowfall = 1 - \%Rainfall \quad (3)$$

Where δ is the isotopic content of the water as compared to VSMOW.

When conducting an isotopic mass balance it is anticipated that the values calculated using hydrogen and oxygen isotopes will usually agree to within 5-10% of each other (Coplen et al., 2000). If the average difference between the two values is significantly greater than 10% within a given dataset, this demonstrates that the isotopic ratio of the water has been influenced by a factor other than the relative contributions of rain and snowfall. The potential causes of this alteration are discussed further in Section 4.6.

4.4.2 Isotopic Analysis of Evaporation

When the values of δ^{2}_{H} and δ^{18}_{O} are plotted for a number of samples a straight line is formed, as in Figure 4-7. The slope of this line is a function of the evaporative history of the water. Water that has undergone evaporation from a free water surface will be located on a line with a shallow slope of 3 to 6,

while water that has not undergone evaporation will fall on a line with a steeper slope of approximately 8. These two lines are known respectively as the local evaporation line (LEL) and the meteoric water line (MWL) (Coplen et al., 2000).

When evaporation occurs in porous media, such as at or near the surface of a waste rock pile, the resultant $LEL_{(Porous)}$ has a slope of 2-3 (Allison 1982). This is due to greater resistance to the diffusion of water vapour in partially saturated media. For example, the $LEL_{(Porous)}$ defined at Mine Doyon, in Quebec has a slope of 2.4, as is shown in Equation 4(Sracek, et al. 2004):

$$\delta^2 H = 2.4 * {}^{18}O - 66.0 \quad (4)$$

Reference isotope data for the Canadian Arctic can be found in literature and on the International Atomic Energy Agency website (IAEA 2014). The two sites closest to Diavik Diamond Mine are Yellowknife (300km SW) and Whatever Lake (600km SE, Informal name). At Yellowknife the local MWL has a slope of approximately 7.0 (IAEA 2014), and samples taken from nearby Pocket Lake had a LEL with a slope of approximately 5.0 (Gibson and Reid 2010). The MWL and LEL at Whatever Lake had slopes of 7.5 and 5.5 respectively (Gibson, Edwards and Bursey 1993). The slope of these lines provides a basis for the analysis of evaporation in the Canadian Arctic, including at Diavik.

4.5 Methodology

Samples of effluent are taken from the north drain every 2-3 days between May and November, when flow is occurring. All sample bottles were triple rinsed with sample water prior to use and were stored in a cool environment after sampling occurred. The samples were kept in HDPE bottles with a minimum of headspace until they were analyzed in 2014. Storing the samples in this manner ensured that the isotopes were not altered (Spangenberg 2012).

In total, 23 effluent samples, three snow samples (taken in April 2014) and two rain samples (from two events in summer 2014) were analyzed. Samples taken between 2011 and 2013 were selected based on

the well defined transition between high and low pH observed in outflow during each of these years (Figure 4-6). The snow samples were taken in the spring prior to the beginning of melting, rather than from individual snowfalls. Experiments using isotopes from a fresh snowfall underestimate the contributions of snowmelt to recharge, because sublimation moves the signature of the snow closer to that of rain prior to infiltration (Earman, et al. 2006). The rainfall samples were collected from clean buckets shortly after each rainfall event.

All samples were analyzed in the Environmental Isotope Laboratory at the University of Waterloo. Samples with a pH of less than 5 were analyzed using chromium reduction and H_2O-CO_2 equilibration. The error associated with these measurements is ± 0.8‰ δ^2_H and ± 0.2‰ δ^{18}_O. Samples with a pH greater than 5 were analyzed on a Los Gatos Research (LGR), "EP LWIA" instrument. The LGR instrument vaporizes a sample and analyzes its isotopic composition using Off-Axis Integrated-Cavity Output Spectroscopy (ICOS). Lab duplicates were run for 9 of the 23 samples and had an average error of 0.3% as compared to the original values.

The results of the lab work were analyzed to determine the relative proportions of melted snow and rain water in outflow from the pile. Additionally, the amount of evaporation occurring in the north batter of the pile was assessed.

4.6 Assumptions

This section summarizes the key assumptions used in the isotope analysis conducted for this chapter. The validity of each assumption is checked in Section 4.9, based on the results presented in Section 4.8.

4.6.1 Interaction with the Rock Pile

Equations 2 and 3 are based on an assumption that the isotopic signature of the water is not significantly altered by interaction with the porous media it is infiltrating. The potential causes for the alteration of isotopes in waste rock include: oxidation reactions associated with ARD, exchange with

CO_2, hydration of silicates, and an exchange with H_2S (Ghomshei and Allen 2000), (Arcadis 2013). The net impact of each of these interactions is shown in Figure 4.8. In general, isotopes are not strongly altered during passage through a waste rock pile; however, it is necessary to confirm the validity of this assumption whenever an experiment is conducted in a new location (ex. Coplen et al. (2000), Allen and Voormeij (2002), and Arcadis (2013)).

4.6.2 Partial Freezing

When a body of water partially freezes the remaining water becomes more depleted in both heavy hydrogen and heavy oxygen isotopes. The first ice to form is enriched in both isotopes, and becomes progressively more depleted as freezing continues. Soughez and Jouzel (1984) experimentally constrained the depletion of δ^2_H to be less than 30‰ and the depletion of δ^{18}_O to be less than 5‰ in partially frozen water taken from a lake in the Canadian Arctic (original composition of -153‰ $\delta^2_H$and-19‰ δ^{18}_O). The isotopic signature of ice is not altered during melting, due to the fact that δ^2_H and δ^{18}_O are relatively immobile in ice(Souchez and Jouzel 1982).

The analysis conducted for this thesis relies on the assumption that the batters freeze and thaw completely each year. This will close the isotopic system (with respect to freezing and thawing), and the average isotopic signature of the effluent will be unaffected. This assumption is supported by thermal data measured within the pile, which demonstrates that the majority of the batters thaw each year (Figure 4-9) (Pham, et al. 2013).

4.7 Limitations

The primary limitation of this analysis is the small number of snow and rain samples analysed, with all precipitation samples being taken in 2014. The isotope ratios of these samples define the end members of the analysis, and are used in Equation 2. Isotope depletion in snow and rain is not constant, and it is recommended that several years of samples be included when differentiating between recharge from snowmelt and from rainfall (Coplen, Herczeg and Barnes 2000). Unfortunately this was not possible at

Diavik, as no historical rain samples were collected. Instead, the samples that were taken are assumed to be representative of average precipitation for all years. Four years of isotope data from Yellowknife were analyzed to estimate the potential error this assumption could cause. On average, the discrete samples deviated from the mean by 17 ‰ δ^{2}_{H} and 2 ‰ δ^{18}_{O}. In a worst case scenario, where both the snow and rain were under or overestimated, the result would be a 13% under/over estimation of snowmelt recharge. In the case where one sample was overestimated and the other was underestimated the result would be a 5% under/over estimation. Additional samples are currently being collected, and will be used to refine this analysis in the future.

4.8 Results

4.8.1 MWL and LEL

Figure 4-10 shows the isotope ratios of all the samples analyzed. The MWL defined by Gibson et al. (1993) at Whatever Lake (W. Lake) is included for comparison. The effluent samples taken from Diavik fall on a line (the 'effluent line') defined by the relationship:

$$\delta^2 H = 8.4 *^{18} O + 21.3 \quad (6)$$

The slope of the effluent line is steeper than the slope of the MWL defined at W. Lake (7.5), but is a good match to the global meteoric water line (GMWL) which has a slope of approximately 8.0.

The MWL at Diavik is defined by connecting only the snow and rain samples, and has the relationship:

$$MWL: \delta^2 H = 7.0 *^{18} O - 21.8 \quad (7)$$

The slope of the MWL is less than that of the effluent line and the GMWL. This is due to the rainfall samples being located slightly below the other lines, which suggests that they may have undergone a small amount of evaporation prior to collection. Evaporation can also occur during rain events that pass

through unsaturated air and this will lead to rain samples plotting below the MWL (Gibson, Reid and Spence 1998).

4.8.2 Snowmelt in the North Drain

The relative proportion of rain and melted snow in each effluent sample was calculated using Equations 2 and 3. The results of this calculation are plotted along with the pH of each sample in Figure 4-11 a-c. Each year the initial circumneutral effluent in the north drain is derived from 60-75% (average 65%) melted snow and 25-40% (average 35%) rain. As the season progresses the proportion of melted snow in the effluent decreases until flow terminates in November. Samples taken in November were derived from 24-33% melted snow (30% average) and 67-76% (70% average) rain. Each year the transition between circum-neutral and low pH outflow water corresponds closely with a decrease in the proportion of the water derived from the infiltration of melted snow. This confirms the hypothesis of Sinclair (2014), who used pH and solute concentrations to suggest that early season discharge can be attributed to snow melt infiltration and preferential flow through the batters of the pile. The more acidic outflow observed during the remainder of the flow season is derived from a combination of snowmelt and rainfall that travelled through the matrix of the pile, rather than through preferential pathways.

Figure 4-12 a-c shows the cumulative volumes of melted snow and rain water passing through the drain each year. These volumes were calculated by assuming a linear change in the proportion of melted snow between samples. The interpolated proportions of rain and melted snow were multiplied by the total daily flow to obtain volumes. In water collected by the north drain in 2011 the cumulative volume of pore water derived from melted snow was greater than that of rain until mid July. In 2012 this transition did not take place until mid August, and in 2013 it occurred in late September. The relative amount of rain and melted snow in the pore water conducted by the north drain each year is interpreted to be a function of rain and snowfall amounts (Figure 4-4). The winter of 2010-2011 was the

driest of the three years, and the summer of 2011 had the highest rainfall. Only 33% of the total outflow in the north drain originated from snowmelt in this year. In 2012 and 2013 there was a greater amount of snowfall and less rain. The percentage of outflow derived from snowmelt on the batters in these years was 39% and 43% respectively. Over the three flow seasons, 40% of the total effluent conducted by the north drain was derived from the infiltration of melted snow, with the remaining 60% derived from the infiltration of rainfall.

4.8.3 Evaporation

Plots of the isotope ratios for effluent samples taken in 2011, 2012 and 2013 are shown in Figure 4-13 a-c. Rather than following a LEL or $LEL_{(Porous)}$, the samples plot along a line with a slope of 8.2 to 8.4. If significant evaporation was occurring following infiltration, the plots shown in Figure 4-13 would have a slope of between 2 and 3 (Allison 1982), (Allison, Barnes and Hughes 1983) and (Sracek, et al. 2004). A slope of 8.2 to 8.4 therefore shows that minimal evaporation occurs following the infiltration of water into the batters of the pile. This differs from infiltration into the pile crest, where strong evaporation occurs (Fretz 2013). The two behaviors can be explained by the differential grain sizes and solar radiation on the crest and batters of the pile. As was previously mentioned, the coarsest material is located at the base of the pile, and the crest of the pile is finer grained than the batters. A visual inspection of the batters shows that they are predominately clast supported, with large void spaces separating the grains. This allows for rapid infiltration through the surface of the batters into the interior of the pile, where cool, dark (low radiation) conditions dictate that evaporation is not likely to occur. Conversely, the crest of the pile contains more matrix material than the batters, and infiltration into the matrix will result in water storage near the surface of the pile, where evaporation can occur.

4.9 Justifying assumptions

The analysis contained in Section 4.8 relied on the assumption that the isotope ratios in the pore water were not being significantly altered by interaction with the waste rock or by partial freezing. In this section the validity of using these assumptions in the type III waste rock pile is assessed.

4.9.1 Interaction with the Rock Pile

The potential alteration of isotopes in the batters of the pile was analyzed by comparing the isotope ratios of the early (circumneutral) and later (acidic) samples. Sinclair (2014) used the geochemistry of the outflow water to conclude that the circumneutral water observed each spring has a shorter residence time in the pile than the later, more acidic outflow water. If interaction with the pile is altering isotopes in the pore water it follows that an increased residence time will lead to a greater alteration. This will lead to a change in the slope and intercept of the effluent water line along one of the paths shown in Figure 4-8. Figure 4-14 a-b shows separate plots of the early (circumneutral) and later (low pH) effluent from each year. The slopes and intercepts of both lines are similar, however both the slope and the intercept of the low pH effluent line is slightly higher than that for the circumneutral samples. This demonstrates that the pile is exerting a small influence on the isotopic composition of the pore water collected by the north drain.

4.9.2 Partial Freezing

Soughez and Jouzel (1982) demonstrated that samples undergoing partial freezing will produce a line with a slope of 4.4 to 6.6 when plotted. Since the plots of the effluent samples created each year have a slope of 8.2 to 8.4 it is concluded that partial freezing is not influencing the isotopes in pore water conducted by the north drain.

4.9.3 Summary of Justifications

In equation 2 the average difference between the values calculated using δ^{2}_{H} and δ^{18}_{O} was 8%, which is within the expected range of error of 5-10% defined by Coplen et al. (2000). This shows that even

through the isotopes in the water are slightly altered by interaction with the pile, the assumptions used in this analysis are valid.

4.10 Conclusions

The objective of this paper was to quantify snowmelt infiltration into the batters of the type III pile at Diavik. 23 samples (2011-2013) were analyzed for stable isotopes of hydrogen and oxygen, and the proportion of snowmelt within each sample was calculated. The results demonstrated a clear correlation between pH and the proportion of the effluent derived from the infiltration of melted snow. In total, 40% of the flow collected by the north drain between 2011 and 2013 was derived from snowmelt. The remainder of the flow was derived from the infiltration of rainfall through the batters of the pile in the current or preceding year. The proportion of recharge attributable to melted snow can be expanded to the other batters on the pile by assuming that the snowpack formed each year is reasonably consistent between each batter. It is acknowledged that this assumption is not completely correct, as the structure of the snowpack is influenced by winds. However, by making this assumption it can be concluded that approximately 40% of the recharge received through the batters of the pile is derived from snowmelt. The remainder of the recharge received through the batters of the pile, and the entire recharge received through the crest of the pile, is derived from rainfall.

The slope of the effluent line showed that minimal evaporation occurs in water infiltrating the northern batter of the type III pile. This differs from infiltration into the crest of the pile, which is heavily influenced by evaporation. There is evidence that the isotope ratios of the pore water are slightly influenced by interaction with the rock pile; however, the net impact of this interaction did not significantly impact the analysis conducted for this research.

4.11 Figures For Chapter 4

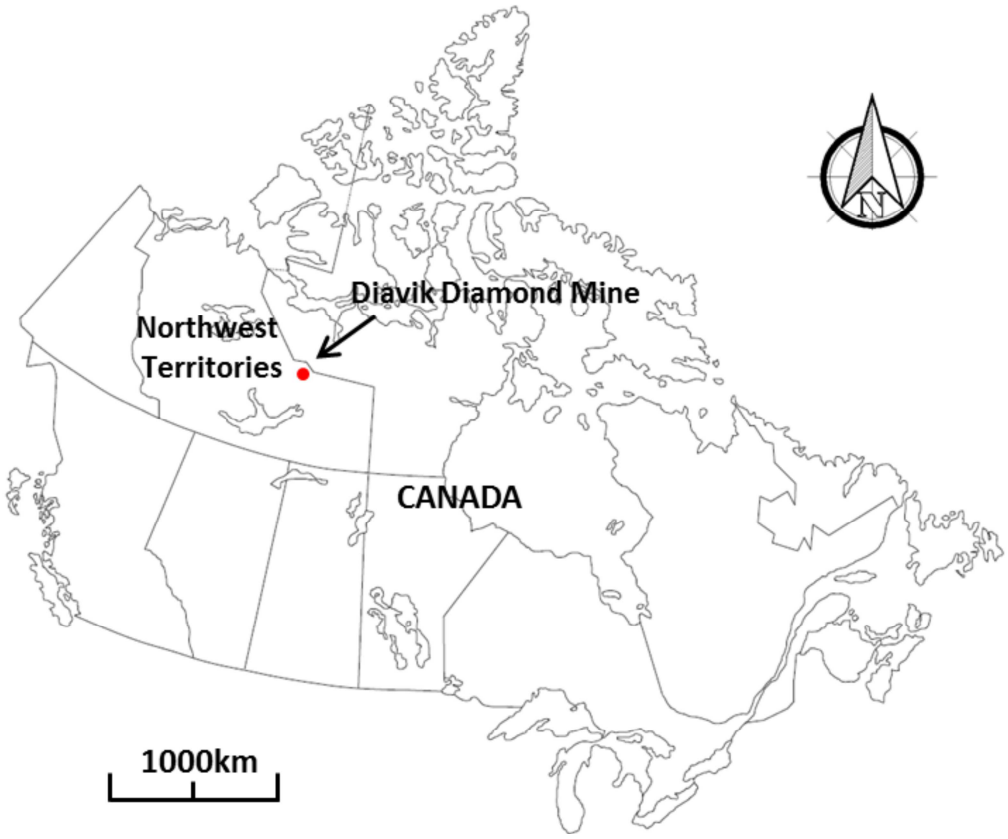

Figure 4-1: Location of Diavik Diamond mine. Image from Fretz (2013)

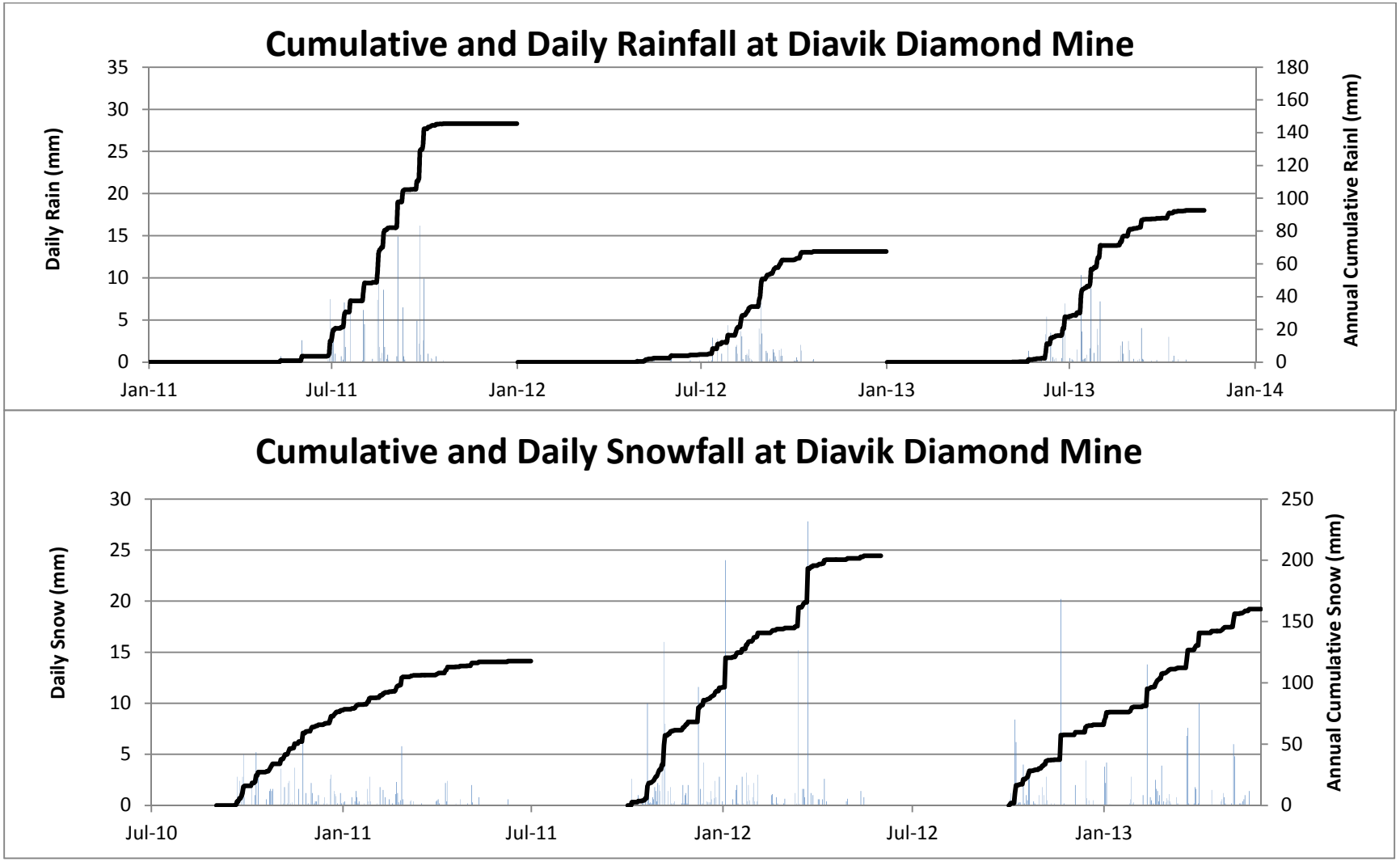

Figure 4-2: Daily and cumulative annual precipitation at Diavik.

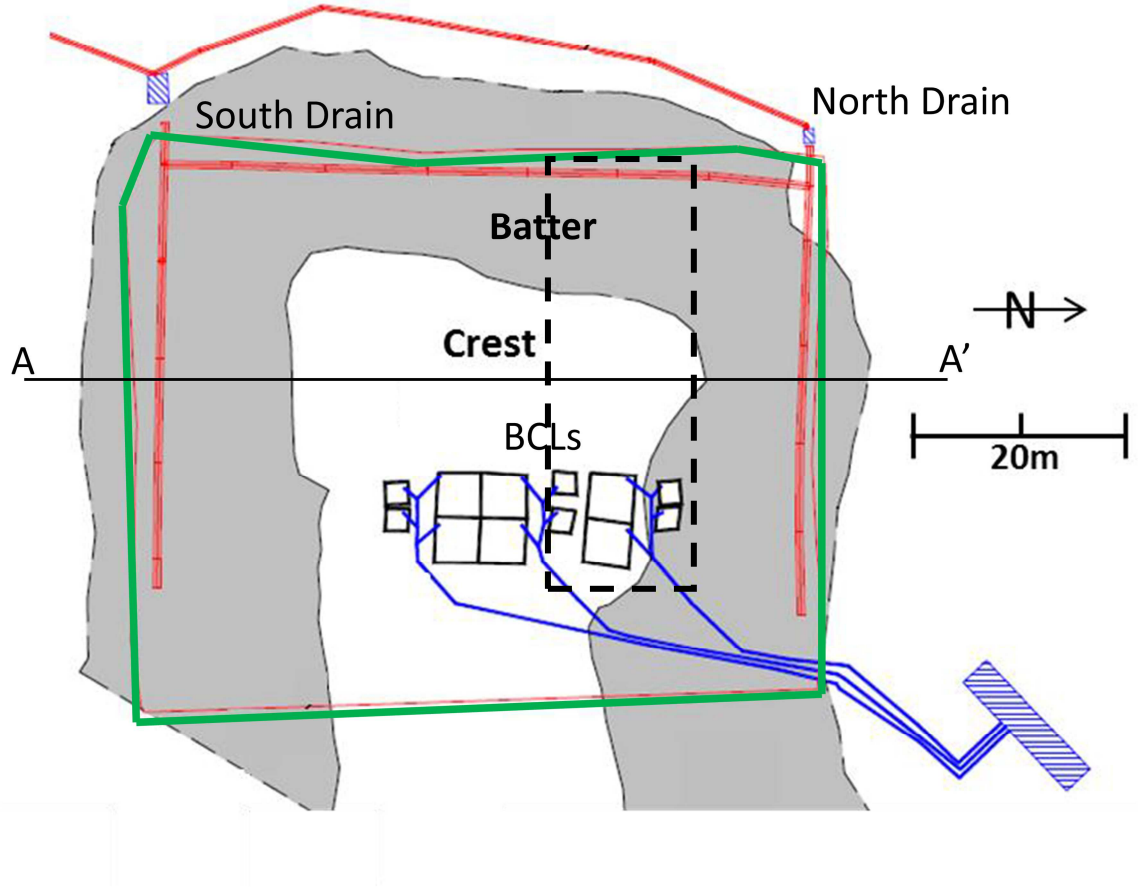

Figure 4-3: The location of the drains and BCLs in the type III pile.

The gray areas show the batters of the pile, the green lines show the extent of the basal liner, the red lines show the basal drainage pipes, and the blue lines show the BCL drainage pipes. The dashed rectangle overlain on the northern edge of the pile shows the approximate portion of the pile that the north drain collects outflow from. Figure 4-4 is taken along line A-A'. Image modified from Fretz (2013)

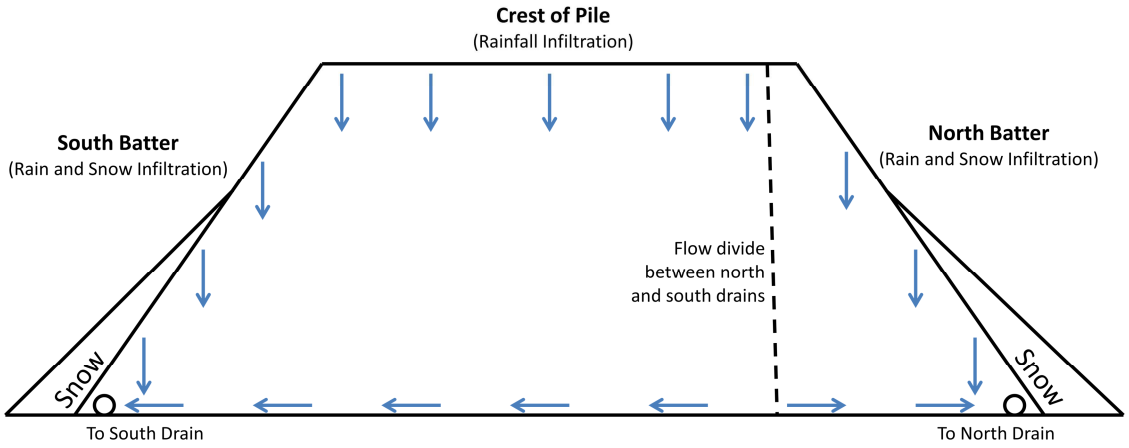

Figure 4-4: Schematic of flow within the TIII pile along A to A'.

The snow shown in this figure is representative of a springtime snowpack immediately prior to melting.

Figure 4-5 a-b: Snowpack on the batters of the type III pile

a. Snowpack on April 25, 2011
b, Snowpack on May 6, 2014

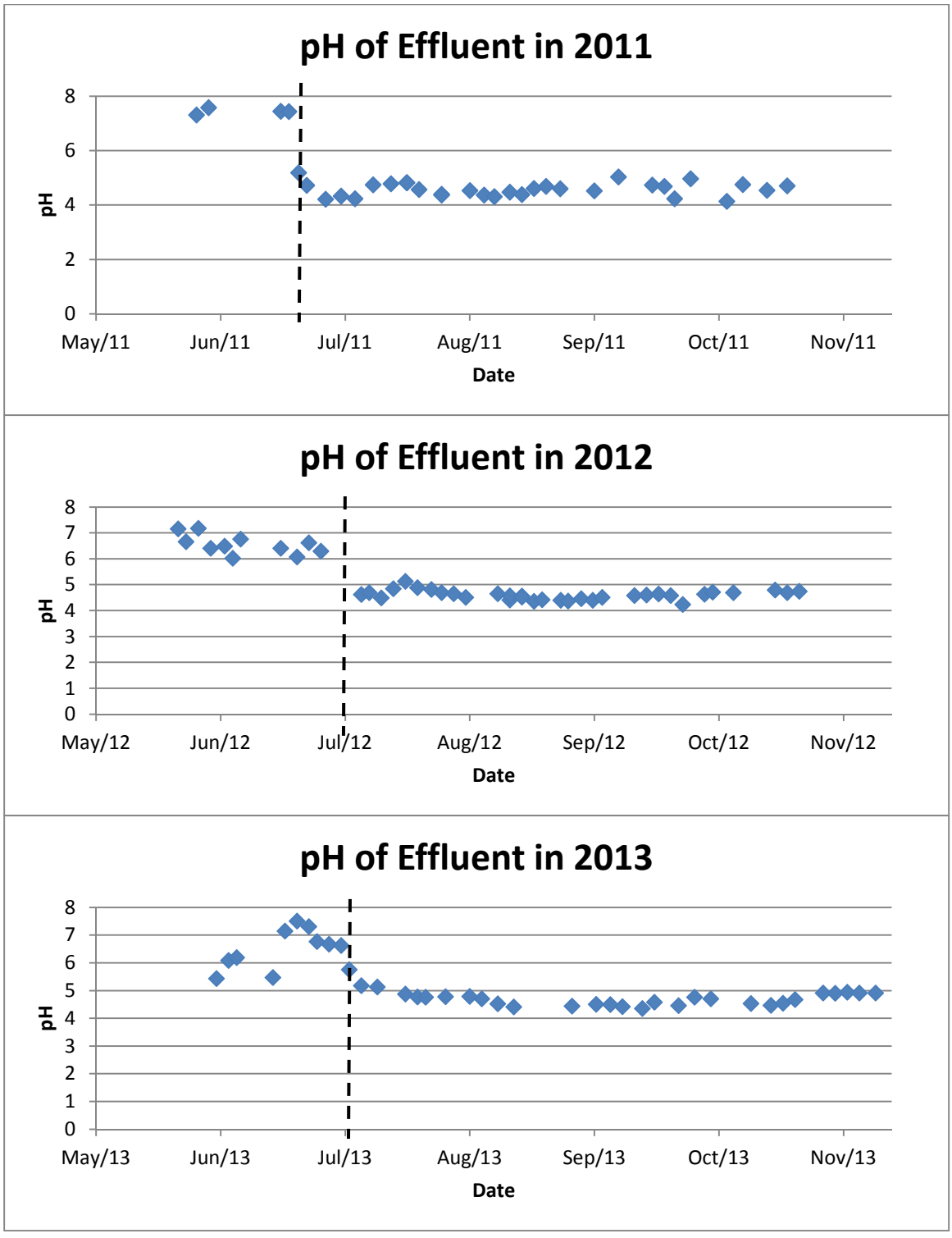

Figure 4-6: The pH of effluent in samples taken from the north basal drain.

The dashed line on each plot shows the divide between early season circumneutral pH outflow and later, more acidic outflow

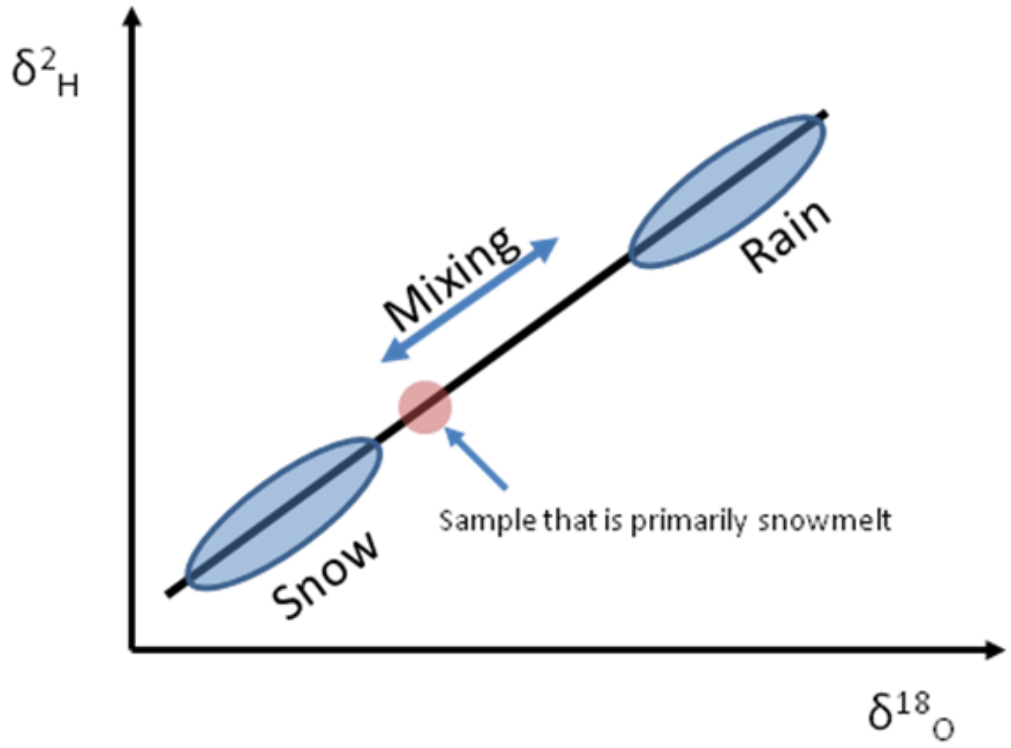

Figure 4-7: Schematic showing the relative isotope ratios of snow and rain.

Snow is more depleted in both ^2H and ^{18}O than rain. A sample comprised of both rain and snowmelt will have an intermediate isotope ratio, as defined in equations 2 and 3.

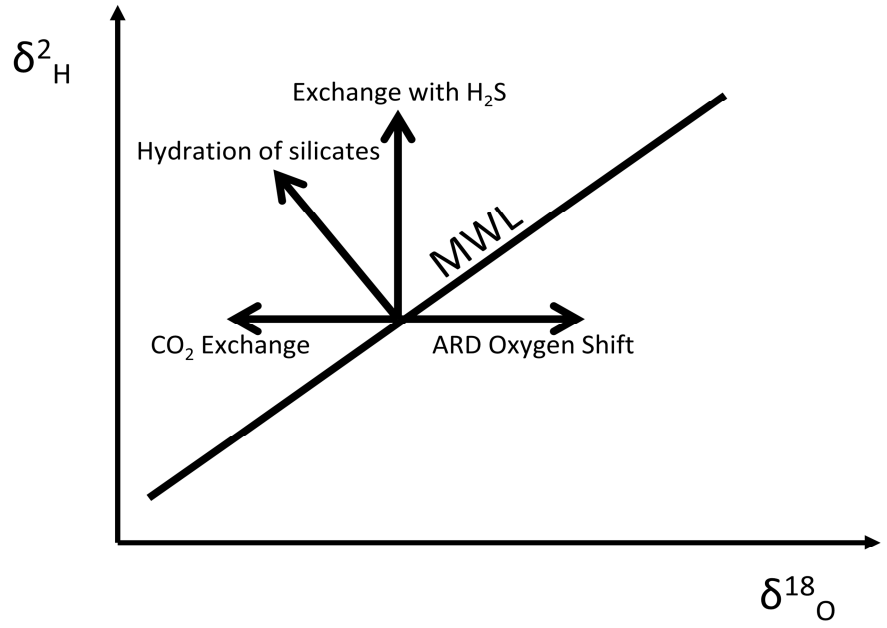

Figure 4-8: Potential sources of isotope alteration in the TIII waste rock pile

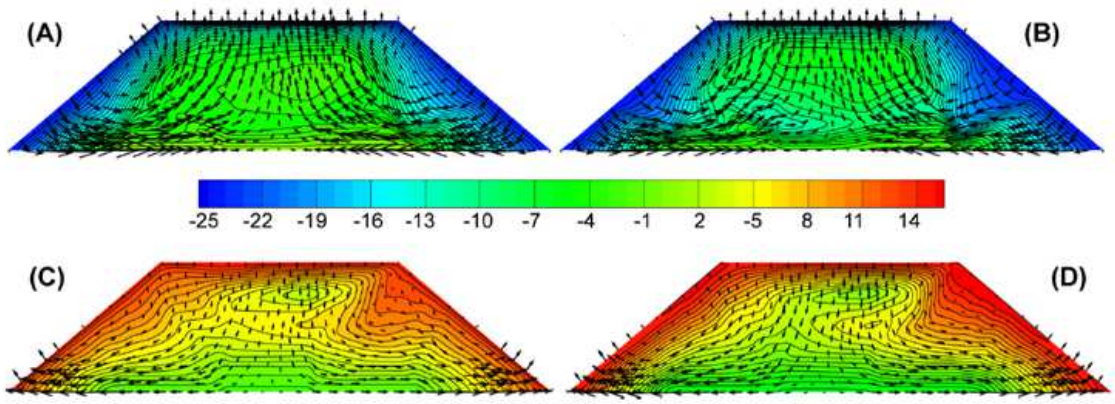

Figure 4-9: Isotherms and density driven air flow vectors in the type III pile

Models show the pile in: (A) January 2007, (B) January 2008, (C) July 2007 and (D) July 2008. Image modified from Pham (2014)

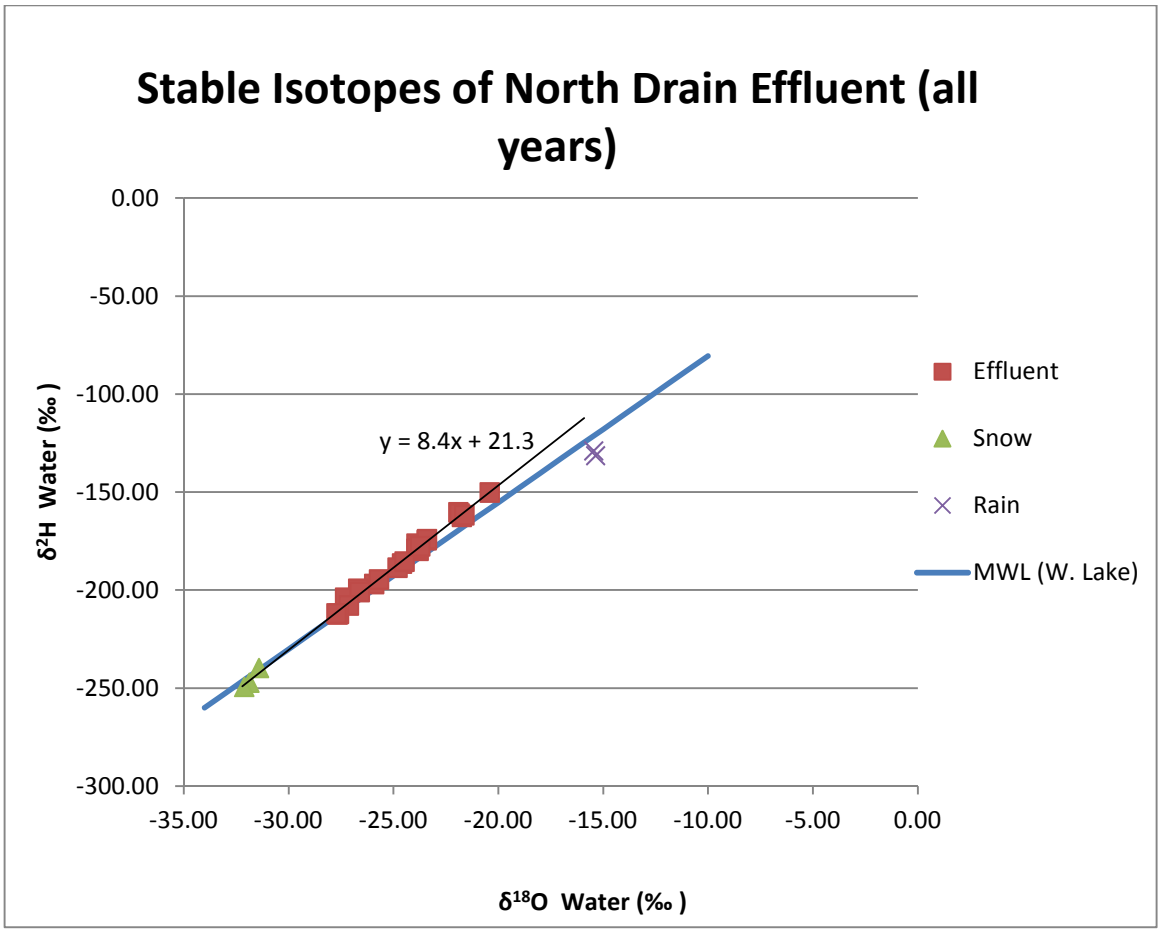

Figure 4-10: Isotopic ratios of rain, snow and effluent at Diavik.

The blue line shows the MWL defined at nearby W. Lake.

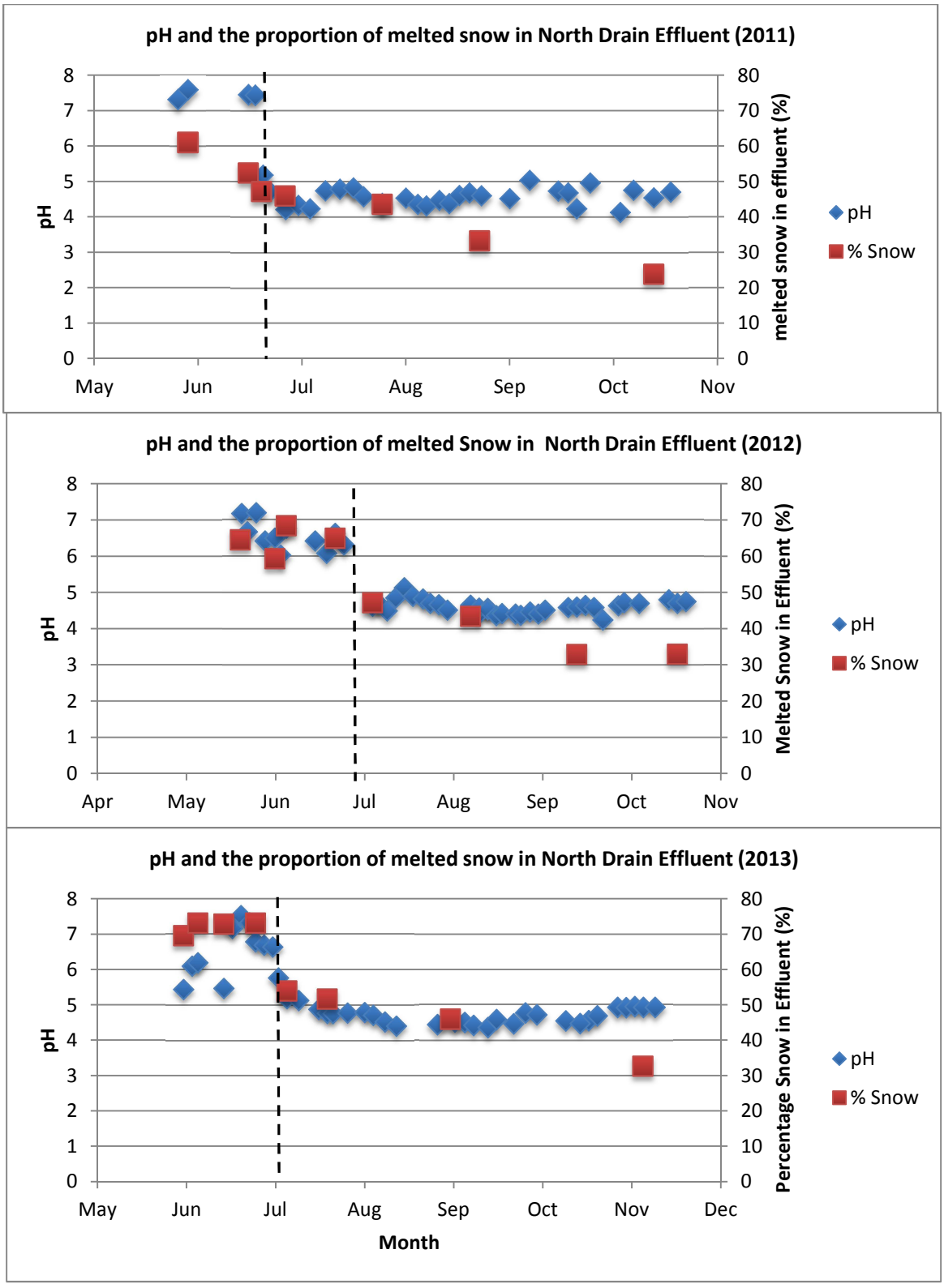

Figure 4-11: Plots showing the percentage of snow and pH of samples

The dashed line on each plot shows the divide between early season (circumneutral) outflow and later (low pH) outflow, as in figure 4-6.

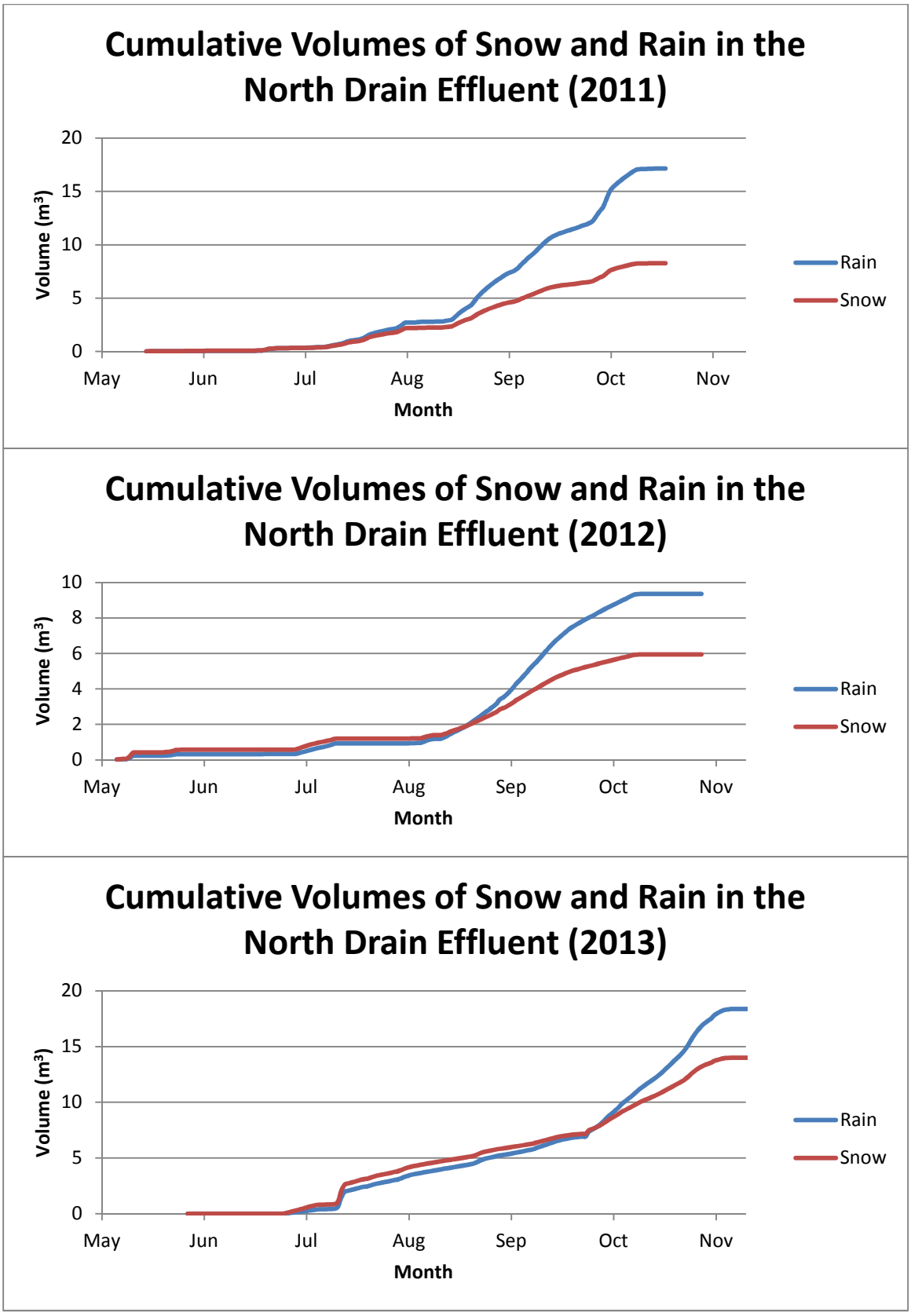

Figure 4-12: Cumulative volumes of rain and snow melt in the north drain effluent.

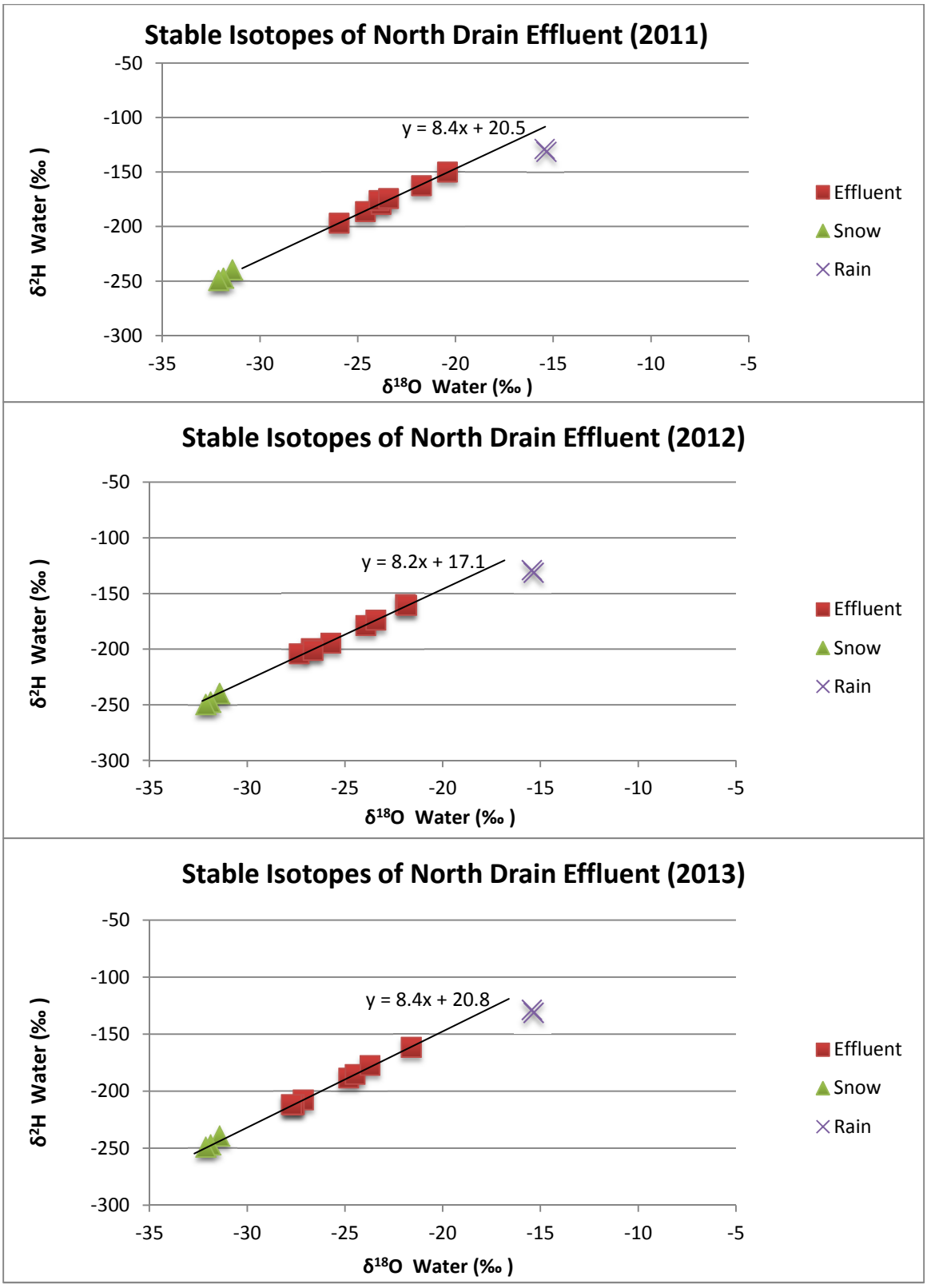

Figure 4-13:Isotope ratios of the effluent from the north drain in 2011-2013.

The isotope ratios and rain and snow (2014) are also plotted.

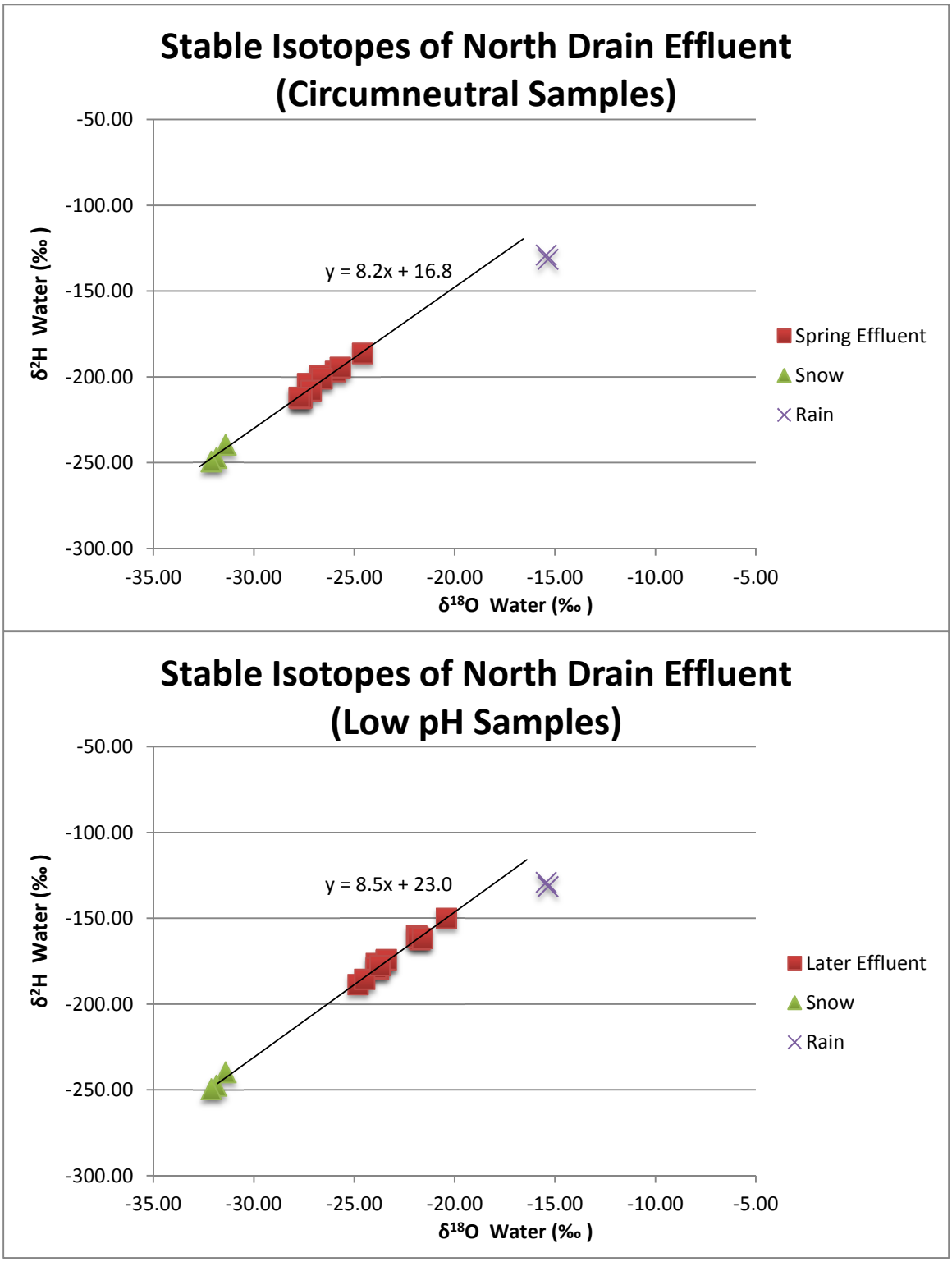

Figure 4-14: Stable isotopes in spring (high pH) and later (low pH) samples.

Chapter 5: Modelling Snowmelt Infiltration into a Covered Waste Rock Pile in the Canadian Arctic

This chapter is written as a self contained article formatted for publication in a journal. In this chapter the infiltration of snowmelt through the batters of the covered experimental waste rock pile is modelled. Estimating the amount of recharge received from snowmelt is important when developing up-scaling relationships between the experimental and full scale piles.

5.1 Summary of Chapter

The goal of this research is to estimate the volume of recharge received through the batters of an experimental waste rock pile due to the infiltration of snowmelt. This is an important component of understanding the hydrological systems that exist within the waste rock. The base of the waste rock pile is underlain by an HDPE liner, which is centred under the pile and occupies 40% of the pile's total surface area. Pore water that reaches the basal liner is directed into a PVC drainage pipe and the volume of water conducted by the pipe is quantified. Only the infiltration that occurs directly above the liner is expected to contribute to outflow from the drainpipe, and the research conducted for this paper is therefore focused primarily on this portion of the pile. Four years of snow survey data were used to calculate the volume of snow on the pile each spring, and demonstrated that on average only 17% of the total snowpack was located above the liner. A melt and sublimation model was then used to estimate the rate of ablation for this portion of the snowpack. Each year melting is initiated in May, and complete melting is estimated to take between 6 and 15 days, depending on the total volume of snow available and the weather during the snowmelt window. In the time period between the snow survey being taken and the complete ablation of the snowpack it is estimated that approximately 13 to 30% of the snow located above the liner is sublimated. The estimated melt rates are used in an infiltration model that describes recharge into frozen soil with the characteristics of the waste rock material. The volume of recharge received through snowmelt is estimated to be between 70-159 m^3 each year, which

is 22 to 54% of the total annual recharge. The modelled volumes of snowmelt each year are used to close a multi-year water balance for the pile between 2007 and 2011.

5.2 Introduction

Waste rock is created when the removal of non-ore bearing rock is required during mining. The weathering of sulfide minerals contained in waste rock can lead to the production of low quality effluent known as acid rock drainage (ARD). ARD can cause significant long term degradation of watersheds and ecosystems, and thus a comprehensive understanding of the flow and geochemistry within waste rock piles is necessary when developing a mine closure plan.

Diavik Diamond Mine (DDMI) is located in the continuous permafrost region of the Canadian Arctic at 64°29'N, 100°18'W (Figure 5-1). Complete excavation of the diamond bearing kimberlite pipes at Diavik requires the removal of 200MT of country rock, which is currently sorted by its sulfide content and stored in a segregated 80m high stockpile. The Diavik waste rock project has the goal of developing a comprehensive understanding of the thermal, hydrological and geochemical evolution of this waste rock. The field portion of the project contains 2m and 15m scale waste rock experiments located at the mine site. Lab based research, including a multiyear humidity cell experiment, is based out of the University of Waterloo. The intention of the project is to develop up scaling relationships between the data collected from each of the experiments, and to use these relationships to create a comprehensive understanding of the thermal, hydrological and geochemicalbehaviour of the full scale pile.

5.3 Scope and Organization

This research is focused on estimating the infiltration of snowmelt into an experimental waste rock pile (known as the covered pile) located at DDMI. A brief background on the construction and hydrology of the pile is presented in Section 5.5. Next, the infiltration of snowmelt into the covered pile is modelled from data obtained during four snow surveys taken in 2010, 2011, 2013 and 2014. For each year, the total volume of snow on the pile is determined and an ablation model is used to estimate melt and

sublimation rates. Following this, an infiltration model is used to estimate the amount of recharge that occurs through the infiltration of snowmelt into the interior of the waste rock pile. Finally, the estimated volumes of snow melt infiltration are used to close a multi-year water balance for the pile.

5.4 Limitations

This research is a modelling exercise based on a comprehensive literature review and four snow surveys taken in 2010, 2011, 2013 and 2014. The snow surveys are used to determine the amount of water contained in the snowpack at the time the survey was taken. From this point onwards the evolution and infiltration of the snowpack is modelled, as no further field measurements were taken during any of the surveys. The infiltration of snowmelt cannot be measured using the existing instrumentation in the pile, as all of the hydrological sensors put in place during construction rely on unfrozen conditions to produce accurate measurements. Additionally, a single year water balance for the pile cannot be constrained, as the potential change in storage within the pile is of a significantly greater magnitude than either the annual outflow or infiltration. Snow surveys were not taken in 2007, 2008, 2009 or 2012, which prevents the direct usage of a multiyear water balance. Instead, a five year water balance for the pile is estimated using the average volume of snowmelt infiltration determined by the results of the modelling. The amount of snowfall infiltrating the surface of the pile varies annually, which introduces uncertainty in the water balance equation; however, this is the best available method to support the results of the modelling.

This research is based on models that were selected with consideration given to the available data. Each of the models utilized was chosen to require a minimum of calibration and is based on studies conducted over time periods ranging from 6 to 25 years in similar environments. The intention of this research is to provide an estimate of snowmelt infiltration into the pile, and to serve as a platform upon which further research can be conducted.

5.5 Background

This section is intended to provide the reader with a background knowledge of the mine site, along with the construction and hydrology of the covered pile.

5.5.1 Diavik Diamond Mine

The climate at DDMI is characterized by long, cold winters and short, cool summers, with an average mean temperature of -8.5^{o}C. Historical precipitation at the mine averaged 280mm per year between 1998 and 2007, with 65% falling as snow (Environment Canada 2010). Since 2007 the annual precipitation on the pile has averaged 250mm per year, with 60% falling as snow (Figure 5-2).

The country rock at Diavik is primarily Archean age granite and pegmatite granite. The rock is characterised by low concentrations of sulfide bearing minerals, except within xenoliths of metasedimentary biotite-schist, which contain pyrrhotite. Waste rock at the mine is classified by sulfur content as type I, type II, or type III material. Type I material has an average sulfur content of <0.04 wt% S, type II material has between 0.04 and 0.08 wt. % S, and the type III material has > 0.08 wt. % S. Each rock type is also characterized by low concentrations of carbonates, and both the type II and type III materials are acid generating.

5.5.2 The Experimental Waste Rock Piles

Three 15m high experimental waste rock piles were constructed for the Diavik project in order to study the hydrology, geochemistry and thermal behaviour of waste rock at Diavik. This research is focused on one of the three piles, known as the covered pile. For a complete description of each of the piles, the reader is referred to Neuner (2009), Smith (2009) and Fretz (2013).

Structure and Construction

The covered waste rock pile has a basal footprint of 100 x 125m. It consists of an acid generating type III core overlain with a cover of low permeability till and type I rock. The type III core has an average sulfur content of 0.083 wt. %S, and was constructed using end dumping and push dumping techniques. The

type III rock was placed below residual saturation, and following placement the batters of the pile were re-sloped to 18^{o} using a bull dozer. Till material from the mine site was used to create a 1.5m thick cover that was placed on top of the re-sloped core using a bulldozer. The till was partially frozen when it was excavated, and had an average gravimetric water content of 8% (L. Smith 2014). Following the placement of the till cover, an additional cover consisting of 3m of dry type 1 material was placed on top of the crest and batters of the pile. A dozer was used on the batters, and the crest was covered by free dumping from haul trucks followed by grading with a dozer.The construction techniques used with the till and type I material resulted in a cover that is not completely uniform; however, anidealized schematic cross section of the covered pile is shown in Figure 5-3.

The core of the type III pile is underlain by an 84 x 59m HDPE liner that covers approximately 40% of the piles total footprint. The liner is graded to direct flow into a perforated, heat traced pipe that passes through the centre of the pile (Figure 5-4). Water collected by the pipe flows into a custom built tipping bucket, which records the volume of effluent passing through it.

Purpose of the Cover

The cover system is designed to prevent the formation and release of ARD from the reactive type III core of the pile. The type 1 material is designed to freeze and thaw annually and act as the active layer of the pile, while the till and type III core remain frozen year round. The low permeability frozen till layer is intended to restrict the ingress of oxygen and water into the core of the pile.

A heat trace located in the base of the pile kept the core of the pile thawed until the heat trace was shut off in 2011. Following this, the core of the pile cooled and froze during 2012 and 2013 (Figure 5-5), which led to a significant alteration of the internal flow regime in the pile.

5.5.3 Hydrology of the Covered Pile

Infiltration of Rainfall into the Type I Material

Infiltration through the surface of the covered pile is divided between snowmelt and rainfall. The annual infiltration of rainfall into the crests of the uncovered experimental waste rock piles was estimated by Fretz (2013) using the Penman Monteith formulation and the results from four 2m scale active zone lysimeters (AZLs). Due to the construction techniques used on the covered pile, the grain size distribution of the batter material is similar to that found on the crests of each pile. Both the crest and the batters of the covered pile are constructed of the same rock, and have had similar compaction through traffic as the uncovered test piles. For this reason, the infiltration of rainfall estimated by Fretz each year has been extended from the crest to the batters of the covered pile. It is acknowledged that this is not a perfect representation of infiltration through the entire surface of the pile, as runoff is more likely to occur on the sloping batters of the pile than on the flat crowns and AZLS. Despite this, the model created by Fretz still contains the best available estimates of infiltration into the pile. The results of the Penman Monteith infiltration model are summarized in Table 5-1 below.

Infiltration of Pore Water through the Till Layer

The type I cover placed on top of the till was intended to keep the till frozen year round to prevent infiltration into the core of the pile. Permanently frozen conditions have not been established in the till as of 2013 (Figure 5-5), and it is anticipated that infiltration through the till layer is occurring during the summer months. A tracer was applied to the east batter of the pile in the summer of 2013 and is intended to determine the effectiveness of the till layer as a barrier to flow. The results of this experiment will be analysed by Jordan Zak (Ongoing). Since the percentage of infiltration that passes through the till layer is currently un-quantified, this paper focuses primarily on infiltration into the type I material.

Table 5-1: Estimates of rainfall infiltration into the covered pile.

Year	Rainfall (mm)	Estimated Net Infiltration (mm)	Estimated Volume Infiltrated (m^3)
2007	92	40	198
2008	154	88	436
2009	74	11	54
2010	98	40	198
2011	146	84	416
2012	68	9	45
2013	91	26	129
Average	**103**	**43**	**211**

Pore Water Storage

The covered pile is unsaturated, and pore water contained within the pile is located in the <5mm fraction of the waste rock. This fraction of the rock is known as the matrix, and is defined by its ability to retain water through capillarity. Previous work estimated that the matrix occupies 18% of the total rock volume in the experimental piles (Figure 5-6) and has a porosity of 25%. This accounts for 5% of the total porosity in the pile (Fretz 2013). The average volumetric moisture content (VMC) in the matrix of the waste rock material increased during the wet up of the pile between 2008-2009, and ranged from 15-25% between 2010 and 2012 (Figure 5-7). In between August 2012 and August 2013 the data from each of the TDR probes showed a strong drying trend. This may be due to low infiltration in 2012 and 2013 (Table 2-1) or may reflect the very gradual onset of freezing conditions in the pile. Ongoing thermal modelling by Pham (2014) shows that the portion of the pile surrounding the TDR probes was consistently around 0^oC during this time period. Experiments conducted by Neuner (2009) demonstrated that some moisture in the pile remains liquid at temperatures just below 0^oC due to capillary forces imparted from the small particles in the matrix (Figure 5-8).

Pore water is also stored in the till of the covered pile, and volumetric moisture contents as high as 40% were observed in the till in July of 2010 and 2011 due to the infiltration of snowmelt (Figure 5-9).

Moisture contents are not directly measured in the type I material, however measurements from tensiometers in the crest of the pile show that the matrix of the type I rock dries noticeably in between infiltration events, and has an average saturation of around 60% immediately prior to winter freeze up each year.

Internal Flow

A rhodamine test conducted on the east batter of the covered pile showed that flow occurs primarily in a vertical direction within the type I material on the covered pile (Figure 5-10). Preferential flow was not induced by the tracer, which was applied at a rate of 8mm hr^{-1}. No overland flow was observed during the rhodamine tracer test; however, overland flow was observed during a different tracer test applied on the same batter at a rate of 6mm hr^{-1}. This resulted from areas of low infiltration capacity, and suggests that overland flow on the batters of the pile can occur at infiltration rates as low as 6mm hr^{-1} during times when the upper surface of the pile is thawed.

Outflow

The daily and cumulative outflow collected from the base of the covered pile increased each year until 2012, and then decreased significantly in 2013 (Figure 5-11). This is interpreted to be a result of the base of the pile cooling and freezing after the heat trace was turned off in 2011 (Figure 5-5). The large amounts of outflow observed from 2008-2012 demonstrate that pore water is able to infiltrate through the till layer. It is anticipated that this infiltration occurs primarily when the till is thawed, while pore water that reaches the till when it is still frozen is more likely to be directed laterally on top of the till.

Summary

A schematic of the hydrology of the pile is shown in Figure 5-12. Each parameter shown in this figure is relatively well constrained, with the exception of infiltration by snowmelt and the proportion of flow passing through the till material.

5.6 Snow Survey Methodology

Snow surveys were taken on the covered pile in the spring of 2010, 2011, 2013 and 2014. Measurements of snow depth were taken by vertically inserting a Plexiglas tube through the snowpack onto the underlying rock. The Plexiglas tube was transparent, and was labeled in 1cm increments to allow for measurements of snow depth. After the depth was measured a snow core was obtained by carefully removing the tube from the snow, and the tube and snow core were weighed to obtain the snow water equivalent (SWE) depth of the snow core. The density of snow was calculated from the length of the snow core and its corresponding SWE.

Each survey consists of measurements taken from a subset of fifty locations on the pile. The locations fit into five uniform elevation bands located between the crest and base of the pile. The surveys taken in 2010 contain only snow depth measurements while the remaining surveys have measurements of both snow depth and SWE. None of the surveys contain all fifty points, as locations which were deemed unsafe, inaccessible or in an artificially created snow bank are not measured. Figure 5-13 is a contour map that shows the snowpack measured in 2014, along with the location of the survey points. Note that only 21 of the survey points are located directly above the basal liner.

5.7 Snowpack Analysis

5.7.1 Snowpack Structure and Density

The snowpack had a consistent spatial distribution each year at the time the snow survey was taken. The snow was very thin to nonexistent at the crest of the pile, and increased in thickness towards the base (Figures 5-13 and 5-14). The distribution of the snowpack is a result of winds scouring the upper portions of the pile and depositing snow onto the batters. Wind speed at Diavik is measured at a MET station located approximately 1km from the test piles, and measurements are taken at a height of 2m above the tundra. Between 2007 and 2013 the average wind velocity at Diavik was 4.9m/s, and the maximum wind speed was 14.5 m/s.

During the snow survey conducted in 2014 the snowpack was observed to be stationary, even during strong winds. This is a result of a wind crust over the top of the snowpack that prevented transport of the underlying snow. It is assumed that this condition is present each spring, and that the snowpack is not strongly altered by wind following the snow survey.

The average density of the snowpack ranged between 290 and 350 kg/m^3 in the three surveys that contained density measurements (2011, 2013 and 2014). This correlates well with other studies conducted in arctic environments, which define a range of snow densities between 200-500kg/m^3(Bell, et al. 2008), (Gustafsson et al. 2012).

5.7.2 Calculating Snow and SWE Volumes

The total volume of snow on the pile each year was calculated using Golden Software Surfer8 and Matlab R2008b and R2012a. A triangle-based linear interpolation was used to create a mesh surface, and the volume under this surface was calculated using an integration approximation. In Surfer8 the volume was calculated as the average of the Trapezoidal Rule, Simpson's Rule, and Simpson's 3/8 Rule. In Matlab the volume of snow was calculated by discretizing the interpolated surface into a matrix of 1m by 1m cells. Each entry in the matrix is equivalent to the height of the snowpack at that point, and the volume of the snowpack can therefore be calculated by summing all of the entries. The integration schemes of both programs were checked by comparing calculated volumes to values previously determined by Ewan McCulloch (a surveyor at Diavik) using AutoCAD, and each technique produced results consistent within 3%.

The SWE of each snowpack was calculated using Equation 1. In 2010, with no density data available, the average snow density value from 2011, 2013 and 2014 was used.

$$SWE = \frac{(snowvolume)*(AverageDensity)}{1000\ kg\ (m^3)^{-1}} \quad (1)$$

Where SWE and snow volume are in m^3 and average density is in kg $(m^3)^{-1}$.

The results of the volumetric analysis are summarized in Table 5-2. An average of 3535m^3 of snow is present on the pile each spring, with only 17% of the total volume of snow overlying the basal liner. This corresponds to an average of590m^3 of snow (191m^3 SWE) of water potentially available for infiltration above the basal liner each year. In comparison, an average of 206m^3 of rainfall is estimated to infiltrate the pile each year (Table 5-1). The amount of rainfall that actually infiltrates the pile ranges between 13 to 60% of the total rainfall, and is a function of the intensity and timing of the rainfall events (Fretz, 2013). Similar to the rainfall, it is anticipated that not all of the available snowmelt will infiltrate the pile, as some will be lost to sublimation and runoff. For this reason, the melt and sublimation of the snowpack have been modelled each year. The results of this model are then used to estimate infiltration into the batters of the pile.

Table 5-2: Snowpack data from each of the spring snow surveys

Year	Mean Density of snow (kg /m^3)	Amount of Snow above Liner (m^3)	Volume SWE Above Liner (m^3)	Total volume of Snow (m^3)	Total volume of SWE (m^3)	Portion of snow above liner (%)
2010	310	430	133	2740	849	16
2011	300	570	179	3590	1077	17
2013	350	810	295	4440	1554	19
2014*	290	550	158	3370	977	16
Average	313	590	191	3535	1114	17

*The snow survey from 2014 was only analysed for volume and structure due to this paper being written in the spring and summer of 2014

5.8 Ablation of the Snowpack

The ablation of the snowpack each spring is controlled by melting and sublimation. The factors controlling melt and sublimation are discussed below, along with a description of the model used to estimate the rate and importance of each process.

5.8.1 Melting

Melting is the conversion of snow into liquid water. The rate of melting is important when calculating infiltration, as it influences the relative proportions of infiltration and runoff.

The rate of snowmelt is a function of available energy. This is often simplified to include just temperature, as melt is usually induced at around zero degrees Celsius, and temperature is the primary control on melting rates. Models based only on temperature are referred to as degree-day models (ex. Kustas et al. (1994), Hock (2003)). More complex snowmelt models incorporate both temperature and solar radiation, and are called combined temperature and radiation models (CTRMs). In general, CRTMs outperform degree day models over small domains where topographic effects dominate (ex. Kustas et al. (1994), Carzorzi and Fontana (1996)). The most complex type of model quantifies not only temperature and radiation, but also wind speed, vapour pressure, and any other factor that may be affecting snowmelt in a given location. These models are referred to as energy balance models, and only outperform the other two model types when each input parameter is precisely constrained (ex. Kane et al. (1991), Kustas et al. (1994)).

5.8.2 Creating a Melt Model for the Covered Pile

It was chosen to use a combined temperature and radiation melt model after considering the available data, the pile's small scale, and the well defined orientation of its batters. The fundamental equation used in the model is the same as that used by Carzorzi and Fontana (1996) (Equation 2).

$$If\ T \geq 0 \qquad M_{h,j} = CMF * EI_{h,j} * T \tag{2}$$

Where T is the temperature (^{0}C), M is the melt rate (mm hr^{-1}) at a given location (h,j), CMF is the combined melt factor discussed below (mm ^{o}C^{-1} EI^{-1} h^{-1}), and EI is the energy index discussed below (MJ m^{-2} d^{-1}).

Combined Melt Factor (CMF)

The CMF is a scaling factor that describes the amount of snow melt induced by a given combination of temperature and radiation. This value varies between 0.016 to 0.024 mm $^{0}C^{-1}$ EI^{-1} h^{-1} due to the decrease in albedo that occurs during snowpack maturation(Carzorzi and Fontana 1996). The snowpack at Diavik is usually a dirty grey colour (low albedo) by springtime (Figure 5-15) and a CMF value of 0.024 mm $^{0}C^{-1}$ EI^{-1} h^{-1} is therefore used in the remainder of this analysis. A sensitivity analysis was conducted that determined that the maximum impact of changing the CMF from 0.024 to 0.016 mm $^{0}C^{-1}$ EI^{-1} h^{-1} was a 3% decrease in the total amount of snow melted (rather than sublimated), and an increase of one day in total melt time.

Energy Index (EI)

The energy index term defines the amount of solar radiation received per day on a unit area of a given aspect and pitch. At a given temperature an increase in radiation will induce additional melting. The variation in the energy index is smaller than the variation in temperature during the melt season, and EI is therefore a secondary control on the rate of melting. The solar radiation received on a horizontal surface is recorded hourly at Diavik, however the EI for each batter will not be the same as that for a horizontal surface. For this reason, the radiation received on each batter was estimated in Matlab R2008b using the algorithm developed by Swift (1976). The required inputs for the algorithm are latitude, slope inclination, slope aspect, Julian day, and measured solar radiation on a horizontal plane. The results of the model are summarized in Figure 5-16. During snowmelt each year the south batter receives up to 38% more radiation than a horizontal surface. The effects on the east and west batter are much smaller, with a maximum of only 4% greater than that of a horizontal surface. The discrepancy between radiation received on the batters and on a horizontal surface decreases to a minimum at the summer solstice, when each surface receives a comparable amount of solar radiation.

5.8.3 Sublimation

Sublimation is the conversion of snow into water vapour, and is induced by a vapour pressure deficit in the air above the snow. Snow that is sublimated following the snow survey will not contribute to infiltration into the pile, and for this reason sublimation must be quantified when calculating infiltration. In this research only the sublimation that occurs in the time period between the snow survey and the completion of melt is considered.

Sublimation is a function of temperature, wind speed and solar radiation (Schulz and Jong 2004). Sublimation from a winter snowpack is largest during transport induced by strong winds (Pomeroy, Marsh and Gray 1997). Conversely, sublimation from a stationary winter snowpack, such as that observed on the covered pile during the snow survey, is very low due to a lack of available energy (low temperatures)(Kane, Gieck and Hinzman 1991). The amount of sublimation that is anticipated during springtime in the Canadian Arctic was constrained by Ohmura (1982) to be between 0.20 and 0.27mm day^{-1} at the approximate elevation of DDMI. This value refers to the time period that occurs each spring prior to the onset of melting known as the dry snow period. During melting (the wet snow period) sublimations of up to 0.82 mm day^{-1} are expected, based on the same study.

5.8.4 Creating a Sublimation Model for the Covered Pile

In a commonly used snow melt runoff model (the HBV model) the amount of sublimation that occurs from a stationary snowpack is equal to the potential evaporation of water under the same conditions (Swedish Meteorological and Hydrological Institute 2006). Potential evaporation rates were previously calculated by Fretz (2013) using the Penman Monteith formulation and the results of that research were modified for this paper to reflect the different amounts of solar radiation received on each batter.

For this research the rate of sublimation on each batter was calculated using the Penman Monteith formulation to estimate potential evaporation, with the added stipulation that below a threshold temperature sublimation occurred at a negligible rate. This assumption is based on the previously

mentioned study conducted by Kane et al. (1991) who showed that sublimation from a stationary snowpack is very low during the winter (cold temperatures) and Ohmura (1982) who showed that dry snow sublimation increased by nearly an order of magnitude between late April and early May on the arctic tundra. The threshold temperature was calibrated based on the expected rate of daily sublimation defined by Ohmura (1982), and a temperature of -4^{0}C was determined to produce the best match. The daily rate of sublimation calculated using this model averaged 0.19 mm day^{-1} during the dry snow period, and increased to 1.4 mm day^{-1} during the wet snow period (snowmelt). The dry snow value is a good match to the expected range of sublimation (0.20-0.27mm day^{-1}), however the wet snow value is outside of the expected range (<0.82 mm day^{-1}). This is due to the fact that the model does not compensate for the high relative humidity found immediately above melting snow (Ohmura, 1982). Since snowmelt occurs over a short time period each year the effects of overestimating sublimation during the wet snow period had a minimal impact on the overall performance of the model.

5.8.5 Combining the Melt and Sublimation Models

The melt and sublimation models described above were combined to create a single model to describe the overall ablation of the snowpack (Equation 3). In this model, the total ablation at a given location (h,j) over a one hour time period (t) is defined as the sum of melt and sublimation. Melting is induced when the average hourly temperature exceeds 0^o C, and sublimation is induced at a rate equal to the potential evaporation when the average hourly temperature exceeds -4^o C.

$$\begin{aligned} &If\, T \geq 0 && Ablation_{h,j}(t) = CMF * EI_{h,j} * T + S_{h,j} \\ &If -4 \leq T < 0 && Ablation_{h,j}(t) = S_{h,j} \\ &If\, T < -4 && Ablation_{h,j}(t) = 0 \end{aligned} \quad (3)$$

Where T is the temperature (^{o}C), CMF is the combined melt factor (mm ^{o}C^{-1} EI^{-1}), EI is the energy index (MJ m^{-2} d^{-1}), and S is the sublimation (mm).

5.9 Creating the Snow Ablation Model

The surface of the snowpack that was measured each year was modelled as a grid, with each entry corresponding to the height of snow in a 1 x 1m square. Matlab R2008b was used to solve equation 3 for each square over sequential one hour time steps. The model required hourly inputs of radiation, potential sublimation, and temperature for each entry in the grid, and modelled the ablation of the snowpack as a function of these parameters. Locations that did not have any snow cover in the preceding time step were not included in the calculations. The volume of snowpack ablation each hour was calculated as the difference between the snow volume at the end of the preceding and current time steps.

5.9.1 Snowfall Occurring After the Model is Initiated

In each of the four years additional snow fell on the covered pile after the snow survey was conducted. It is anticipated that a portion of this snowfall will remain on the batters of the pile, while the remainder will be transported away from the pile by wind. The percentage of a given snowfall that remains on the pile and overlays the basal liner has not been quantified; however, studies conducted in similar environments suggest that it is likely between 30 and 85% (Pomeroy, Marsh and Gray 1997). Based on these studies, it is assumed that 50% of all the snowfall that occurred after the snow survey was conducted remained on the batters of the covered pile overlying the basal liner. This snow was added to the model on the day when it occurred. No accumulation is expected to remain on the crest of the pile, based on in field observations made by Fretz (2013) and Krentz (this thesis).

5.9.2 Results from the Snow Ablation Model

The results from the snow ablation model are summarized in Table 5-2 and Figures 5-17, 5-18 and 5-19. The SWE available at the time of the snow survey ranges from 133 to 295m^3 depending on the year. Snow that fell after the snow survey adds 10-49m^3 of SWE onto the pile, which corresponds to an additional 6-36% of the total snow. Melting was initiated in May each year, and the snowpack above the liner is estimated to be completely ablated within 6 to 15 days following the onset of melting.

Similar melt rates were modelled each year, and the variability in total melt time was primarily a function of the amount of snow available. The thicker snowpack that exists at the base of the pile will take much longer to ablate completely; however, this was not modelled as snow that does not overly the basal liner is not anticipated to contribute to flow collected from the pile. Once melt was initiated in 2010 and 2011 there was no more than one day in a row where melt did not occur. In 2013 there was a single day of melt which occurred 13 days prior to onset of continuous melting (not included in Table 5-2).

The rate of melting influences the amount of infiltration and runoff that is expected to occur, and for this reason the peak melt rate predicted by the model each year is included in Table 5-3.

Table 5-3: Results from the melt model.

Year	Snow at Survey (m^3 SWE)	Additional Spring Snow (m^3 SWE)	Total Snow (m^3 SWE)	Sub* (%)	Total Melt (m^3)	Melt Period (Date)	Calculated Peak Melt Rate (mm/hr)
2010	133	48	181	30	127	26-31 May	9
2011	179	10	189	16	159	6-15 May	4
2013	295	49	344	13	299	17-31 May	6
Average	202	36	238	20	195	16-26 May	6

* Sublimation

5.10 Snowmelt Infiltration

It is anticipated that infiltration of snowmelt into the matrix material of the covered pile will be limited by the presence of ice that constricts or blocks flow pathways (Granger, Gray and Dyck 1984). The infiltration of snowmelt into the matrix of the pile is not recorded by the TDRs, ECH_2O probes or tensiometers installed in the pile, as these only output accurate measurements when the pile is thawed. Instead, infiltration of snowmelt into the matrix of the pile was modelled for this research using a parametric equation developed by Gray et al. (2001) to describe the infiltration of melt water into unsaturated, frozen mineral soils. In the classification scheme used by Gray et al. (2001) unsaturated

soils where flow is controlled by capillarity are referred to as 'limited' soils, due to their limited ability to infiltrate melt water.

It is anticipated that infiltration that occurs through macropores in the cover will be small in comparison to infiltration through the matrix. This is based on the results of the rhodamine test discussed in Section 5.5.3 (Figure 5-10), and the peak melt rates predicted in Table 5-3. Macropore flow that does occur will be directed away from the basal liner by the frozen till layer, as pore water cannot be held in storage without capillarity and the till is not expected to have persistent macropore pathways.

5.10.1 Storage Capacity of the Type I Layer

Since the frozen till layer is anticipated to act as a barrier to flow, infiltration of melt water into this layer is not anticipated until after the till thaws. The maximum amount of water that can infiltrate and be held in storage is therefore a function of the available air filled porosity in the matrix of the type I material. Gray et al (1986) demonstrated that the storage capacity of a frozen limited soil is lower than that of the same soil when it is unfrozen due to ice blocking the interconnectivity of pores in the material. On average, that study determined that the water storage potential of a frozen limited soil was approximately 60% of the total air filled porosity (Equation 4).

$$W_{SP} = 0.6 * \emptyset(1 - S_1)Z_p \quad (4)$$

Where W_{SP} is the water storage potential (m), $\emptyset$ is the porosity (-), S_1 is the initial saturation of the soil above, and Z_P is the depth of the type I material (m).

Janowicz et al. (2002) determined that the initial saturation term in Equation 4 can be represented by the pre-freeze-up soil moisture. The initial saturation of the type I material each year was therefore estimated using the soil tension measurements taken in the preceding autumn, which showed that each year the initial saturation of the material was approximately 0.6. Taken over the 3m depth of the type I material this equates to a W_{sp} of 36mm available for infiltration.

5.10.2 Parametric Infiltration Model for the Covered Pile

Zhao and Grey (1999) and Grey et al. (2001) utilized the results from two and a half decades of field research conducted at the University of Saskatchewan to develop a parametric equation describing the infiltration of snowmelt into frozen soils with limited infiltration capacity (Equation 5). This equation is based on research conducted in prairie, boreal forest, arctic and alpine environments and in general applies independently of soil texture. The factors affecting infiltration into limited soils include the surface saturation during melting (assumed to be 1), the initial soil saturation (described above), the initial soil temperature and the infiltration opportunity time. The equation developed by Zhao and Gray (1999) and Gray et al. (2001) is a refinement of equations presented previously by Zhao and Gray (1997), and is partially based on work conducted by Granger et al (1984) and Gray et al. (1985).

$$INF = C_1 S_0^{2.92} * (1 - S_1)^{1.64} * (\frac{273.15 - T_1}{273.15})^{-0.45} * t_0^{0.44} \quad (5)$$

where INF is the cumulative infiltration (mm), C_1 is a scaling parameter (1.14 mm $hr^{-0.44}$), S_o is surface saturation (unitless), S_1 is average soil saturation at the start of infiltration (unitless), T_1 is the average temperature of the soil being infiltrated at the start of melting (^oC), and t_o is the average infiltration opportunity time (hr).

A temperature profile of the pile is shown in Figure 5-20 a-b (Pham 2014). Based on these figures a temperature of -1^0C was used in the parametric equation each year. The infiltration opportunity time was defined by the melt model, and ranges between 47 hours in 2010 to 240 hours in 2013.

5.10.3 Results of the Infiltration Model

A plot of cumulative infiltration into the batters of the covered pile versus infiltration opportunity time is shown in Figure 5-21. The estimated amount of infiltration of snowmelt into the matrix for 2010, 2011 and 2013 is shown in Table 5-4. The percentage of the total available melt water that infiltrated the matrix of the pile ranged from 51-72% over the three years. Between 55 and 97% of the available

matric storage in the TI material was used, depending on the year. It is anticipated that the majority of the remaining melt water was removed through localised overland flow on the batters of the pile. Some of this flow is anticipated to have occurred underneath the snowpack, and as such would not have been observed. The infiltration model that was used defines a maximum frozen infiltration rate of 3mm hr^{-1}, which means that any melt rate that exceeds 3mm hr^{-1} is anticipated to induce overland flow. Based on the snowmelt and infiltration models, the type I material in the covered pile is anticipated to receive between 22 and 54% of its total annual recharge from snowmelt. The variation in this value is due to the different rain and snowfall amounts observed each year at DDMI.

Table 5-4: Infiltration of snowmelt into the matrix

Year	t_o (hr)	Water Available For Infiltration (mm)	Modelled infiltration (mm)	Modelled Infiltration (% of total available)	W_{SP} Used(%)	Estimated Infiltration of Snowmelt (m3)	Estimated Infiltration of Rainfall (m3)	Estimated Recharge from snowmelt (%)
2010	47	29	18	62	55	79	198	29
2011	120	36	26	72	75	114	416	22
2013	240	69	35	51	97	152	129	54
Average	136	45	26	62	76	115	248	35

5.11 Five Year Water Balance

The water balance for the covered pile was calculated using Equation 6 to assess the results of the modeling.

$$E_B + \Delta S = I_R + I_S \quad (6)$$

Where E_B is the basal effluent (m^3), ΔS is the change in storage (m^3), I_R is the infiltration of rainfall and I_s is the infiltration of snowmelt (m^3).

In this equation it is assumed that all of the water that infiltrates into the matrix of the type I material eventually passes through the till layer and remains above the basal liner until is collected by the basal

drain and accounted for as outflow. Storage of water asmulti-year ice is not considered, as the pile thawed completely each year prior to 2011 (Figure 5-5). Storage of pore water within void spaces is also not considered, as this water will either enter the matrix material or be collected by the basal drain relatively quickly.

As mentioned previously, determining a single year water balance for the pile is not practical due to the very large potential change in pore water storage within the pile each year. Over the five year period between 2007 and 2011 storage in the pile attained a pseudo-steady state, and each parameter in Equation 6 has a similar magnitude. Snow surveys were not taken in 2007, 2008 or 2009, and for this reason the average estimated snowmelt infiltration from Table 5-4 is used in the water balance for these years ($115 m^3$). It is acknowledged that this introduces uncertainty into the water balance, as the infiltration of snowmelt varies each year; however, this approximation is necessary to close the water balance for the pile. The estimated infiltration of rainfall and snowmelt, along with the measured outflow collected from the pile each year is shown in Table 5-5. The change in storage between 2007 and 2013 was measured using the tensiometers, ECH_2O probes and TDR sensors in the pile, and is presented in the final column of Table 5-5. Using this approximation the water balance closes over the five year period, which suggests that the calculated volumes of rainfall and snowmelt infiltration are reasonable.

Table 5-5: Five year water balance for the covered pile.

Year	Infiltration Rainfall (Estimated) (m^3)	Infiltration Snowmelt (Estimated) (m^3)	Outflow (Measured) (m^3)	Change in Storage (Measured) (m^3)
2007	198	115	2	
2008	436	115	30	
2009	55	115	46	
2010	198	79	110	
2011	416	114	195	
Total	**1303**	**538**	**383**	**1458**

5.12 Conclusions

Four years of snow data from a covered waste rock pile at Diavik Diamond mine are analysed in this paper. The snowpack that was measured each year had a consistent spatial distribution, with the thickest snow being located at the base of the pile and only 17% of the total snowpack overlying the basal liner. Only the portion of the snowpack that overlies the basal liner was considered in the remainder of the analysis. Melting of the snowpack was initiated in May each year and complete melting of the snow above the liner took between 6 and 15 days. In the time period between the snow survey being taken and the complete ablation of the snowpackapproximately 13 to 30% of the snowpack was sublimated each year. The volume of melt water that infiltrated the matrix of the pile was modelled as a function of potential infiltration time, and is estimated to range from between 51 to 72% of the total melt water. The majority of the remaining water is anticipated to be lost to overland flow. In 2010, 2011 and 2013 between 22 and 54% of the total recharge received by the pile is estimated to have been derived from snowmelt. The importance of snowmelt to the total recharge received by the pile is a function of the snow available for melting, the length of the melt period and the total annual infiltration of rainfall. A five year water balance for the pile was closed using the modeled volumes of snowmelt infiltration, and showed that the estimates of rain and snowfall infiltration presented in this paper are reasonable.

5.13 Figures for Chapter 5

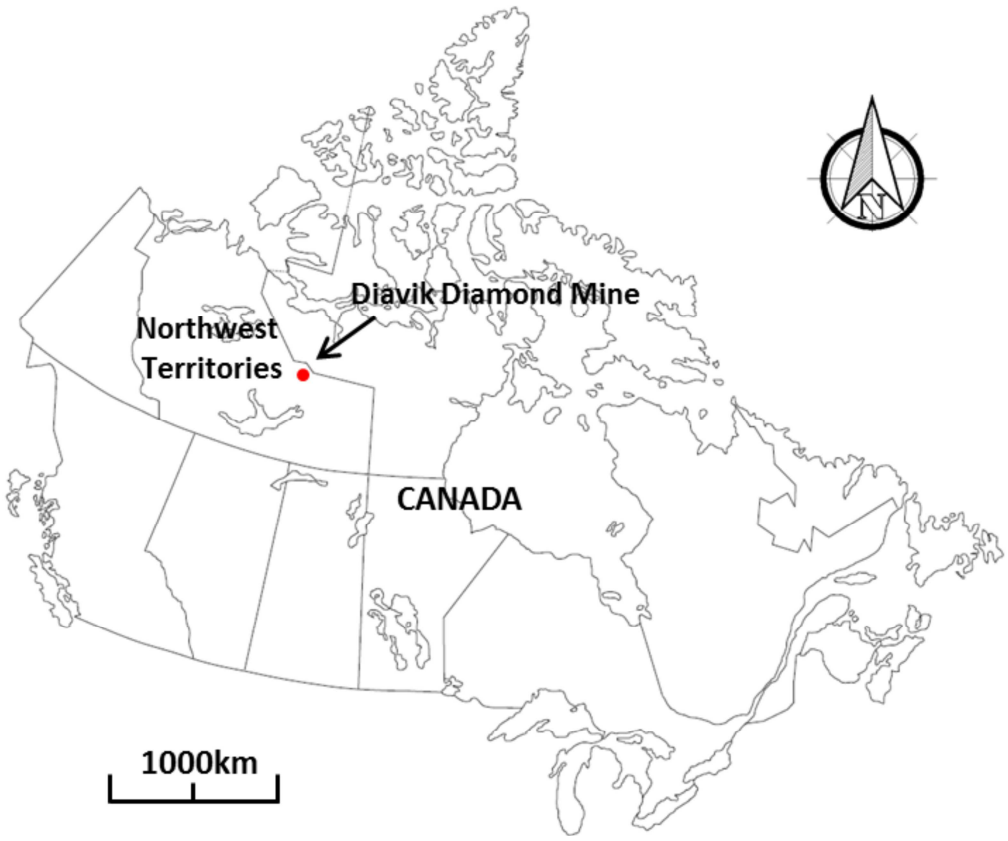

Figure 5-1: Location of Diavik Diamond Mine. Image from Fretz (2013)

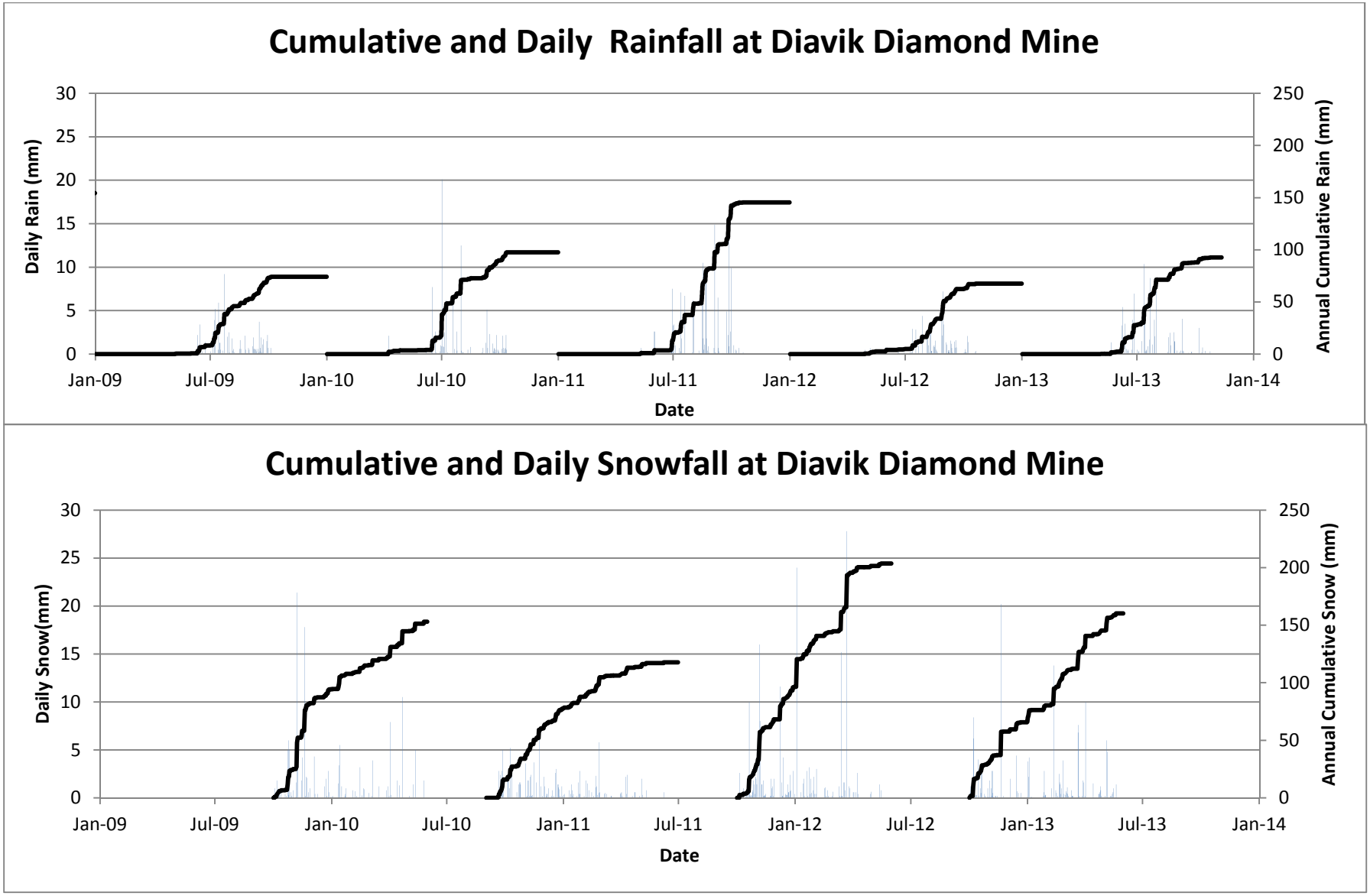

Figure 5-2: Daily and cumulative annual precipitation at Diavik

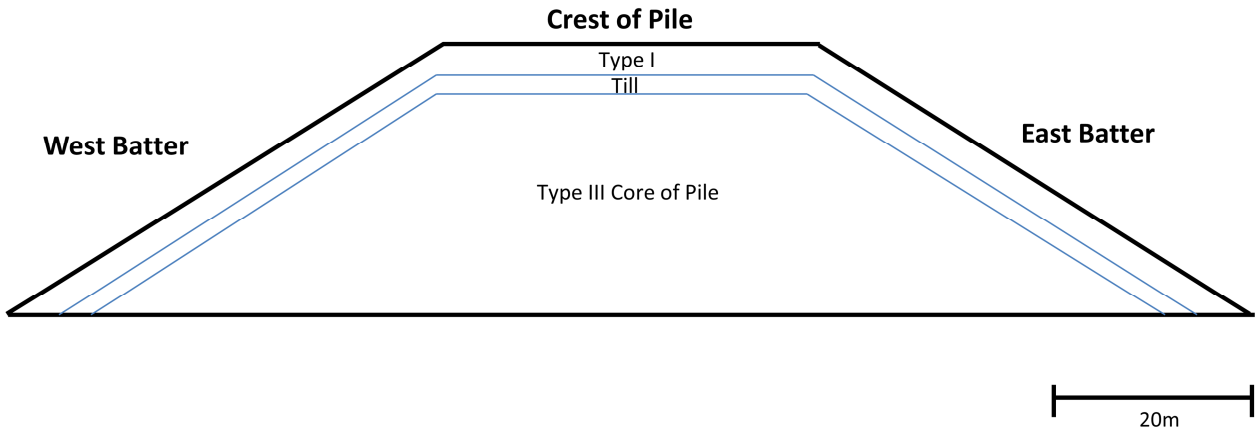

Figure 5-3: Schematic cross section of the covered pile.

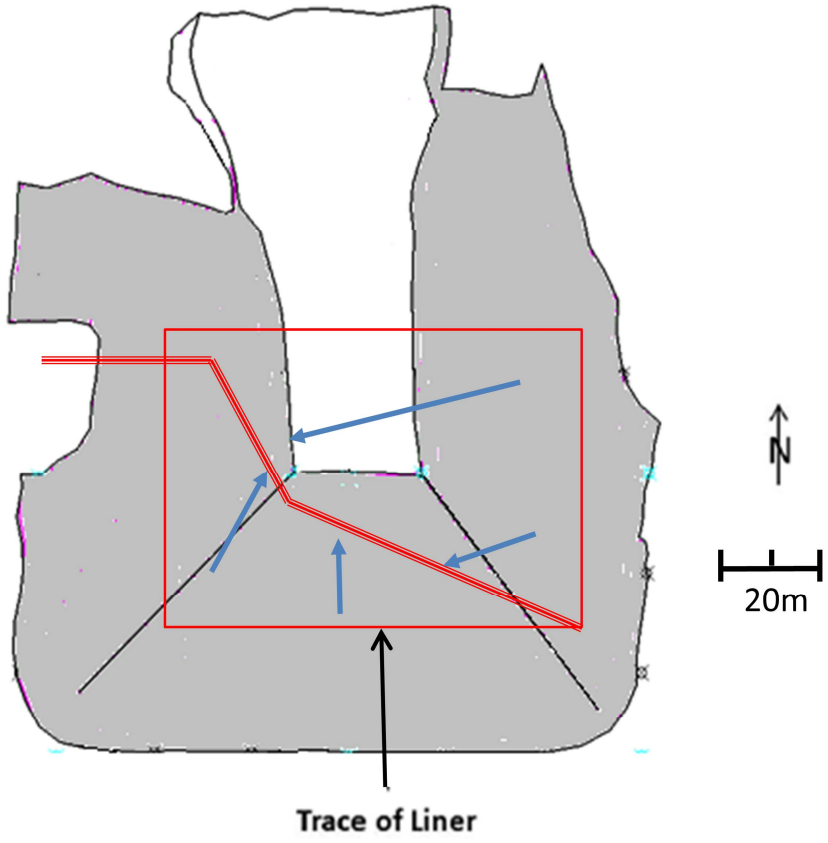

Figure 5-4: Schematic of the covered pile drainage scheme

The batters are grey, the crest is white, and the basal liner is shown by the red rectangle. The thick diagonal red line shows the basal drain, and the blue arrows show the intended direction of flow along the basal liner.

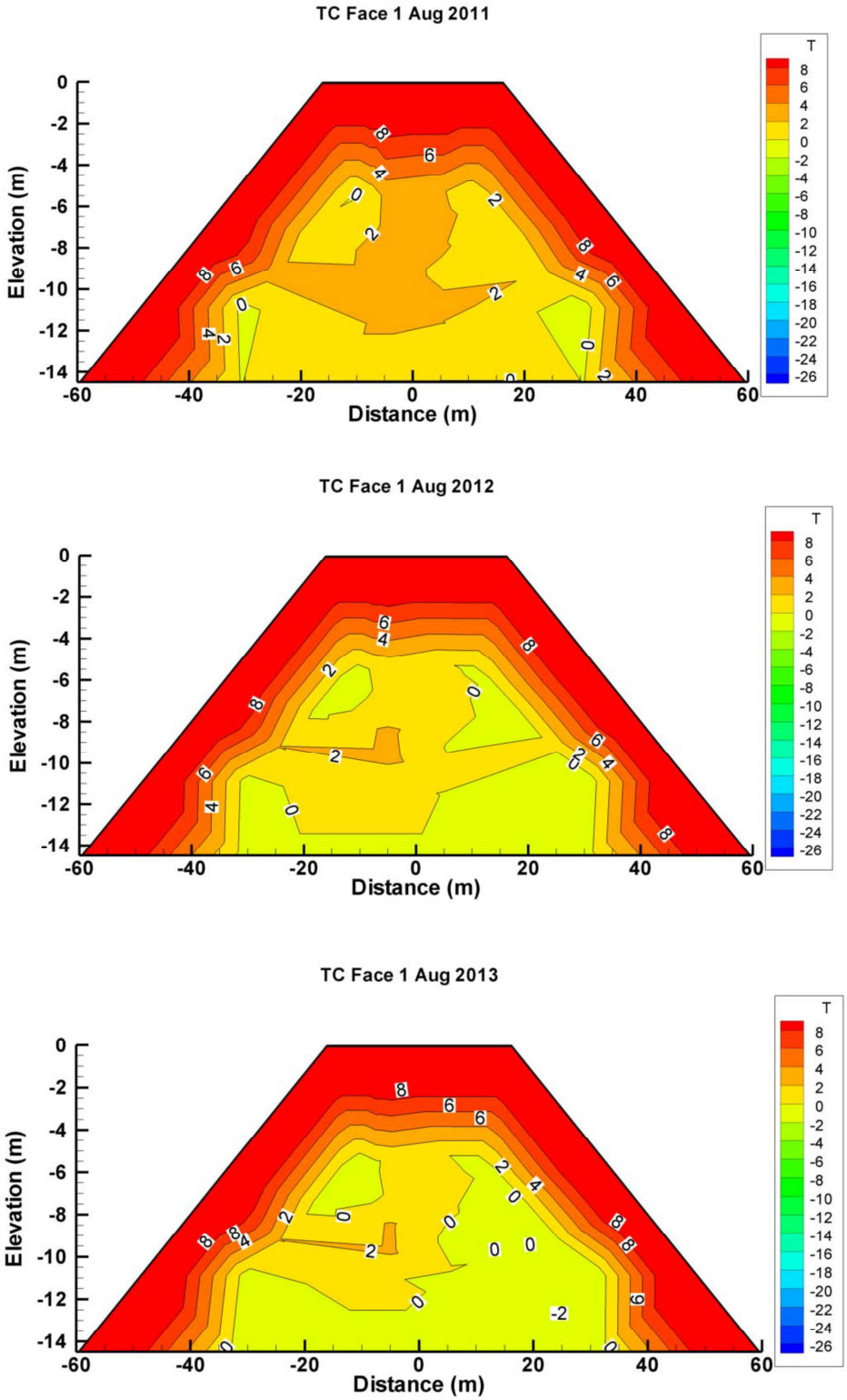

Figure 5-5: Thermal profile of the covered pile

Between 2011 and 2013 the core of the pile cooled, and now much of the base of the pile remains frozen year round

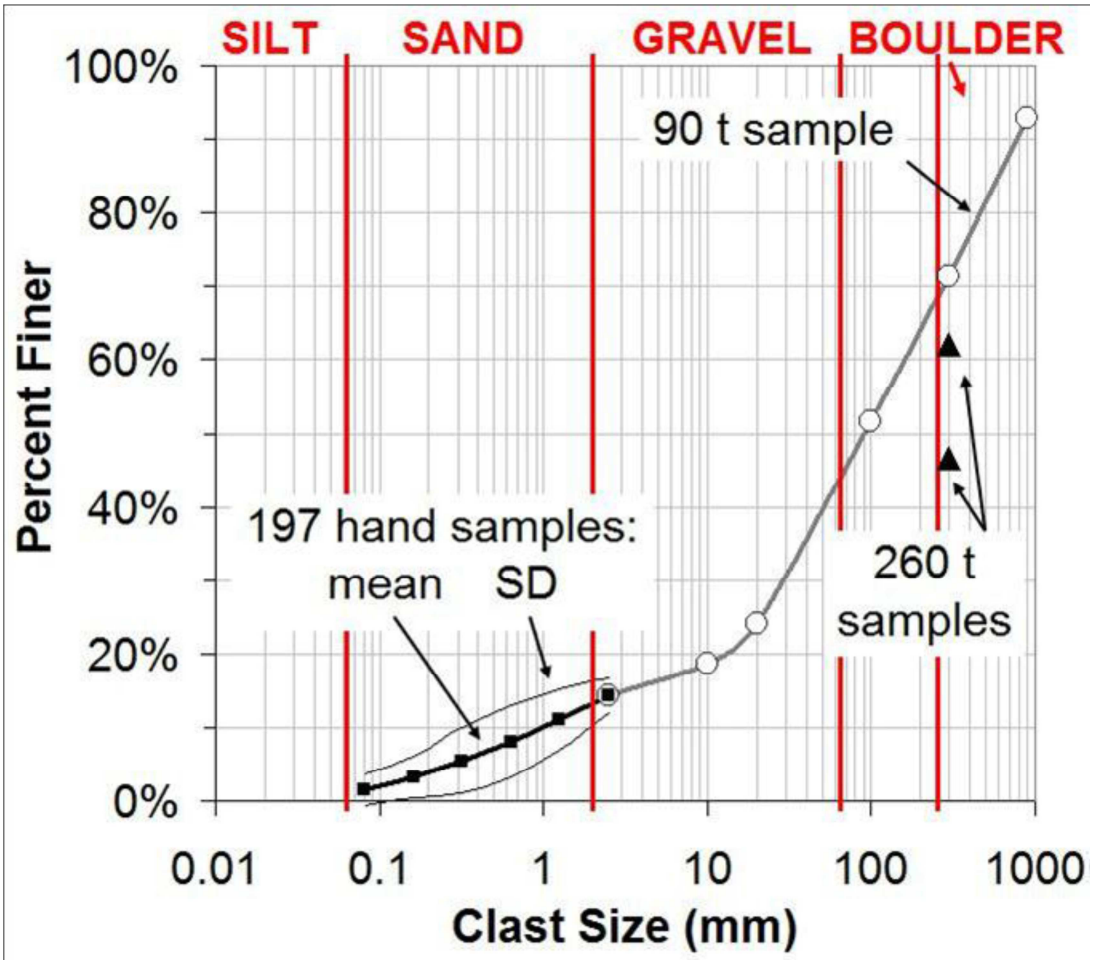

Figure 5-6: Grain size distribution of the waste rock piles. Image from Neuner (2009)

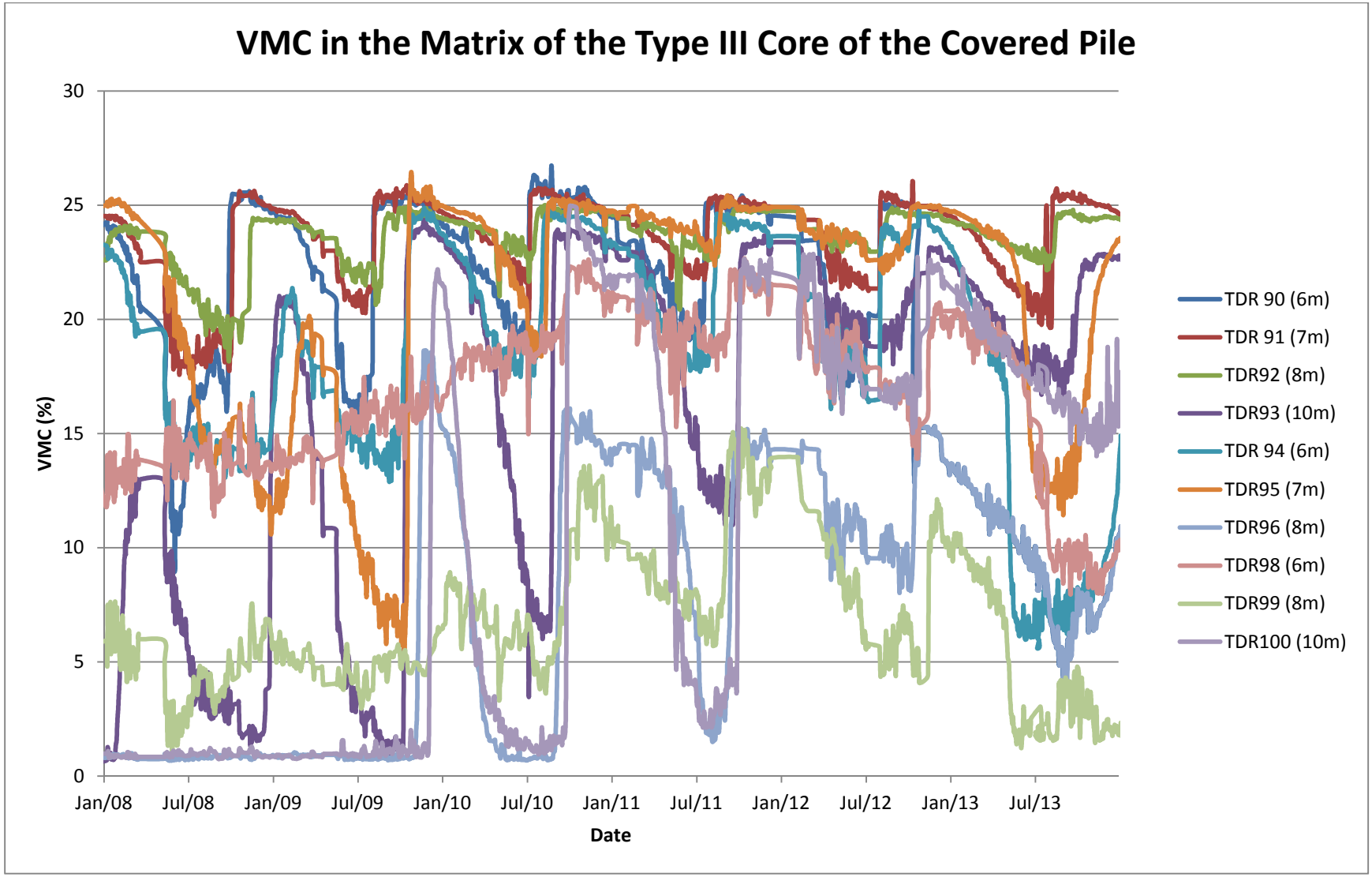

Figure 5-7: Volumetric moisture contents measured by TDR probes in the covered pile.

Note the effects of freezing and thawing as described in the write up. Image from Fretz (2013)

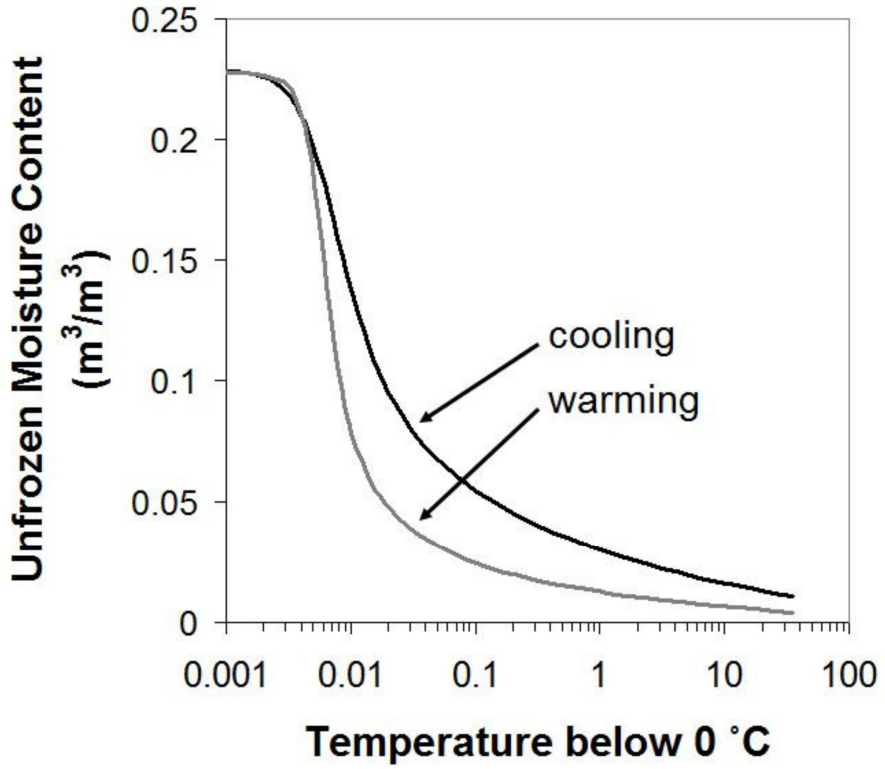

Figure 5-8: The estimated portion of moisture in the matrix material that remains liquid at below freezing temperatures due to capillary forces

Image from Neuner (2009)

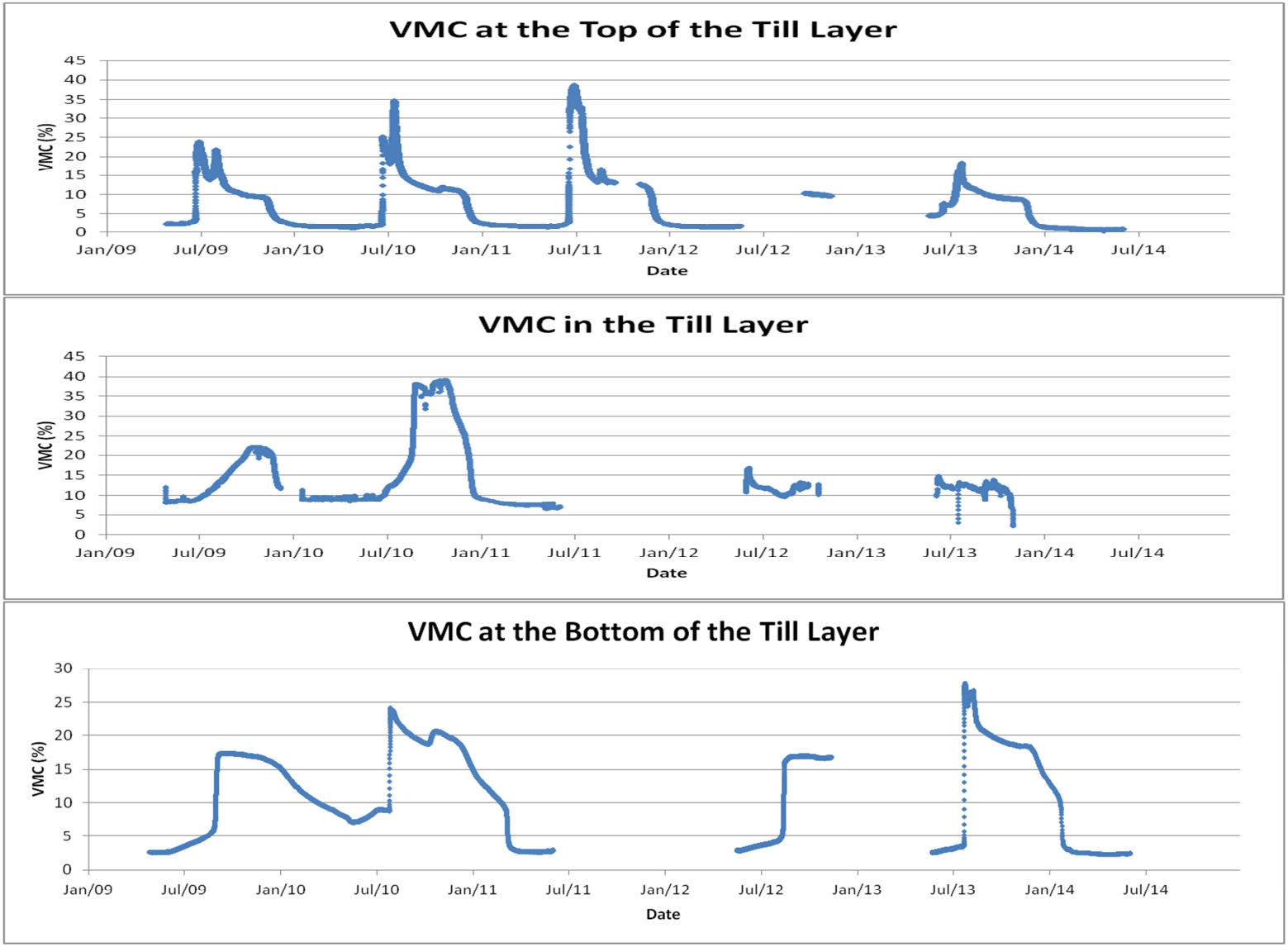

Figure 5-9 a-c: Volumetric moisture contents measured by ECH2O probes in the till

Figure 5-10: A rhodamine tracer test conducted on the east batter of the covered pile.

The results of this excavation showed that flow primarily occurs on a vertical direction in the type I material on the covered pile

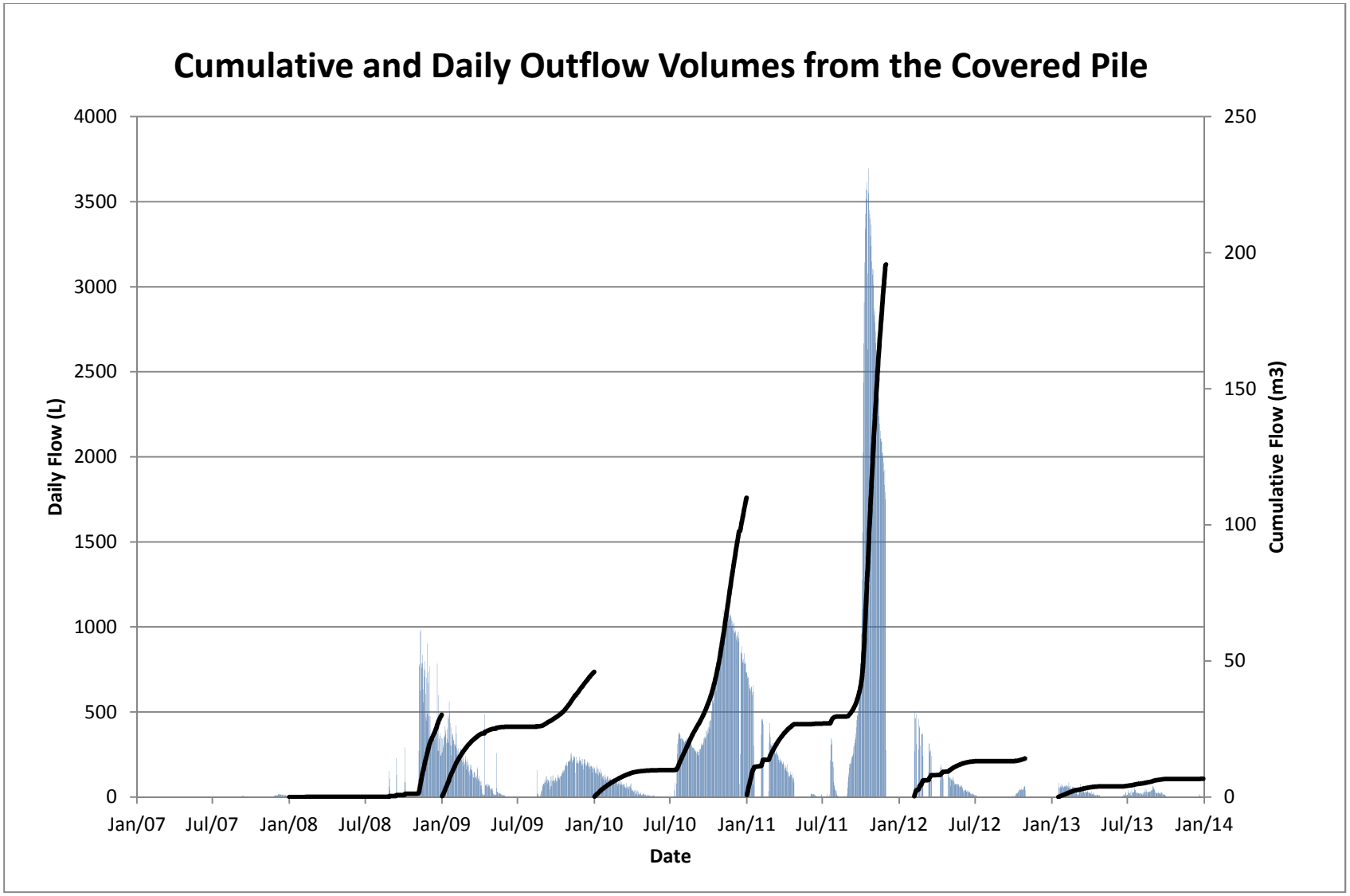

Figure 5-11: Daily and cumulative outflow volumes measured at the covered pile basal drain

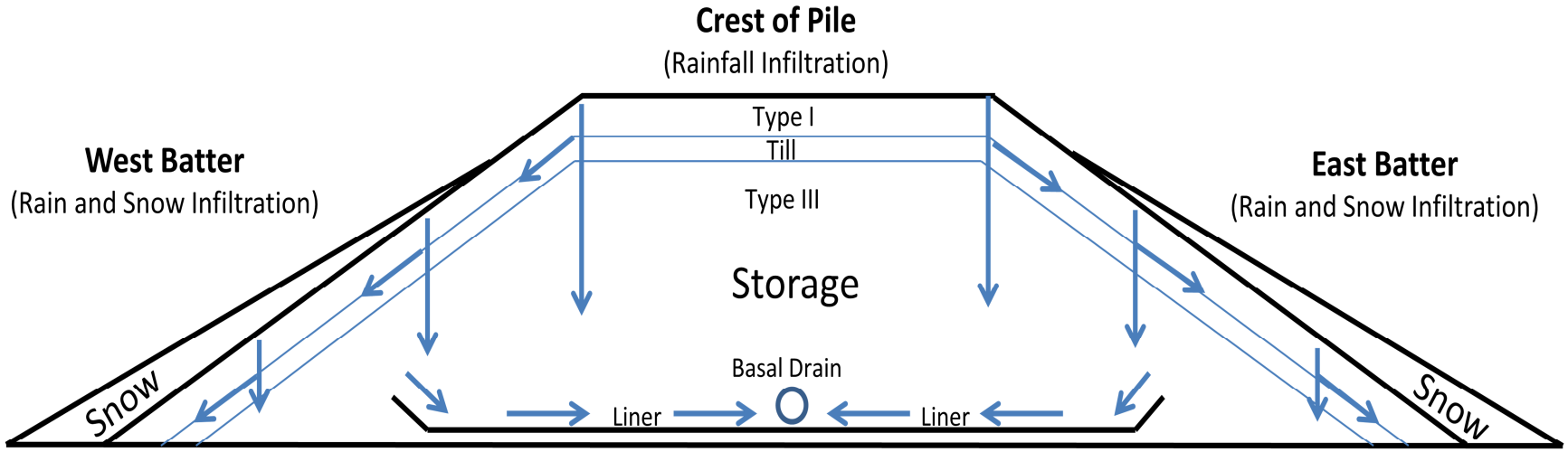

Figure 5-12: Schematic of the infiltration, internal flow and storage in the matrix of the covered pile.

Infiltration through the till layer is anticipated to be the greatest during times when the till is thawed. This figure assumes that the core of the pile is thawed, which allows for internal flow. When the core of the pile is completely frozen internal flow through the basal drain is terminated.

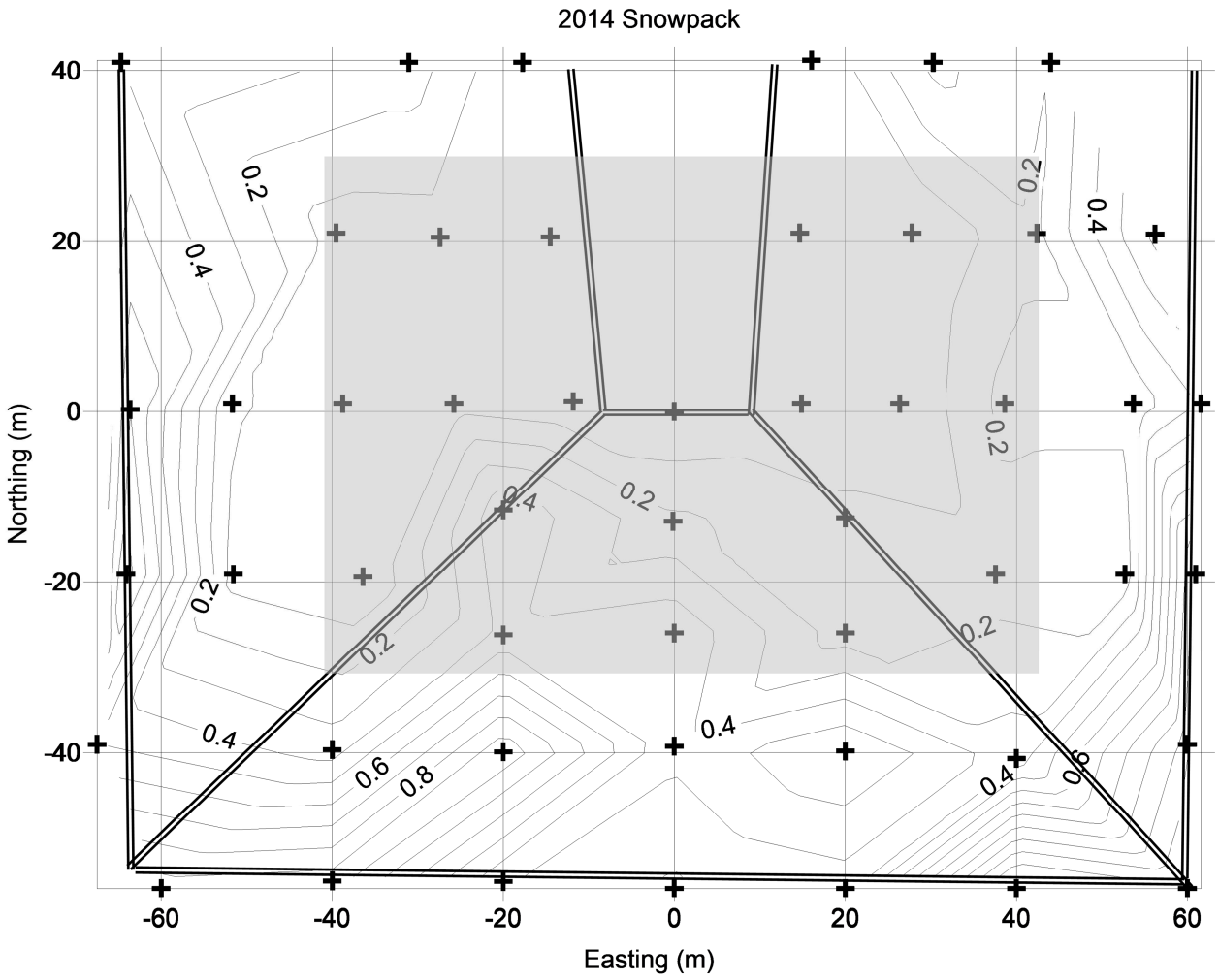

Figure 5-13: Snowpack contours on April 8, 2014.

The double lines show the crest and batters of the pile, while the grey rectangle shows the extent of the basal liner. The survey points are shown as black crosses.

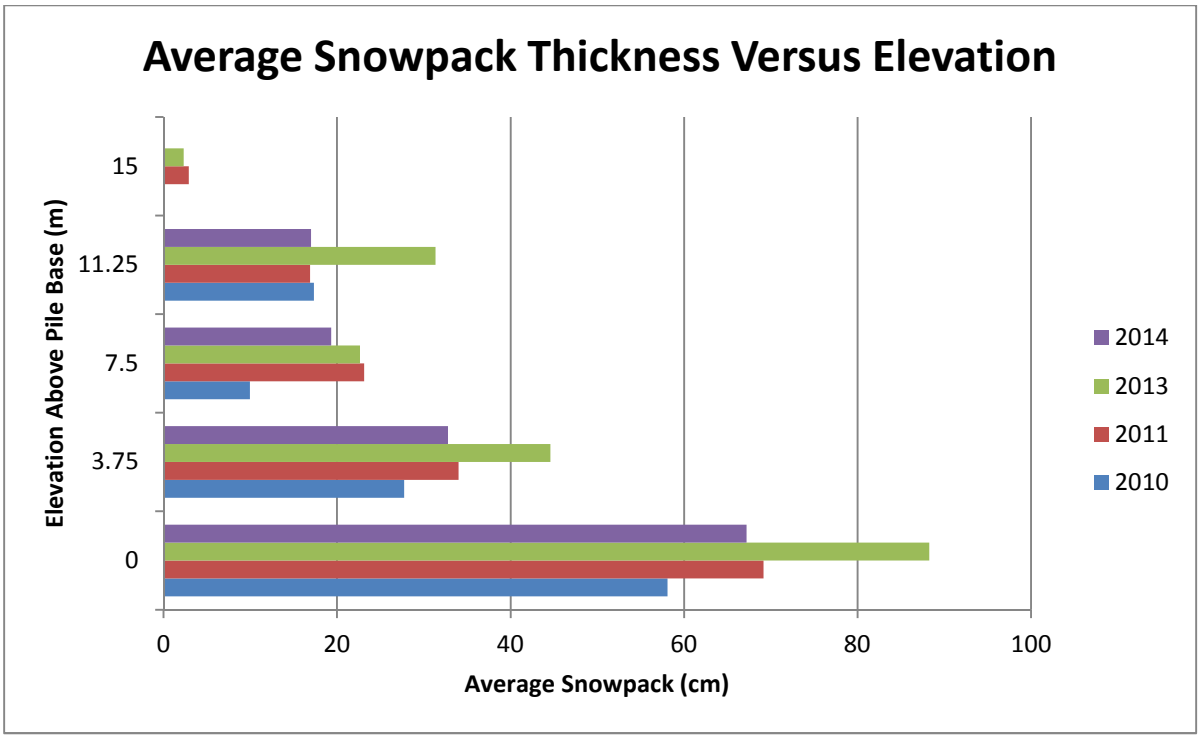

Figure 5-14: Average snowpack thickness versus elevation on the covered pile

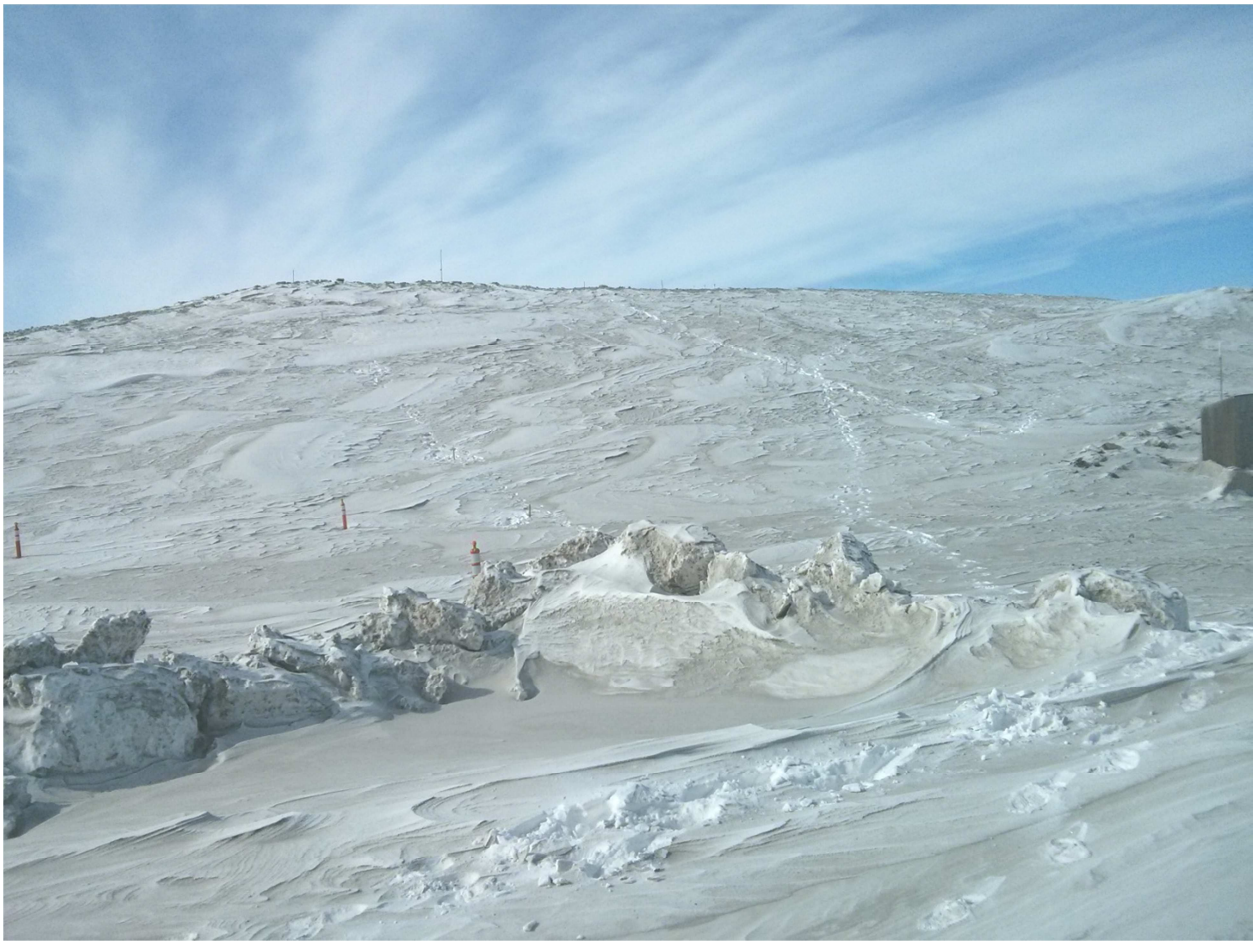

Figure 5-15: Dirty grey snowpack on the eastern batter of the covered pile.

Photo taken on April 10, 2014.

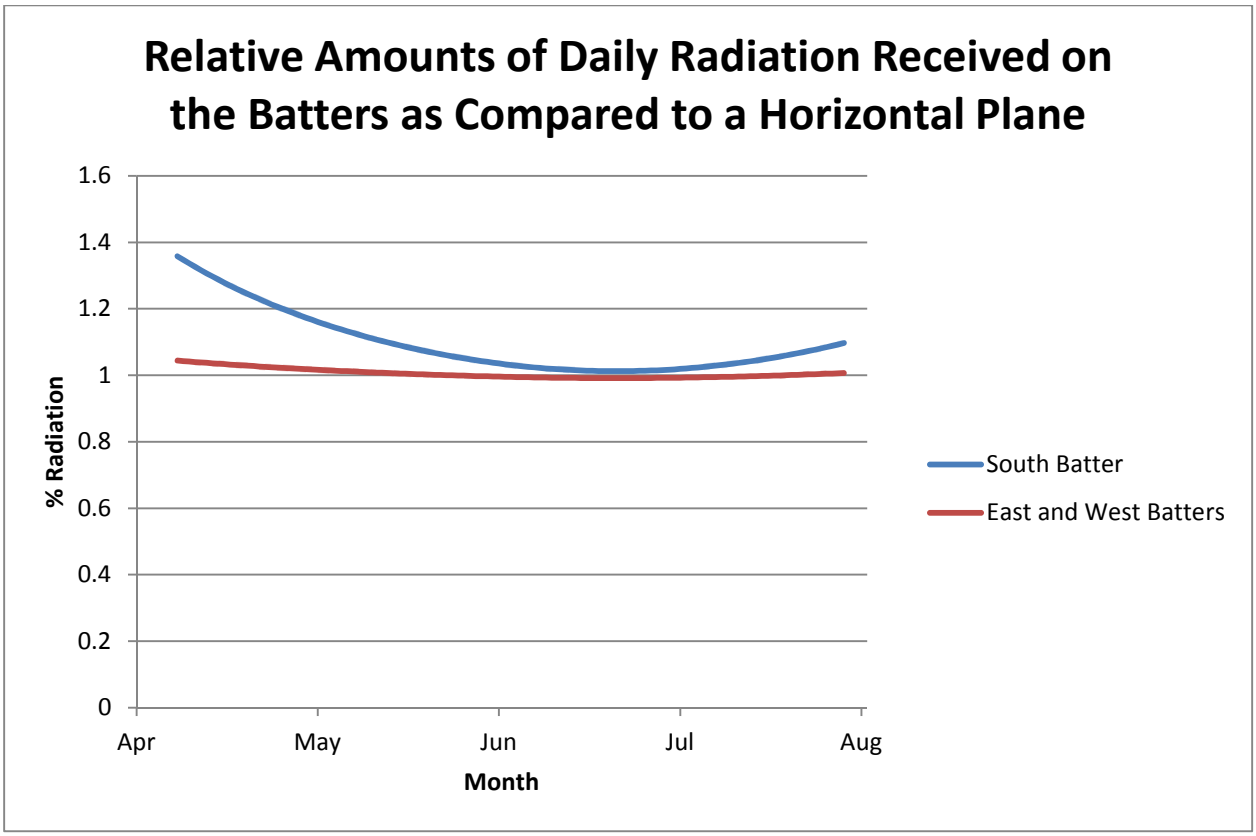

Figure 5-16: The daily radiation received on each of the batters, expressed as a percentage of the radiation received on a horizontal plane

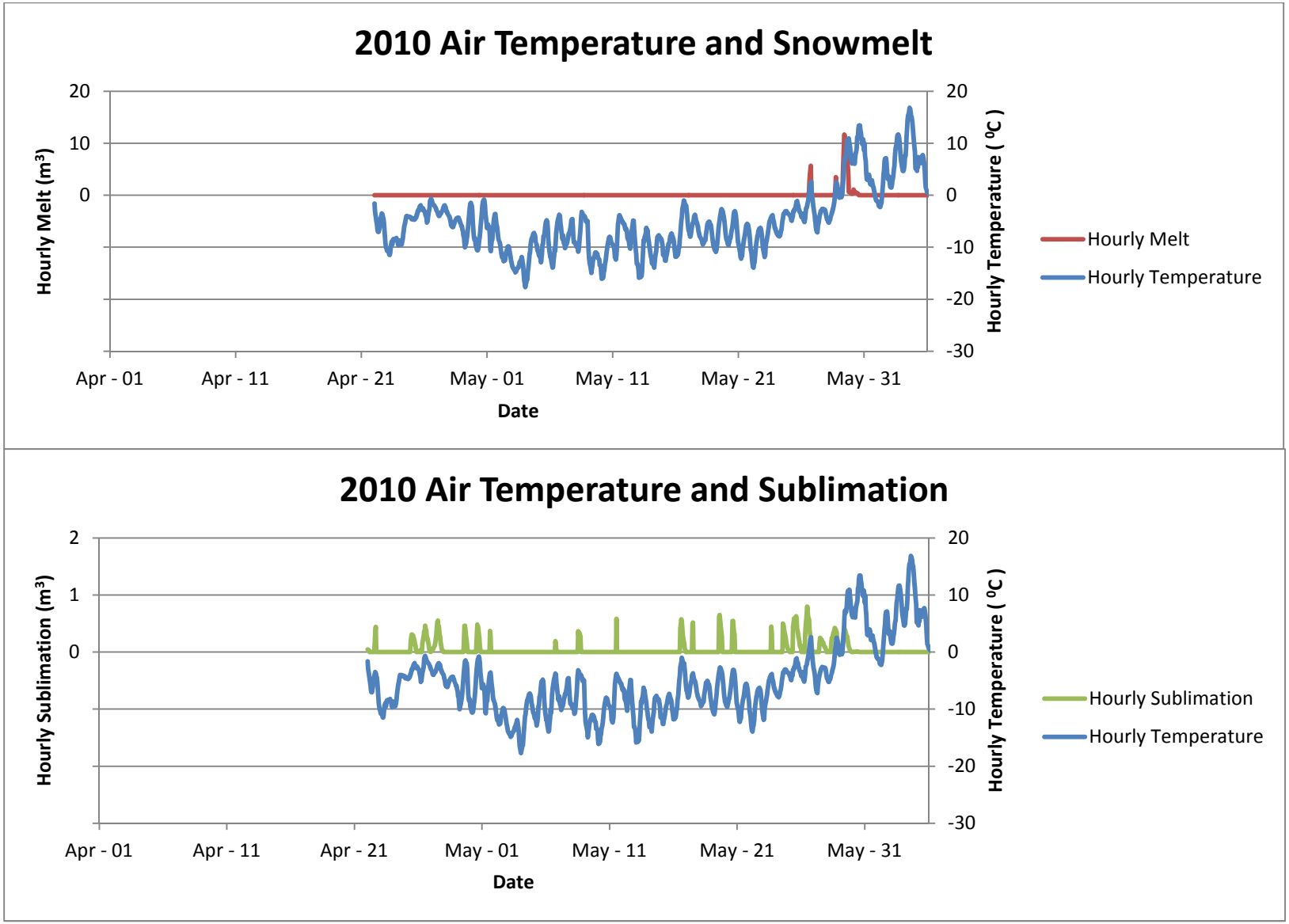

Figure 5-17: Hourly Temperature, melt and sublimation on the covered pile in 2010

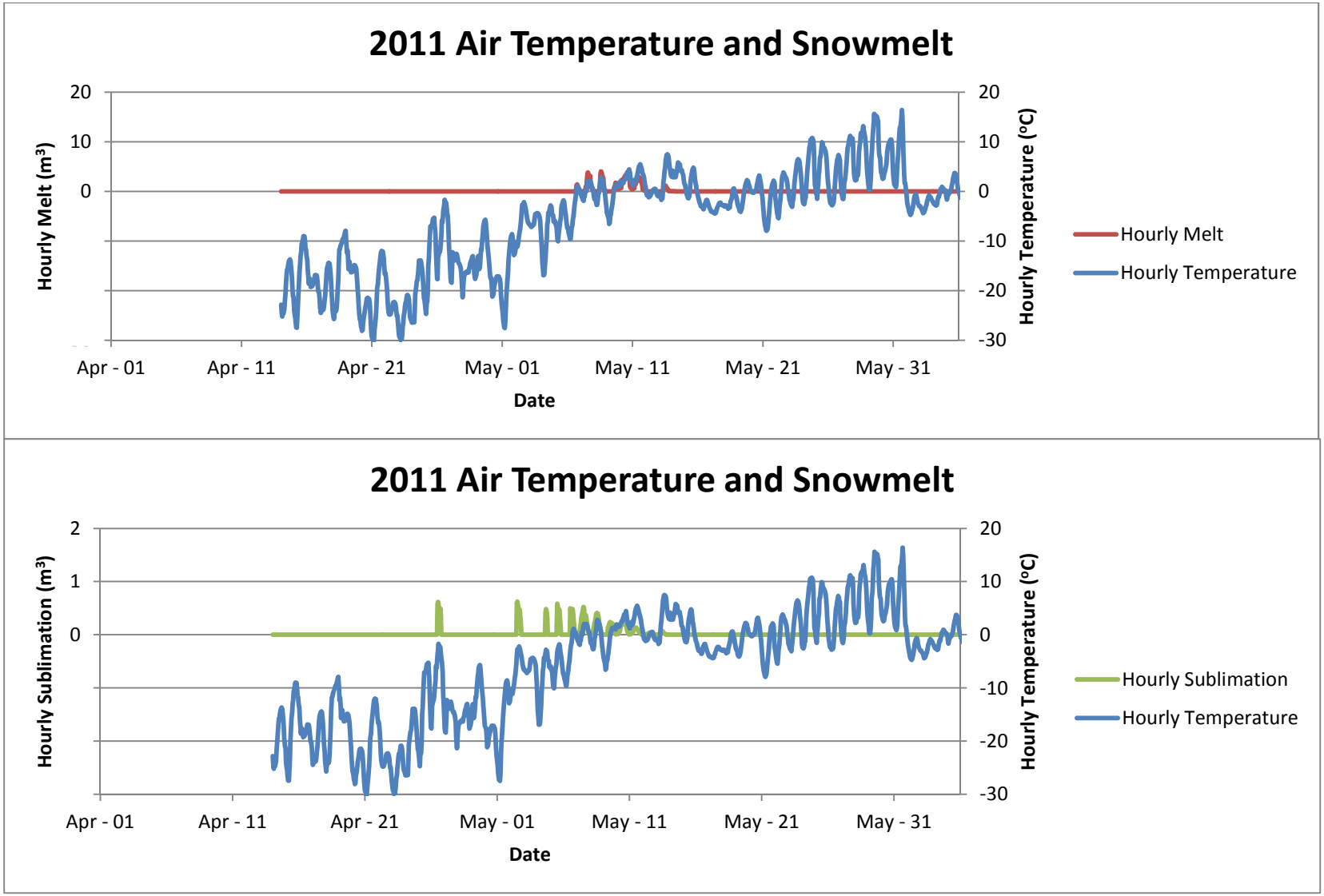

Figure 5-18: Hourly Temperature, melt and sublimation on the covered pile in 2011.

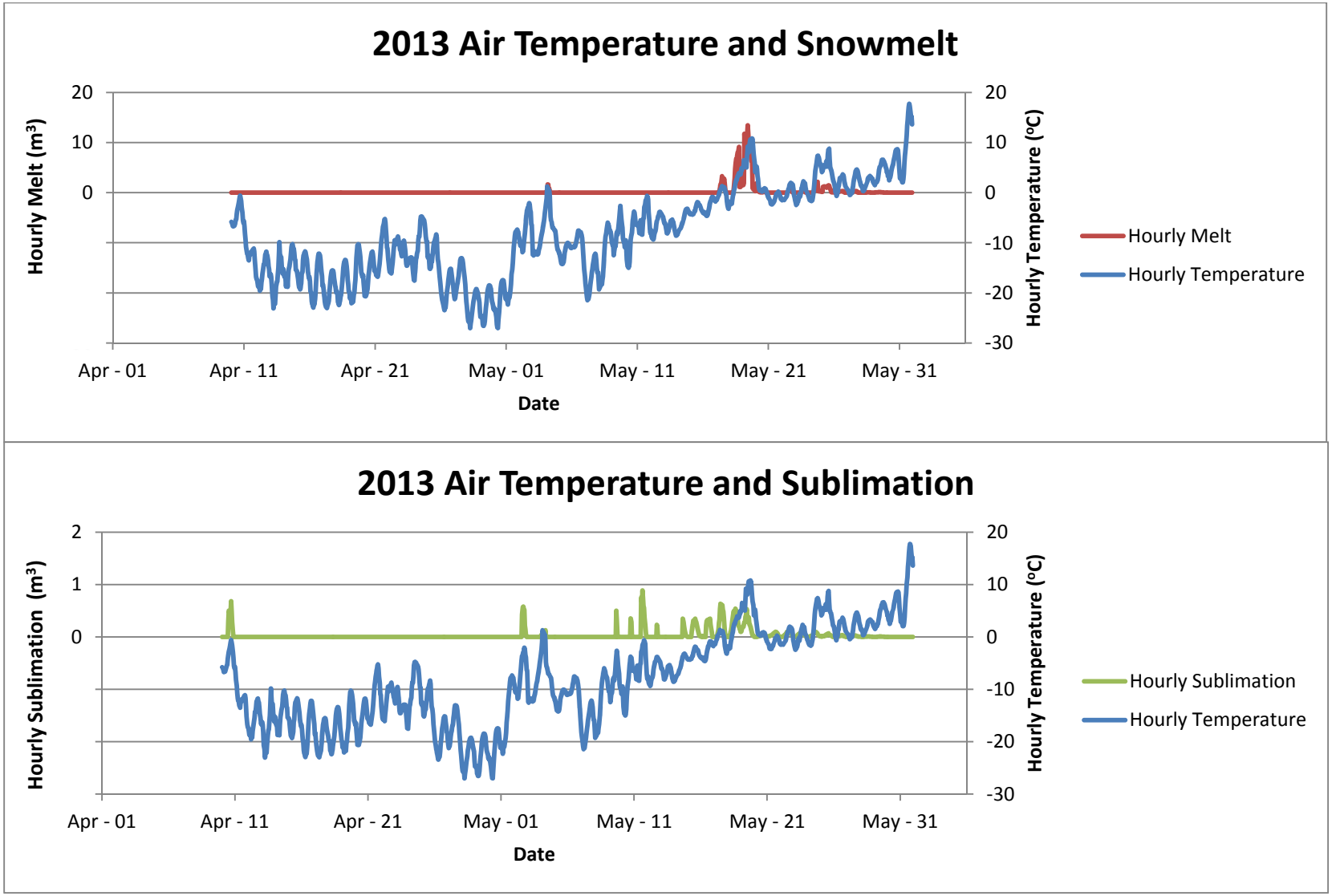

Figure 5-19: Hourly Temperature, melt and sublimation on the covered pile in 2013.

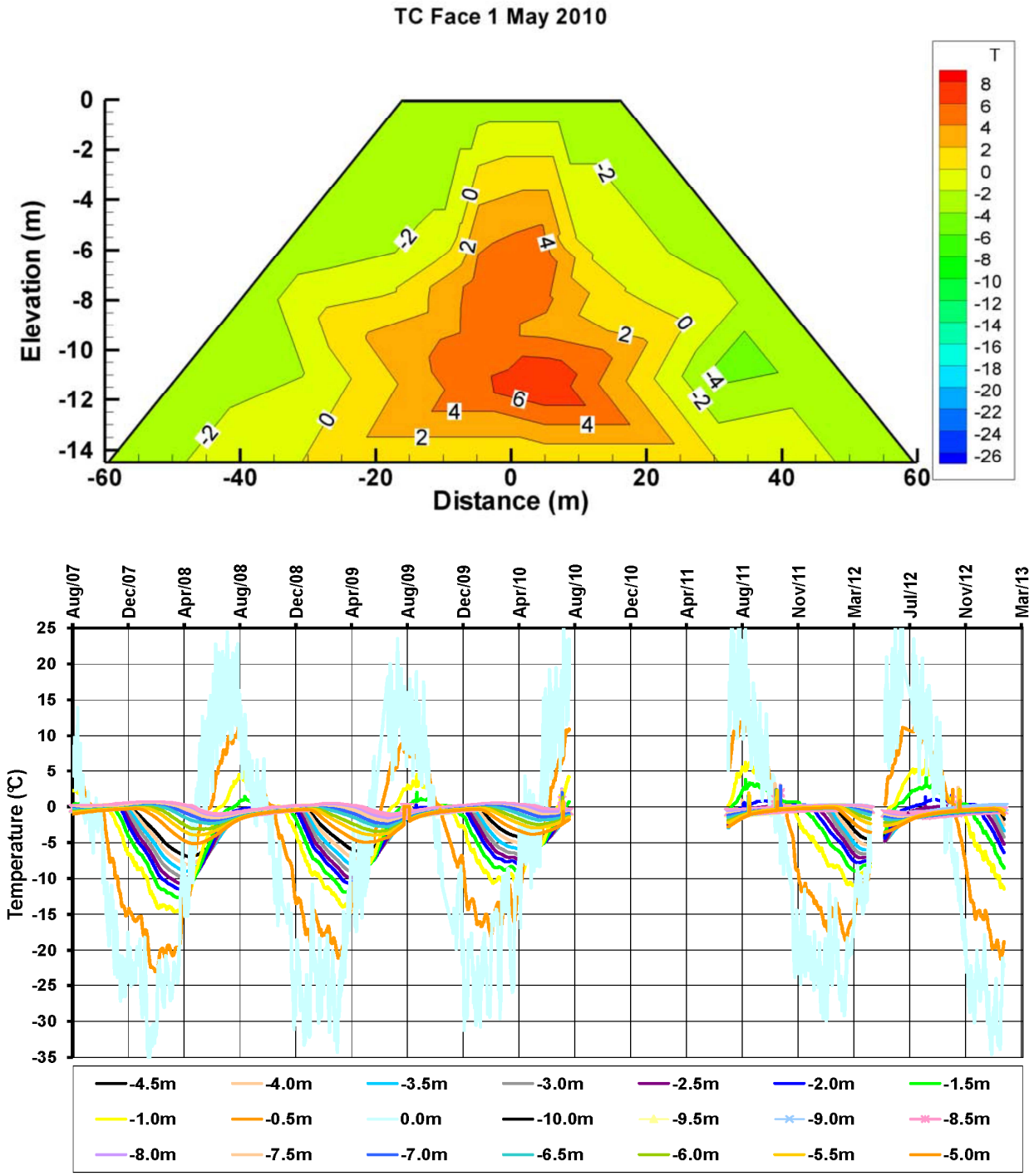

Figure 5-20 a-b: Temperatures in the covered pile. Images from Pham (2014).

a) Temperature profile of the covered pile on May 15, 2010.

b) Temperatures recorded at different depths in the covered pile.

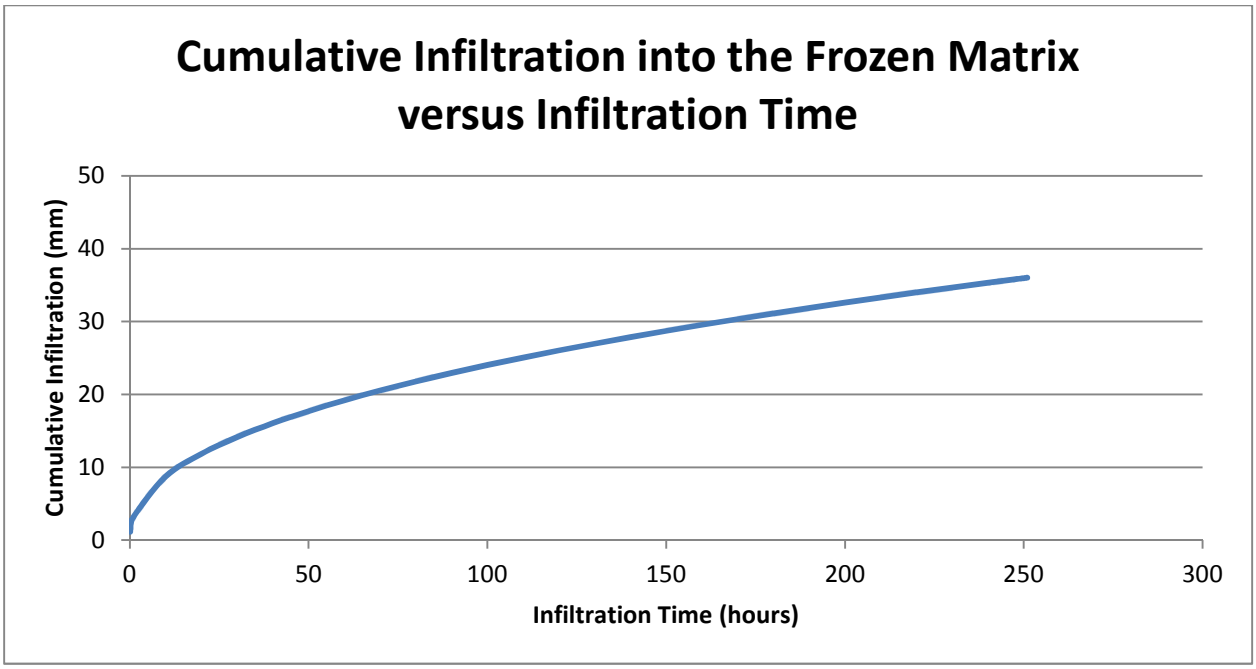

Figure 5-21: Cumulative infiltration versus infiltration time on the covered pile.

Chapter 6: Conclusions and Recommendations

6.1 Conclusions

The goal of the Diavik waste rock project is to develop a comprehensive understanding of the hydrological, geochemical, microbiological and thermal evolution of waste rock piles located at Diavik Diamond Mine. Three experimental waste rock piles and four active zone lysimeters were constructed at DDMI for this purpose, and data from these experiments has been collected continuously since 2007. This thesis focused on understanding the hydrology of two of the waste rock piles, and is a continuation of work conducted by Neuner (2009)and Fretz (2013). The primary findings of this research are highlighted below:

1. The thermal regime of the type III pile was impacted by a disruption in output from the heat trace between December 2012 and September 2013. In 2013 outflow from the basal lysimeters was not observed until the heat trace was restored, and less than 100m^3 of outflow was recorded from the south basal drain. The north basal drain conducted above average flow in 2013. The outflow observed from the pile, along with the results of a tracer test (discussed below) suggest that the core of the type III pile may be frozen year round, and may be storing water as ice within void spaces.

   Storage in the matrix of the type III pile appears to have remained in a pseudo-steady state between 2008 and 2013, with some drying occurring in portions of the pile. The TDR probes used to measure VMC demonstrate that the upper nine meters of the pile continue to thaw each summer; however, they do not provide any information regarding temperature or the storage of water below 9m depth.
2. The thermal regime of the covered pile was altered by turning off a heat trace in June, 2011. Significant outflow from the pile continued until the end of 2011, followed by a significant decrease in outflow observed in 2012 and 2013. This is interpreted to be the result of frozen

conditions at the base of the pile preventing flow along the basal liner. The till layer of the covered pile continues to thaw each year, and it is anticipated that infiltration into the core of the pile will continue as long as long as the till thaws each year.

Between August 2012 and August 2013 each of the TDR probes showed a strong drying trend and some of the TDRs froze. The drying trend may be due to low infiltration in 2012 and 2013 or may reflect the gradual onset of freezing conditions in the core of the pile.

3. A tracer was applied to the crest of the type III pile in September, 2007, and as of 2013 only 38% of this tracer has been recovered through the basal drains and the BCLs. The recovery of the tracer was significantly lower than anticipated in 2013. This is interpreted to be a result of freezing conditions in the core of the pile, which were likely induced or accelerated by the disruption of power to the heat trace in the pile between December 2012 and September 2013. The recovery observed between 2007 and 2012 was extrapolated until an estimated time for 50% recovery was reached. This extrapolation was used to estimate that pore water in the matrix material of the type III pile has an average residence time of 6 years, and travels 2.3 metres per year. Flow and transport are seasonally transient in the pile, and only occur during times when the matrix material of the pile is thawed. During the time periods when the pile was thawed the tracer was observed to travel at an average velocity of 0.3 to 0.5m/month, averaged over the 6 year time period of the experiment. Previous work has demonstrated that pore water is primarily contained within the matrix of the type III pile, and these velocities are representative of matrix flow.

   The tracer was applied at a high rate with the intention of inducing preferential flow through the pile, and flow velocities as fast as 0.7m/day were observed in the upper 9m of the pile following the experiment.

Outflow collected by the north basal drain did not contain any tracer between 2007 and 2013, and this demonstrates that this drain does not collect pore water from the full northern half of the pile as it was intended to. Instead the drain is collecting water primarily from the north batter. This result explains the disparity in flow volumes collected between the north and south drains.

4. A stable isotope analysis demonstrated that approximately 40% of the total water collected by the north drain between 2011 and 2013 was derived from the infiltration of snowmelt, with the remaining 60% derived from the infiltration of rainwater. The analysis also showed a strong correlation between the pH of the outflow, and the relative proportion of snowmelt in the water. Circumneutral effluent that is collected from the pile each spring contains an average of 65% snowmelt, and is the result of melt water travelling through preferential pathways to the base of the pile. The proportion of snow melt in outflow from the pile decreases throughout the year to an average of 30% immediately prior to winter freeze up. The isotope analysis also showed that almost no evaporation occurs following the infiltration of snowmelt into the north batter of the type III pile. This is interpreted to be a result of the clast supported nature of the batters, and the cooler conditions found in the interior of the pile.
5. The recharge received by the covered pile is divided between the infiltration of snowmelt and rainfall. Strong winds each winter lead to a consistent spatial distribution of snow on the covered pile, with the thickest snowpack located at the base of the pile and a thin to nonexistent snowpack on the upper batters and crest. A snowmelt and infiltration model was applied to portion of the snowpack that overlaid the basal liner, and it is estimated that snowfall contributed between 22 and 54% of the total recharge received by this portion of the pile during the years that were examined. The importance of snowmelt in the total recharge is a function of the total snow available for infiltration, the length of the melt period, and the amount of

rainfall infiltration each year. The estimates of snowmelt and rainfall infiltration were used to close a water balance for the covered pile between 2007 and 2013.

6.1.1 Application of this Research to the Full Scale Pile

The research conducted for the Diavik waste rock project is intended to facilitate a thorough understanding of the hydrological, geochemical, thermal and microbiological behavior of waste rock at DDMI. The results of the waste rock project will be applied in the closure plan for the mine, and as such it is necessary to relate the results of this research to the full scale waste rock pile.

Flow Velocity and Residence Times

Quantifying the residence time and flow velocity of pore water in the type III rock pile will facilitate an improved understanding of reaction rates within the waste rock, and will assist in future efforts to model the combined hydrology and geochemistry of the full scale rock pile.

Core and Batter Flow

The crest of the full scale pile has a large surface area relative to its batters. For this reason, it is volumetrically considered a core dominated system, while the experimental piles are batter dominated. Despite this the majority of the core of the full scale pile is frozen, with fluid flow restricted to an active zone that forms on the outer edges of the pile each year. The ability to differentiate between batter flow (north drain), core flow (BCLs) and combined core and batter flow (south drain) will therefore be beneficial when developing up-scaling relationships between the experimental and the full scale piles. The core dominated nature of the full scale pile will also lead to different patterns of snowmelt infiltration compared to the experimental piles. Quantifying the contribution of snowmelt to recharge will improve the up-scaling relationships developed to estimate the total infiltration into the full scale pile.

6.2 Recommendations

The following recommendations are intended to assist in guiding future research on both the Diavik waste rock project and on future experimental waste rock piles.

1. An excavation of the type I pile conducted in 2014 showed that a large portion of the basal core of the pile is frozen year round. The data from this excavation should be used to determine the factors influencing the formation of multi-year ice, and if similar ice should be expected in the type III pile.
2. The recovery of bromide from the type III pile should continue to be monitored until 90% recovery is achieved.
3. The amount of snow present on the batters of the type III pile should be assessed in the spring of 2015 using a LiDAR scanner or similar. Ideally the daily or weekly ablation of the snowpack will be monitored in the same manner.
4. A tracer test was conducted on the batters of the covered pile to determine the efficiency of the till liner as a barrier to flow (described in Appendix B). Continuing the analysis of this tracer test will lead to a greater understanding of the hydrology of the covered waste rock pile.
5. Additional rain and snow samples should be taken for isotopic analysis. This will lead to greater accuracy when quantifying the infiltration of snowmelt into the batter above the north drain.
6. In future experiments all instrumentation should cover the entire height of the pile, from the crest to the base. This will ensure that flow, chemistry and freezing within the pile can be accurately observed.
7. In future experiments additional basal collection lysimeters would be useful for differentiating between core and batter flow, and for understanding the effects of heterogeneity on flow within the pile.

8. In future experiments it is recommended to use the drainage pattern found in the type III pile to minimize the effects of freezing in the core of the pile. When possible clean crush should be used to protect drain lines, in order to avoid the storage of water in the crush material.

Bibliography

Allen, D. M., and D. A. Voormeij. “Oxygen-18 and Deuterium Fingerprinting of Tailings Seepage at the Sullivan Mine.” *Mine Water and the Environment*, 2002: 168-182.

Allen, Diana M., and Michele E. Lepitre. “Use of Pb, 18O, and 2H Isotopes in Mining-related Environmental Studies.” *Mine Water and the Environment*, 2004: 119-132.

Allison, G. B. "The relationship between 18O and deuterium in water in sand columns undergoing evaporation." *Journal of Hydrology*, 1982: 163-169.

Allison, G. B., C.J. Barnes, and M. W. Hughes. "The distribution of deuterium and 18O in dry soils: 2. Experimental." *Journal of Hydrology*, 1983: 377-397.

Arcadis. "Isotope Applications in Mining Provide Advantages to Mine Site Evaluations." Report, 2013.

Bailey, Brenda L., Lianna J.D. Smith, David W. Blowes, Carol J. Ptacek, Leslie Smith, and David C. Sego. “The Diavik Waste Rock Project: Persistence of contaminants from blasting agents in waste rock effluent.” *Applied Geochemistry*, 2013: 256-270.

Bell, Christina, et al. “Spatial and temporal variability in the snowpack of a High Arctic ice cap: implications for mass-change measurements.” *Annals of Glaciology*, 2008: 159-169.

Carzorzi, F., and Dalla G. Fontana. “Snowmelt modelling by combining air temperature and a distributed radiation index.” *Journal of hydrology*, 1996: 169-187.

Chi, X. "Characterizing low-sulfide instrumented waste-rock piles: Image grain-size analysis and wind-induced gas transport." *M.Sc. Thesis. University of Waterloo, Waterloo, Canada*, 2010.

Coplen, Tyler B., Andrew L. Herczeg, and Chris Barnes. *Isotope Engineering - Using Stable Isotopes of the Water Molecule to Solve Practical Problems.* New York: Springer Science + Business Media, 2000.

Davis, Stanley N., Glenn M. Thompson, Harold W. Bentley, and Gary Stiles. “Ground-Water Tracers - A Short Review.” *Ground Water* 18, no. 1 (1980): 14-23.

Earman, Sam, Andrew R. Campbell, Fred M. Phillips, and Brent D. Newman. "Isotopic exchange between snow and atmospheric water vapor: Estimation of the snowmelt component of groundwater recharge in the southwestern United States." *Journal of Geophysical Research*, 2006.

Environment Canada. "Monthly data report for Ekati A, Northwest Territories." 2010. <http://climate.weatheroffice.ec.gc.ca/climateData/.

Environment Canada. "Monthly data report for Ekati A, Northwest Territories." 2013.

Fala, O., J. Molson, M. Aubertin, and B. Bussier. "Numerical modeling of flow and capilalry barrier effects in unsaturated waste rock piles." *Mine Water and The Environment*, 2005: 172-185.

Fretz, Nathan. “Multi year hydrologic response of experimental waste rock piles in a cold climate: active zone developement, net infiltration, and fluid flow.” *Master's Thesis, University of British Columbia*, 2013.

Ghomshei, M. M., and D. M. Allen. “Hydrochemical and stable isotope assessment of tailings pond leakage, NIckel Plate Mine, British Columbia.” *Environmental Geology*, 2000b: 937-944.

Ghomshei, M. M., and D. M. Allen. “Potential Application of oxygen-18 and deuterium in mining effluent and acid rock drainage studies.” *Environmental Geology*, 2000: 767-773.

Gibson, J. J., and R. Reid. "Stable isotope fingerprint of open-water evaporation losses and effeective drainage area fluctuations in a subarctic shield watershed." *Journal of Hydrology*, 2010: 142-150.

Gibson, J. J., R. Reid, and C. Spence. "A six-year isotopic record of lake evaporation at a mine site in the Canadian subarctic: results and validation." *Hydrological Processes*, 1998: 1779-1792.

Gibson, J. J., T.W.D. Edwards, and G.G. Bursey. “Extimating Evaporation Using Stable Isotopes: Quantitative Results and Sensitivity Analysis for Two Catchments in North America.” *Nordic Hydrology*, 1993: 79-94.

Granger, RJ, DM Gray, and GE Dyck. "Snowmelt Infiltration to frozen Prairie soils." *Canadian Journal of Earth Sciences*, 1984: 669-677.

Gray, D. M., Brenda Toth, Litong Zhao, J. W. Pomeroy, and R. J. Granger. “Estimating areal snowmelt infiltration into frozen soils.” *Hydrological Processes*, 2001: 3095-3111.

Gray, DM, PG Landine, and RJ Granger. "Simulating infiltration into frozen Prairie soils in streamflow models." *Canadian Journal of Earth Sciences*, 1985: 464-472.

Gray, DM, RJ Granger, and PG Landine. "Modelling snowmelt infiltration and runoff in a Prairie Environment." *Proceedings of the Cold Ragions Hydrology Symposium.* 1986. 427-438.

Gustafsson, David, Nils Sundstrom, and Angela Lundberg. “Estimation of Snow Water Equivalent of Dry Snowpacks Using a Multi-Offset Ground Penetrating Radar System.” *69th Eastern Snow Conference.* Claryville, New York, 2012. 197-205.

Hock, Regine. “Temperature index melt modelling in mountain areas.” *Journal of Hydrology*, 2003: 104-115.

IAEA . “Statistical Treatment of Data on Environmental Isotopes in Precipitation.” Technical Report, Vienna, 1992.

IAEA. 2014. http://www.iaea.org/ (accessed August 25, 2014).

Janowicz, JR, DM Gray, and JW Pomeroy. "Characterisation of Snowmelt Infiltration Scaling Parameters Within a Mountainous Subarctic Watershed." *Proceedings of the 59th Eastern Snow Conference.* Stowe, Vermont, 2002. 67-81.

Johnson, Barrie D., and Kevin B. Hallberg. "Acid mine drainage remediation options: a review." *Science of theTotal Environment*, 2005: 3-14.

Kane, Douglas L, Robert E. Gieck, and Larry D. Hinzman. “Snowmelt Modelling at Small Alaskan Arctic Watershed.” *Journal of Hydrologic Engineering*, 1991: 204-210.

Kustas, William P., Albert Rango, and Remko Uijlenhoet. “A simple energy budget algorithm for the snowmelt runoff model.” *Water Resources Research*, 1994: 1515-1527.

Langman, Jeff B., Mandy L. Moore, Carol J. Ptacek, Leslie Smith, David Sego, and David W. Blowes. "Diavik Waste Rock Project: Evolution of Mineral Weathering, Element Release, and Acid Generation and Neutralization during a Five-Year Humidity Cell Experiment." *Minerals*, 2014: 257-278.

Li, Fadong, Xianfang Song, Changyuan Tang, Changming Liu, Jingjei Yu, and Wanjun Zhang. “Tracing infiltration and recharge using stable isotope in Taihang Mt., North China.” *Environmental Geology*, 2007: 687-696.

Mackay, D. M., D. L. Freyberg, and P. V. Roberts. “A Natural Gradient Experiment on Solute Transport in a Sand Aquifer 1. Approach and Overview of Plume Movement.” *Water REsource Research* 22, no. 13 (1986): 2017-2029.

Marcoline, Joseph R. “Investigations of water and tracer movement in covered and uncvoered unsaturated waste rock.” *Ph.D. Dissertation, University of British Columbia, Vancouver, Canada*, 2008.

Neuner, Matthew. "Water Flow Through Unsaturated Mine Waste Rock in a Region of Permafrost." *Master's Thesis, University of British Columbia*, 2009.

Neuner, Matthew, et al. "The Diavik waste rock project: Water flow through mine waste rock in a permafrost terrain." *Applied Geochemistry*, 2013: 222-233.

Nichol, C. F. "Transient flow and transport in unsaturated heterogeneous media: Field experiments in mine wast rock." *Ph.D. Dissertation. University of British Columbia, Vancouver, Canada*, 2002.

Nichol, Craig, Leslie Smith, and Roger Beckie. “Field-scale experiments of unsaturated flow and solute transport in a heterogeneous porous medium.” *Water Resources Research* 41 (2005).

Ohmura, Atsumu. “Evaporation From the Surface of the Arctic Tundra on Axel Heiberg Island.” *Water Reasources Research*, 1982: 291-300.

Peterson, Holly. “Unsaturated Hydrology, Evaporation, And Geochemistry of Neutral and Acid Rock Drainage in Highly Heterogeneous Mine Waste Rock at the Antamina Mine, Peru.” *PhD Thesis, University of British Columbia*, 2014.

Pham, H. "Diavik Waste Rock Project: Temperature Data." *Annual Waste Rock Project Group Meeting.* Waterloo, 2014.

Pham, H. “Heat transfer in waste-rock piles constructed in a continuous permafrost region.” *Ph.D. Dissertation. University of Alberta, Edmonton, Canada*, 2012.

Pham, Hoang. "Personal Communication, Email." 2014.

Pham, Nam H., David C. Sego, Lukas Arenson, David W. Blowes, Richard T. Amos, and Leslie Smith. "The Diavik Waste Rock Project: Measurement of the thermal regime of a waste-rock test pile in a permafrost environment." *Applied Geochemistry*, 2013: 234-245.

Pomeroy, J. W., P. Marsh, and D. M. Gray. “Application of a Distributed Blowing Snow Model to the Arctic.” *Hydrological Processes*, 1997: 1451-1464.

Schulz, Oliver, and Carmen De Jong. "Snowmelt and Sublimation: field experiments and modelling in the High Atlas Mountains of Morocco." *Hydrology and Earth System Sciences*, 2004: 1076-1089.

Sinclair, Sean. “Influence of Freeze-Thaw Dynamics and Spatial Contributions on Geochemical Loading from a Low Sulfide Waste-Rock Pile.” *Master's Thesis, University of Waterloo*, 2014.

Sinclair, Sean. “Personal Communication (email).” February 2013b.

Smith, L. J. D. "Building and characerizing low sulfide instrumented waste rock piles: Pile design and construction, particle size and sulfur characterization, and initial geochemical response." *P.hD. dissertation. University of Waterloo*, 2009.

Smith, Lianna J.D., Michael C. Moncur, Matthew Neuner, Michael Gupton, and Blowes W. David. "The Diavik Waste Rock Project: Design, construction, and instrumentation of field-scale experimental waste-rock piles." *Applied Geochemistry*, 2013: 187-199.

Smith, Lianna. "Personal Communication." September 9, 2014.

Smith, Lianna. "Test Piles Project 2006 Construction Summary." Internal Document, 2006.

Souchez, R. A., and J. Jouzel. "Melting-refreezing at the Glacier Sole and the isotopic composition of the ice." *Journal of Glaciology*, 1982: 35-42.

Soughez, R. A., and J. Jouzel. "On the isotopic composition in dD and d180 of water and ice during freezing." *Journal of Glaciology*, 1984: 369-372.

Spangenberg, Jorge E. “Caution on the storage of waters and aqueous solutions in plastic containers for hydrogen and oxygen stable isotope analysis.” *Rapid Communications in Mass Spectrometry*, 2012: 2627-2636.

Sracek, O., M. Choquette, P. Gelinas, R. Lefebvre, and R. V. Nicholson. “Geochemical Characterization of acid mine drainage from a waste rock pile, Mine Doyon, Quebec, Canada.” *Journal of Contaminant Hydrology*, 2004: 45-71.

Stockwell, Justin, Leslie Smith, John L. Jambor, and Roger Beckie. "The relationship between fluid flow and mineral weathering in heterogeneous unsaturated porous media: A physical and geochemical characterization of a waste rock pile." *Applied Geochemistry*, 2006: 1347-1361.

Swedish Meteorological and Hydrological Institute. *The HBV model.* 2006 йил 03-05. http://www.smhi.se/sgn0106/if/hydrologi/hbv.htm (accessed 2014 йил 20-May).

Swift, Lloyd W. Jr. "Algorithm for Solar Radiation on Mountain Slopes." *Water Resources Research* 12, no. 1 (02 1976).

Yazdani, J., L. Barbour, and G. W. Wilson. "Soil water characteristic curve for mine waste rock containing coarse material." *PRedecdings of the 6th Environmental Engineering Sprecialty Conference of the Canadian Society of Civil Engineers.* London, ON, Canada, 2000.

Zhao, Litong, and D. M. Gray. "A parametric expression for estimating infiltration into frozen soils." *Hydrological Processes*, 1997: 1761-1775.

Appendix A: Hydrology Dataset

The complete hydrology dataset from 2007 to 2013 is contained in this appendix. This dataset is an update to the data presented in Fretz (2013), and is structured in a similar manner.

A.1 Rainfall and Infiltration

Natural rainfall at the test piles was calculated as the average rainfall measured from four tipping buckets located on the crest of the waste rock piles. The type III waste rock pile also received significant applied rainfall events in 2006 and 2007, which were measured using a grid of coffee cups. The annual infiltration into the crests of the piles was calculated using the Penman Monteith method outlined in Fretz (2013).

Snowfall is not measured at the test piles; however, the environment team at Diavik runs a MET station located approximately 1km from the test piles, and daily snowfalls amounts are recorded there. Figure A-1 summarizes the natural rainfall and snowfall observed at the test piles between 2007 and 2013. Tables A-1 and A-2 summarizes the natural rainfall and the calculated infiltration of natural rainfall into the crests of the piles between 2007 and 2013. Table A-3 summarizes the total snowfall measured each winter at the MET station.

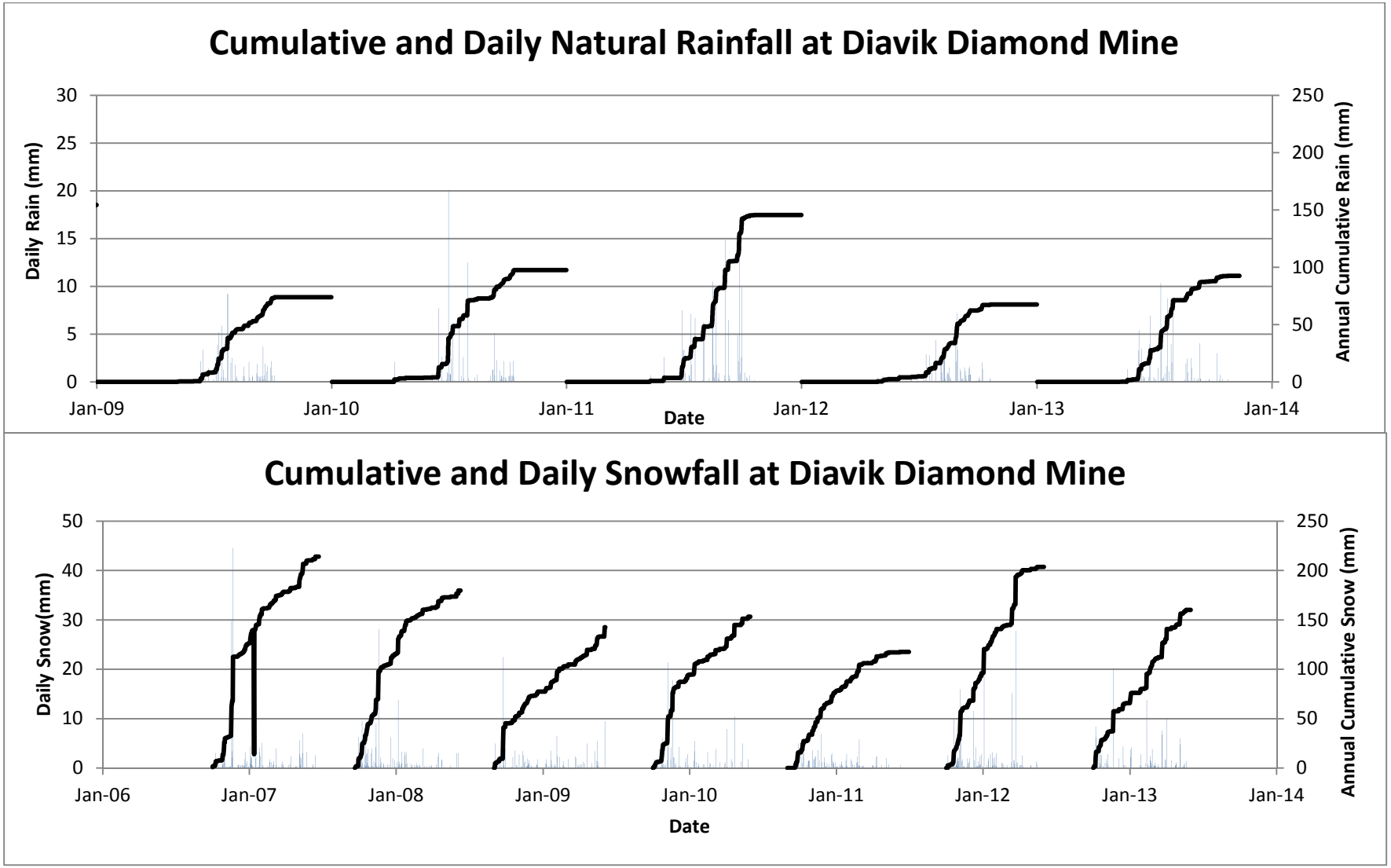

Figure A-1:Daily and annual natural rainfall and snowfall at the test piles

Table A-1: Rainfall and calculated Infiltration into the crown of the type I pile and covered pile

Year	Natural Rainfall (mm)	Estimated Net Infiltration (mm)
2006	-	-
2007	92	40
2008	154	88
2009	74	11
2010	98	40
2011	146	84
2012	68	9
2013	91	26

Table A-2: Rainfall and calculated infiltration into the crown of the type III pile

Year	Natural Rainfall (mm)	Applied Rainfall (mm)	Estimated Net Infiltration (mm)
2006		58	51
2007	92	61	92
2008	154	-	88
2009	74	-	11
2010	98	-	40
2011	146	-	84
2012	68	-	9
2013	91	-	26

Table A-3: Winter snowfall measured at Diavik Diamond Mine

Winter	Cumulative Snowfall (mm)
2006/2007	214
2007/2008	180
2008/2009	143
2009/2010	153
2010/2011	118
2011/2012	204
2012/2013	160

A.2 Type I Test Pile

The dataset from the type I pile consists of measurements of volumetric moisture contents from TDR probes and outflow from the basal drain and BCLs.

The type I dataset was influenced by a flooding event in December, 2012. The data logger that records outflow from the main basal drain and the BCLs in the type I pile was destroyed by the flood, and was replaced prior to the onset of flow in 2013. The power source for the data logger attached to the TDRs was also damaged during the flood. Until power was restored, 12 volt car batteries were used to power the data logger and the TDRs. This system failed several times over the summer, and led to the disruption of TDR data from the type I pile in 2013. Once regular power was restored the data logger once again began collecting reliable data from the TDRs.

The flood also disrupted power to the heat trace for the BCLs and basal drain. Following this event, very little outflow has been observed from the type I pile. An excavation conducted in the summer of 2014 demonstrated that the base of the type I pile contained significant volumes of ice. The formation of ice in the waste rock piles is currently being examined by Jordan Zak (Ongoing)

Figure A-2 shows the location of the TDR probes in the type I pile, and figureA-3 shows the VMC measured at each probe between 207 and 2013. Figure A-4 shows the location of the basal drain and BCLs in the type I pile. Figure A-5 shows the daily and cumulative annual outflow from the type 1 basal drain, and Figure A-6 shows the daily outflow from each BCL cluster. Table A-4 shows the start and stop dates of the type I basal drain, and table A-5 shows the start and stop dates of the BCLs.

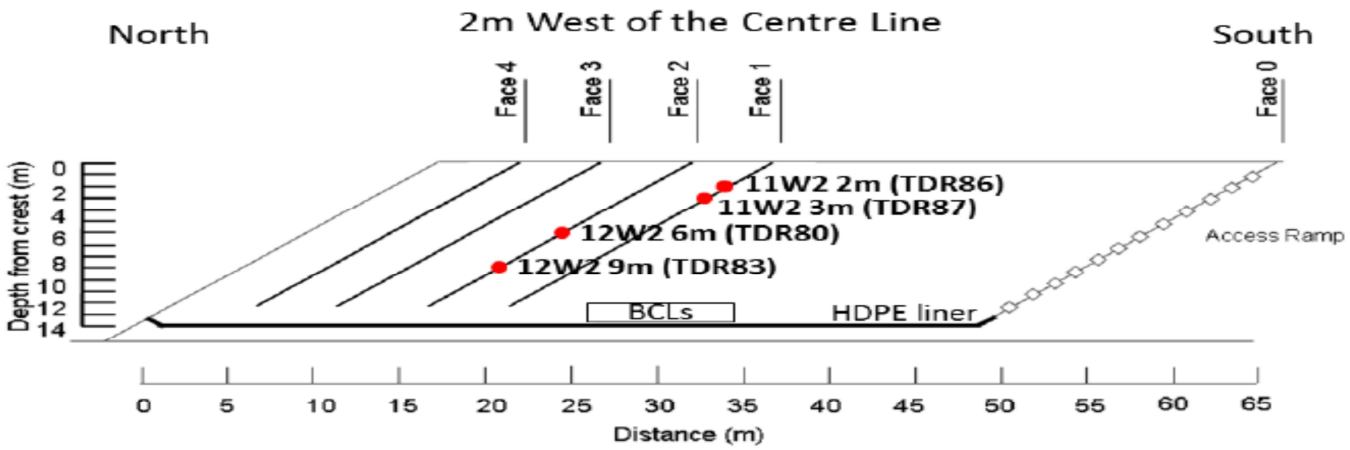

Figure A-2: Location of TDR probes in the type I pile.
Image from Fretz (2013)

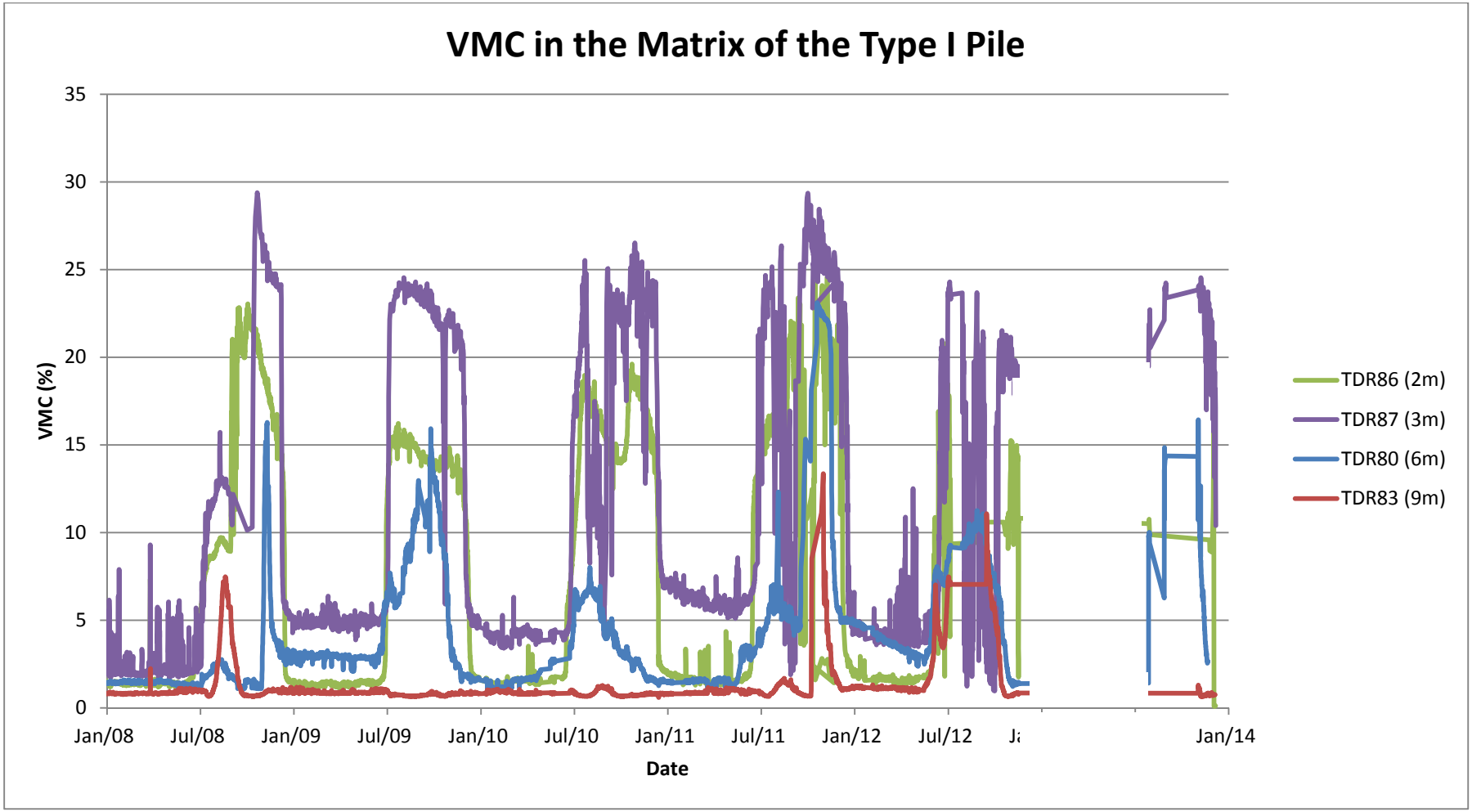

Figure A-3: Volumetric moisture contents measured at the TDR probes in the type I pile.
Data collection was disrupted in 2013 due to a flood that disrupted power to the data logger used with the TDRs.

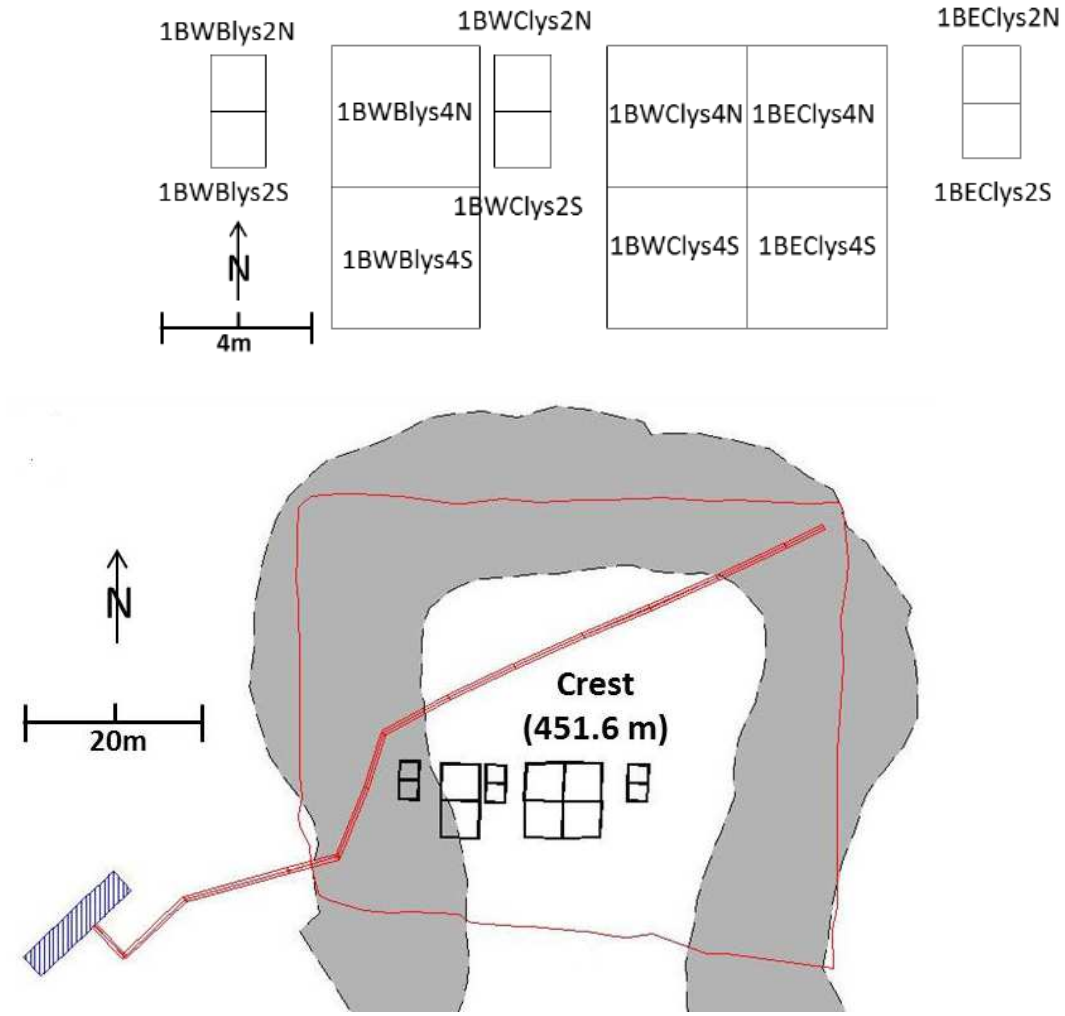

Figure A-4: Drainage system in the type I pile.
The upper schematic shows the name of each BCL, and the lower image is an as-built drawing of the type I test pile drainage scheme.

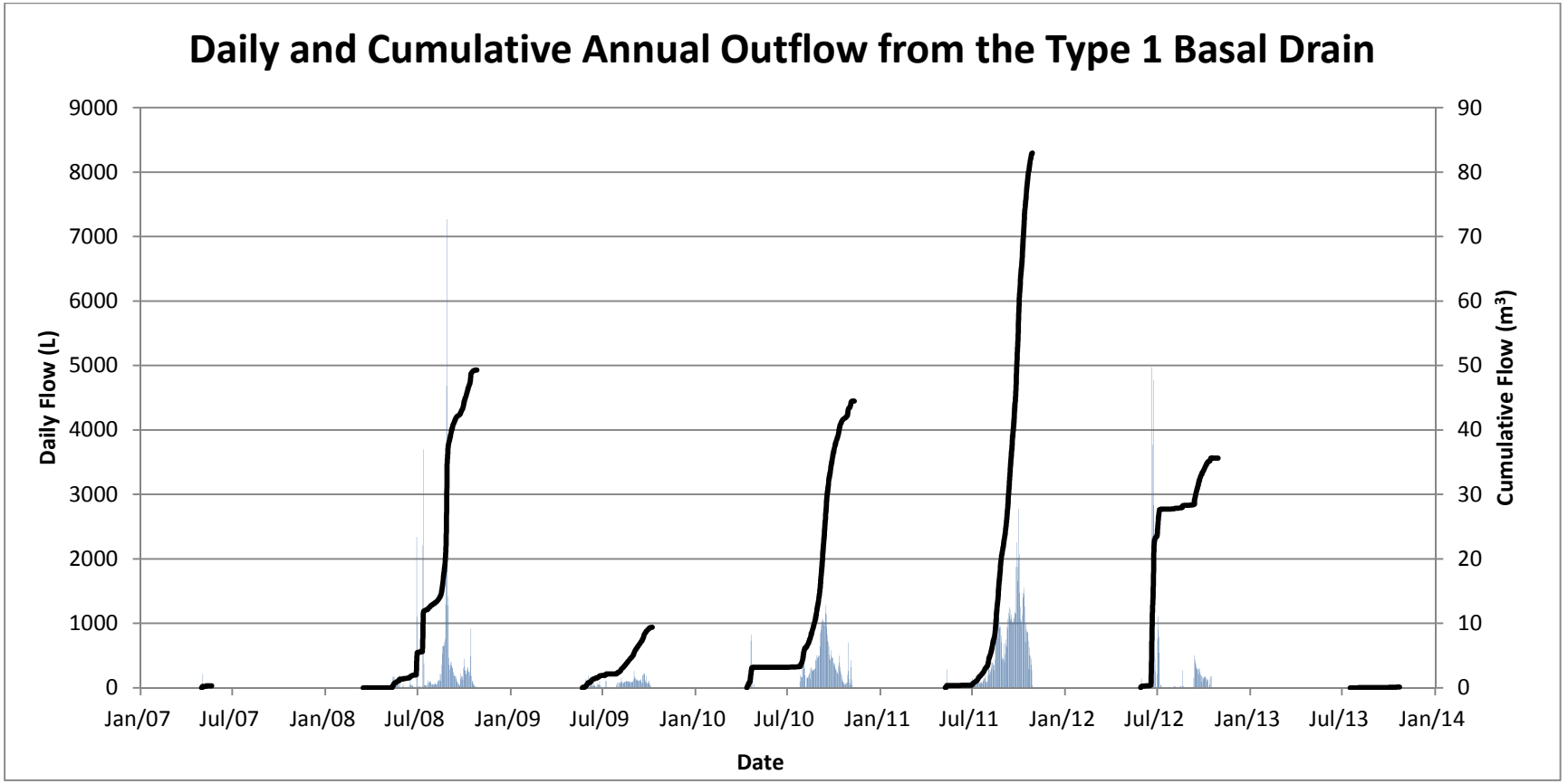

Figure A-5: Daily and cumulative outflow from the type I basal drain

Table A-4: Basal outflow and start/stop dates for the type I Drain

Type I Drain			
Year	Flow Start	Flow Stop	Discharge (m^3)
2007	1-May	Unknown	Unknown
2008	10-May	25-Oct	50
2009	22-May	6-Oct	10
2010	12-Apr	10-Nov	44
2011	9-May	28-Oct	83
2012	29-May	29-Oct	36
2013	17-Jul	22-Oct	0.1

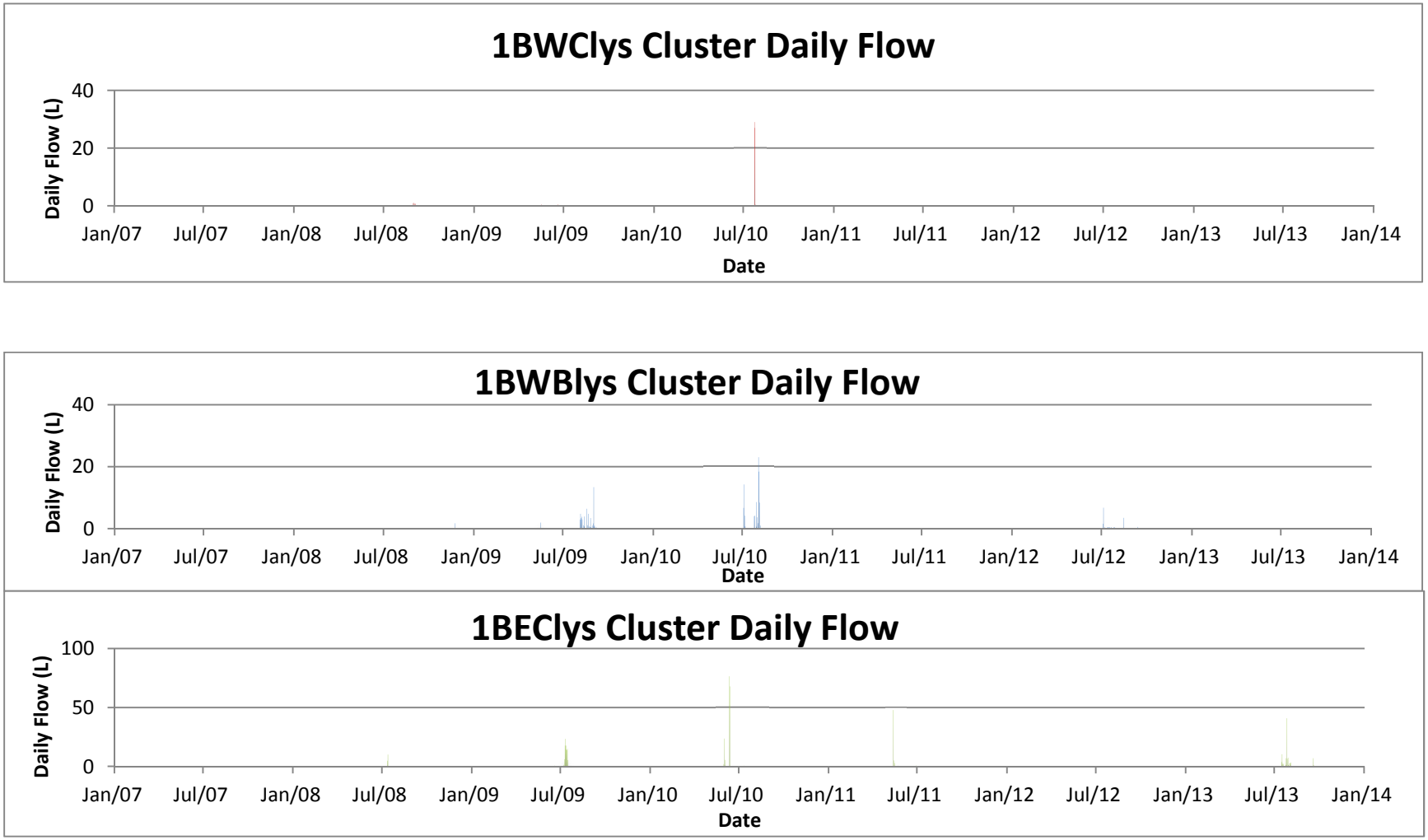

Figure A-6: Outflow from the basal collection lysimeters in the type I pile

Table A-5: Basal outflow and start/stop dates for the type I BCLs

Type I BCLs			
Lysimeter Cluster	Flow Start	Flow Stop	Discharge (L)
2007			
All	No Flow		
2008			
1BWB	-	-	2
1BWC	27-Aug	3-Sep	4
1BEC	29-Jun	6-Sep	18
2009			
1BWB	7-Jul	29-Sep	62
1BWC	7-Jul	10-Jul	1
1BEC	7-Jul	29-Sep	123
2010			
1BWB	3-Jul	18-Aug	99
1BWC	27-Jun	2-Aug	56
1BEC	1-Jun	16-Aug	177
2011			
1BWB	No Flow		
1BWC	No Flow		
1BEC	5-May	21-May	61
2012			
1BWB	5-Jul	12-Sep	20
1BWC	No Flow		
1BEC	No Flow		
2013			
1BWB	No Flow		
1BWC	No Flow		
1BEC	11-Jul	24-Sep	106

A.3 Type III Test Pile

The dataset from the type III pile consists of volumetric moisture contents measured with TDR probes, outflow measured at the basal drain and BCLs, and hydraulic head measured using tensiometers.

The type III dataset was influenced by a flooding event in December, 2012. The data logger that records outflow from BCLs in the type III pile was destroyed by the flood, and was replaced prior to the onset of flow in 2013. The power source for the data logger attached to the TDRs and the tensiometers in the pile was also damaged during the flood. Until power was restored, 12 volt car batteries were used to power the data logger and the TDRs. This system worked better in the type III pile than in the type I pile, and the disruption to the type III dataset was smaller than the disruption to the type I dataset. When regular power was restored the data logger once again began collecting reliable data from the TDRs. The pressure transducers used with the tensiometers were bench tested in early 2013, and did not perform as anticipated. This led to them not being installed until August 2013. The number of erroneous points recorded by the tensiometers was very high in 2013, likely due to power fluctuations caused by changing batteries. As of 2014 all of the pressure transducers are working correctly.

The flood also disrupted power to the heat trace for the BCLs and basal drains. This had a smaller impact on outflow from the type III basal drains than it did on the type I basal drain, likely due to the different drainage patterns used in the two piles. Outflow was not observed at the type III BCLs until power was restored to the heat trace.

Figure A-7 shows the location of TDR probes in the pile, and figure A-8 shows the VMCs measured at each probes between 207 and 2013. Figure A-9 shows the location of the basal drains and BCLs in the type III pile. Figure A-10 shows the daily and cumulative annual outflow from the north and south basal drains. Figure A-11 shows the daily outflow from each BCL cluster. Figure A-12 shows the calculated

hydraulic head in the upper 1.2m of the pile for each year between 2010 and 2013. Table A-6 and Table A-7 show the start and stop dates along with flow volumes for the basal drains and BCLs respectively.

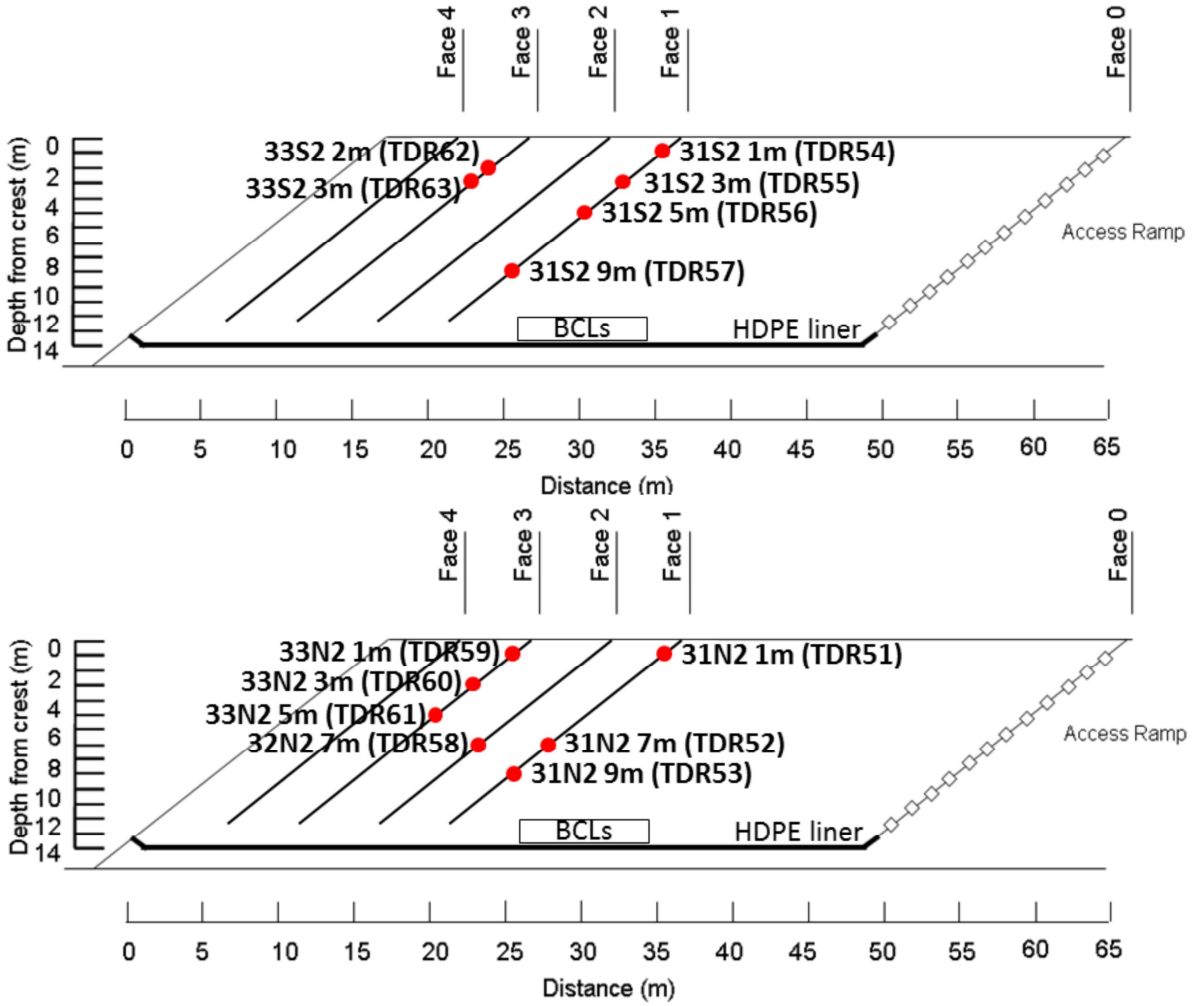

Figure A-7: Location of the TDR probes in the type III pile.
Image from Fretz (2013)

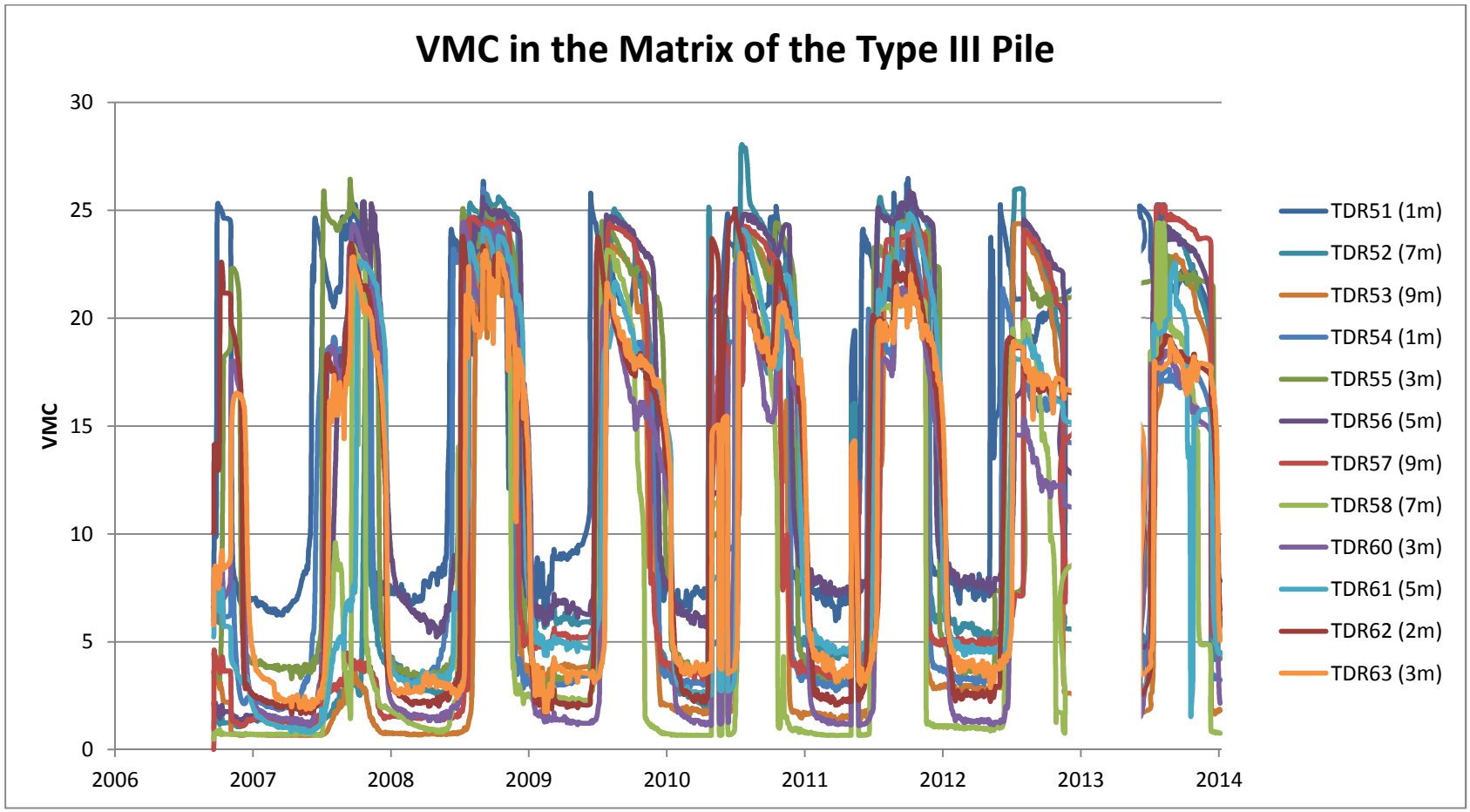

Figure A-8: Volumetric moisture contents measured at the TDR probes in the type III pile.

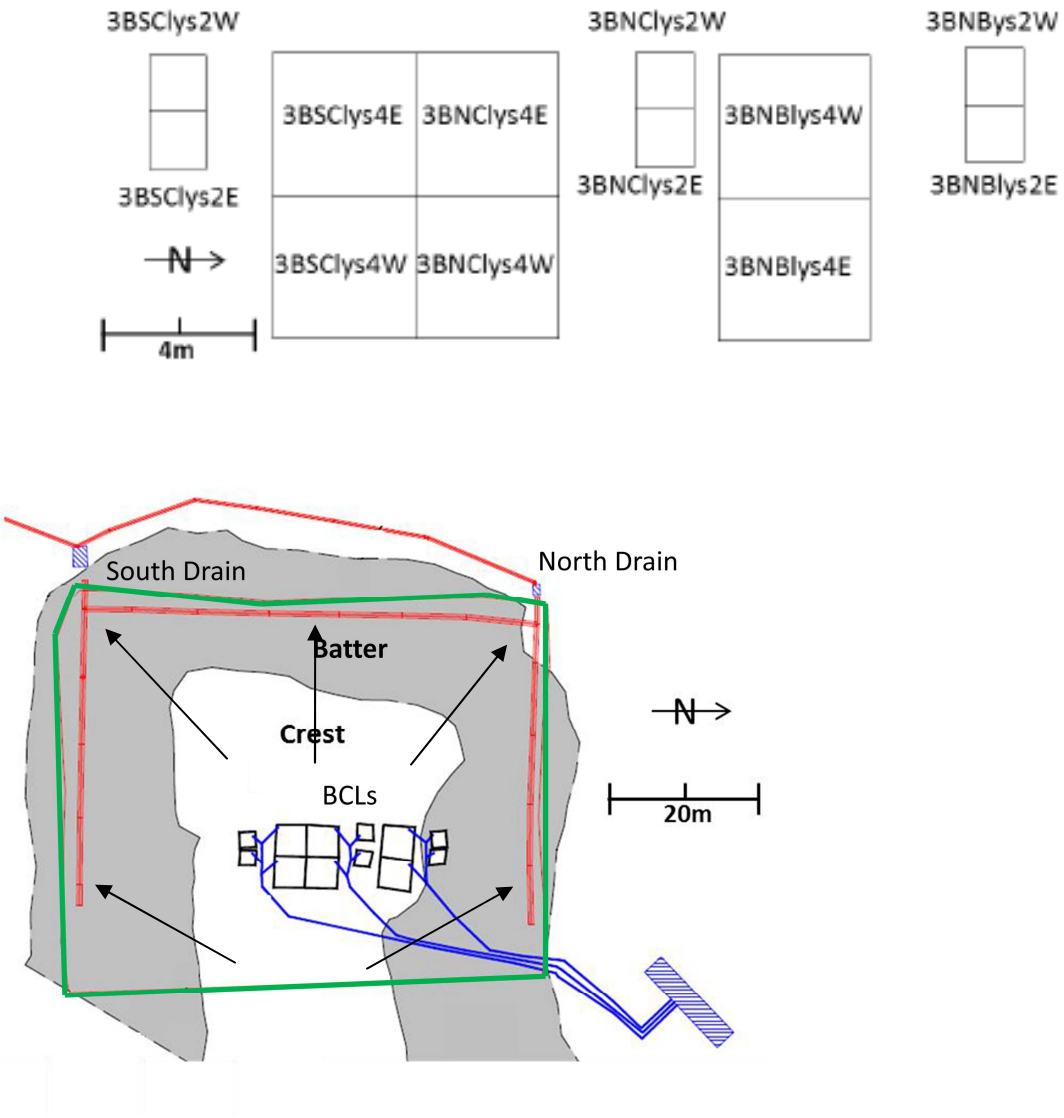

Figure A-9: Drainage system in the type III pile.
The upper schematic shows the name of each BCL, and the lower image is an as-built drawing of the type III test pile drainage scheme.

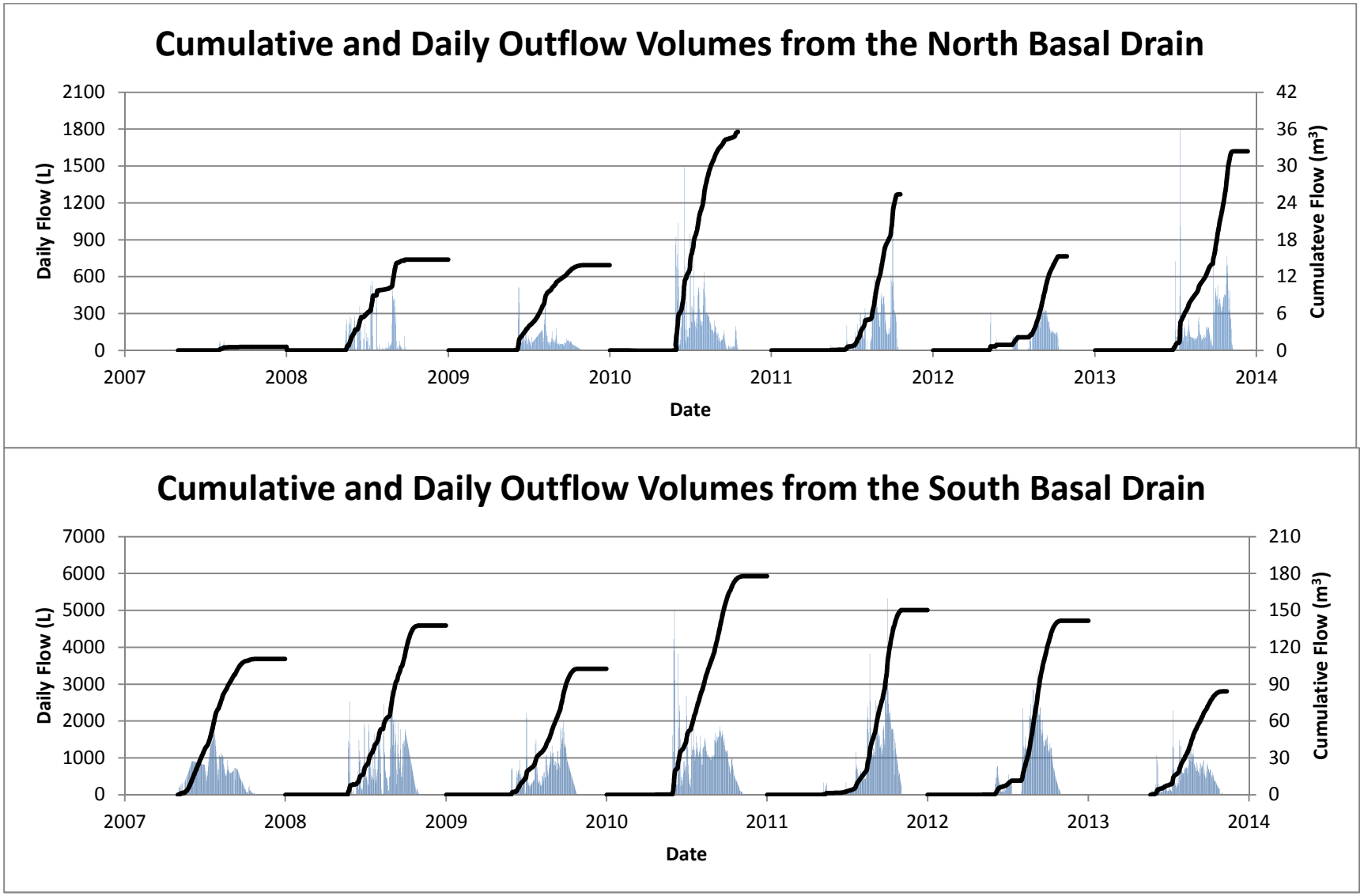

Figure A-10: Daily and cumulative outflow from the north and south drains

Table A-6: Basal outflow and start/stop dates for the combined north and south basal drains

Type III Basal Drain Outflow (Combined)			
Year	Flow Start	Flow Stop	Discharge (m^3)
2007	3-May	1-Nov	110
2008	2-May	30-Oct	150
2009	29-May	30-Oct	117
2010	20-Apr	6-Nov	213
2011	9-May	4-Nov	176
2012	28-Apr	29-Oct	156
2013	25-May	10-Nov	116

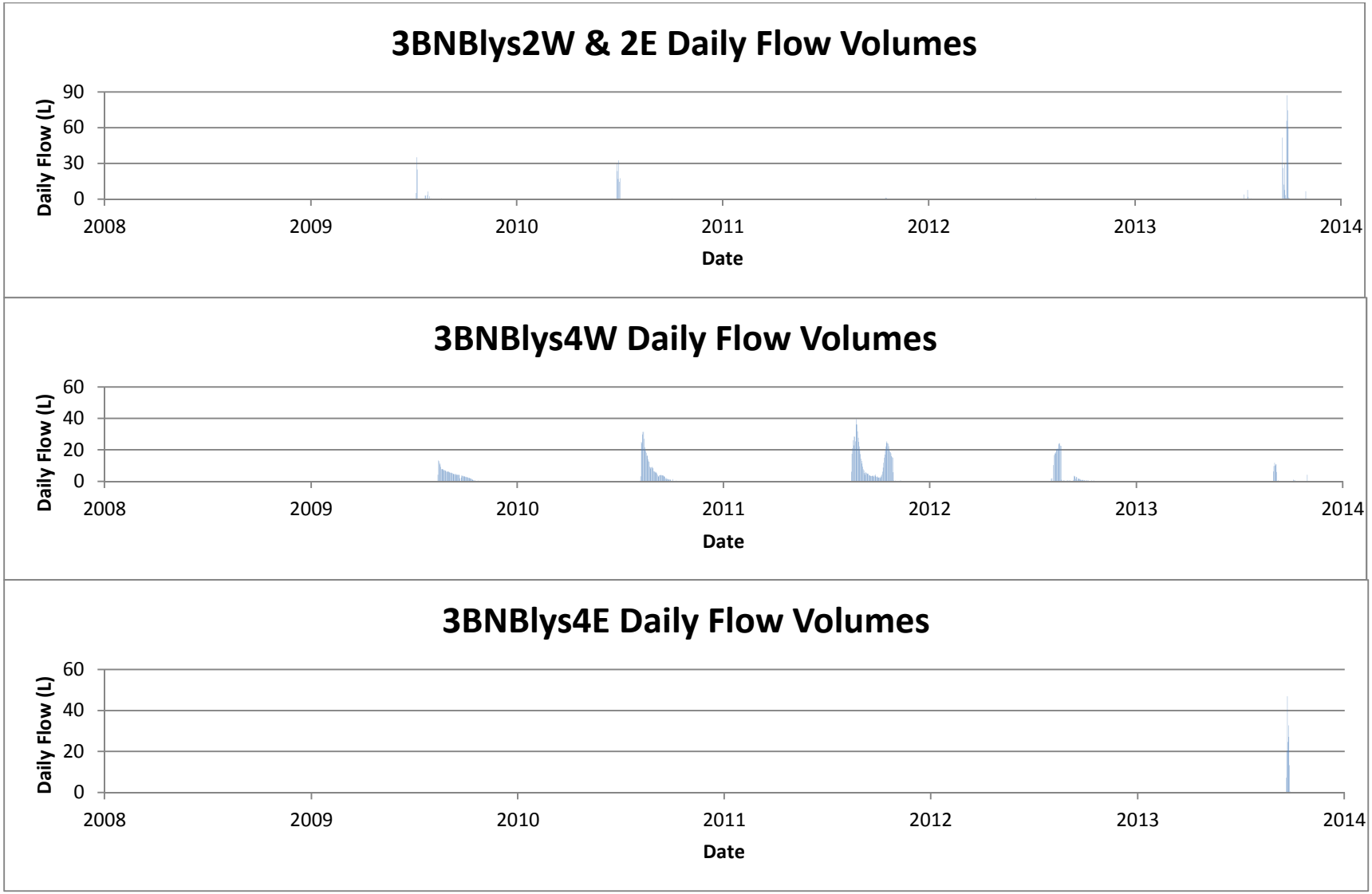

Figure A-11: Outflow from the basal collection lysimeters in the type III pile.
Continued on next page

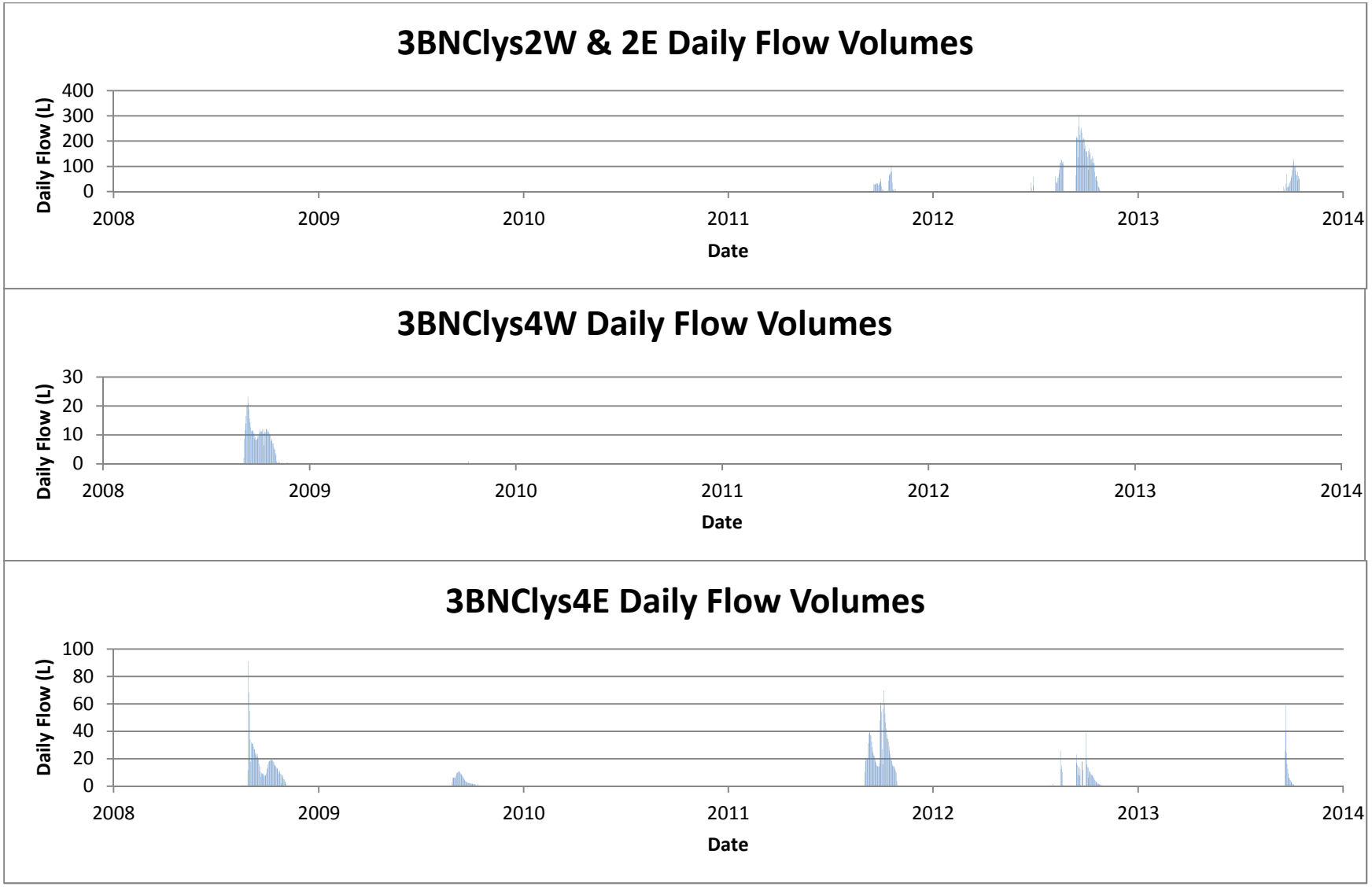

Figure A-11: Outflow from the basal collection lysimeters in the type III pile. Continued on next page

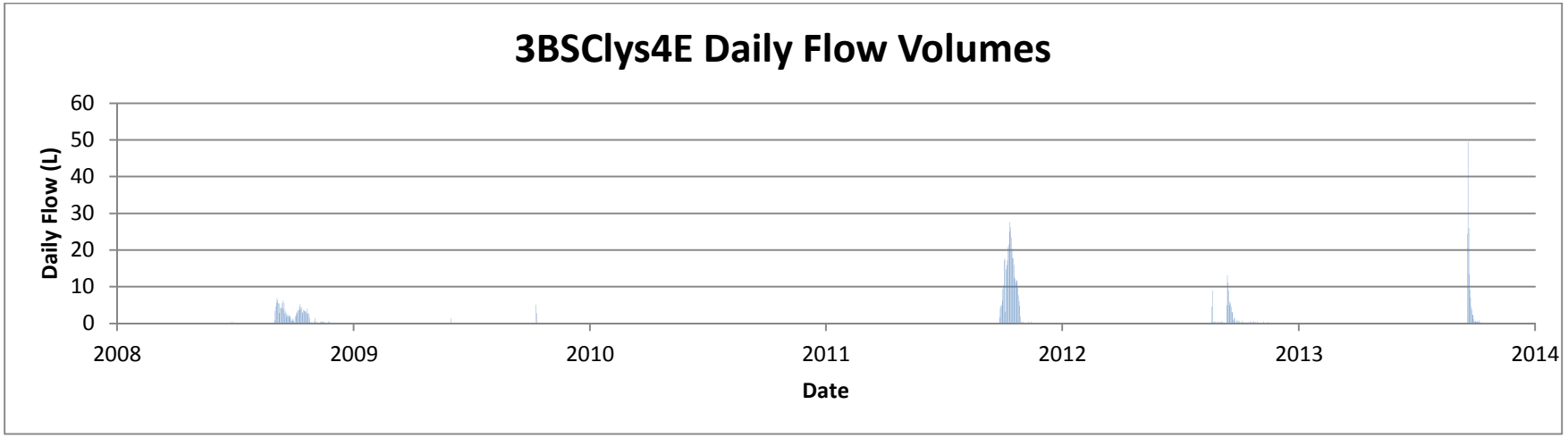

Figure A-11: Outflow from the basal collection lysimeters in the type III pile.

Table A-7: Outflow volumes and start/stop dates for the type III BCLs.
Note that in 2013 significant flow was not observed in the BCLs until September

Type III BCLs			
Lysimeter Cluster	Flow Start	Flow Stop	Discharge (L)
2007			
All	No Flow		
2008			
3BNBlys2W/2E	No Flow		
3BNBlys4W	No Flow		
3BNBlys4E	No Flow		
3BNClys2W/2E	No Flow		
3BNClys4W	6-Sep	4-Nov	629
3BNClys4E	16-Aug	4-Nov	1211
3BSClsy4W	No Flow		
3BSClys4E	31-Aug	4-Nov	187
3BSClys2W/2E	No Flow		
2009			
3BNBlys2W/2E	6-Jul	7-Oct	86
3BNBlys4W	7-Jul	22-Oct	307
3BNBlys4E	No Flow		
3BNClys2W/2E	No Flow		
3BNClys4W	7-Jul	10-Oct	1
3BNClys4E	7-Jul	17-Oct	228
3BSClsy4W	No Flow		
3BSClys4E	7-Jul	11-Oct	10
3BSClys2W/2E	No Flow		
2010			
3BNBlys2W/2E	27-Jun	20-Oct	138
3BNBlys4W	6-Aug	9-Oct	493
3BNBlys4E	No Flow		
3BNClys2W/2E	No Flow		
3BNClys4W	No Flow		
3BNClys4E	29-Sep	24-Oct	3
3BSClsy4W	No Flow		
3BSClys4E	No Flow		
3BSClys2W/2E	No Flow		
2011			
3BNBlys2W/2E	16-Oct	21-Oct	5
3BNBlys4W	15-Aug	11-Nov	963
3BNBlys4E	No Flow		

Lysimeter Cluster	Flow Start	Flow Stop	Discharge (L)
3BNClys2W/2E	15-Sep	13-Nov	1105
3BNClys4W	No Flow		
3BNClys4E	1-Sep	11-Nov	1611
3BSClsy4W	No Flow		
3BSClys4E	26-Sep	13-Nov	436
3BSClys2W/2E	No Flow		
2012			
3BNBlys2W/2E	9-Jul	8-Aug	3
3BNBlys4W	5-Jul	17-Oct	330
3BNBlys4E	No Flow		
3BNClys2W/2E	20-Apr	12-Nov	7940
3BNClys4W	No Flow		
3BNClys4E	9-Jul	7-Nov	467
3BSClsy4W	No Flow		
3BSClys4E	19-Aug	14-Nov	
3BSClys2W/2E	No Flow		
2013			
3BNBlys2W/2E	12-Jul	1-Nov	443
3BNBlys4W	31-Aug	1-Nov	75
3BNBlys4E	19-Sep	27-Sep	173
3BNClys2W/2E	11-Jul	11-Nov	1586
3BNClys4W	No Flow		
3BNClys4E	20-Sep	12-Oct	195
3BSClsy4W	No Flow		
3BSClys4E	17-Jul	22-Oct	149
3BSClys2W/2E	No Flow		

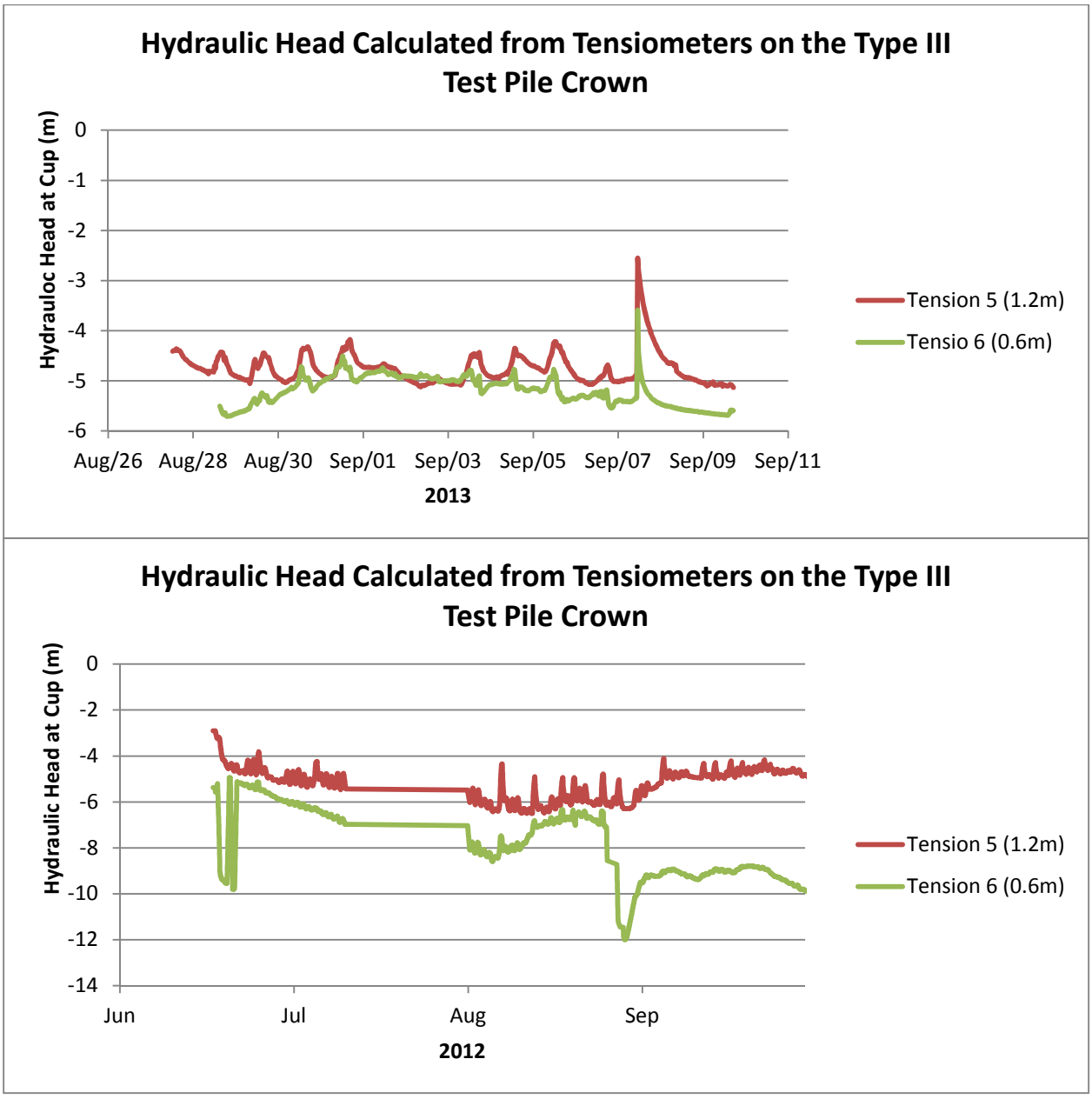

Figure A-12: Hydraulic head calculated from tensiometers on the type III test pile crown
(Continued on next page)

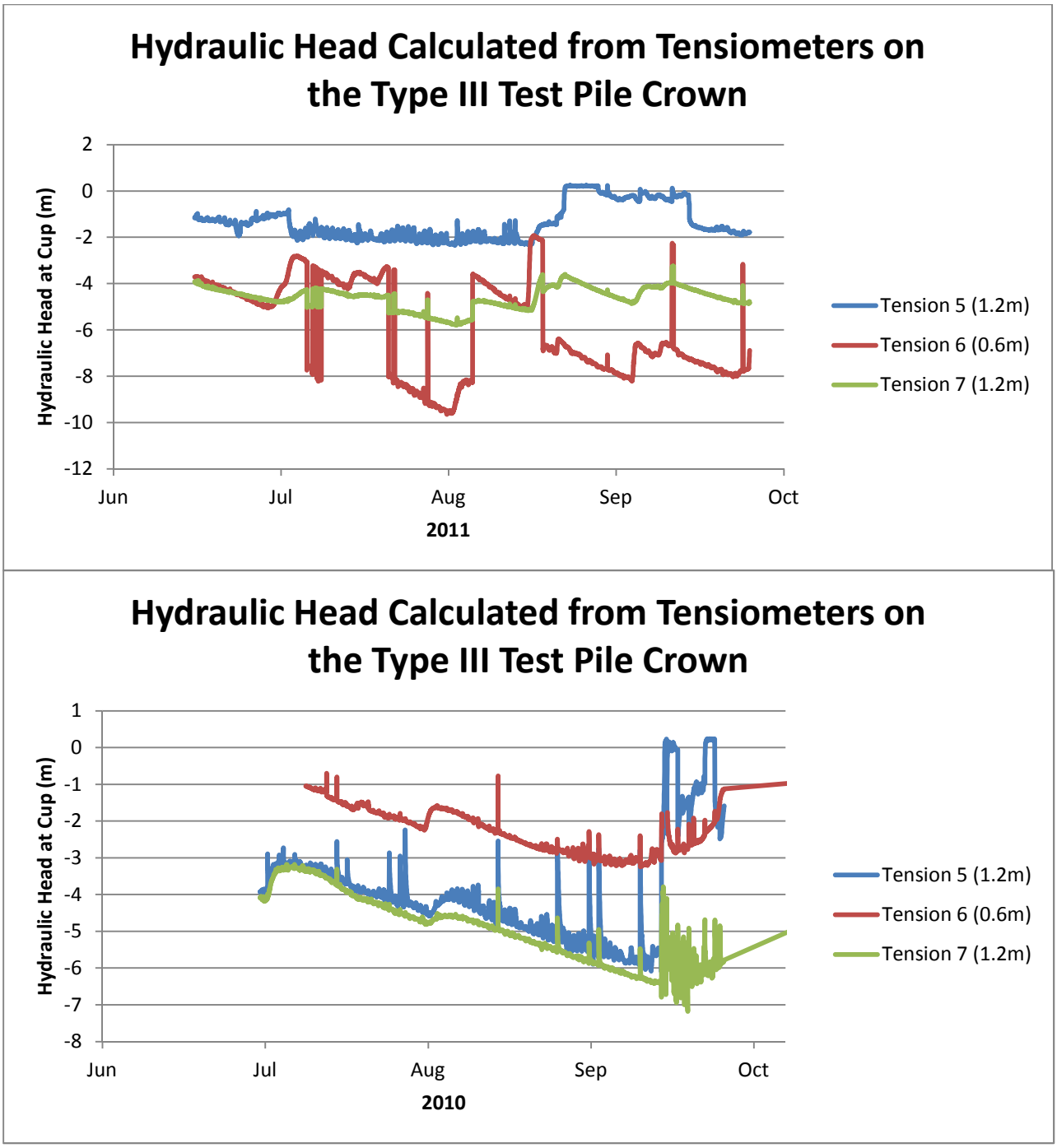

Figure A-12: Hydraulic head calculated from tensiometers on the type III test pile crown

A.4 Covered Test Pile

The dataset from the covered pile consists of volumetric moisture contents measured with TDR probes, outflow measured at the basal drain, hydraulic heads measured using tensiometers, and temperature and VMC data measured using ECH_2O probes. Two tracer tests were also conducted on the east batter of the pile in the summer of 2013, and outflow from three collection lysimeters was observed that summer. The volumetric recovery of the tracer is provided in this section; however, a summary of each test can be found in Appendix B.

Outflow from the covered pile was influenced by turning a heat trace off in June 2011. After this event the pile slowly cooled and froze, and outflow from the pile was significantly reduced. The covered pile was not affected by the flooding event in December, 2012.

Figure A-13 and A-14 show the location of the TDR probes in the covered pile and the VMC measured at each probe between 2007 and 2013 respectively. Annual outflow from the pile is shown in Figure A-16, and Figure A-17 shows the cumulative outflow measured per flow season (as flow is observed throughout the winter). Figure A-18 shows the hydraulic head measured using tensiometers on the crest of the pile. Figure A-19 shows the VMCs and temperatures measured by ECH2O probes within the pile. Figure A-20 shows the volume of water collected by the lysimeters on the eastern batter of the pile. Figures A-19 to A-22 show the snowpack contours created by surfer for 2010, 2011, 2013 and 2014 respectively. Table A-8 shows the start and stop dates along with flow volumes for the basal drain. Tables A-9 to A-12 show the measured snow depths and densities in 2010, 2011, 2013 and 2014 respectively.

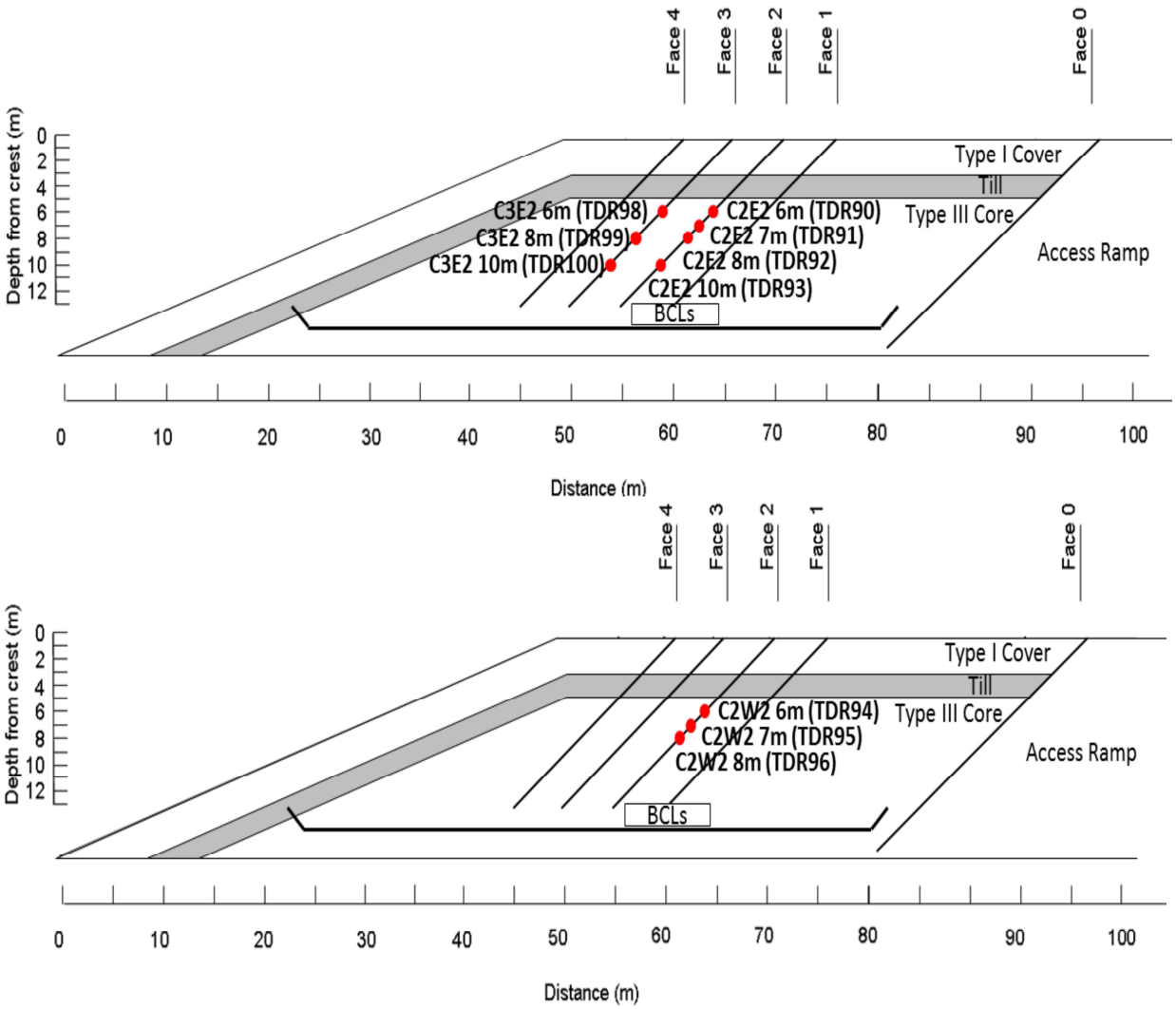

Figure A-13: Location of the TDR probes in the covered pile.

The upper image shows probes located 2m east of centre, and the bottom shows probes located 2m west of centre. Image from Fretz (2013)

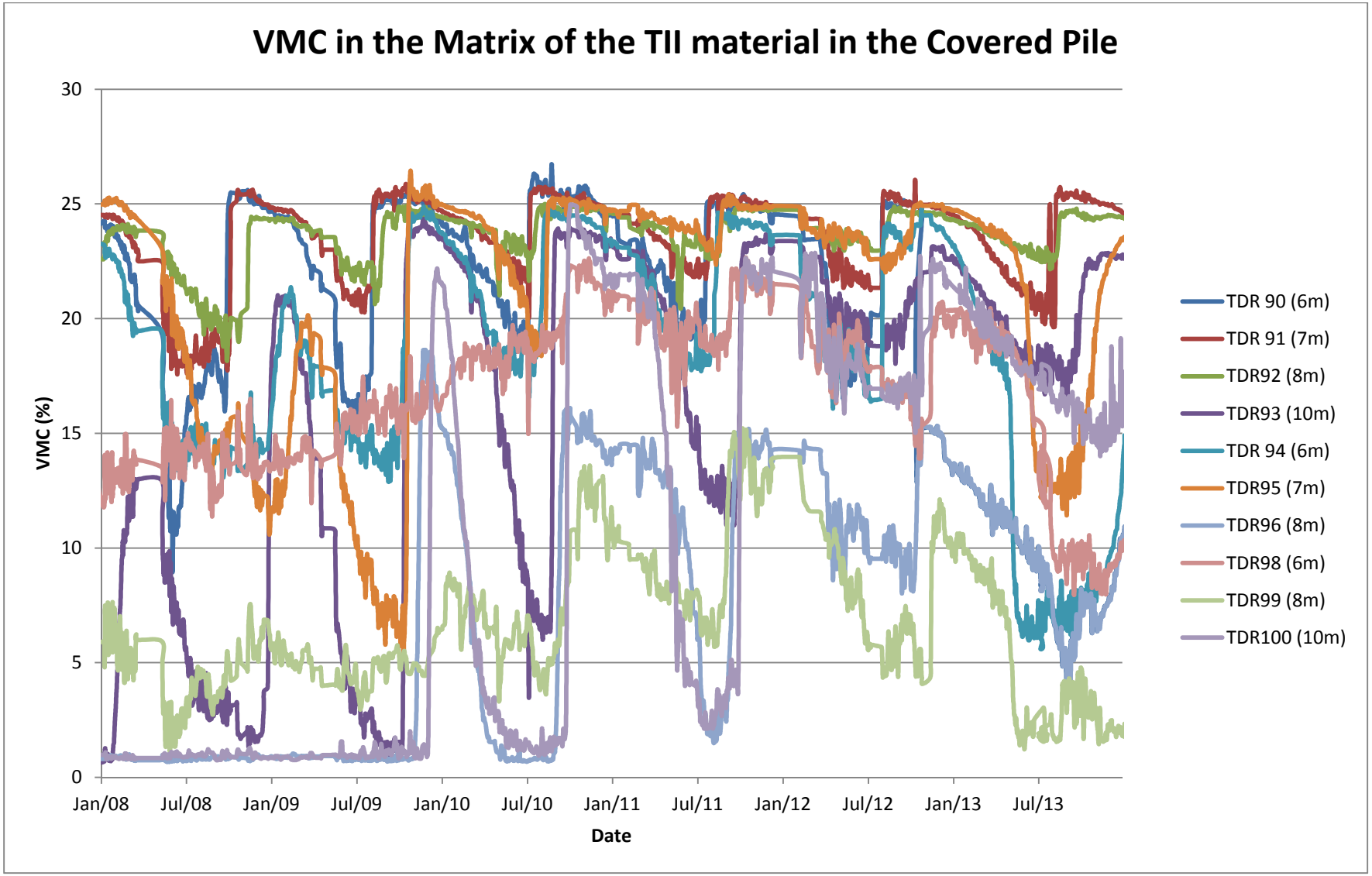

Figure A-14: Volumetric moisture contents measured at the TDR probes in the covered pile

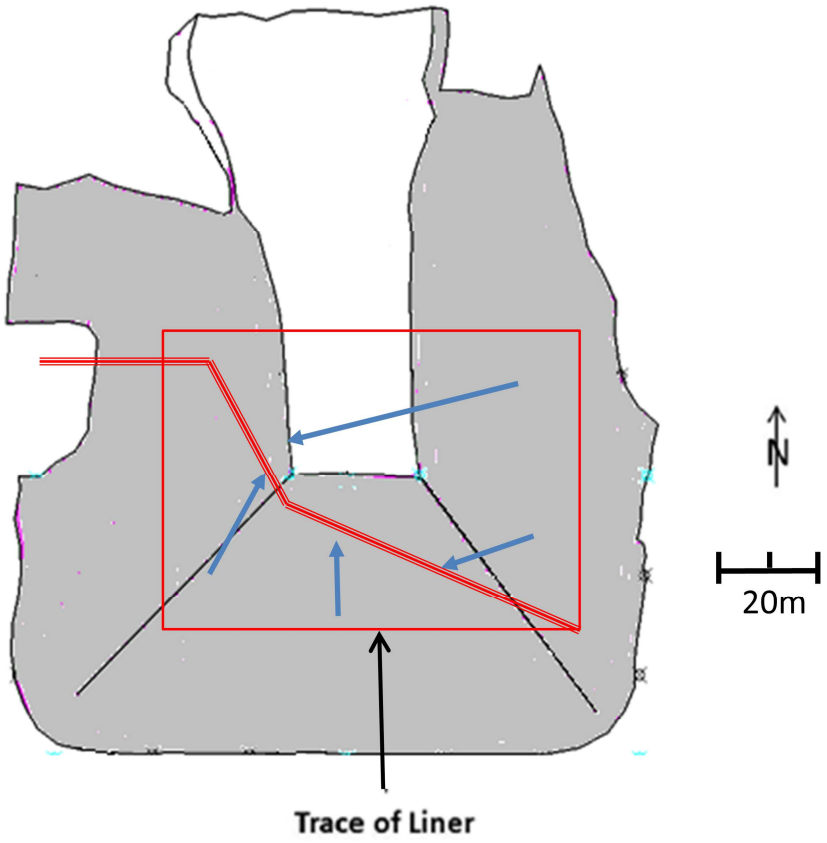

Figure A-15: As built drawing of the covered test pile.
White represents the crown of the pile, grey represents the batters. The thick diagonal red line shows the basal drain location, and the thin red line shows the extent of the HDPE liner. The blue arrows show intended flow directions. The BCLs in the covered pile are not shown, since they have never conducted flow.

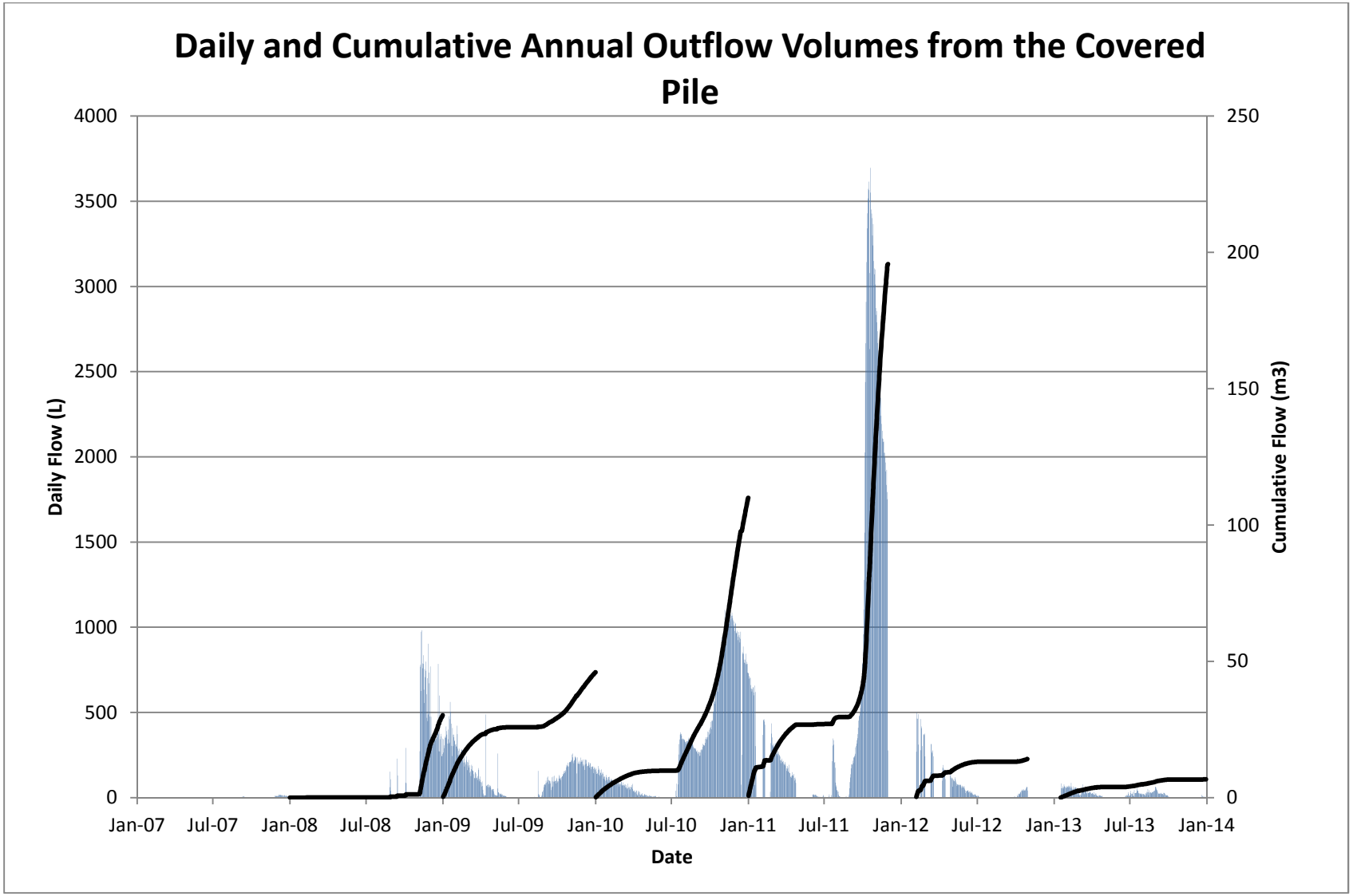

Figure A-16: Daily and cumulative annual outflow from the covered pile basal drain

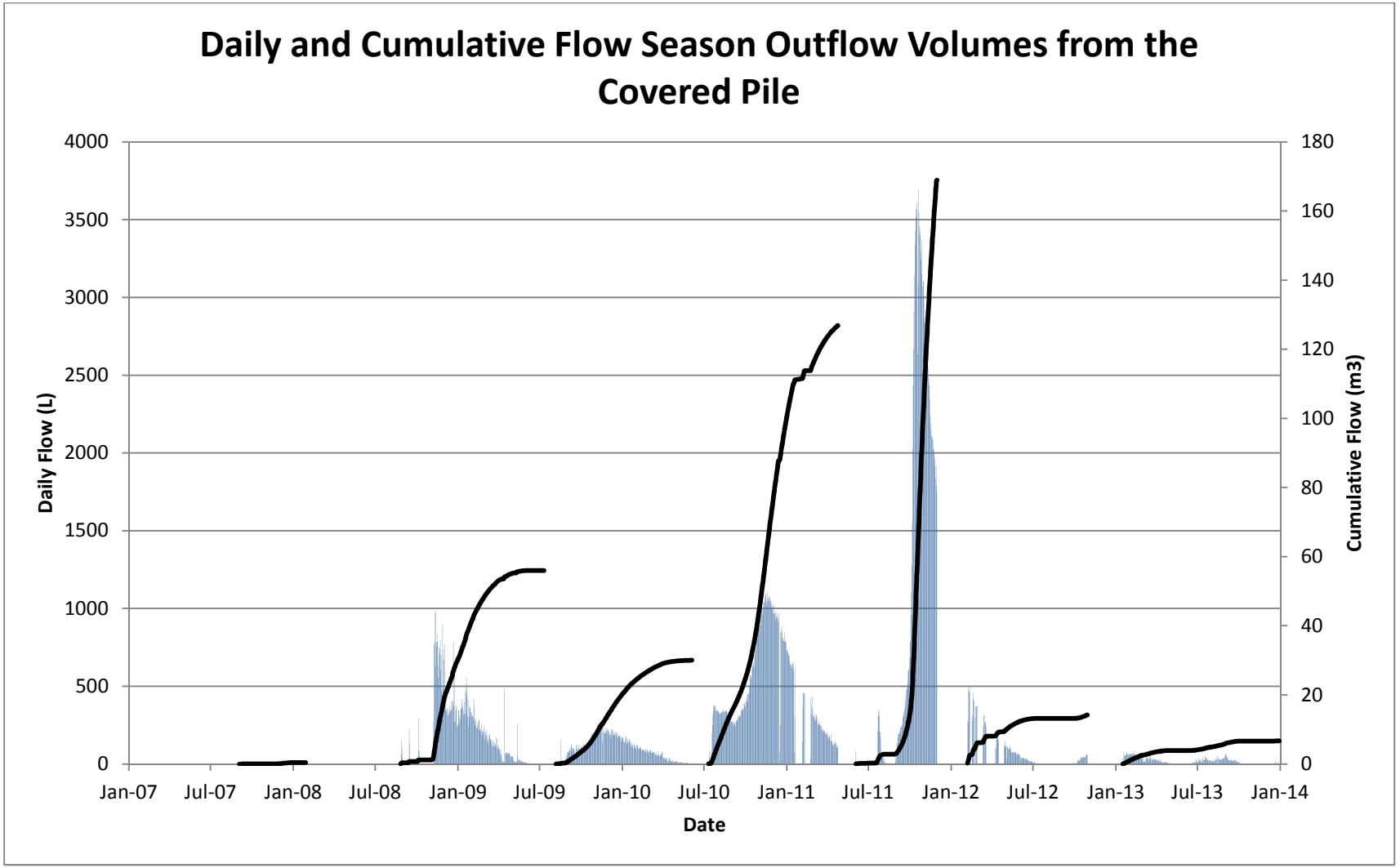

Figure A-17: Daily and cumulative flow season outflow from the covered pile.
In this figure, the cumulative values are defined by the onset and termination of flow, which does not occur on an annual basis as it does in the other drains.

Table A-8: Outflow volumes and start/stop dates for the covered pile.

Covered Pile Drain		
Flow Start	Flow Stop	Discharge (m^3)
3-Sep-07	28-Jan-08	0.5
26-Aug-08	10-Jul-09	56
6-Aug-09	4-Jun-10	30
11-Jul-10	24-Apr-11	127
3-Jun-11	30-Nov-11	169
6-Feb-12	29-Oct-12	14
16-Jan-13	Ongoing	7

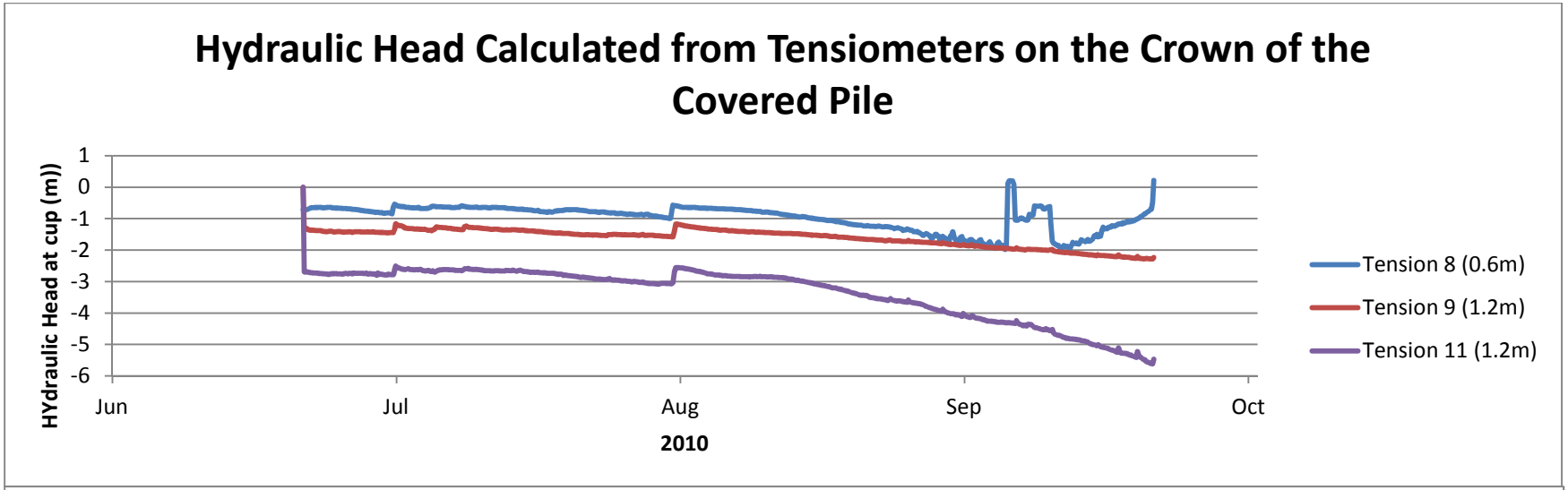

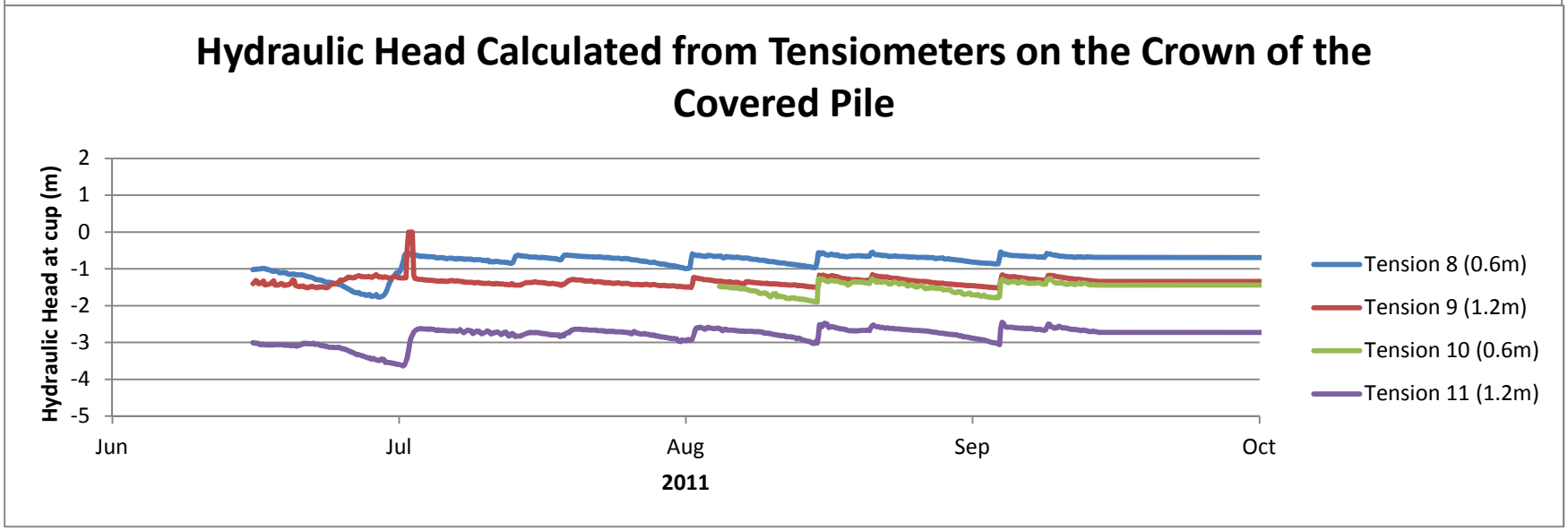

Figure A-18: Hydraulic Head calculated from tensiometers on the crown of the covered pile
(Continued on next page).

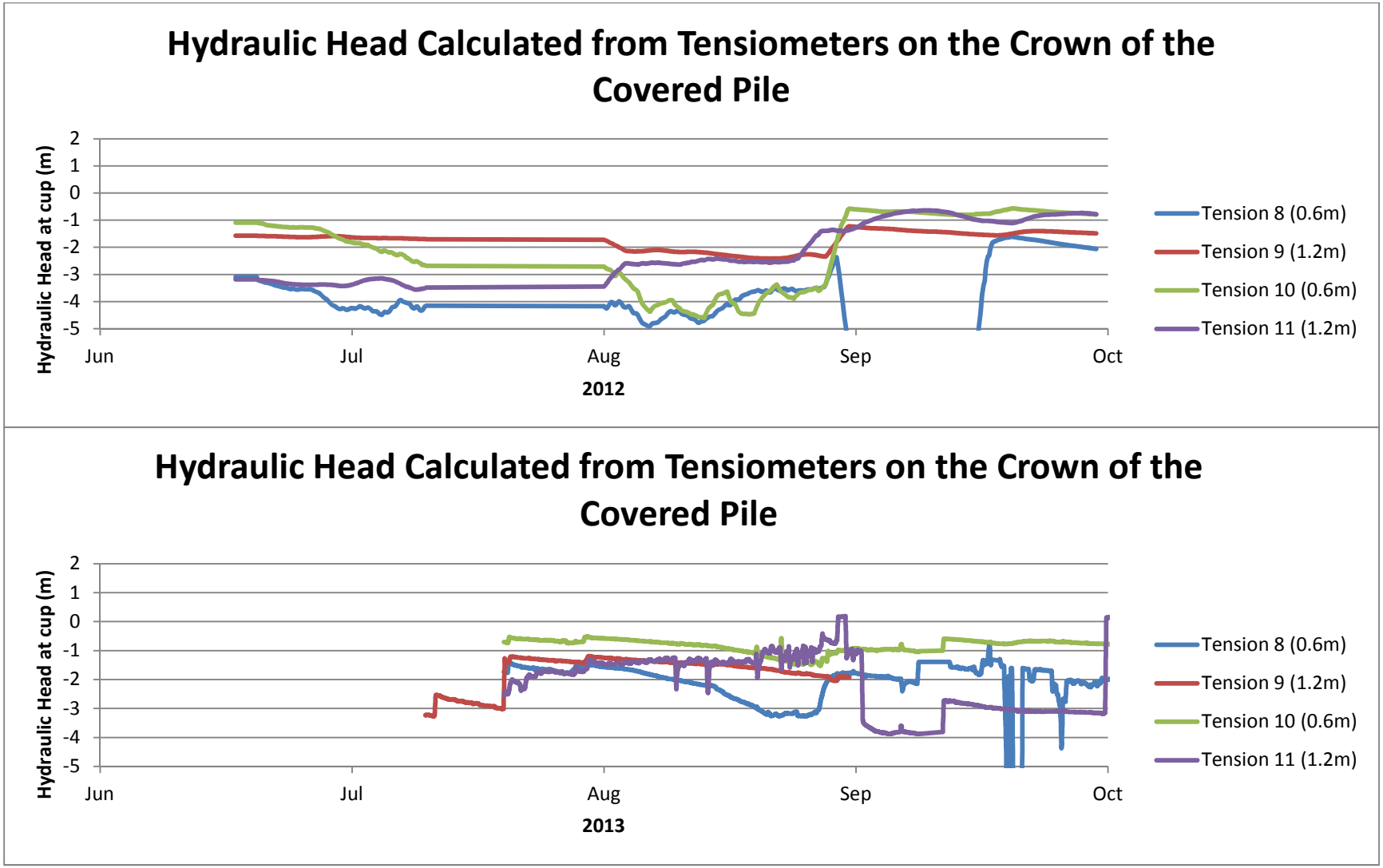

Figure A-17: Hydraulic head calculated from tensiometers on the crown of the covered pile.

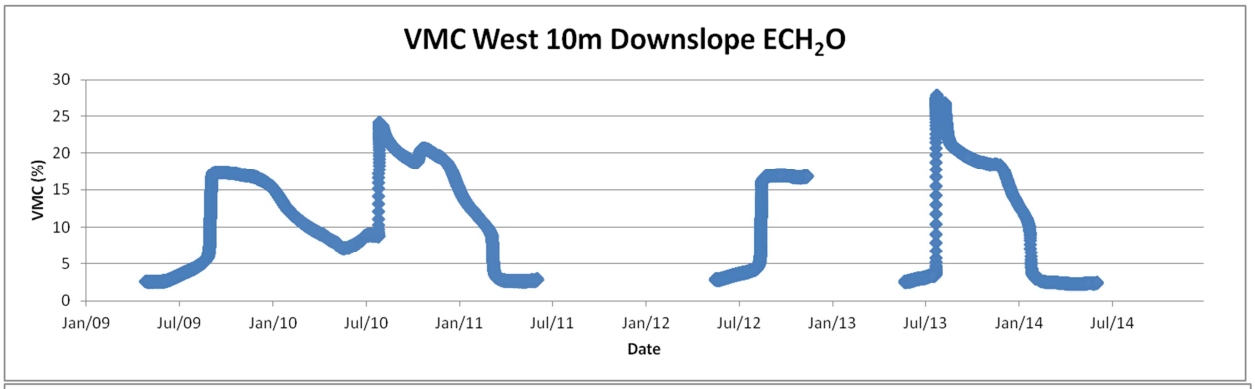

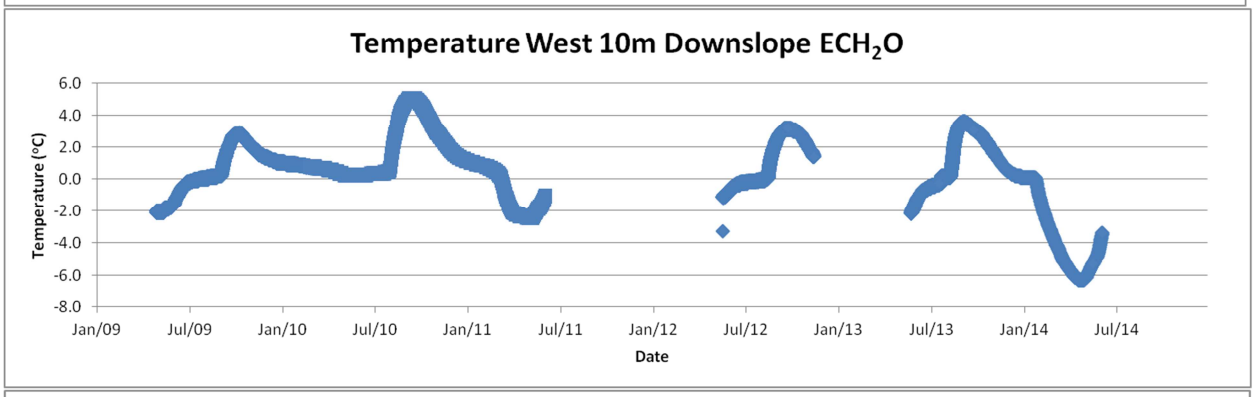

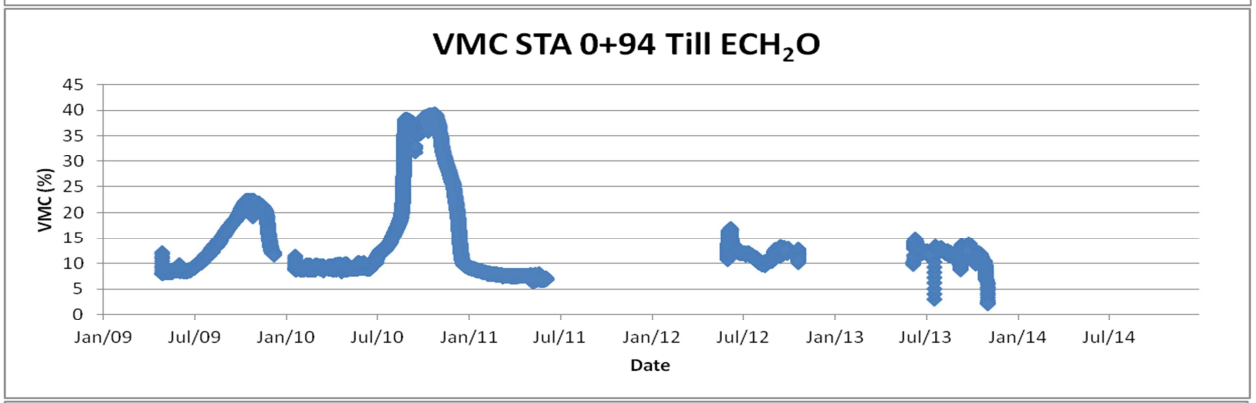

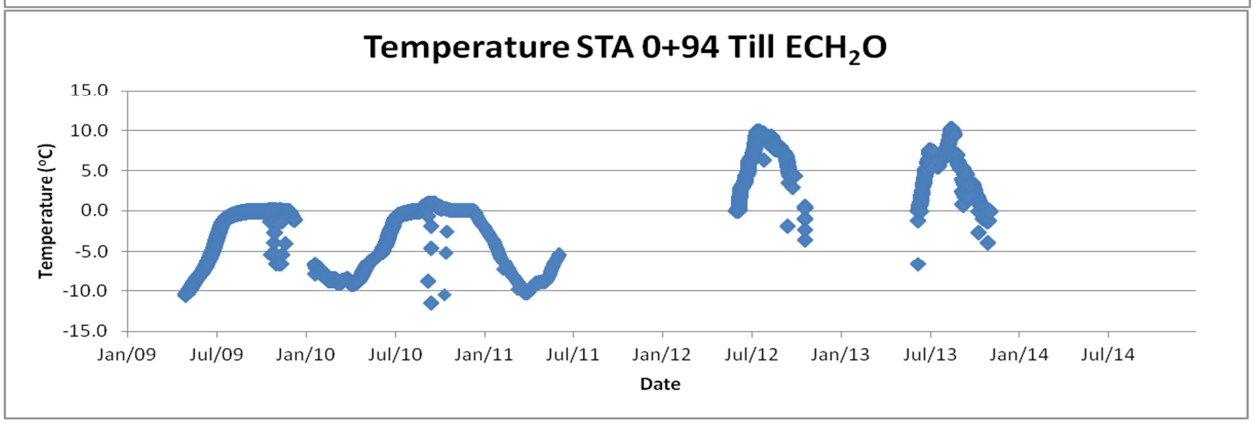

Figure A-19: VMC and temperature measured using the ECH2O probes
(continued on next page)

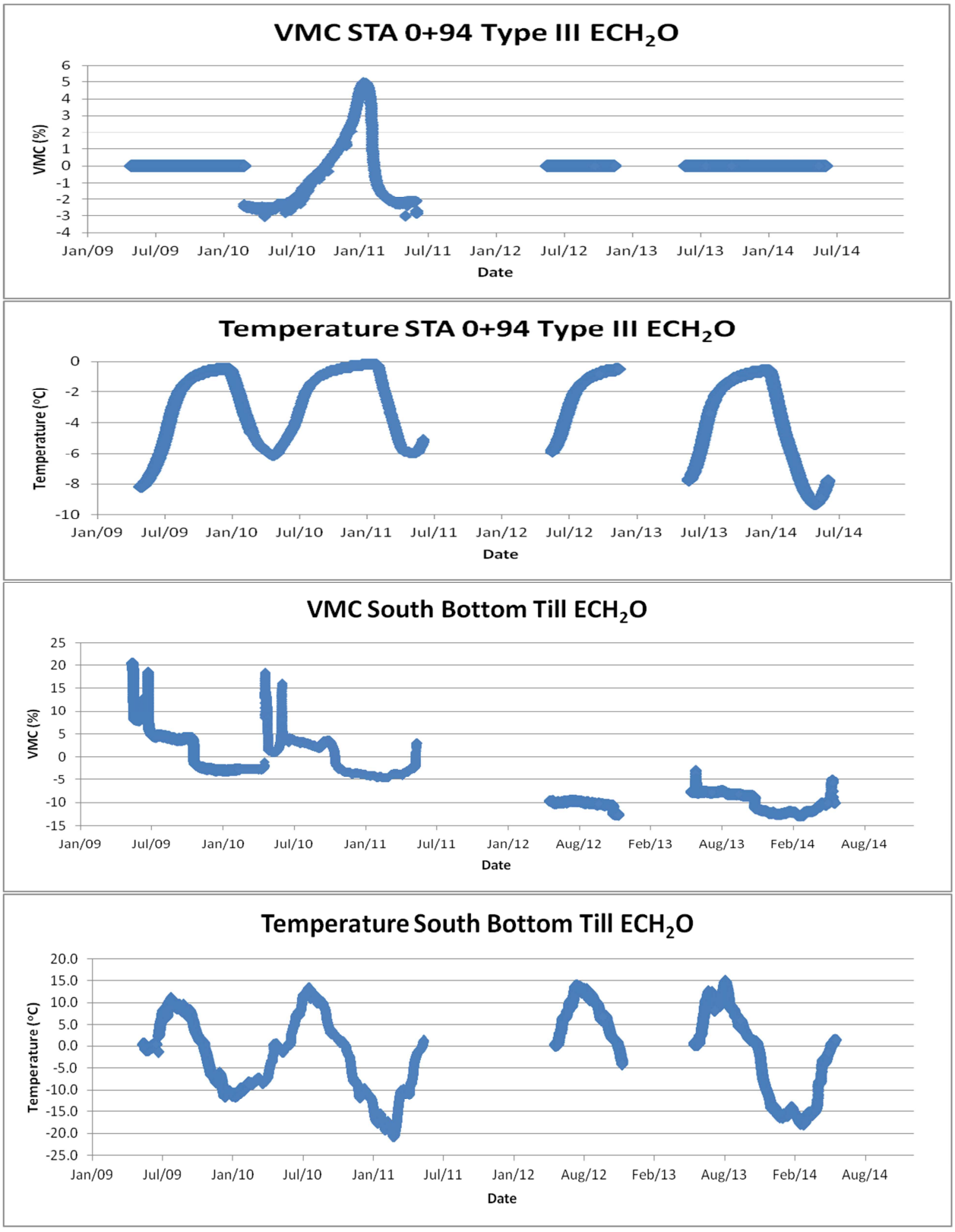

Figure A-18: VMC and temperature measured using the ECH2O probes (continued on next page)

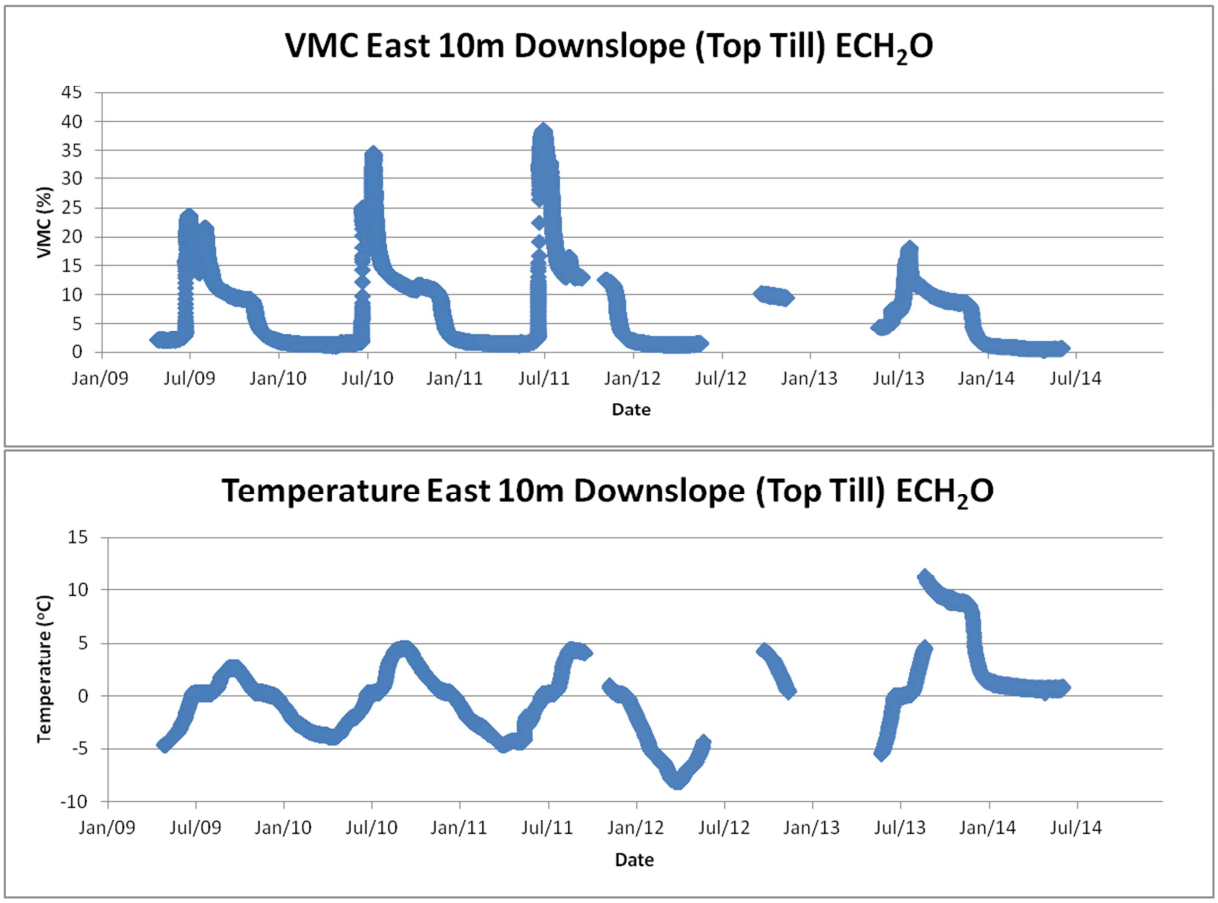

Figure A-18: VMC and temperature measured using the ECH2O probes

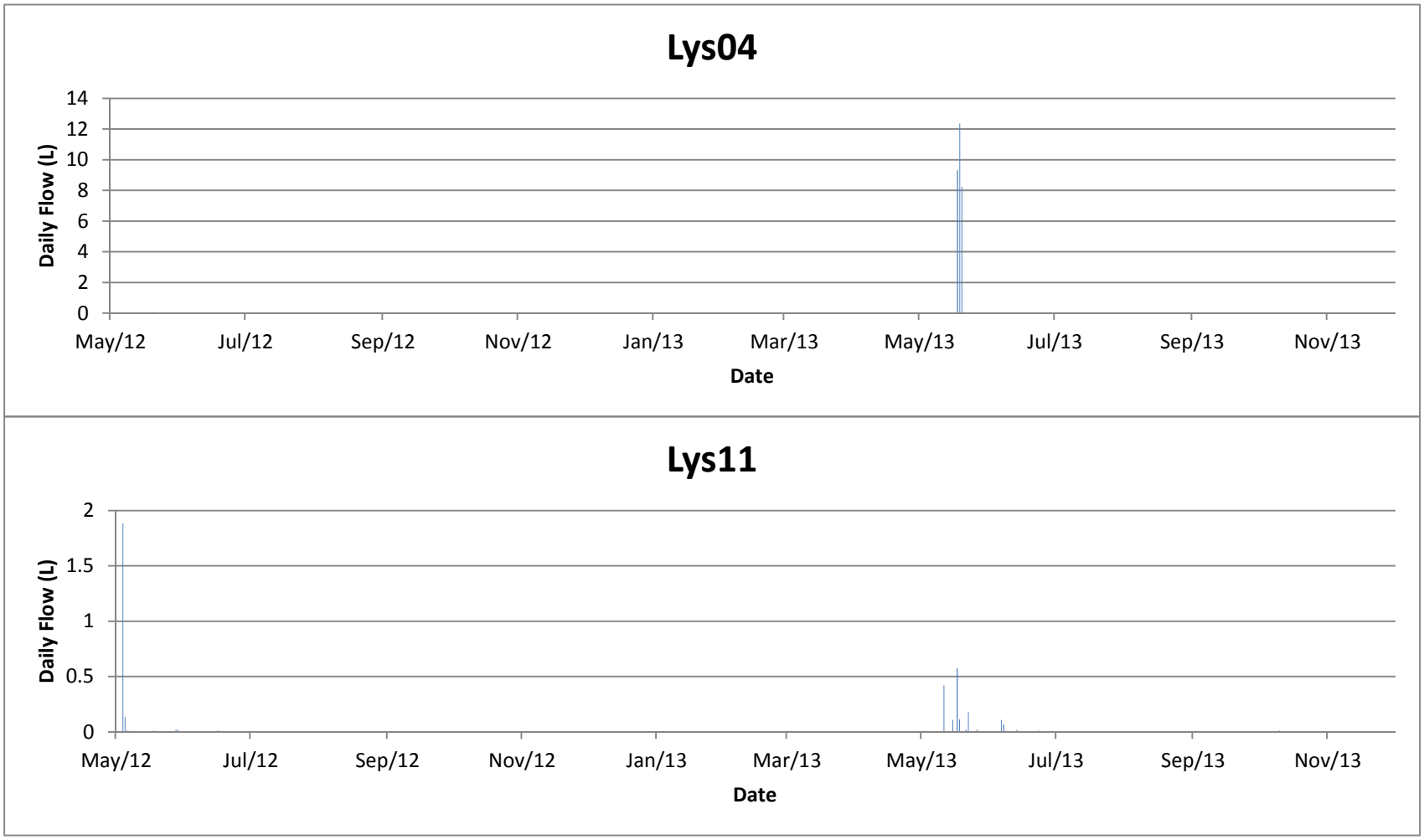

Figure A-20: Water collected by the lysimeters on the east batter of the covered pile. The LysTill lysimeter has not collected significant water since the tracer was applied

Table A-9: Snow survey 21 April, 2010

Snow Depth Survey			
By:	Jeff Bain and Stefan Gopaul		
		21-Apr-10	
Location	**Picket #**	**Depth (cm)**	
WN2A		40-50	
WN2A		35-45	
WN1		0	
WN1a		0	
wc1	18	0	
ec1		0	
EN2A		0	
EN2		10 + 10 cm ice	
EC2		5 cm ice, 0-20 cm snow nearby	
SE2		0-15	
SE3		0-10	
?	29	35	
?	19	0	
?	30	0	
WC2	17	15-20	
WN3	13	40-45	
WC3	16	0-10	
WC4		45-50	
WS4		65-70	
WS3		0	10 cm nearby
SC3		10 cm ice, 15 cm snow	
between SC3 and WC3 a ~10 m wide drift @80 cm deep running from to to toe			
SW4		65	
SC4		5	
SE3		5	
SE4		0	
ES3		0-5	
EC3		0-5	slush and ice
EN3		0-10	
EN3A		0	
EN4		25+ some ice	
?	24	20-25	
ES5		65	
ES4		0	
ES5a		55	near plowed material/drift
Location	**Picket #**	**Depth (cm)**	
SE4a		5-10 + some ice	

SE5a		20-25	
SE4		0	
SC4		0-10	slush and ice
SC5		10	
SW5		5-10	
SW5a		10-25	icy, near toe of large drift
WC5		90-110	

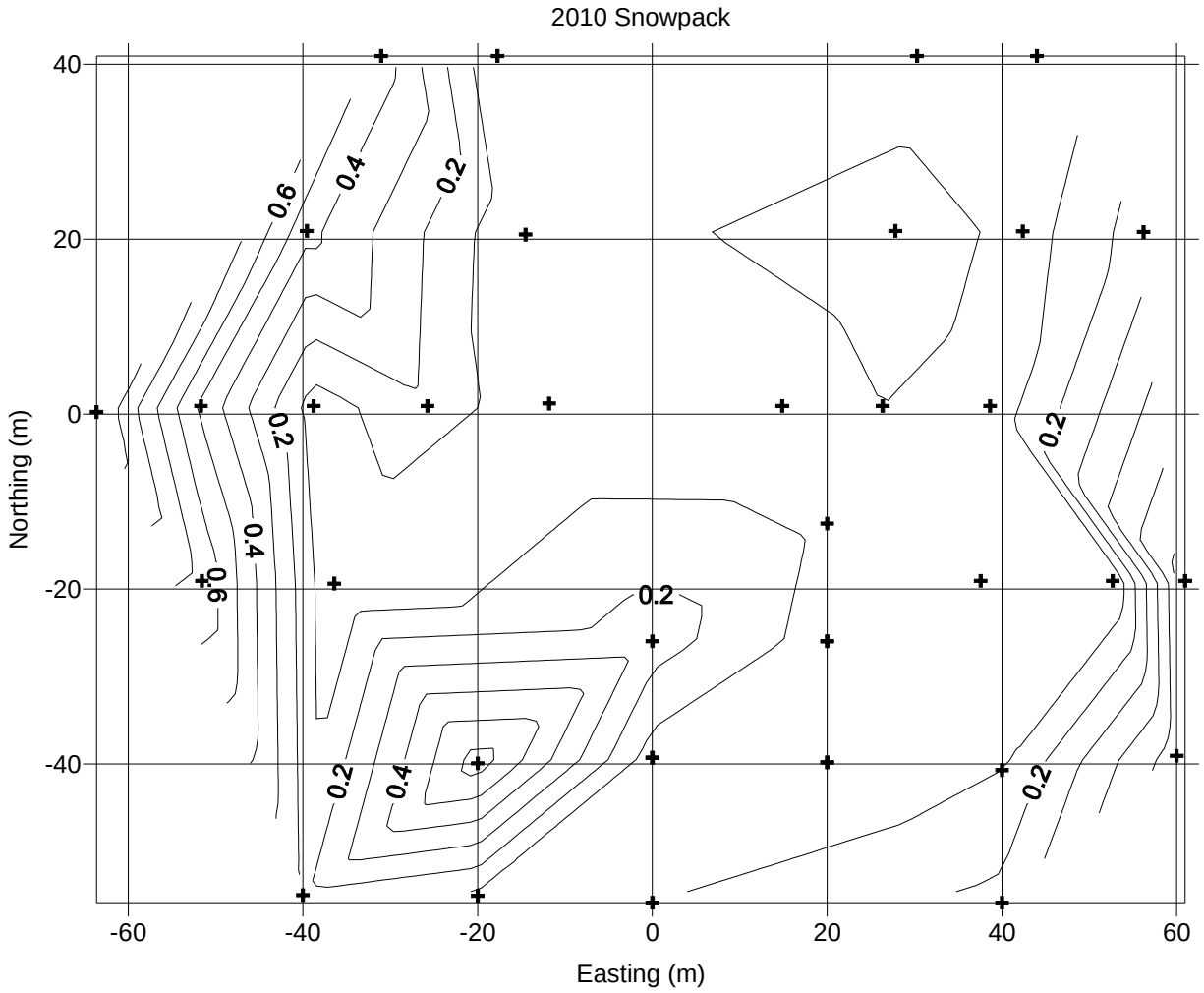

Figure A-21: Snowpack contours April 21, 2010

Table A-10: Snow survey 13 April, 2011

13-Apr-11		Jeff Bain	Surveyor: Gavin Hodgson		
small core tube empty		12	cm H2O		(core max length 30-35 cm)
long core tube empty		38	cm H2O		
Location	Snow depth	Length of snow core	Equivalent cm of water	Corrected cm water	Notes
WN1a	0-1				
WN2a	15		15	3	short
	no location, but depth is probably near 50 cm between 1a and 2a				
WN5a	43	30	42	4	long
WN3	20		18	6	short
WN2	42	38	49	11	long
WN1	0				
WC1	0-5				rocks
WC2	25		19	7	short
WC3	21	16	17	5	short
WC4	23		16	4	short
WC5	73	52	52	14	long
WS5	120		65	27	long
WS5a	plowed area		n/a		
SW5a	71	65	62	24	long
SW5	68	62	55	17	long
SC5	35		n/a		long
SE5	33	31	48	10	long
SE5a	120	100	70	32	long
SE4a	47		51	13	long
ES5a	42		54	16	long

Location	Snow depth	Length of snow core	Equivalent cm of water	Corrected cm water	Notes
ES5	103	100	65	27	long
ES4	15		18	6	short
EC4	33		22	10	short
EC5	45		50	12	long
EN4	65	38	49	11	long
EN3a	17				
EN3	10				
EC3	35				
ES3	36				
SE3	20				
SE4	26				
SC4	23				
SW4	43				
SW4a	35				
WS4	36				
WS3	100? 10?		n/a		
SW2	7				
SW3	25				
SC3	28				
SC2	2-3				
SE2	2-3				
EC2	35	20	21	9	short
EN2	20		18	6	short
EN2a	0-3				
EN1a	0-3				
EN1	0-3				
EC1	2-5				bouldery, crevaces
SC1	2-5				snow pack starts 1-2 m below this point

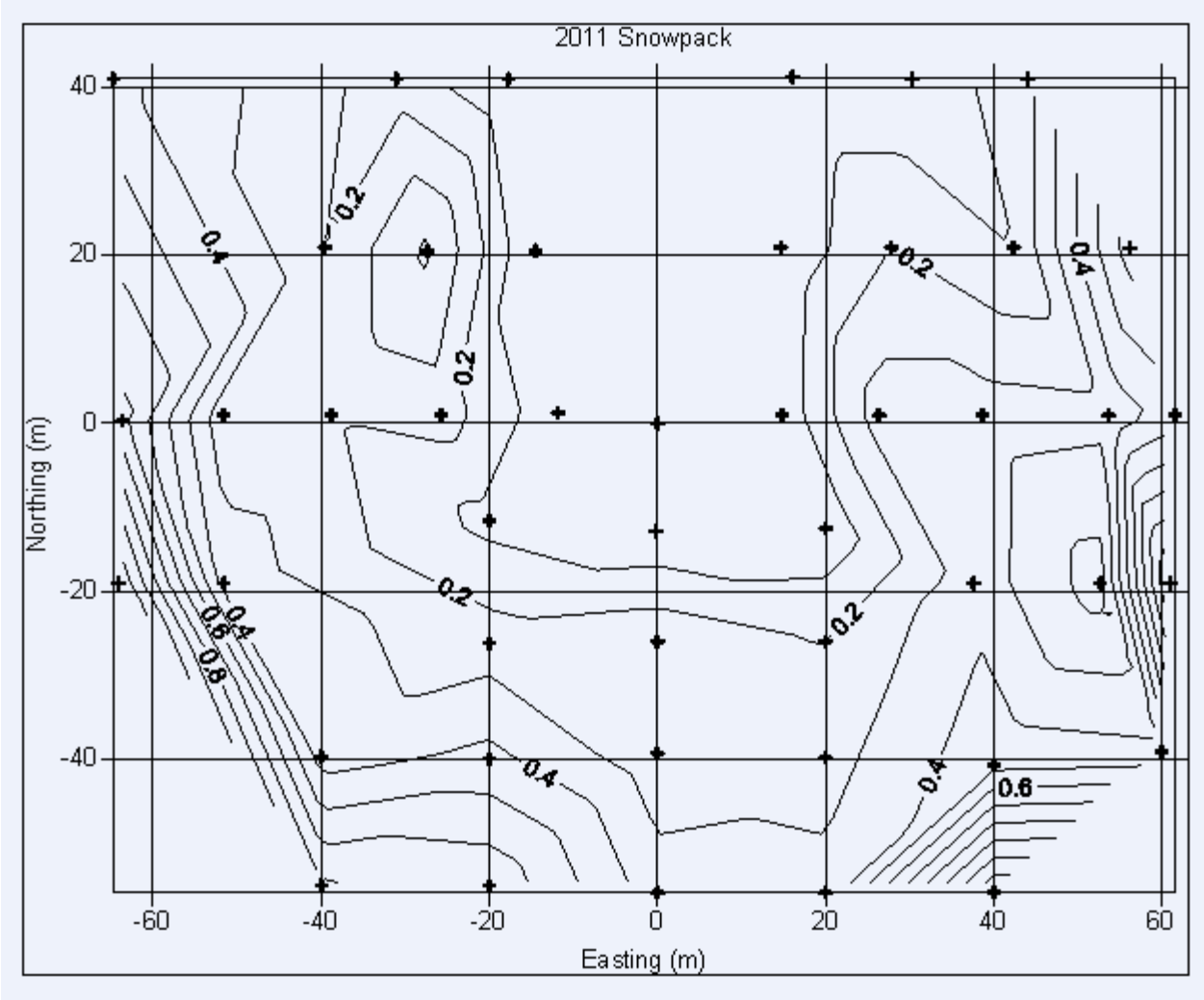

Figure A-22: Snowpack contours April 13, 2011

Table A-11: Snow survey April 10, 2013

Corrected mass = core mass - empty tube mass						
Empty tube mass = 38 cm H2O (**Says 40 in the book but I think you said on the SOP it said 38?)						
Location	**Location**	**Snow Depth (cm)**	**Core Length (cm)**	**Core mass (cm H2O)**	**Corrected Mass (cm H2O)**	**Notes**
B28982	WN5A	70	64	56.5	18.5	
B28981	WN2A	80	74	61	23	
B2898C	WN1A	1	N/A	N/A		
B2897E	WN1	3	N/A	N/A		
B2897F	WN2	78	71	61	23	
B28980	WN3	55	44	54	16	
B2896C	WC2	26	14	44	6	
B2896C	WC2	30	19	45	7	Second coring for location
B2896D	WC3	43	38	50	12	
B2896E	WC4	55	51	53	15	
B2896F	WC5	110	91	65	27	
B2896F	WC5	110	104	69	31	Second coring for location
B28986	WS5	155	91	65	27	
B28986	WS5	150	145	84	46	Second coring for location
B28984	WS4	63	44	52	14	
B28984	WS4	70	49	54	16	Second coring for location
B28983	WS3	19	18.5	45	7	*
B28953	SW2	2	N/A	N/A	N/A	
B28955	SW3	45	35	52	14	
B28955	SW3	45	35	50	12	Second coring for location

Location	Location	Snow Depth (cm)	Core Length (cm)	Core mass (cm H2O)	Corrected Mass (cm H2O)	Notes
B28956	SW4A	35	35	50	12	
B28987	WS5A	90	74	60	22	
B28957	SW5A	74	45	55	17	
B28957	SW5A	74	62	60	22	Second coring for location
B28952	SW4	98	70	67	29	Very hard ice at 65 cm
B28952	SW4	95	86	75	37	Second coring for location
B28954		61	53	57	19	
B28954		59	56	58	20	Second coring for location
B2892E	SC5	30	29	47	9	
B2892E	SC5	28	27	47	9	Second coring for location
B2894F	SE5	46	44	52	14	
B28923	SC4	26	24	45	7	
B28921	SC3	33	29	47	9	
B28922	SC2	20	20	49	11	
B2891C	SC1	4	N/A	N/A	N/A	
B28970	EC1	4	N/A	N/A	N/A	
B2894C	SE2	16	16	42	4	
B2894D	SE3	5	N/A	N/A	N/A	
B2894E	SE4	11	11	42	4	
B28950	SE5A	101	98	72	34	
B28951	SE4A	20	18	44	6	
B28989	ES3	28	25	49	11	
B2898A	ES4	8	8	41	3	
B2898B	ES5	110	108	71	33	
B28975	EC5	62	58	56	18	

Location	Location	Snow Depth (cm)	Core Length (cm)	Core mass (cm H2O)	Corrected Mass (cm H2O)	Notes
B28976	EC4	28	27	47	9	
B289BA	EC3	18	18	45	7	
B28971	EC2	24	24	46	8	
B28978	EN1	1	N/A	N/A	N/A	
B28977	EN2	9	9	42	4	
B28979	EN3	2	N/A	N/A	N/A	
B2897A	EN4	70	65	61	23	
B2897D	EN3A	25	24	47	9	
B2897C	EN2A	25	24	45	7	
B2897B	EN1A	1	N/A	N/A	N/A	

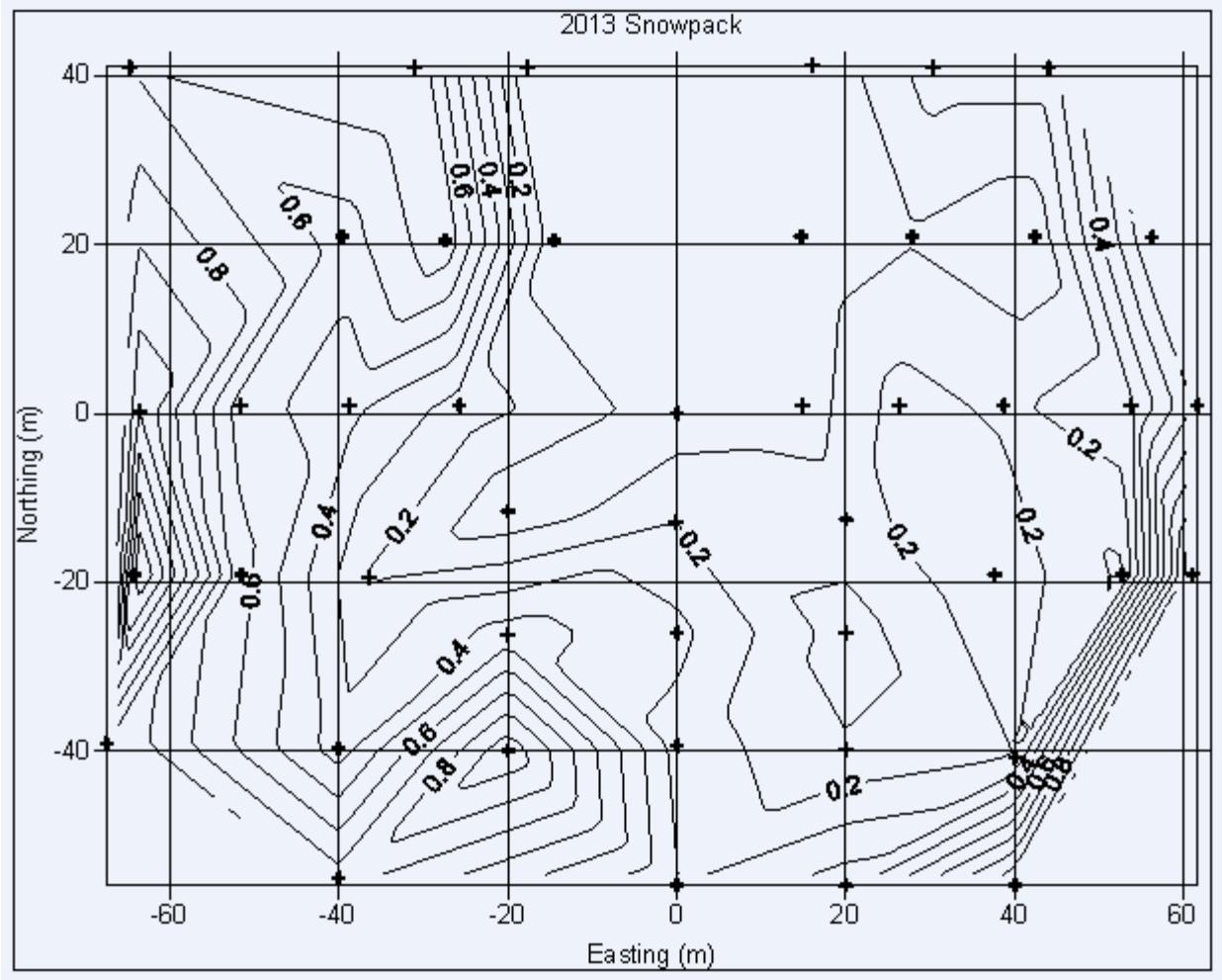

Figure A-23: Snowpack contuors April 10, 2013

Table A-12: Snow survey April 8, 2014

Date		Crew	Surveyor
4/8/2014		AK/AT	Paul Myrick
Small Core Tube Empty		Not Used	cm H2O
Long Core Tube Empty		34	cm H2O

Location	Snow Depth	Length of Snow Core	Eq. cm H2O	Corrected cm H2O	Notes
WN5A	40	33	42	8	
WN2A	26	26	41	7	
WN2	5				
WN1A		No Snow			
WN1		No snow			
WN3	5	5	35	1	
WC3	6	4	35	1	
WC2	6	4	35	1	
WC1		No Snow			
WC4	11	11	37	3	
WC5	70	50	46	12	
WS5	85	82	60	26	
WS4	6	6	36	2	
WS3		No Snow			
WS5A	50	45	47	13	
SW5A	95	90	63	29	
SW5B		In a snow bank			
SW4A	35	35	46	12	
SW5	41	36	45	11	
SW4	98	98	69	35	
SW3	43	43	49	15	
SW2	48	48	46	12	
SC2	22	22	35	1	
SC1		No Snow			
SC3	48	34	43	9	
SC4	43	40	44	10	
SC5	28	25	40	6	
SE5	35	30	45	11	
SE4	60	60	53	19	
SE3	15	15	39	5	
SE2	13	10	36	2	

Location	Snow Depth	Length of Snow Core	Eq. cm H2O	Corrected cm H2O	Notes
SE4A	50	50	51	17	
SE5A	140	111	70	36	
SE5B		In a snow bank			
ES5A		In a snow bank			
ES5	104	40	41	7	
ES4	12	12	38	4	
ES3	15	15	37	3	
EC5	41	36	45	11	
ec4	23	17	39	5	
ec3	23	17	38	4	
ec2		No Snow			
ec1		No Snow			
en1		No Snow			
en2		No Snow			
en3	18	16	40	6	
en4	63	56	52	18	
en3a	20	20	40	6	
en2a	33	33	44	10	
en1a		No Snow			

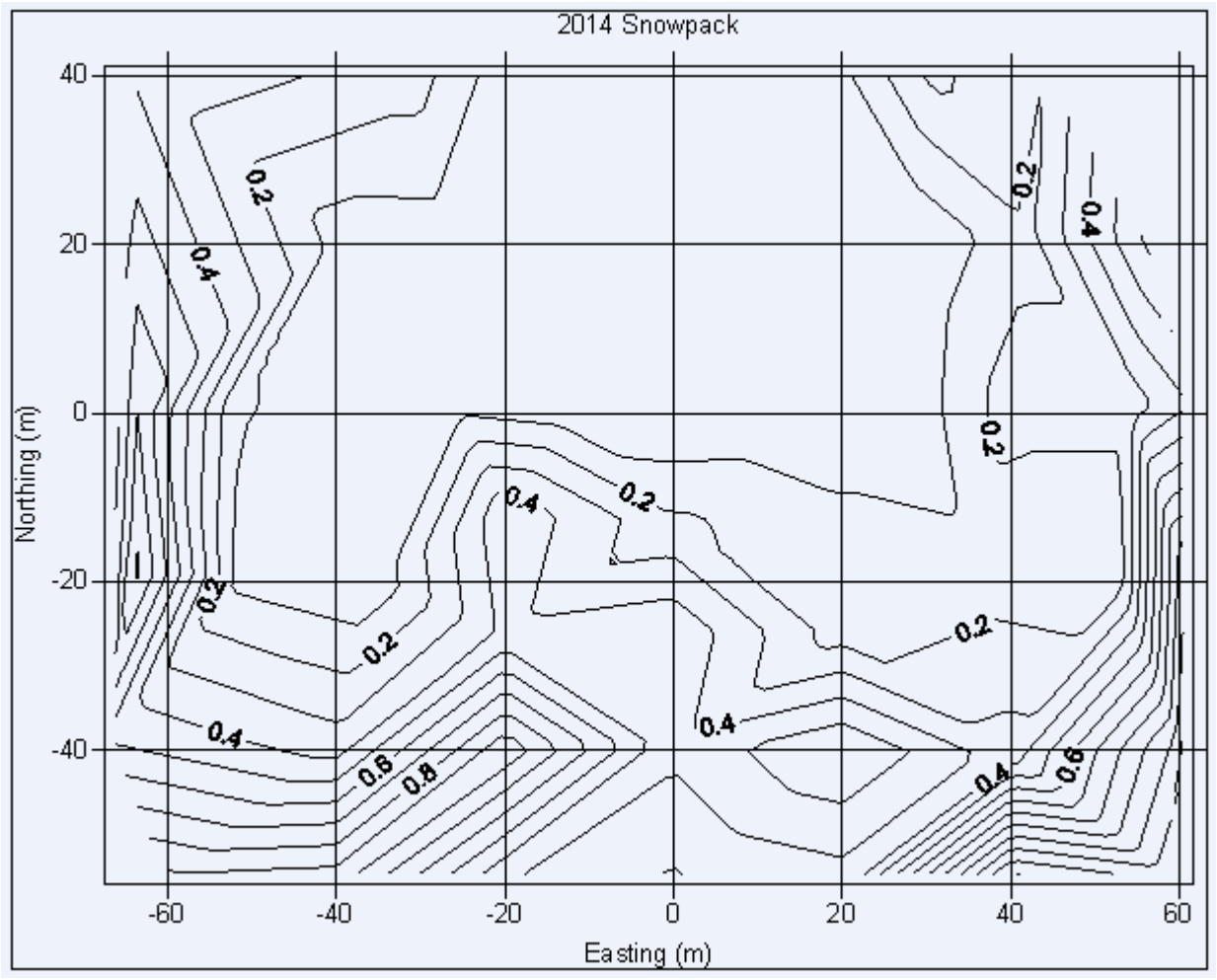

Figure A-24: Snowpack contours April 8, 2014

A.5 Active Zone Lysimeters

The dataset from the AZLs consists of outflow measured from each drain, hydraulic heads measured using tensiometers, and temperature and VMC data measured using ECH_2O probes.

The dataset collected from the AZLs was influence by the flood in December 2012. Power to the datalogger used for the AZLs was interrupted, and a car battery was used as an interim measure to allow data collection to continue. The datalogger failed in September, 2013 and was successfully replaced in early October. The leads on one of the ECH2O probes failed at around the same time as the datalogger, and could not be recovered. During the time period when the datalogger was not functional outflow from the AZLs was collected in 20L pails and measured every 2-3 days using a 1L graduated cylinder.

Outflow from the AZLs was very low in 2012 and 2013. In 2012 the infiltration estimated using the Penman Monteith equation was very low; however, in 2013 it is estimated that over 20mm of infiltration occurred, and outflow from 3 of the 4 AZLs remained low. In the summer of 2013 a video camera was used to examine the drain lines, and no damage was observed within the drain pipes between the data collection trailer and the sharp turn in the drain lines after entering the pile (figure A-25).

Since 2010 two of the three tensiometers have cracked, and are no longer able to hold water. New tensiometer tubes have been installed at the AZls, and it is recommended that they are used in 2015.

Figure A-25 is an as-built drawing of the AZls. Figure A-26 shows the temperatures and VMCs measured by EHC2O probes at the AZLs. Figures A-27 and A-28 show the daily outflow from the type I and type III AZLs respectively. Figure A-29 shows the calculated infiltration versus outflow (in mm) from each of the AZLs. Figure A-30 shows the hydraulic heads measured using tensiometers at the AZLs. Table A-13 shows the start and stop dates along with the total volume of outflow from each AZL.

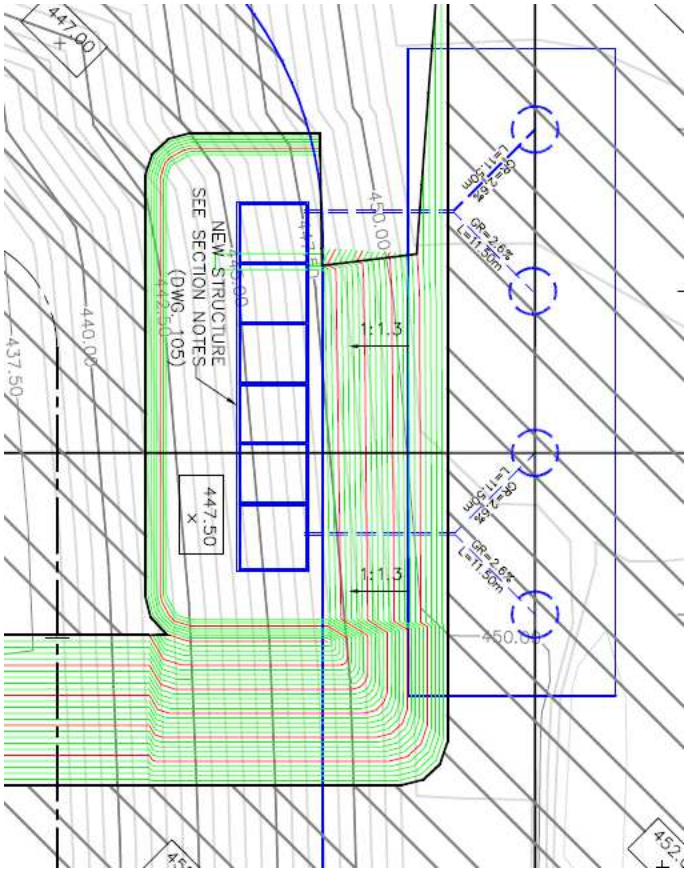

Figure A-25: As-built drawing of the AZLs.
A video camera was successfully used to determine that the drainage lines from two of the AZLs were unbroken, up until the sharp turn in each drain line

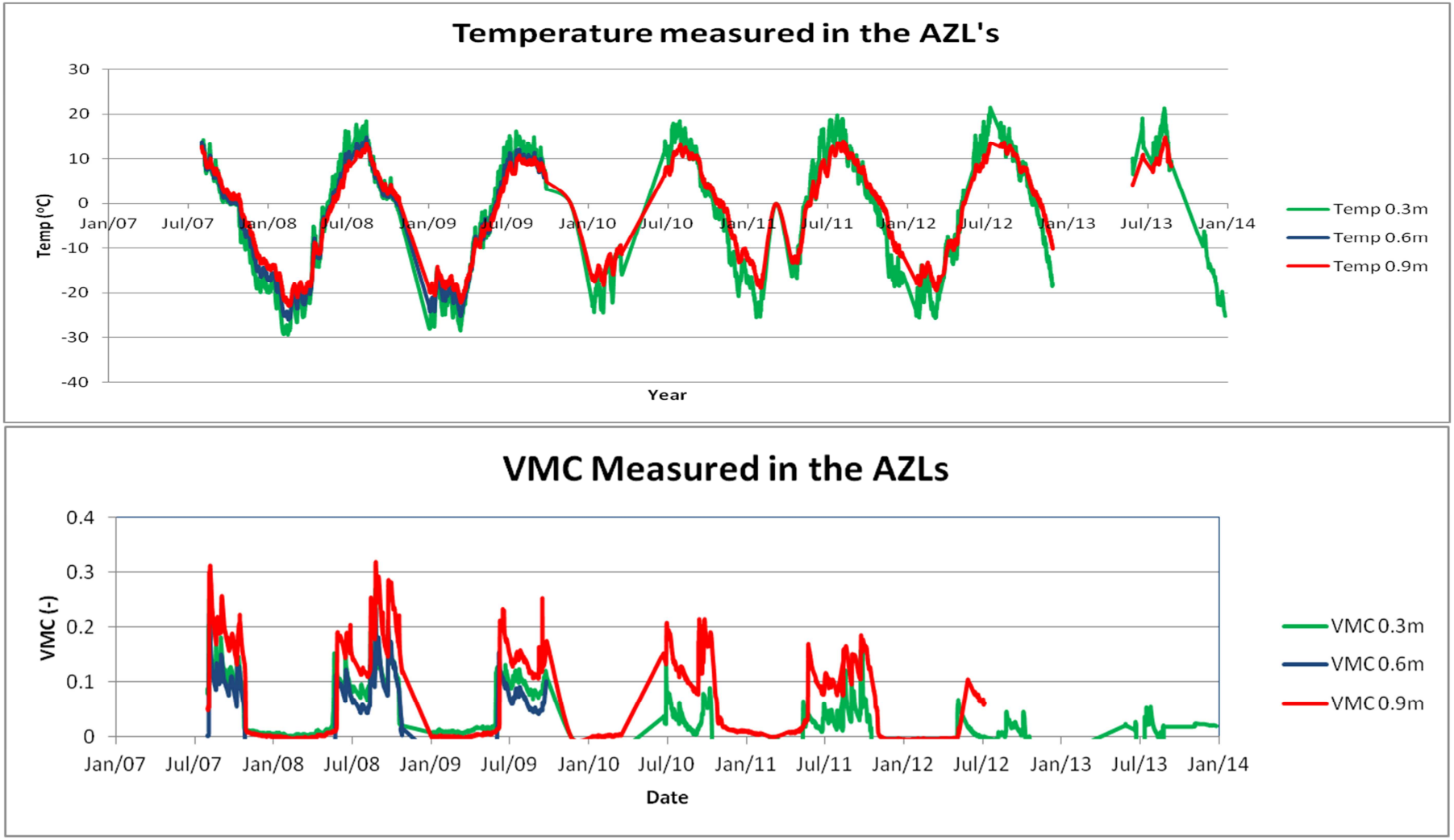

Figure A-26: Temperatures and VMCs measured in the AZLs

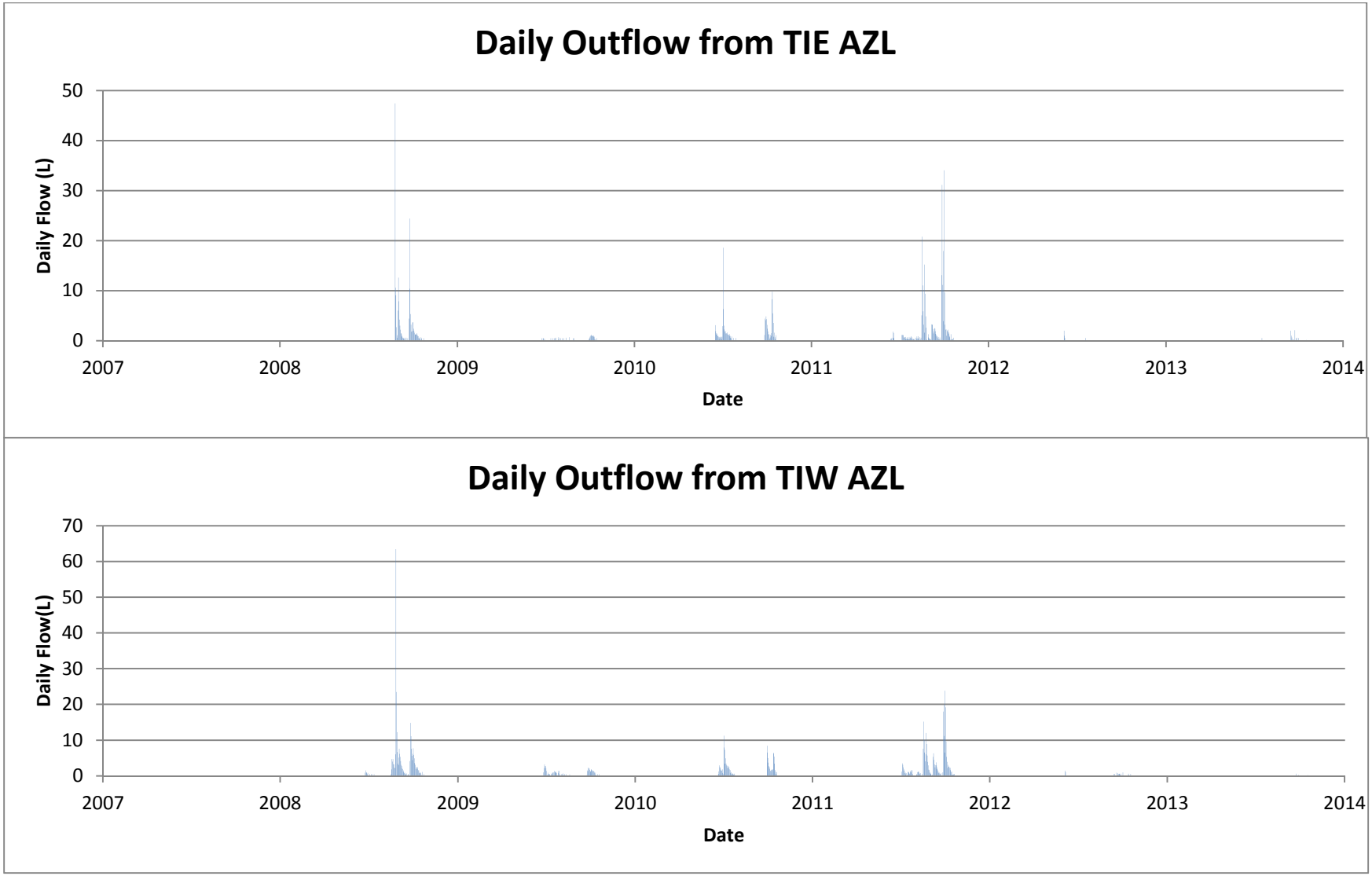

Figure A-27: Daily outflow from the type I AZLs

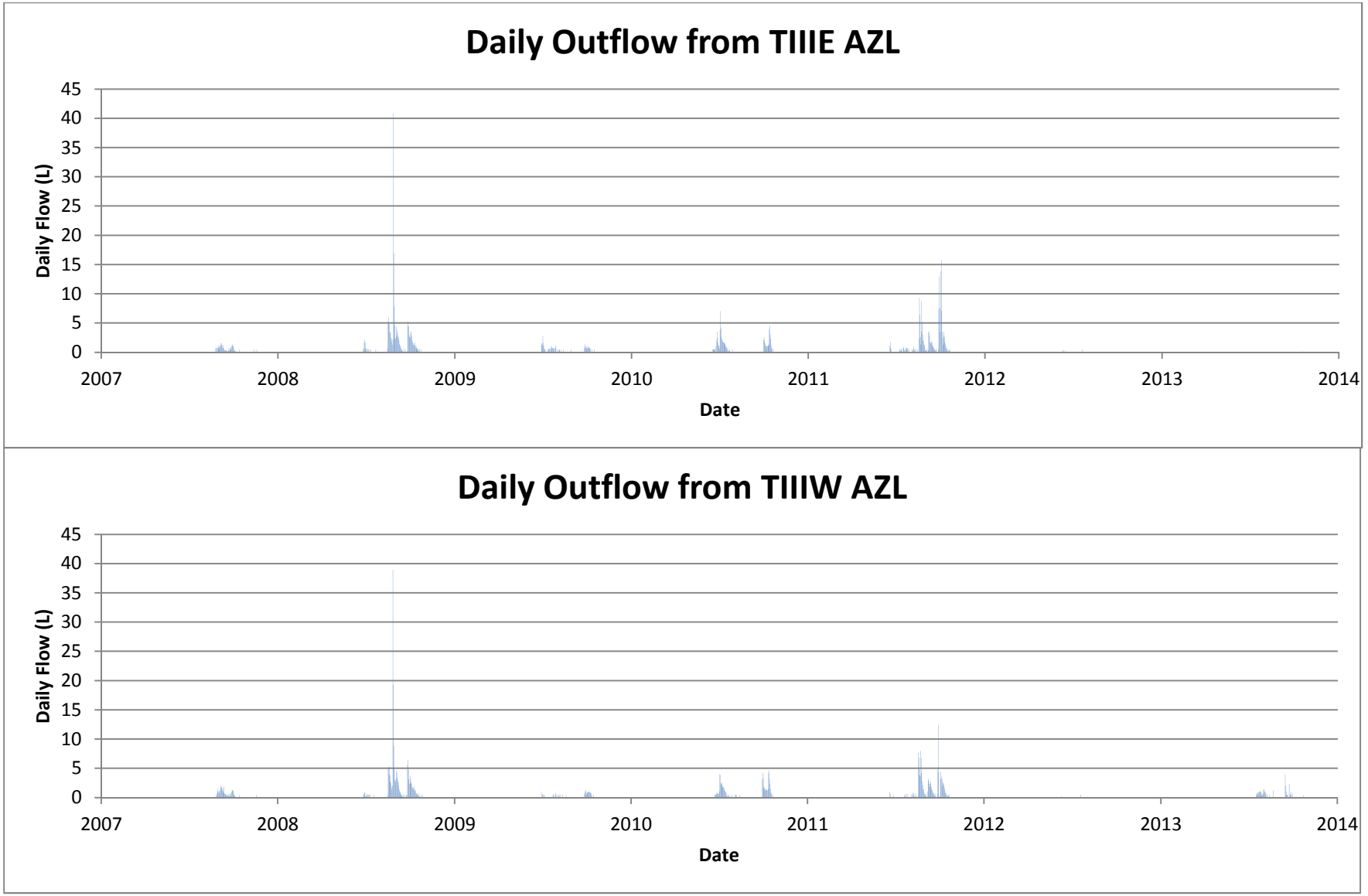

Figure A-28: Daily Outflow from the type III AZLs

Table A-13: Outflow volumes and start/stop dates for the AZLs.

AZLs			
AZL	Flow Start	Flow Stop	Discharge (L)
2007			
TI West	No Flow		
TI East	No Flow		
TIII West	28-Aug	10-Oct	36
TIII East	25-Aug	10-Nov	31
2008			
TI West	17-Aug	21-Oct	297
TI East	25-Aug	23-Oct	194
TIII West	27-Jun	23-Oct	203
TIII East	26-Jun	21-Oct	202
2009			
TI West	26-Jun	15-Oct	66
TI East	26-Jun	15-Oct	22
TIII West	1-Jul	25-Oct	23
TIII East	28-Jun	25-Oct	38
2010			
TI West	21-Jun	19-Oct	147
TI East	10-Jun	19-Oct	134
TIII West	10-Jun	21-Oct	84
TIII East	17-Jun	21-Oct	88
2011			
TI West	4-Jun	20-Oct	309
TI East	5-Jun	24-Oct	283
TIII West	5-Jun	24-Oct	146*
TIII East	5-Jun	20-Oct	185
2012			
TI West	4-Jun	17-Oct	11
TI East	4-Jun	19-Jul	4
TIII West	9-Jun	19-Jul	1
TIII East	9-Jun	19-Jul	2
2013			
TI West	18-Jul	17-Oct	1
TI East	16-Jul	30-Oct	9*
TIII West	17-Jul	30-Oct	35
TIII East	< 1L flow		

*Unknown amount of missing flow

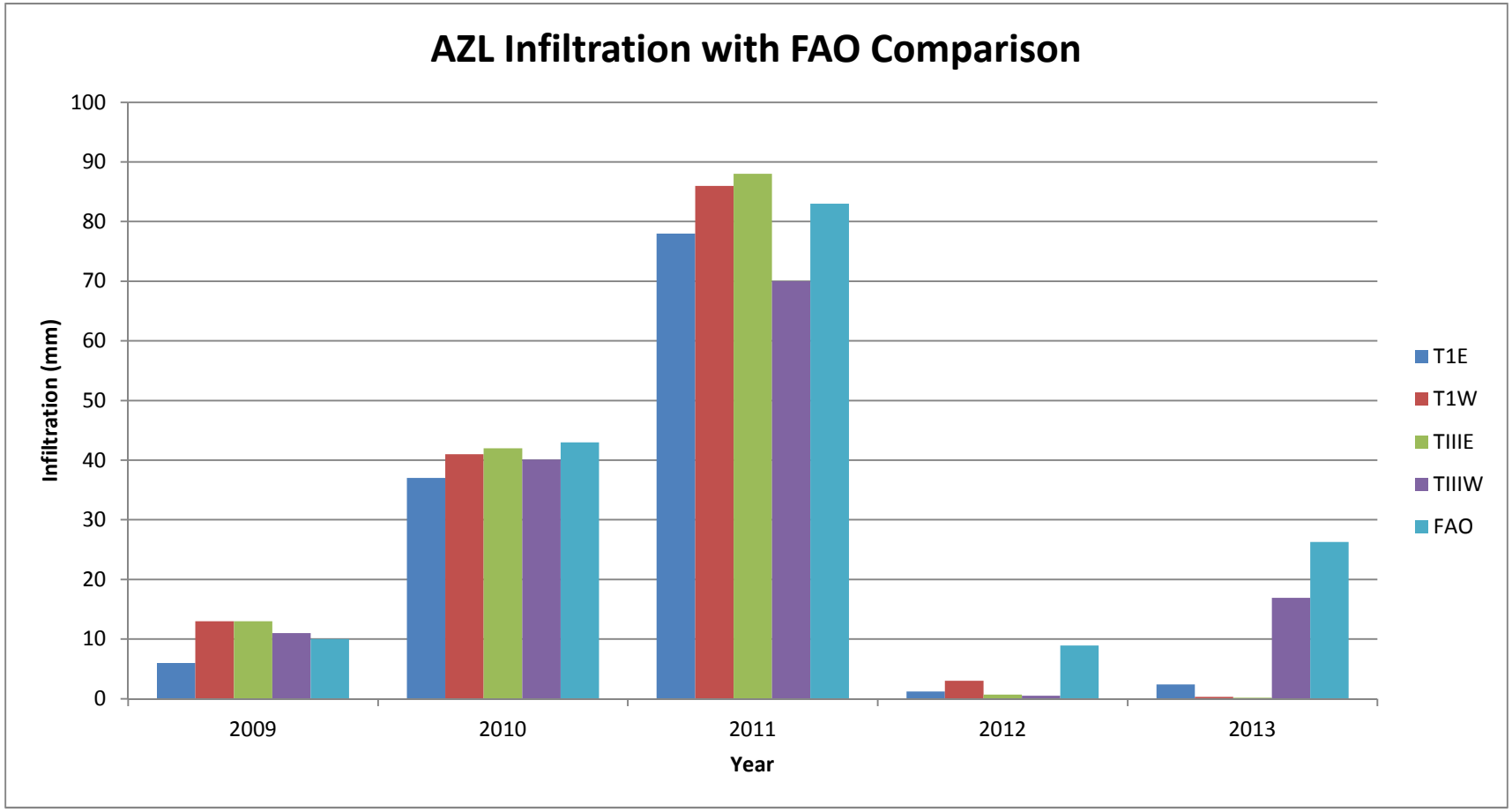

Figure A-29: Infiltration into the AZLs compared to the FAO calculated amount of infiltration

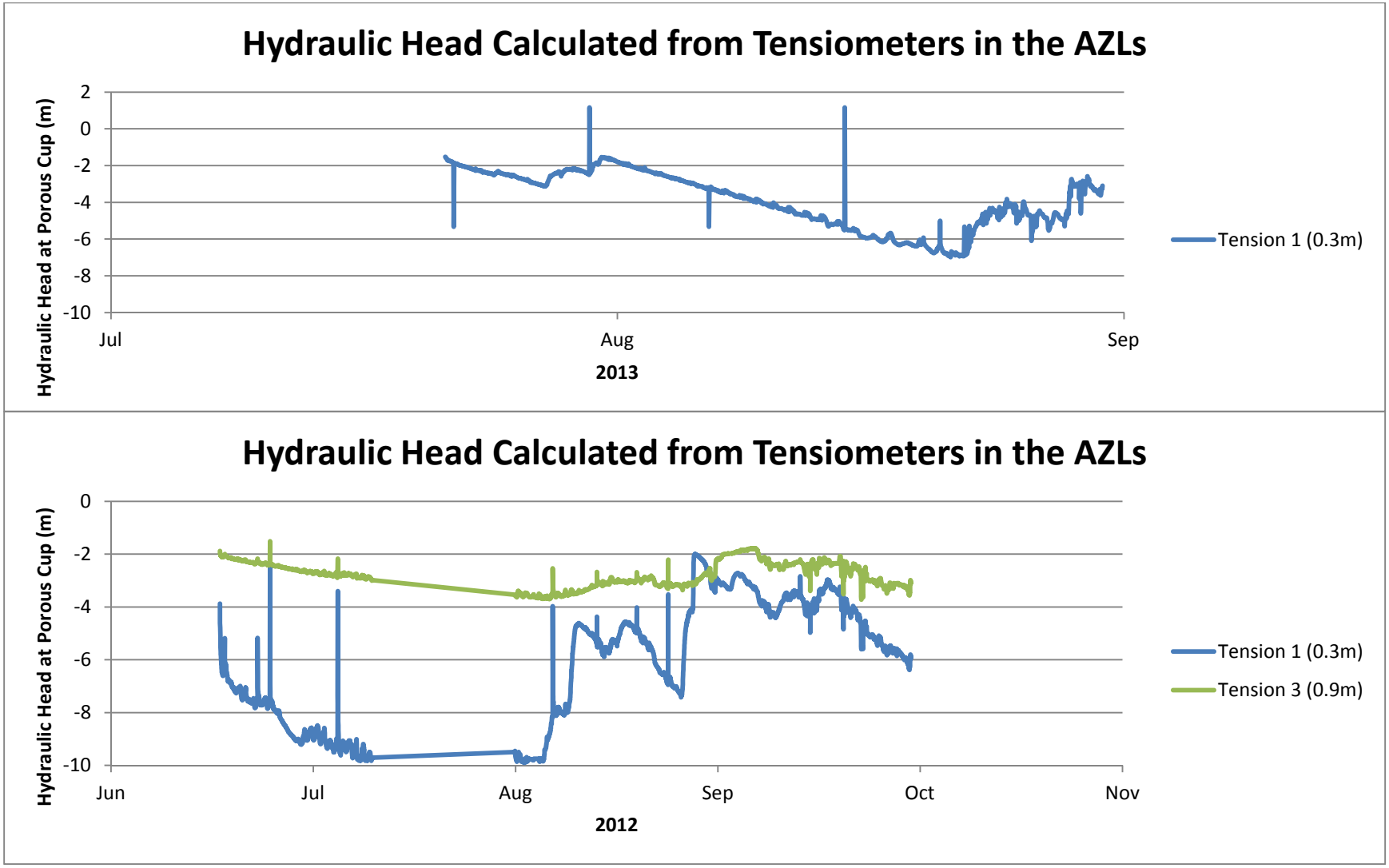

Figure A-30: Hydraulic head calculated from tensiometers in the AZLs (continued on next page)

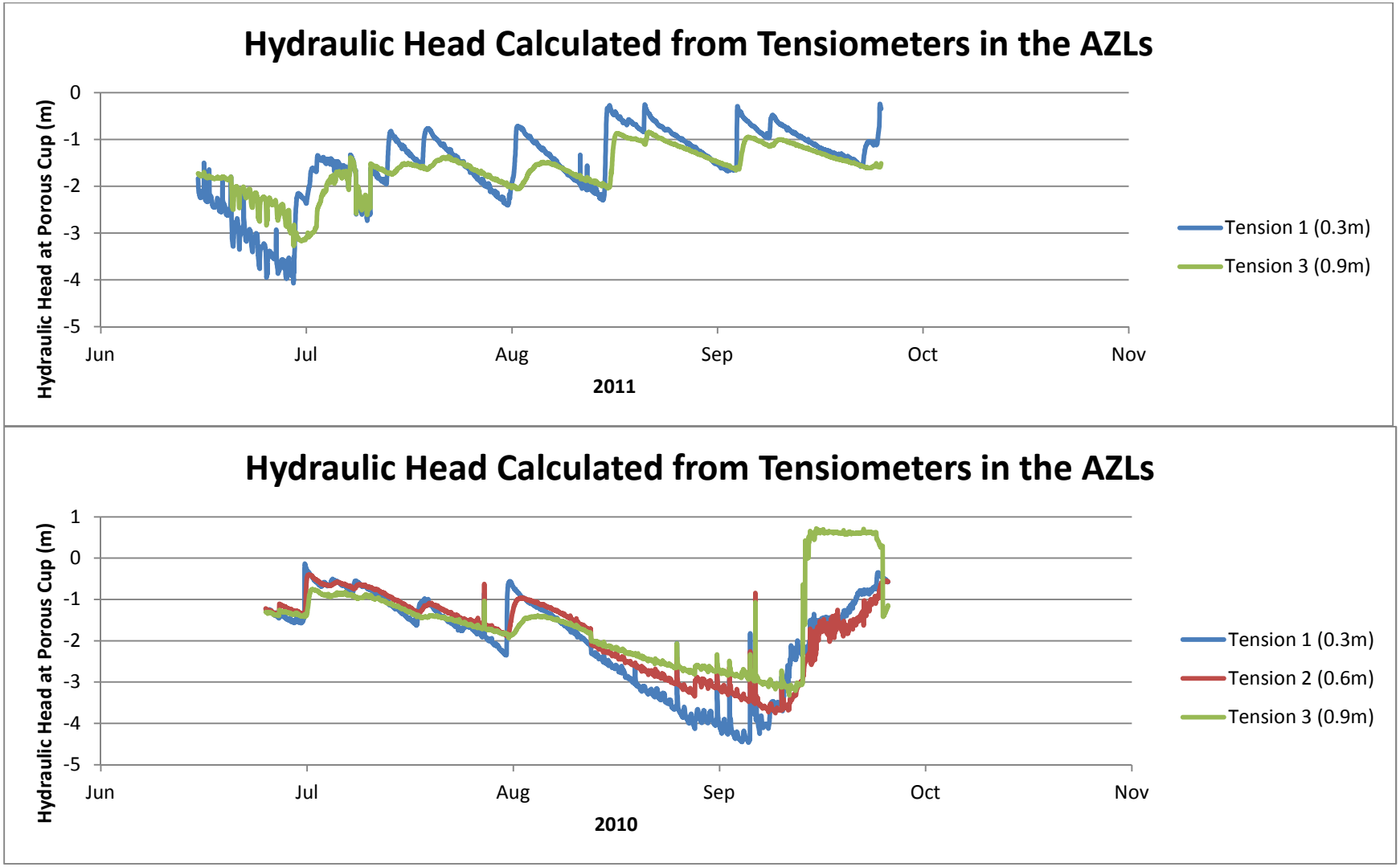

Figure A-30: Hydraulic head calculated from tensiometers in the AZLs

Appendix B: Summary of Tracer Tests Conducted on the Covered Pile

B.1 Rhodamine Tracer Test (East Batter, Covered Pile)

This test was conducted on June 21 and 22, 2013. Ten ounces of 'Bright Dyes Red Dye' was mixed with 400L of water. This water was applied to a $6m^2$ patch on the southern edge of the eastern slope of the covered pile. The test was run for five hours at a volumetric rate of 50L/h. This is equivalent to a precipitation event of 8mm/hour for the area tested. Tracer application began at 2:00pm on June 21st, and finished at 7:00pm on the same day. A cross section of the tracer test was excavated at 8:30am on June 22, and observations were taken until 9:30am on the same day.

The dye had infiltrated uniformly throughout the matrix to an average depth of 55cm. Preferential flow around larger rocks was observed on the upper portion of only one rock (5cm diameter). The remainder of the 3m wide excavation showed only matrix flow. The cross section was extended 1m north from the tracer test into clean material. The interface between the tracer and the clean rock showed that flow was vertical in this dimension. Overland flow was only observed as a result of a kinked hose, and a tear in the hose. Both issues were corrected within fifteen minutes and had minimal impact.

Figure B-1 shows the cross section excavated. The dye has stained the upper material pink, while the clean material below is brown. Pink material located below the horizontal stained/clean interface is debris from the excavation.

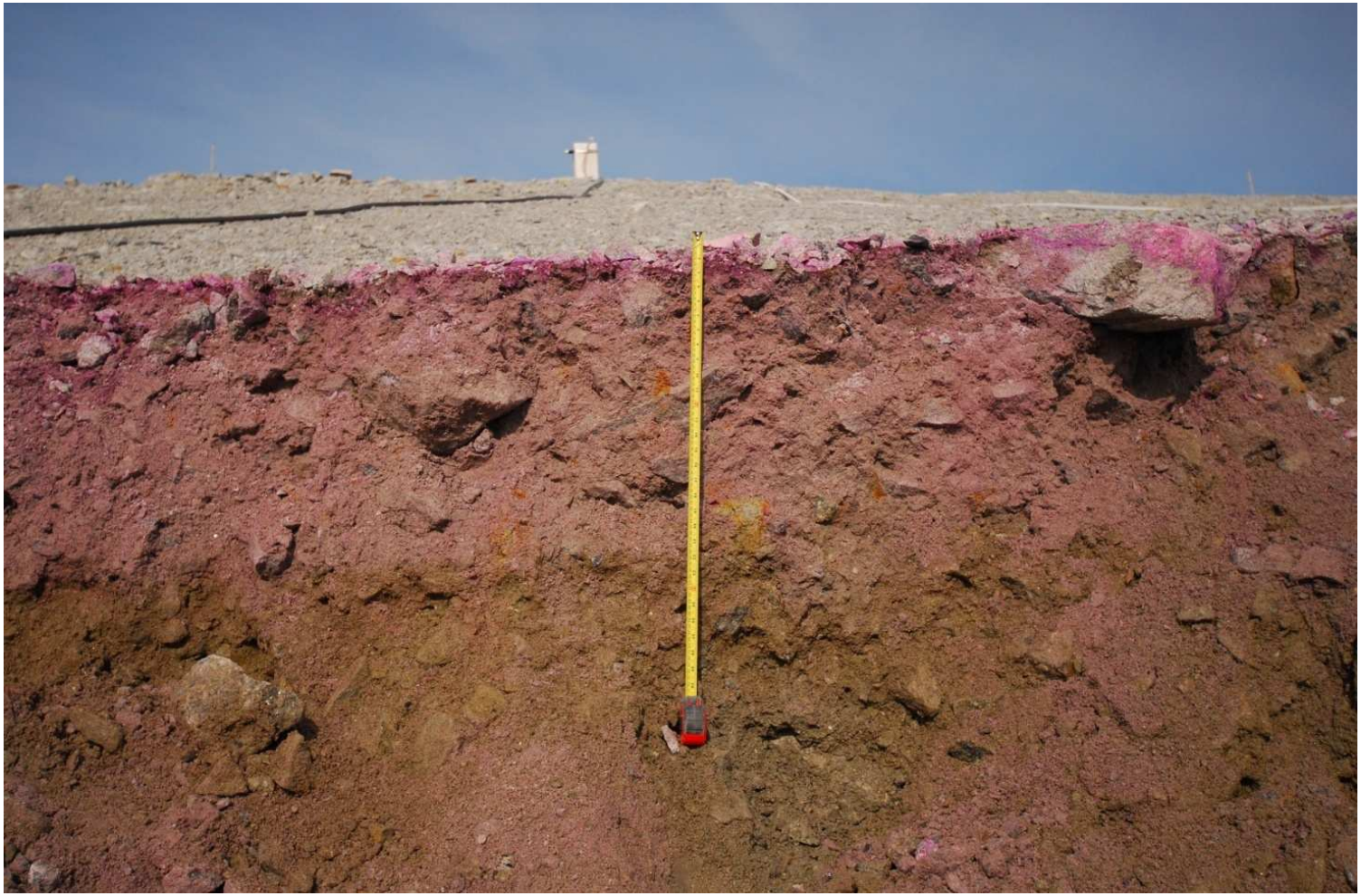

Figure B-1: Rhodamine staining in the type I material on the covered pile

B.2 Anion and Deuterium Tracer Tests (East Batter, Covered Pile)

Two tracer tests were conducted on the covered pile on July 27 and July 29, 2013. The intention of the tests is to quantify the amount of infiltration passing through the till layer on the covered pile. The first tracer test released deuterium and sodium chloride tracers directly above the uppermost edge of the collection lysimeters installed on the east face of the covered pile. The second test released a sodium bromide tracer near the crest of the pile directly in line with the collection lysimeters (Figure B-2).

B.2.1 Sodium Chloride and Deuterium Tracer Test (July 27, 2013)

To create the tracer 1.93kg of Sifto table salt and 59.4g of deuterium were mixed with approximately 450L of water to create a tracer with a chloride concentration of 2600mg/L and a deuterium concentration of around +500 ‰ Vienna Mean Ocean Water Standard. These concentrations match those used in tracer tests conducted in 2007 (Neuner, et al., 2009). Three 500mL background samples and three 500mL tracer samples were taken and analysed.

The tracer was released from a 25 foot long weeper hose onto a 4m by 1.5m infiltration area located 18m upslope from the point where the collection pipes exit the pile (Figure B-1). An average volumetric flow rate of 50L/hr (equivalent to an 8.3mm/hr rainfall) was maintained for 8 hours, for a total release of 400L. This rate was chosen based on the results of a rhodamine tracer test and excavation previously conducted on the same slope (June 21 and 22, 2013) which showed no overland or preferential flow at this flow rate.

The weather during the tracer test was cool and overcast, with rain falling for approximately 4 of the 8 hours. Tarps were used to cover the tracer area to minimize dilution and prevent overland flow resulting from the combined tracer and natural precipitation. Despite this, some overland flow was observed from low infiltration capacity areas. The covered pile tipping bucket recorded 1.4mm of rain during the tracer test.

B.2.2 Bromide Tracer Test (July 29, 2013)

To create the tracer 1.74kg of sodium bromide from Anachemia Science was mixed with approximately 450L of water to create a tracer with a bromide concentration of around 3000mg/L. This concentration matches that used in tracer tests conducted in 2007 (Neuner, et al., 2009). Three 500mL background samples and three 500mL tracer samples were taken.

The tracer was released onto a 4m by 1.5m infiltration area located 8 meters down slope from the crest of the pile (Figure B-2). The infiltration system was gravity fed, and it was not possible to maintain a flow rate of 50L/hr this high on the pile. Instead an average flow rate of 38L/hr (6.3mm/hr) was maintained for 10.5 hours, for a total release of 400L. Despite the lower flow rate some overland flow was observed during the test. This was partially rectified by frequently changing the hoses location within the infiltration area, and by avoiding the lowest permeability regions of the infiltration area.

The weather during this test was warm and sunny with scattered clouds. Tarps were placed over the tracer area to minimize the effects of evaporation.

Figure B-3 shows the set up used in both tracer tests. Figure B-4 shows the tarps used to prevent the infiltration of rainfall on July 27, 2013 and evaporation on July 28, 2013. Figure B-5 shows the weeping hose used to apply the tracer.

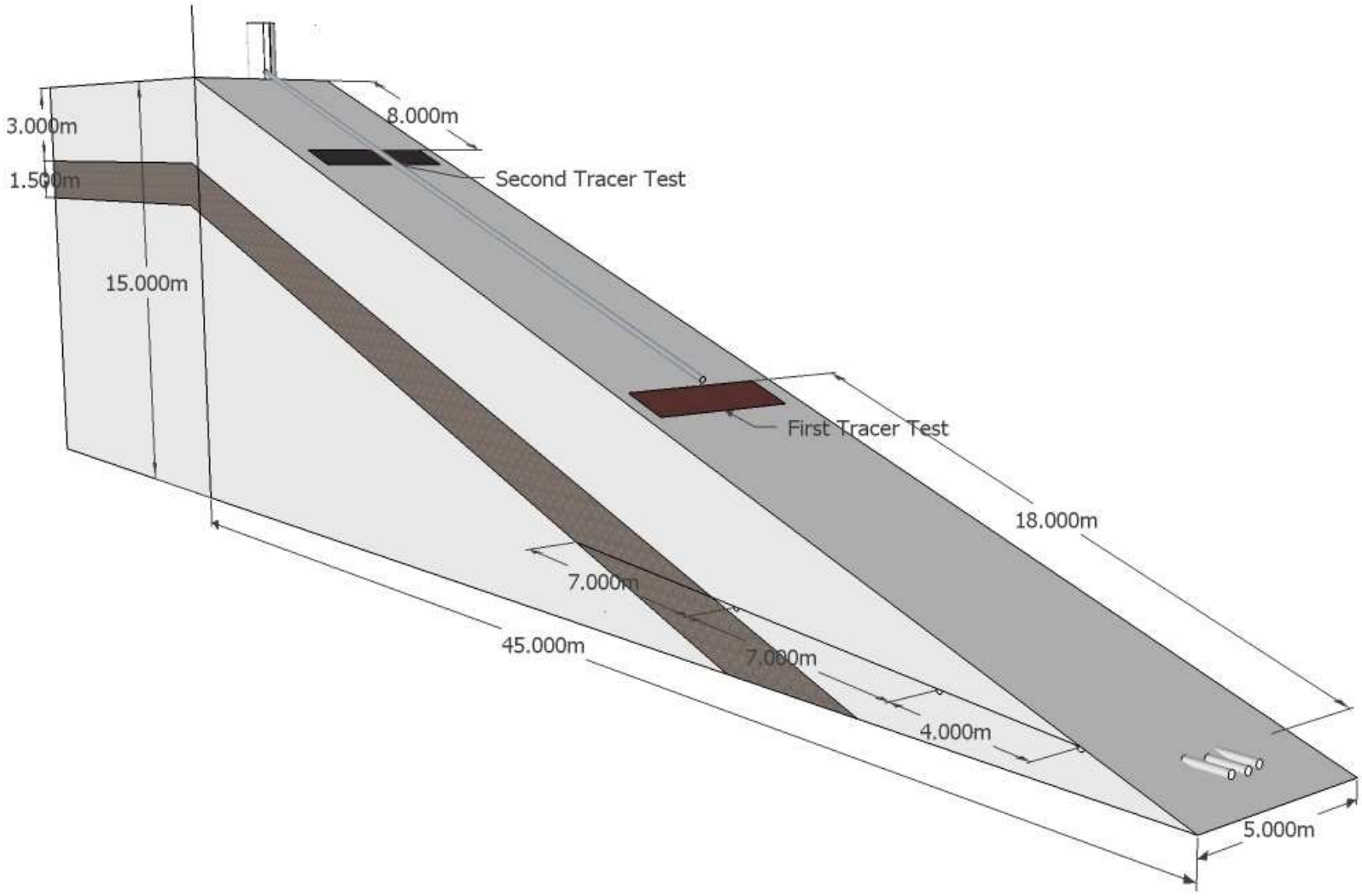

Figure B-2: Location of the tracer tests

Figure B-3: Tracer test with weeper hose.

Figure B-4: Tracer area covered by tarps

Figure B-5: Weeping hose

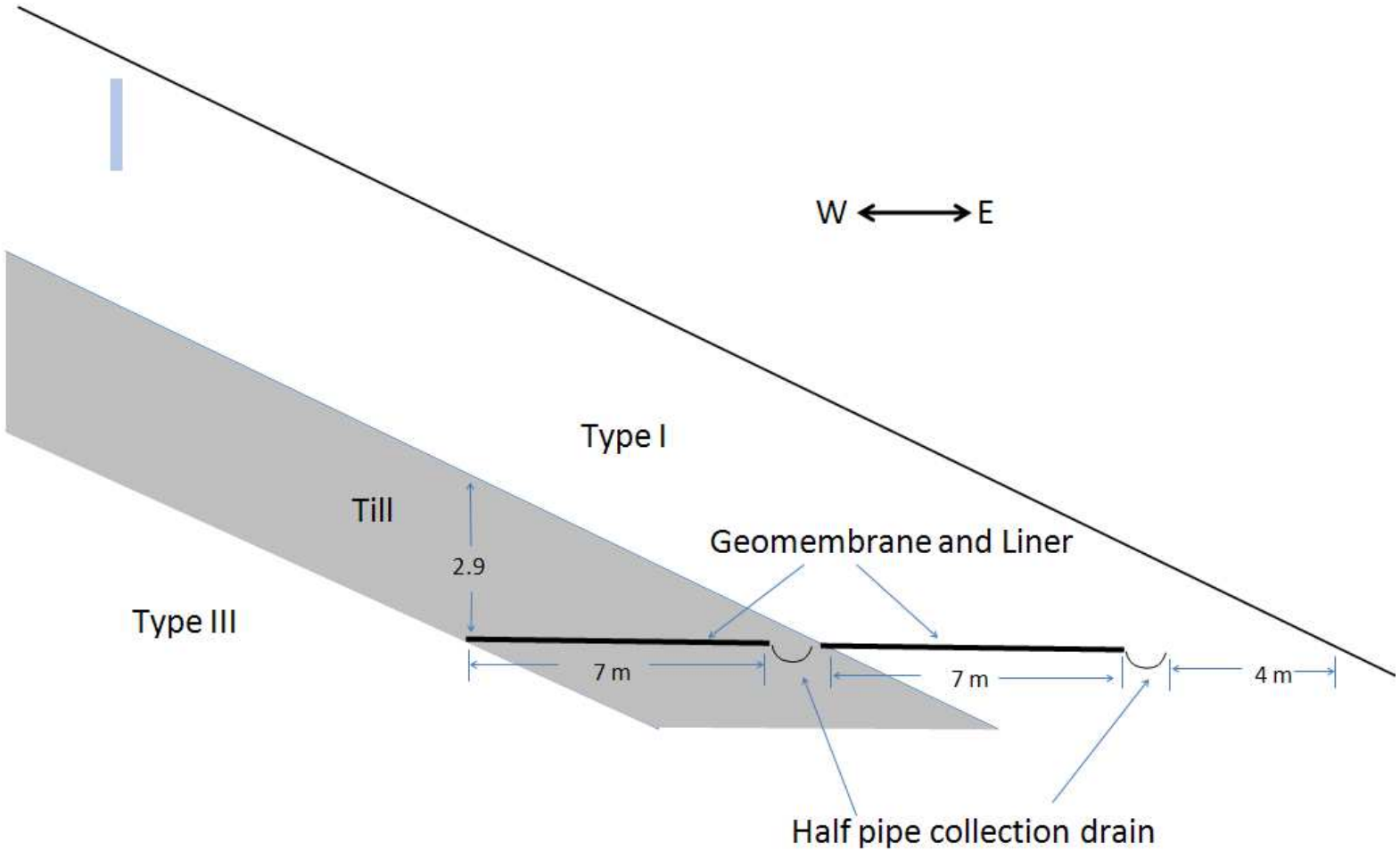

Covered pile slope drain cross section.

Figure B-6: Cross section of the covered pile lysimeters.
Image taken from the construction summary prepared by Jeff Bain

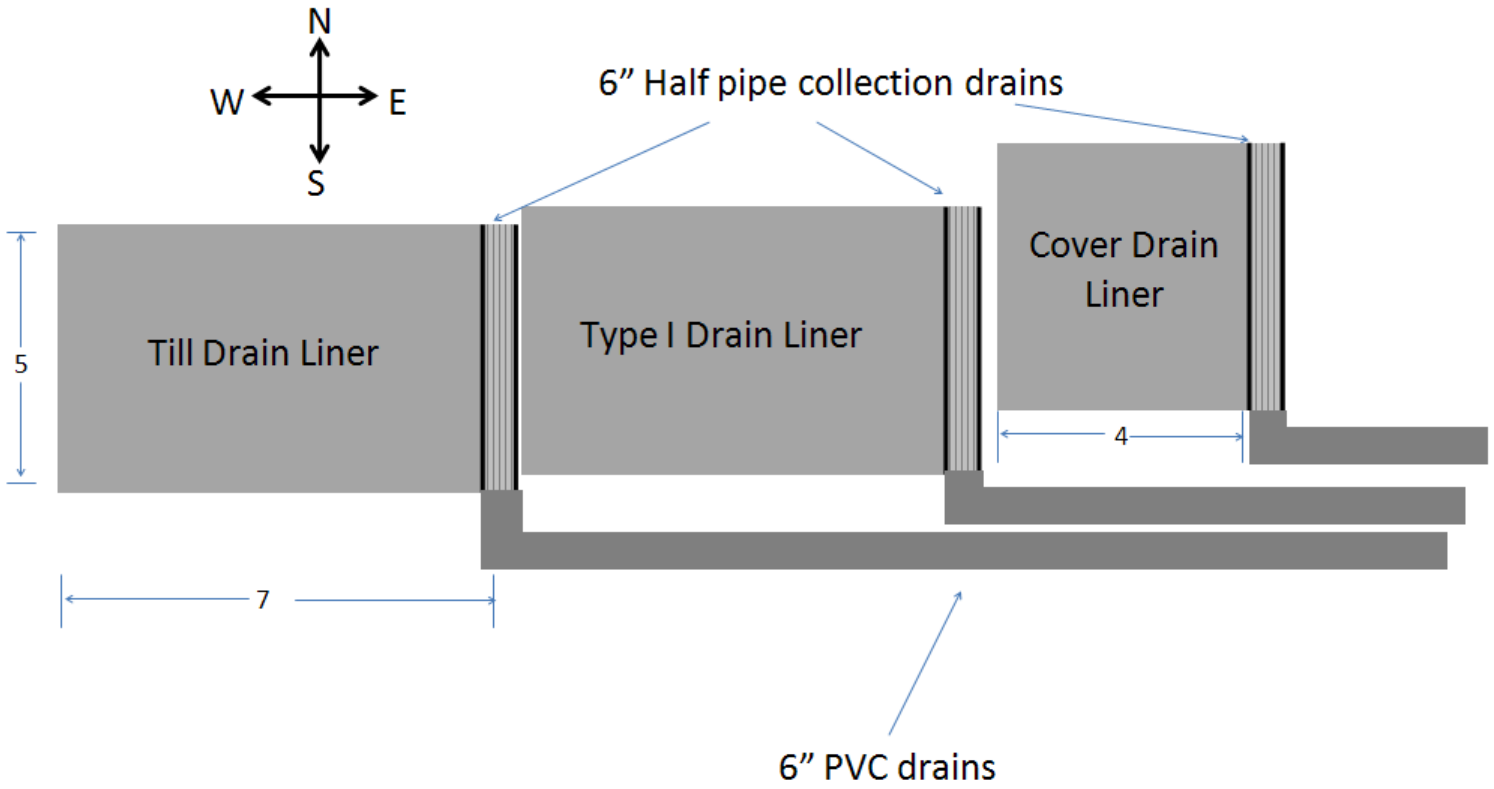

Covered pile slope drain plan view.

- Liners slope to east.
- Half pipe drains slope to south.
- Till and Type 1 drain liners are 5 x 7 m; Cover drain liner is 5 x 4 m

Figure B-7: Overview of the covered pile lysimeters.
Image taken from the construction summary prepared by Jeff Bain

B.3 Deuterium Tracer Test (South Batter, Type III Pile)

This test was conducted on the south batter of the type 3 pile on April 8 and 9, 2014. The intention of the test was to quantify preferential and matric flow velocities through the batters, especially as they pertain to snowmelt in the spring. Since it is not possible to walk on the batters, a deuterium tracer was mixed and then frozen in ice cube trays. The individual cubes were then thrown onto the south batter of the pile from below.

A total of nine litres of ice (518 cubes) with a deuterium concentration of 13.2g deuterium per litre of Diavik tap water was thrown. The ice cubes were 100 times more concentrated than in previous tracer tests, so this is the signal equivalent of 900L of water. Water at this deuterium concentration has a melting point of 0.4 degrees Celsius.

The ice cubes were thrown onto the batter at a constant height 4.5 meters above the basal liner. A horizontal rope was used as a target for throwing. To place the horizontal rope on the pile it was strung between two longer ropes, and these were thrown from the crest of the pile to the base. They were then moved apart until the horizontal rope was stretched tight. The horizontal rope was placed 14.3 meters below the crest of the pile, as measured along the piles batters. This was calculated to be 4.5 meters above the basal liner. A strong, inconsistent wind off of the pile made accuracy difficult, even though the ice cubes were not thrown very far. Approximately 80% of the ice cubes thrown landed within 1.5 meters of the intended location. The ice cubes were not evenly distributed along the length of the rope, as portions of the snow were too stiff to allow the ice cubes to penetrate and stick. The distribution of ice cubes on the batter is shown in Figure 2 (below).

It is anticipated that some of the deuterium will travel through preferential pathways and be seen very quickly in the basal drain. The remainder of the deuterium will travel with a matric flow velocity through

the batter. The velocity is anticipated to be quicker than the 3m/year seen through the core of the pile due to the fact that the lower batters preferentially contain larger sized materials. The value calculated from this tracer test will be the first flow velocity measured through the batters of the pile.

All samples taken from the south drain must now have an extra bottle for deuterium analysis. The samples should be unfiltered and non acidic, with no head space in the standard 60mL HDPE bottles.

The environment crew at Diavik has agreed to take pictures of the south batter of the pile until the arrival of the test piles crew onsite in May, 2014. This will provide important information regarding the ice cubes location in relation to the snow line prior to the onset of melting.

Figure B-8: Distribution of ice cubes on the batter.
The horizontal rope seen in the picture was the target height for the ice cubes. Figure taken April 9, 2014

Figure B-9: Snow on the batter April 20, 2014 (Photo taken by environment crew)

Figure B-10: Snow on the batter April 27, 2014 (Photo taken by the environment crew).

Appendix C: Matlab Codes

The Matlab codes written for this thesis are provided in this appendix for reference. The datalogger program used in datalogger 3Ba was changed following the flood in 2012, and the new Matlab script used for processing the data can be found in this appendix. The Matlab codes used to process the daily outflow recorded at each of the other dataloggers remain unchanged from those presented in Fretz (2013). The radiation model developed by Swift (1976) and the snowmelt model used each year is also provided.

C.1 New Scripts for 3Ba datalogger

C.1.1 Get Raw Tips

```
%Script: getRawTips3Ba
%Author: Andrew Krentz - based on scripts written by Matthew Neuner and
%Steven Momeyer that were used for interpreting the 3Ba data prior to
%flooding in the winter of 2012-2013

%%

function [T1_Raw,tb_1,tb_2,tb_3,tb_4,tb_5,tb_6,tb_7,tb_8,tb_9,tb_10,...
   tb_11,tb_12,tb_13] = getRawTips3Ba_NEW(inName)

%inName: Write directory of file here.
%This script opens raw data files from the datalogger and sorts the tipping
%buckets based on ArrayID
%Creates an array for each tipping bucket with Date in column 1 and time
%between tips (in days) in column 2.

%tb_1 = 3BNBlys2W & 3BNBlys2E
%tb_2 = 3BNBlys4W
%tb_3 = 3BNBlys4E
%tb_4 = 3BNClys2W & 3BNClys2E
%tb_5 = 3BNClys4W
%tb_6 = 3BNClys4E
%tb_7 = 3BSClys2W & 3BSClys2E
%tb_8 = 3BSClys4W
%tb_9 = 3BSClys4E
%tb_10 = 1BWBlys Cluster
%tb_11 = 1BWClys Cluster
%tb_12 = 1BEClys Cluster
%tb_13 = 1Bxxdrn13
%T1_Raw = no important data, disregard

%File format constants.
%"TIMESTAMP","RECORD","TB(1)","TB(2)","TB(3)","TB(4)","TB(5)","TB(6)","TB(7%)","TB(8)","TB(9)","TB(10)","TB(1
1)","TB(12)","TB(13)","TB_total(1)","TB_total(2)","TB_total(3)","TB_total(4)","TB_total(5)","TB_total(6)","TB_total(
7)","TB_total(8)","TB_total(9)","TB_total(10)","TB_total(11)","TB_total(12)","TB_total(13)"
%This section identifies the column that each tipping bucket's data is
%stored in
dateFormatString = '"%f-%f-%f
%f:%f:%f",%f,%f,%f,%f,%f,%f,%f,%f,%f,%f,%f,%f,%f,%f,%f,%f,%f,%f,%f,%f,%f,%f,%f,%f,%f,%f,%f,%f,%f,%f,%f,%f,%f,%f,%f,%f\n';
nColumns = 33;
minuteColumn = 5;
hourColumn = 4;
secondsColumn = 6;
daysColumn = 3;
monthsColumn = 2;
yearsColumn = 1;
TB1Column = 8;
TB2Column = 9;
```

```
TB3Column = 10;
TB4Column =11;
TB5Column = 12;
TB6Column = 13;
TB7Column =14;
TB8Column = 15;
TB9Column = 16;
TB10Column = 17;
TB11Column = 18;
TB12Column = 19;
TB13Column = 20;

%Filter for taking derivatives.
diffFilter = [1,-1];

%Read data from file.
%Data = txt2mat(file location, header rows, columns, format string);
Data = txt2mat(inName,4,nColumns,dateFormatString);

%Calculate the time in days using matlab's datenum.
dateVec = [Data(:,yearsColumn) Data(:,monthsColumn) Data(:,daysColumn)...
   Data(:, hourColumn) Data(:, minuteColumn) Data(:,secondsColumn)];
tRaw = datenum(dateVec);

%Outputs all data before sorting and creating separate arrays for each ID.
tRaw(:,2) = Data(:,TB1Column);
T1_Raw = [tRaw(:,1), tRaw(:,2)];
tb_1 = [tRaw(:,1), tRaw(:,2)];
D = tb_1(:,1);
B = tb_1(:,2);
tb_1 = D(B==1);
if size(tb_1) > 0
   m = size(tb_1);
   Difference = diff(tb_1);
   Difference(m,1) = 0.0001;
   C = cat(2,tb_1,Difference);
   tb_1 = C;
else tb_1 = ('No Flow');
end

tRaw(:,2) = Data(:,TB2Column);
tb_2 = [tRaw(:,1), tRaw(:,2)];
D = tb_2(:,1);
B = tb_2(:,2);
tb_2 = D(B==1);
if size(tb_2) > 0
   m = size(tb_2);
   Difference = diff(tb_2);
   Difference(m,1) = 0.0001;
   C = cat(2,tb_2,Difference);
   tb_2 = C;
else tb_2 = ('No Flow');
```

```
end

tRaw(:,2) = Data(:,TB3Column);
tb_3 = [tRaw(:,1), tRaw(:,2)];
D = tb_3(:,1);
B = tb_3(:,2);
tb_3 = D(B==1);
if size(tb_3) > 0
   m = size(tb_3);
   Difference = diff(tb_3);
   Difference(m,1) = 1E-4;
   C = cat(2,tb_3,Difference);
   tb_3 = C;
else tb_3 = ('No Flow');
end

tRaw(:,2) = Data(:,TB4Column);
tb_4 = [tRaw(:,1), tRaw(:,2)];
D = tb_4(:,1);
B = tb_4(:,2);
tb_4 = D(B==1);
if size (tb_4) > 0
   m = size(tb_4);
   Difference = diff(tb_4);
   Difference(m,1) = 1E-4;
   C = cat(2,tb_4,Difference);
   tb_4 = C;
else tb_4 = ('No Flow');
end

tRaw(:,2) = Data(:,TB5Column);
tb_5 = [tRaw(:,1), tRaw(:,2)];
D = tb_5(:,1);
B = tb_5(:,2);
tb_5 = D(B==1);
if size (tb_5) > 0;
   m = size(tb_5);
   Difference = diff(tb_5);
   Difference(m,1) = 1E-4;
   C = cat(2,tb_5,Difference);
   tb_5 = C;
else tb_5 = ('No Flow');
end

tRaw(:,2) = Data(:,TB6Column);
tb_6 = [tRaw(:,1), tRaw(:,2)];
D = tb_6(:,1);
B = tb_6(:,2);
tb_6 = D(B==1);
if size(tb_6) > 0
   m = size(tb_6);
   Difference = diff(tb_6);
```

```
   Difference(m,1) = 1E-4;
   C = cat(2,tb_6,Difference);
   tb_6 = C;
else tb_6 = ('No Flow');
end

tRaw(:,2) = Data(:,TB7Column);
tb_7 = [tRaw(:,1), tRaw(:,2)];
D = tb_7(:,1);
B = tb_7(:,2);
tb_7 = D(B==1);
if size(tb_7) > 0;
   m = size(tb_7);
   Difference = diff(tb_7);
   Difference(m,1) = 1E-4;
   C = cat(2,tb_7,Difference);
   tb_7 = C;
else tb_7 = ('No Flow');
end

tRaw(:,2) = Data(:,TB8Column);
tb_8 = [tRaw(:,1), tRaw(:,2)];
D = tb_8(:,1);
B = tb_8(:,2);
tb_8 = D(B==1);
if size(tb_8) > 0
   m = size(tb_8);
   Difference = diff(tb_8);
   Difference(m,1) = 1E-4;
   C = cat(2,tb_8,Difference);
   tb_8 = C;
else tb_8 = ('No Flow');
end

tRaw(:,2) = Data(:,TB9Column);
tb_9 = [tRaw(:,1), tRaw(:,2)];
D = tb_9(:,1);
B = tb_9(:,2);
tb_9 = D(B==1);
if size(tb_9) > 0;
   m = size(tb_9);
   Difference = diff(tb_9);
   Difference(m,1) = 1E-4;
   C = cat(2,tb_9,Difference);
   tb_9 = C;
else tb_9 = ('No Flow');
end

tRaw(:,2) = Data(:,TB10Column);
tb_10 = [tRaw(:,1), tRaw(:,2)];
D = tb_10(:,1);
B = tb_10(:,2);
```

```
tb_10 = D(B==1);
if size(tb_10)>0
   m = size(tb_10);
   Difference = diff(tb_10);
   Difference(m,1) = 1E-4;
   C = cat(2,tb_10,Difference);
   tb_10 = C;
else tb_10 = ('No Flow');
end

tRaw(:,2) = Data(:,TB11Column);
tb_11 = [tRaw(:,1), tRaw(:,2)];
D = tb_11(:,1);
B = tb_11(:,2);
tb_11 = D(B==1);
if size(tb_11) > 0;
   m = size(tb_11);
   Difference = diff(tb_11);
   Difference(m,1) = 1E-4;
   C = cat(2,tb_11,Difference);
   tb_11 = C;
else tb_11 = ('No Flow');
end

tRaw(:,2) = Data(:,TB12Column);
tb_12 = [tRaw(:,1), tRaw(:,2)];
D = tb_12(:,1);
B = tb_12(:,2);
tb_12 = D(B==1);
if size(tb_12) > 0;
   m = size(tb_12);
   Difference = diff(tb_12);
   Difference(m,1) = 1E-4;
   C = cat(2,tb_12,Difference);
   tb_12 = C;
else
   tb_12 = ('No Flow');
end

tRaw(:,2) = Data(:,TB13Column);
tb_13 = [tRaw(:,1), tRaw(:,2)];
D = tb_13(:,1);
B = tb_13(:,2);
tb_13 = D(B==1);
if size(tb_13) > 0;
   m = size(tb_13);
   Difference = diff(tb_13);
   Difference(m,1) = 1E-4;
   C = cat(2,tb_13,Difference);
   tb_13 = C;
else tb_13 = ('No Flow');
end
```

```
end
```

C.1.2 Calculate Rates and Volumes for the Type I Drain

```
%Script: calcRates_Volumes_TIDrain
%Author: Modified by Nathan Fretz from Matthew Neuner and Steven Momeyer
%Project: Diavik Waste-Rock Project

%%

function [TIDrain_Rates,TIDrain_DailyVolumes]...
   = calcRates_Volumes_TIDrain(var)

%This script creates 2 arrays:
%TIDrain_Rates has the Date in column 1, Time between tips (in days) in
%column 2, mL/s in column 3, L/d in column 4, L in column 5.
%TIDrain_DailyVolumes has the Date in column 1 and daily L in column 2.

%Convert time between tips in days to seconds.
secs = var(:,2).* 86400;

%Averages time between tips for two adjacent tips to
%remove effects from unbalanced tipping bucket and discrepancy in bucket
%volume.
i = 1;
secs(i,2) = secs(i,1);
i=i+1;
while i < size(secs,1)+1
  secs(i,2) = ((secs(i,1)+secs(i-1,1))/2);
  i=i+1;
end

%Convert time between tips to flow rate (mL/s).
%Contact Matthew Neuner for equation used for 2007.
%Contact Steven Momeyer for equation used in 2008 and 2009.
%The Type I Drain (1Bxxdrn13) tipping bucket was replaced on July 19, 2011
%between 14:00 and 15:00.
%Equation for all 2010 data (Nathan Fretz): %y = 828.46x^-1.052
 %Flow = secs(:,2).^-1.052 .*828.46;

%Equation for 2011 data after July 19, 2011 15:00 (Nathan Fretz):
            %y = 664.16x^-1.035
%Flow = secs(:,2).^-1.035 .*664.16;

%Equation for 2013 data used for all of 2013 season
            %y = 597.8x^-1.014
Flow = secs(:,2).^-1.014.*597.8;
TIDrain_Rates = [var(:,1),var(:,2),Flow];

%Add 4th column and convert flow from mL/s to L/d.
TIDrain_Rates(:,4) = Flow(:,1).*86400.*0.001;

%Add 5th column consisting of volume of each tip (L).
```

```
TIDrain_Rates(:,5) = TIDrain_Rates(:,2).*TIDrain_Rates(:,4);

%Calculate the volume of water (L) over a specified peroid.
%The interval is specified in minutes.
%This gives you a nx3 matrix: date, volume, number of rows included.
interval = 1440; %1 day in minutes.
mins = round((TIDrain_Rates(:,1)- datenum ('Jan 01 2000'))*1440); %Converts
%data to number of minutes since Jan 1, 2000.
mins = ceil(mins/interval); %ceil rounds towards + infinity
lastmins = mins(1);
x = [0,0];
TIDrain_DailyVolumes = [];
for i= 2:size(TIDrain_Rates,1)
      if mins(i) ~= lastmins
       TIDrain_DailyVolumes = [TIDrain_DailyVolumes;...
          (mins(i-1)*interval)/1440 + datenum('Jan 01 2000'),x];
       x = [TIDrain_Rates(i,5),1]; %5 refers to the column containing flow
       %in L.
       lastmins = mins(i);
   else  x = x + [TIDrain_Rates(i,5),1]; %5 refers to the column
       %containing flow in L.
       end
end
   TIDrain_DailyVolumes = [TIDrain_DailyVolumes;...
      (mins(i-1)*interval)/1440 + datenum('Jan 01 2000'),x];
   TIDrain_DailyVolumes(:,1) = TIDrain_DailyVolumes(:,1)-interval/(1440*2);
   %Subtracts half of interval (in minutes). This is done for graphing
   %purposes, so that a bar graph is plotted correctly.

   %Create 6th column of cumulative L.
   TIDrain_DailyVolumes(:,4) = cumsum(TIDrain_DailyVolumes(:,2));
   %Create 7th column of cumulative m^3.
   TIDrain_DailyVolumes(:,5) = TIDrain_DailyVolumes(:,4)./1000;

end
```

C.1.3 Calculate Rates and Volumes for the BCLs

```
%Script: calcRates_Volumes_BCLs
%Author: Modified by Nathan Fretz from Matthew Neuner and Steven Momeyer
%Project: Diavik Waste-Rock Project

%%

function [BCL_Rates,BCL_DailyVolumes]...
   = calcRates_Volumes_BCLs(var)

%This script creates 2 arrays:
%BCL_Rates has the Date in column 1, Time between tips (in days) in
%column 2, mL/s in column 3, L/d in column 4, L in column 5.
%BCL_DailyVolumes has the Date in column 1 and daily L in column 2.
```

```
%Convert time between tips in days to seconds.
secs = var(:,2).* 86400;

%Averages time between tips for two adjacent tips to
%remove effects from unbalanced tipping bucket and discrepancy in bucket
%volume.
i = 1;
secs(i,2) = secs(i,1);
i=i+1;
while i < size(secs,1)+1
  secs(i,2) = ((secs(i,1)+secs(i-1,1))/2);
  i=i+1;
end

%Convert time between tips to flow rate (mL/s).
%Contact Matthew Neuner for equation used for 2007.
%Contact Steven Momeyer for equation used in 2008 and 2009.
%Equation for all 2010 and 2011 data:
            %y = 2.6425x^-1.1124
Flow = secs(:,1).^-1.1124 .*2.6425; %secs(:,2) for average time btw tips.

BCL_Rates = [var(:,1),var(:,2),Flow];

%Add 4th column and convert flow from mL/s to L/d.
BCL_Rates(:,4) = Flow(:,1).*86400.*0.001;

%Add 5th column consisting of volume of each tip (L).
BCL_Rates(:,5) = BCL_Rates(:,2).*BCL_Rates(:,4);

%Calculate the volume of water (L) over a specified peroid.
%The interval is specified in minutes.
%This gives you a nx3 matrix: date, volume, number of rows included.
interval = 1440; %1 day in minutes.
mins = round((BCL_Rates(:,1)- datenum ('Jan 01 2000'))*1440); %Converts
%data to number of minutes since Jan 1, 2000.
mins = ceil(mins/interval); %ceil rounds towards + infinity
lastmins = mins(1);
x = [0,0];
BCL_DailyVolumes = [];
for i= 2:size(BCL_Rates,1)
     if mins(i) ~= lastmins
      BCL_DailyVolumes = [BCL_DailyVolumes;...
         (mins(i-1)*interval)/1440 + datenum('Jan 01 2000'),x];
      x = [BCL_Rates(i,5),1]; %5 refers to the column containing flow
      %in L.
      lastmins = mins(i);
   else  x = x + [BCL_Rates(i,5),1]; %5 refers to the column
      %containing flow in L.
      end
end
```

```
   BCL_DailyVolumes = [BCL_DailyVolumes;...
      (mins(i-1)*interval)/1440 + datenum('Jan 01 2000'),x];
   BCL_DailyVolumes(:,1) = BCL_DailyVolumes(:,1)-interval/(1440*2);
   %Subtracts half of interval (in minutes). This is done for graphing
   %purposes, so that a bar graph is plotted correctly.

   %Create 4th column of cumulative L.
   BCL_DailyVolumes(:,4) = cumsum(BCL_DailyVolumes(:,2));
   %Create 5th column of cumulative m^3.
   BCL_DailyVolumes(:,5) = BCL_DailyVolumes(:,4)./1000;

end
```

C.2 Radiation Model (Based on Swift, 1976)

```
%this file calculates radiation on a slope of the covered pile based on an
%input of latitude, slope inclination, slope aspect, day of year, and
%measured total daily radiation

%all measurements are in degrees, use sind, cosd, tand
%all inputs go in this section (except julian day and radiation, which are
%imported from excel below)
I = 18.4; %slope angle in degrees - at Daivik it is 18.4
A = 90; % slope azimuth in degrees (90 = east, 180 = south, 270 = west)
Lo = 64.4961; % latitidue of site in degrees - at Diavik it is 64.4961
Ro = 1.95; %solar constant in cal/cm2/min - using Drummond et al.

L1 = asind(cosd(I)*sind(Lo)+sind(I)*cosd(Lo)*cosd(A));

D1 = cosd(I)*cosd(Lo)-sind(I)*sind(Lo)*cosd(A);
if(D1==0)
   D1 = 1.0E-10;
end

L2 = atand(sind(I)*sind(A)/D1);
if(D1<0)
   L2 = L2 +180;
end

%1 starts here

%This section imports an excel file with the Julian day in collumn one, and
%the total daily radiation, measured in g calorie /cm2/day
ndata = xlsread('C:\Documents and Settings\akrentz\Desktop\Thesis\Thesis\Work\Radiation
Calculations\Julian_Radians.xlsx','2010');
J_vector = ndata(:,1);
R2_vector = ndata(:,2);
tot_days = length(ndata);

for i=1:length(ndata)
J =J_vector(i);
```

```
R2 = R2_vector(i);


%J = 98; % test value Julian Day
%R2 = 341; % test value measured radiation

D = asind(0.39785*sind(278.9709+0.9856*J+1.9163*sind(356.6153+0.9856*J))); % use complex function for D


E = 1-0.0167*cosd((J-3)*0.986); %func1(1.0,0.0167,-3)
R1 = (60 * Ro/(E*E)); % not sure if this is actually E*E or not

T = acosd(-tand(L1)*tand(D)); %func2(L1)
T7 = T - L2;
T6 = -T - L2;

T = acosd(-tand(Lo)*tand(D)); %func2(Lo)
T1 = T;
To = -T;

if(T7<T1)
   T3 = T7;
else
   T3 = T1;
end

if(T6 > To)
   T2 = T6;
else
   T2 = To;
end

%The R4 substitution starts here
if(T3<T2)
   T2 = 0;
   T3 = 0;
end
T6 = T6+360;

if(T6<T1)
   T8 = T6;
   T9 = T1;
   R4_dum1 = R1*(sind(D)*sind(L1)*(T3-T2)/15+cosd(D)*cosd(L1)*(sind(T3+L2)-sind(T2+L2))*12/pi);
   R4_dum2 = R1*(sind(D)*sind(L1)*(T9-T8)/15+cosd(D)*cosd(L1)*(sind(T9+L2)-sind(T8+L2))*12/pi);
   R4 = R4_dum1 + R4_dum2;
else
   T7 = T7 - 360;
   if (T7 > To)
      T8 = To;
      T9 = T7;
```

```
      R4_dum1 = R1*(sind(D)*sind(L1)*(T3-T2)/15+cosd(D)*cosd(L1)*(sind(T3+L2)-sind(T2+L2))*12/pi);
      R4_dum2 = R1*(sind(D)*sind(L1)*(T9-T8)/15+cosd(D)*cosd(L1)*(sind(T9+L2)-sind(T8+L2))*12/pi);
      R4 = R4_dum1 + R4_dum2;
   else
      R4 = R1*(sind(D)*sind(L1)*(T3-T2)/15+cosd(D)*cosd(L1)*(sind(T3+L2)-sind(T2+L2))*12/pi);
   end
end

%R4 = R1*(sind(D)*sind(L1)*(T3-T2)/15+cosd(D)*cosd(L1)*(sind(T3+L2)-sind(T2+L2))*12/pi);
%simple case R4 equation not needed here
T4 = T2/15;
T5 = T3/15;

V = 0;
W = Lo;
x = T1;
y = To;

R3 = R1*(sind(D)*sind(W)*(x-y)/15+cosd(D)*cosd(W)*(sind(x+V)-sind(y+V))*12/pi);
F = R4/R3;
R5_col_2 = F * R2;
R5(i,1) = i;
R5(i,2) = R5_col_2;
R6 = R5 / cosd(I);
end


%Check variables
%I
%A
%J
%R2
%D
%T4
%T5
%R4
%R3
%F
%R5
%R6
```

C.3 Snowmelt Models

Each year the additional snowfall that fell after the snow survey was manually added to the basic snowmelt script. The Matlab script for each year is presented below:

C.3.1 2010

```
%this program imports snowpack data from excel in the format: relative X (m),
%relative Y (m), relative Z (m) and creates an interpolation of the
%snowpack - IT IS ***MAYBE**** NECESSARY TO IMPORT THE HEIGHTS OF THE SNOWPACK PLUS THE
%PILE, AND THEN SUBTRACT THE PILE HEIGHT FOR INTERPOLATION REASONS
%****SNOWPACK DATA MUST BE EXPRESSED IN SWE****
CMF = 0.016; %change to get full range %the CMF ranges from 0.016 to 0.024

%first import the xls file - all units in metres - snowpack plus pile height
ndata = xlsread('C:\Documents and
Settings\akrentz\Desktop\Thesis\Thesis\Work\Snowfall\Snow_survey\Surfer_SnowPacks\2010.xlsx','Snow_and_Pi
le_Above_Liner');

%now seperate out the X,Y and Z coordinates
x=ndata(:,1);
y=ndata(:,2);
z=ndata(:,3);

%Define the grid you want in the x (tix) and y (tiy) direction. Now there
%is a matrix Z1 that contains the interpolated height at 1m intervals
%within the domain specified
tix = -42:1:42;%defines the x domain and the discretization used
tiy = -29:1:29; %defines the y domain and the discretization used
[X1,Y1] = meshgrid(tix,tiy); %this defines the domain for the interpolated surface
Z1=griddata(x,y,z,X1,Y1);% this creates the interpolated surface

%check if the interpolation worked - you can only check one plot at a time,
%use % signs to block out the other plots
%mesh(X1,Y1,Z1), hold %this plots the surface that was previously created
%plot3(x,y,z,'o'), hold off %this plots the measurement points onto the surface

%Calculate the total volume of the snow and pile
```

```
total_volume_snow_and_pile=nansum(nansum(Z1));


%Now import the xls file for the pile only - all units in metres - pile only
pile_data = xlsread('C:\Documents and
Settings\akrentz\Desktop\Thesis\Thesis\Work\Snowfall\Snow_survey\Surfer_SnowPacks\2010.xlsx',
'Pile_Above_Liner');
x1=pile_data(:,1);
y1=pile_data(:,2);
z1=pile_data(:,3);

%Create interpolated surface
Z2=griddata(x1,y1,z1,X1,Y1);
%check if the interpolation worked - you can only check one plot at a time,
%use % signs to block out the other plots
%mesh(X1,Y1,Z2), hold; %this plots the surface that was previously created
%plot3(x,y,z,'o'), hold off; %this plots the measurement points onto the surface

%Calculate the total volume of the pile
total_volume_pile = nansum(nansum(Z2));

%calculate the volume of snow available - this should match the value in
%the write up +/- 3%
total_snow = total_volume_snow_and_pile - total_volume_pile;


%Now create a matrix that contains only the snow - to apply the snowmelt
%model too
Z3 = Z1-Z2;
Indices = (Z3<0.001); % find the elements showing less than 1/10cm snow (interpolation error)
Z3(Indices) = 0; % make these cells = zero
Z3(isnan(Z3))= 0; % make NaN cells = 0



%check that the total volume of snow has not been changed by removing the
%interpolation values
total_snow_check = nansum(nansum(Z3));%checks total snow volume.  Should = total_snow


% Plot this model to check if it worked
%mesh(X1,Y1,Z3), hold; %this plots the surface that was previously created

%Now divide the matrix into different aspects (east, south, west)
Z3_East = Z3(:,1:30);
Z3_South = Z3(:,31:57);
Z3_West = Z3(:,58:85);
%mesh(Z3_South);
```

```
%print a file showing the interpolated matrix. This is just a check. Skip
%this step once confident to avoid making too many excel files
%xlswrite('/Users/Andrew/Dropbox/Work/Snowfall/Snow_survey/Surfer_SnowPacks/Matlab_created_files/2010_
Snow_Meshgrid.xls',Z3);
%xlswrite('/Users/Andrew/Dropbox/Work/Snowfall/Snow_survey/Surfer_SnowPacks/Matlab_created_files/2010_
Snow_Meshgrid_East.xls',Z3_East);
%xlswrite('/Users/Andrew/Dropbox/Work/Snowfall/Snow_survey/Surfer_SnowPacks/Matlab_created_files/2010_
Snow_Meshgrid_South.xls',Z3_South);
%xlswrite('/Users/Andrew/Dropbox/Work/Snowfall/Snow_survey/Surfer_SnowPacks/Matlab_created_files/2010_
Snow_Meshgrid_West.xls',Z3_West);

%Now import the radiation data for the year of concern - the model must
%start the day after the survey was taken
Radiation = xlsread('C:\Documents and Settings\akrentz\Desktop\Thesis\Thesis\Work\Radiation
Calculations\Radiation_all_years_and_slopes_for_matlab.xlsx','2010');
East_Radiation = Radiation(:,4);
West_Radiation = Radiation(:,5);
South_Radiation = Radiation(:,6);

%Now caculate the volume of snow on each batter and check that all of the
%snow has been included
snow_east_batter_initial = nansum(nansum(Z3_East));
snow_west_batter_initial = nansum(nansum(Z3_West));
snow_south_batter_initial = nansum(nansum(Z3_South));
total_snow_check_1 = snow_east_batter_initial + snow_west_batter_initial + snow_south_batter_initial; % should
= total_snow_check


%Now import the hourly temperature and evaporation/sublimation data from excel
Hourly_Temperature = xlsread('C:\Documents and Settings\akrentz\Desktop\Thesis\Thesis\Work\Radiation
Calculations\Hourly_Temp_Evap\2010_Temperature_Hourly_For_Matlab.xlsx','2010');
east_sublimation(:,1) = Hourly_Temperature(:,1); % date and time
east_sublimation(:,2) = Hourly_Temperature(:,6); % sublimation rate
west_sublimation(:,1) = Hourly_Temperature(:,1);
west_sublimation(:,2) = Hourly_Temperature(:,7);
south_sublimation(:,1) = Hourly_Temperature(:,1);
south_sublimation(:,2) = Hourly_Temperature(:,8);

for i = 1:length(Hourly_Temperature)
    if Hourly_Temperature(i,4) <= -4
    east_sublimation(i,2) = 0;
    west_sublimation(i,2) = 0;
    south_sublimation(i,2) = 0;
    end
end



%now apply the melt model to the east batter, stepping through time in one
%hour increments
```

```
k = length(Hourly_Temperature); %counter that equals the total amount of hours considered
L = 1; %counter for days
time = Hourly_Temperature(:,2); % time counter, 100 to 2300 hours
Melt_Rate_East = zeros(k,2); % preallocate array for speed
night_radiation = min(East_Radiation); % this is the minimum energy value, which is used to describe nighttime
melting



for i = 1:k
   if time(i) < 0400 % modified equation to reflect short nights
      Melt_Rate_East(i,2) = CMF*night_radiation*Hourly_Temperature(i,4); % correct for low radiation at night -
need to alter this
      else if time(i) > 1800 % modified equation to reflect short nights
       Melt_Rate_East(i,2) = CMF*night_radiation*Hourly_Temperature(i,4); % correct for low radiation at night -
need to alter this
         else
       Melt_Rate_East(i,2) = CMF*East_Radiation(L) * Hourly_Temperature(i,4);
         end
   end

   if(Melt_Rate_East(i,2) < 0)
      Melt_Rate_East(i,2) = 0;
   end

   if time(i) == 2400
      L = L + 1;
   end
end
Melt_Rate_East(:,1) = Hourly_Temperature(:,1);

% Now calculate snow loss on the east batter - measure hourly
d = size(Z3_East);
Z3_East_Original = Z3_East;
k = length(Hourly_Temperature);



for i = 1:k
Z3_New_East = Z3_East_Original - Melt_Rate_East(i,2)/1000;
   for l = 1:d(1,1)
      for m = 1:d(1,2)
       if Z3_New_East(l,m) < 0
         Z3_New_East(l,m) = 0;
       end
      end
   end

  % mesh(Z3_New_East); %make a movie of snowmelt
   %axis([0 30 0 60 0 0.5]);%make a movie of snowmelt
   %M(k) = getframe;%make a movie of snowmelt
   %axis([0 10 0 10 0 1]);%make a movie of snowmelt
```

```
volume_east_snowmelt(i,3) = nansum(nansum(Z3_East_Original))-nansum(nansum(Z3_New_East));
Z3_East_Original = Z3_New_East;

%now apply sublimation
sublimation_matrix_east = Z3_East_Original - (east_sublimation(i,2)/1000);
for l = 1:d(1,1)
      for m = 1:d(1,2)
       if sublimation_matrix_east(l,m) < 0
         sublimation_matrix_east(l,m) = 0;
       end
      end
end
volume_sublimation_east(i,2) = nansum(nansum(Z3_East_Original))-nansum(nansum(sublimation_matrix_east));
Z3_East_Original = sublimation_matrix_east;
if i == 1
   Z3_East_Original = Z3_East_Original + 0.0105/2; % snowfall on April 22, 2010
end
if i == 265
   Z3_East_Original = Z3_East_Original + 0.0002/2; %snowfall on May 3, 2010
end
if i == 409
   Z3_East_Original = Z3_East_Original + 0.0014/2; %snowfall on May 9, 2010
end
if i == 481
   Z3_East_Original = Z3_East_Original + 0.005/2; %snowfall on May 12, 2010
end
if i == 817
   Z3_East_Original = Z3_East_Original + 0.0018/2; %snowfall on May 16, 2010
end
end
volume_sublimation_east(:,1) = Hourly_Temperature(:,1);

%movie(M,1)%make a movie of snowmelt
volume_east_snowmelt(:,2) = Hourly_Temperature(:,4);
volume_east_snowmelt(:,1) = Hourly_Temperature(:,1);

%now apply the melt model to the west batter, stepping through time in one
%hour increments

k = length(Hourly_Temperature); %counter that equals the total amount of hours considered
L = 1; %counter for days
time = Hourly_Temperature(:,2); % time counter, 100 to 2300 hours
Melt_Rate_West = zeros(k,2); % preallocate array for speed
night_radiation = min(West_Radiation); % this is the minimum energy value, which is used to describe nighttime
melting



for i = 1:k
   if time(i) < 0400 % modified equation to reflect short nights
```

```
      Melt_Rate_West(i,2) = CMF*night_radiation*Hourly_Temperature(i,4); % correct for low radiation at night -
need to alter this
      else if time(i) > 1800 % modified equation to reflect short nights
       Melt_Rate_West(i,2) = CMF*night_radiation*Hourly_Temperature(i,4); % correct for low radiation at night -
need to alter this
         else
       Melt_Rate_West(i,2) = CMF*West_Radiation(L) * Hourly_Temperature(i,4);
         end
   end

   if(Melt_Rate_West(i,2) < 0)
      Melt_Rate_West(i,2) = 0;
   end

   if time(i) == 2400
      L = L + 1;
   end
end
Melt_Rate_West(:,1) = Hourly_Temperature(:,1);

% Now calculate snow loss on the west batter - measure hourly
d = size(Z3_West);

Z3_West_Original = Z3_West;
k = length(Hourly_Temperature);

for i = 1:k
Z3_New_West = Z3_West_Original - Melt_Rate_West(i,2)/1000;
   for l = 1:d(1,1)
      for m = 1:d(1,2)
       if Z3_New_West(l,m) < 0
         Z3_New_West(l,m) = 0;
       end
      end
   end

volume_west_snowmelt(i,3) = nansum(nansum(Z3_West_Original))-nansum(nansum(Z3_New_West));

Z3_West_Original = Z3_New_West;
%now apply sublimation
sublimation_matrix_west = Z3_West_Original - (west_sublimation(i,2)/1000);
for l = 1:d(1,1)
      for m = 1:d(1,2)
       if sublimation_matrix_west(l,m) < 0
         sublimation_matrix_west(l,m) = 0;
       end
      end
end
volume_sublimation_west(i,2) = nansum(nansum(Z3_West_Original))-
nansum(nansum(sublimation_matrix_west));
Z3_West_Original = sublimation_matrix_west;
```

```
if i == 1
   Z3_West_Original = Z3_West_Original + 0.0105/2; % snowfall on April 22, 2010
end
if i == 265
   Z3_West_Original = Z3_West_Original + 0.0002/2; %snowfall on May 3, 2010
end
if i == 409
   Z3_West_Original = Z3_West_Original + 0.0014/2; %snowfall on May 9, 2010
end
if i == 481
   Z3_West_Original = Z3_West_Original + 0.005/2; %snowfall on May 12, 2010
end
if i == 817
   Z3_West_Original = Z3_West_Original + 0.0018/2; %snowfall on May 16, 2010
end
end
volume_sublimation_west(:,1) = Hourly_Temperature(:,1);
volume_west_snowmelt(:,2) = Hourly_Temperature(:,4);
volume_west_snowmelt(:,1) = Hourly_Temperature(:,1);

%now apply the melt model to the South batter, stepping through time in one
%hour increments

k = length(Hourly_Temperature); %counter that equals the total amount of hours considered
L = 1; %counter for days
time = Hourly_Temperature(:,2); % time counter, 100 to 2300 hours
Melt_Rate_South = zeros(k,2); % preallocate array for speed
night_radiation = min(South_Radiation); % this is the minimum energy value, which is used to describe nighttime
melting



for i = 1:k
   if time(i) < 0400 % modified equation to reflect short nights
      Melt_Rate_South(i,2) = CMF*night_radiation*Hourly_Temperature(i,4); % correct for low radiation at night -
need to alter this
      else if time(i) > 1800 % modified equation to reflect short nights
       Melt_Rate_South(i,2) = CMF*night_radiation*Hourly_Temperature(i,4); % correct for low radiation at night -
need to alter this
         else
       Melt_Rate_South(i,2) = CMF*South_Radiation(L) * Hourly_Temperature(i,4);
         end
   end

   if(Melt_Rate_South(i,2) < 0)
      Melt_Rate_South(i,2) = 0;
   end

   if time(i) == 2400
      L = L + 1;
   end
end
```

```
Melt_Rate_South(:,1) = Hourly_Temperature(:,1);

% Now calculate snow loss on the South batter - measure hourly
d = size(Z3_South);

Z3_South_Original = Z3_South;
k = length(Hourly_Temperature);

for i = 1:k
Z3_New_South = Z3_South_Original - Melt_Rate_South(i,2)/1000;
   for l = 1:d(1,1)
      for m = 1:d(1,2)
       if Z3_New_South(l,m) < 0
         Z3_New_South(l,m) = 0;
       end
      end
   end



volume_South_snowmelt(i,3) = nansum(nansum(Z3_South_Original))-nansum(nansum(Z3_New_South));
Z3_South_Original = Z3_New_South;

%now apply sublimation
sublimation_matrix_south = Z3_South_Original - (south_sublimation(i,2)/1000);
for l = 1:d(1,1)
      for m = 1:d(1,2)
       if sublimation_matrix_south(l,m) < 0
         sublimation_matrix_south(l,m) = 0;
       end
      end
end
volume_sublimation_south(i,2) = nansum(nansum(Z3_South_Original))-
nansum(nansum(sublimation_matrix_south));
Z3_South_Original = sublimation_matrix_south;
if i == 1
   Z3_South_Original = Z3_South_Original + 0.0105/2; % snowfall on April 22, 2010
end
if i == 265
   Z3_South_Original = Z3_South_Original + 0.0002/2; %snowfall on May 3, 2010
end
if i == 409
   Z3_South_Original = Z3_South_Original + 0.0014/2; %snowfall on May 9, 2010
end
if i == 481
   Z3_South_Original = Z3_South_Original + 0.005/2; %snowfall on May 12, 2010
end
if i == 817
   Z3_South_Original = Z3_South_Original + 0.0018/2; %snowfall on May 16, 2010
end
end
volume_sublimation_south(:,1) = Hourly_Temperature(:,1);
```

```
volume_South_snowmelt(:,2) = Hourly_Temperature(:,4);
volume_South_snowmelt(:,1) = Hourly_Temperature(:,1);

Final_East_Spreadsheet(:,1:4) = Hourly_Temperature(:,1:4);
Final_East_Spreadsheet(:,5) = Melt_Rate_East(:,2);
Final_East_Spreadsheet(:,6) = volume_east_snowmelt(:,3);
Final_East_Spreadsheet(:,7) = east_sublimation(:,2);
Final_East_Spreadsheet(:,8) = volume_sublimation_east(:,2);

Final_West_Spreadsheet(:,1:4) = Hourly_Temperature(:,1:4);
Final_West_Spreadsheet(:,5) = Melt_Rate_West(:,2);
Final_West_Spreadsheet(:,6) = volume_west_snowmelt(:,3);
Final_West_Spreadsheet(:,7) = west_sublimation(:,2);
Final_West_Spreadsheet(:,8) = volume_sublimation_west(:,2);

Final_South_Spreadsheet(:,1:4) = Hourly_Temperature(:,1:4);
Final_South_Spreadsheet(:,5) = Melt_Rate_South(:,2);
Final_South_Spreadsheet(:,6) = volume_South_snowmelt(:,3);
Final_South_Spreadsheet(:,7) = south_sublimation(:,2);
Final_South_Spreadsheet(:,8) = volume_sublimation_south(:,2);
```

C.3.2 2011

```
%this program imports snowpack data from excel in the format: relative X (m),
%relative Y (m), relative Z (m) and creates an interpolation of the
%snowpack - IT IS ***MAYBE**** NECESSARY TO IMPORT THE HEIGHTS OF THE SNOWPACK PLUS THE
%PILE, AND THEN SUBTRACT THE PILE HEIGHT FOR INTERPOLATION REASONS
%****SNOWPACK DATA MUST BE EXPRESSED IN SWE****

CMF = 0.016; %change to get full range %the CMF ranges from 0.016 to 0.024

%first import the xls file - all units in metres - snowpack plus pile height
ndata = xlsread('C:\Documents and
Settings\akrentz\Desktop\Thesis\Thesis\Work\Snowfall\Snow_survey\Surfer_SnowPacks\2011.xlsx','Snow_and_Pi
le_Above_Liner');

%now seperate out the X,Y and Z coordinates
x=ndata(:,1);
y=ndata(:,2);
z=ndata(:,3);

%Define the grid you want in the x (tix) and y (tiy) direction. Now there
%is a matrix Z1 that contains the interpolated height at 1m intervals
%within the domain specified
tix = -42:1:42;%defines the x domain and the discretization used
tiy = -29:1:29; %defines the y domain and the discretization used
[X1,Y1] = meshgrid(tix,tiy); %this defines the domain for the interpolated surface
Z1=griddata(x,y,z,X1,Y1);% this creates the interpolated surface

%check if the interpolation worked - you can only check one plot at a time,
%use % signs to block out the other plots
%mesh(X1,Y1,Z1), hold %this plots the surface that was previously created
```

```
%plot3(x,y,z,'o'), hold off %this plots the measurement points onto the surface

%Calculate the total volume of the snow and pile
total_volume_snow_and_pile=nansum(nansum(Z1));


%Now import the xls file for the pile only - all units in metres - pile only
pile_data = xlsread('C:\Documents and
Settings\akrentz\Desktop\Thesis\Thesis\Work\Snowfall\Snow_survey\Surfer_SnowPacks\2011.xlsx',
'Pile_Above_Liner');
x1=pile_data(:,1);
y1=pile_data(:,2);
z1=pile_data(:,3);

%Create interpolated surface
Z2=griddata(x1,y1,z1,X1,Y1);
%check if the interpolation worked - you can only check one plot at a time,
%use % signs to block out the other plots
%mesh(X1,Y1,Z2), hold; %this plots the surface that was previously created
%plot3(x,y,z,'o'), hold off; %this plots the measurement points onto the surface

%Calculate the total volume of the pile
total_volume_pile = nansum(nansum(Z2));

%calculate the volume of snow available - this should match the value in
%the write up +/- 3%
total_snow = total_volume_snow_and_pile - total_volume_pile;


%Now create a matrix that contains only the snow - to apply the snowmelt
%model too
Z3 = Z1-Z2;
Indices = (Z3<0.001); % find the elements showing less than 1/10cm snow (interpolation error)
Z3(Indices) = 0; % make these cells = zero
Z3(isnan(Z3))= 0; % make NaN cells = 0



%check that the total volume of snow has not been changed by removing the
%interpolation values
total_snow_check = nansum(nansum(Z3));%checks total snow volume.  Should = total_snow


% Plot this model to check if it worked
%mesh(X1,Y1,Z3), hold; %this plots the surface that was previously created

%Now divide the matrix into different aspects (east, south, west)
Z3_East = Z3(:,1:30);
Z3_South = Z3(:,31:57);
Z3_West = Z3(:,58:85);
```

```
%mesh(Z3_South);



%print a file showing the interpolated matrix. This is just a check. Skip
%this step once confident to avoid making too many excel files
%xlswrite('/Users/Andrew/Dropbox/Work/Snowfall/Snow_survey/Surfer_SnowPacks/Matlab_created_files/2010_
Snow_Meshgrid.xls',Z3);
%xlswrite('/Users/Andrew/Dropbox/Work/Snowfall/Snow_survey/Surfer_SnowPacks/Matlab_created_files/2010_
Snow_Meshgrid_East.xls',Z3_East);
%xlswrite('/Users/Andrew/Dropbox/Work/Snowfall/Snow_survey/Surfer_SnowPacks/Matlab_created_files/2010_
Snow_Meshgrid_South.xls',Z3_South);
%xlswrite('/Users/Andrew/Dropbox/Work/Snowfall/Snow_survey/Surfer_SnowPacks/Matlab_created_files/2010_
Snow_Meshgrid_West.xls',Z3_West);

%Now import the radiation data for the year of concern - the model must
%start the day after the survey was taken
Radiation = xlsread('C:\Documents and Settings\akrentz\Desktop\Thesis\Thesis\Work\Radiation
Calculations\Radiation_all_years_and_slopes_for_matlab.xlsx','2011');
East_Radiation = Radiation(:,4);
West_Radiation = Radiation(:,5);
South_Radiation = Radiation(:,6);



%Now caculate the volume of snow on each batter and check that all of the
%snow has been included
snow_east_batter_initial = nansum(nansum(Z3_East));
snow_west_batter_initial = nansum(nansum(Z3_West));
snow_south_batter_initial = nansum(nansum(Z3_South));
total_snow_check_1 = snow_east_batter_initial + snow_west_batter_initial + snow_south_batter_initial; % should
= total_snow_check



%Now import the hourly temperature and evaporation/sublimation data from excel
Hourly_Temperature = xlsread('C:\Documents and Settings\akrentz\Desktop\Thesis\Thesis\Work\Radiation
Calculations\Hourly_Temp_Evap\2011_Temperature_Hourly_For_Matlab.xlsx','2011');
east_sublimation(:,1) = Hourly_Temperature(:,1); % date and time
east_sublimation(:,2) = Hourly_Temperature(:,6); % sublimation rate
west_sublimation(:,1) = Hourly_Temperature(:,1);
west_sublimation(:,2) = Hourly_Temperature(:,7);
south_sublimation(:,1) = Hourly_Temperature(:,1);
south_sublimation(:,2) = Hourly_Temperature(:,8);

for i = 1:length(Hourly_Temperature)
    if Hourly_Temperature(i,4) <= -4
    east_sublimation(i,2) = 0;
    west_sublimation(i,2) = 0;
    south_sublimation(i,2) = 0;
    end
end
```

```
%now apply the melt model to the east batter, stepping through time in one
%hour increments

k = length(Hourly_Temperature); %counter that equals the total amount of hours considered
L = 1; %counter for days
time = Hourly_Temperature(:,2); % time counter, 100 to 2300 hours
Melt_Rate_East = zeros(k,2); % preallocate array for speed
night_radiation = min(East_Radiation); % this is the minimum energy value, which is used to describe nighttime
melting



for i = 1:k
   if time(i) < 0400 % modified equation to reflect short nights
      Melt_Rate_East(i,2) = CMF*night_radiation*Hourly_Temperature(i,4); % correct for low radiation at night -
need to alter this
      else if time(i) > 1800 % modified equation to reflect short nights
       Melt_Rate_East(i,2) = CMF*night_radiation*Hourly_Temperature(i,4); % correct for low radiation at night -
need to alter this
         else
       Melt_Rate_East(i,2) = CMF*East_Radiation(L) * Hourly_Temperature(i,4);
         end
   end

   if(Melt_Rate_East(i,2) < 0)
      Melt_Rate_East(i,2) = 0;
   end

   if time(i) == 2400
      L = L + 1;
   end
end
Melt_Rate_East(:,1) = Hourly_Temperature(:,1);

% Now calculate snow loss on the east batter - measure hourly
d = size(Z3_East);
Z3_East_Original = Z3_East;
k = length(Hourly_Temperature);



for i = 1:k
Z3_New_East = Z3_East_Original - Melt_Rate_East(i,2)/1000;
   for l = 1:d(1,1)
      for m = 1:d(1,2)
       if Z3_New_East(l,m) < 0
         Z3_New_East(l,m) = 0;
       end
      end
```

```
   end

  % mesh(Z3_New_East); %make a movie of snowmelt
   %axis([0 30 0 60 0 0.5]);%make a movie of snowmelt
   %M(k) = getframe;%make a movie of snowmelt
   %axis([0 10 0 10 0 1]);%make a movie of snowmelt

volume_east_snowmelt(i,3) = nansum(nansum(Z3_East_Original))-nansum(nansum(Z3_New_East));
Z3_East_Original = Z3_New_East;

%now apply sublimation
sublimation_matrix_east = Z3_East_Original - (east_sublimation(i,2)/1000);
for l = 1:d(1,1)
      for m = 1:d(1,2)
       if sublimation_matrix_east(l,m) < 0
         sublimation_matrix_east(l,m) = 0;
       end
      end
end
volume_sublimation_east(i,2) = nansum(nansum(Z3_East_Original))-nansum(nansum(sublimation_matrix_east));
Z3_East_Original = sublimation_matrix_east;
if i == 120
   Z3_East_Original = Z3_East_Original + 0.0004/2; % snowfall on April 19, 2011
end
if i == 216
   Z3_East_Original = Z3_East_Original + 0.0006/2; %snowfall on April 23, 2011
end
if i == 384
   Z3_East_Original = Z3_East_Original + 0.0002/2; %snowfall on April 30, 2011
end
if i == 480
   Z3_East_Original = Z3_East_Original + 0.002/2; %snowfall on May 4, 2011
end
if i == 504
   Z3_East_Original = Z3_East_Original + 0.0003/2; %snowfall on May 5, 2011
end
if i == 648
   Z3_East_Original = Z3_East_Original + 0.0008/2; %snowfall on May 11, 2011
end
end
volume_sublimation_east(:,1) = Hourly_Temperature(:,1);

%movie(M,1)%make a movie of snowmelt
volume_east_snowmelt(:,2) = Hourly_Temperature(:,4);
volume_east_snowmelt(:,1) = Hourly_Temperature(:,1);

%now apply the melt model to the west batter, stepping through time in one
%hour increments

k = length(Hourly_Temperature); %counter that equals the total amount of hours considered
L = 1; %counter for days
```

```
time = Hourly_Temperature(:,2); % time counter, 100 to 2300 hours
Melt_Rate_West = zeros(k,2); % preallocate array for speed
night_radiation = min(West_Radiation); % this is the minimum energy value, which is used to describe nighttime
melting



for i = 1:k
   if time(i) < 0400 % modified equation to reflect short nights
      Melt_Rate_West(i,2) = CMF*night_radiation*Hourly_Temperature(i,4); % correct for low radiation at night -
need to alter this
      else if time(i) > 1800 % modified equation to reflect short nights
       Melt_Rate_West(i,2) = CMF*night_radiation*Hourly_Temperature(i,4); % correct for low radiation at night -
need to alter this
         else
       Melt_Rate_West(i,2) = CMF*West_Radiation(L) * Hourly_Temperature(i,4);
         end
   end

   if(Melt_Rate_West(i,2) < 0)
      Melt_Rate_West(i,2) = 0;
   end

   if time(i) == 2400
      L = L + 1;
   end
end
Melt_Rate_West(:,1) = Hourly_Temperature(:,1);

% Now calculate snow loss on the west batter - measure hourly
d = size(Z3_West);

Z3_West_Original = Z3_West;
k = length(Hourly_Temperature);

for i = 1:k
Z3_New_West = Z3_West_Original - Melt_Rate_West(i,2)/1000;
   for l = 1:d(1,1)
      for m = 1:d(1,2)
       if Z3_New_West(l,m) < 0
         Z3_New_West(l,m) = 0;
       end
      end
   end

volume_west_snowmelt(i,3) = nansum(nansum(Z3_West_Original))-nansum(nansum(Z3_New_West));

Z3_West_Original = Z3_New_West;
%now apply sublimation
sublimation_matrix_west = Z3_West_Original - (west_sublimation(i,2)/1000);
for l = 1:d(1,1)
      for m = 1:d(1,2)
```

```
       if sublimation_matrix_west(l,m) < 0
         sublimation_matrix_west(l,m) = 0;
       end
      end
end
volume_sublimation_west(i,2) = nansum(nansum(Z3_West_Original))-
nansum(nansum(sublimation_matrix_west));
Z3_West_Original = sublimation_matrix_west;
if i == 120
   Z3_West_Original = Z3_West_Original + 0.0002/2; % snowfall on April 19, 2011
end
if i == 216
   Z3_West_Original = Z3_West_Original + 0.0006/2; %snowfall on April 23, 2011
end
if i == 384
   Z3_West_Original = Z3_West_Original + 0.0002/2; %snowfall on April 30, 2011
end
if i == 480
   Z3_West_Original = Z3_West_Original + 0.002/2; %snowfall on May 4, 2011
end
if i == 504
   Z3_West_Original = Z3_West_Original + 0.0003/2; %snowfall on May 5, 2011
end
if i == 648
   Z3_West_Original = Z3_West_Original + 0.0008/2; %snowfall on May 11, 2011
end
end
volume_sublimation_west(:,1) = Hourly_Temperature(:,1);
volume_west_snowmelt(:,2) = Hourly_Temperature(:,4);
volume_west_snowmelt(:,1) = Hourly_Temperature(:,1);

%now apply the melt model to the South batter, stepping through time in one
%hour increments

k = length(Hourly_Temperature); %counter that equals the total amount of hours considered
L = 1; %counter for days
time = Hourly_Temperature(:,2); % time counter, 100 to 2300 hours
Melt_Rate_South = zeros(k,2); % preallocate array for speed
night_radiation = min(South_Radiation); % this is the minimum energy value, which is used to describe nighttime
melting



for i = 1:k
   if time(i) < 0400 % modified equation to reflect short nights
      Melt_Rate_South(i,2) = CMF*night_radiation*Hourly_Temperature(i,4); % correct for low radiation at night -
need to alter this
      else if time(i) > 1800 % modified equation to reflect short nights
       Melt_Rate_South(i,2) = CMF*night_radiation*Hourly_Temperature(i,4); % correct for low radiation at night -
need to alter this
         else
       Melt_Rate_South(i,2) = CMF*South_Radiation(L) * Hourly_Temperature(i,4);
         end
```

```
   end

   if(Melt_Rate_South(i,2) < 0)
      Melt_Rate_South(i,2) = 0;
   end

   if time(i) == 2400
      L = L + 1;
   end
end
Melt_Rate_South(:,1) = Hourly_Temperature(:,1);

% Now calculate snow loss on the South batter - measure hourly
d = size(Z3_South);

Z3_South_Original = Z3_South;
k = length(Hourly_Temperature);

for i = 1:k
Z3_New_South = Z3_South_Original - Melt_Rate_South(i,2)/1000;
   for l = 1:d(1,1)
      for m = 1:d(1,2)
       if Z3_New_South(l,m) < 0
          Z3_New_South(l,m) = 0;
       end
      end
   end



volume_South_snowmelt(i,3) = nansum(nansum(Z3_South_Original))-nansum(nansum(Z3_New_South));
Z3_South_Original = Z3_New_South;

%now apply sublimation
sublimation_matrix_south = Z3_South_Original - (south_sublimation(i,2)/1000);
for l = 1:d(1,1)
      for m = 1:d(1,2)
       if sublimation_matrix_south(l,m) < 0
          sublimation_matrix_south(l,m) = 0;
       end
      end
end
volume_sublimation_south(i,2) = nansum(nansum(Z3_South_Original))-
nansum(nansum(sublimation_matrix_south));
Z3_South_Original = sublimation_matrix_south;
if i == 120
   Z3_South_Original = Z3_South_Original + 0.0002/2; % snowfall on April 19, 2011
end
if i == 216
   Z3_South_Original = Z3_South_Original + 0.0006/2; %snowfall on April 23, 2011
end
```

```
if i == 384
   Z3_South_Original = Z3_South_Original + 0.0002/2; %snowfall on April 30, 2011
end
if i == 480
   Z3_South_Original = Z3_South_Original + 0.002/2; %snowfall on May 4, 2011
end
if i == 504
   Z3_South_Original = Z3_South_Original + 0.0003/2; %snowfall on May 5, 2010
end
if i == 648
   Z3_South_Original = Z3_South_Original + 0.0008/2; %snowfall on May 5, 2010
end
end
volume_sublimation_south(:,1) = Hourly_Temperature(:,1);
volume_South_snowmelt(:,2) = Hourly_Temperature(:,4);
volume_South_snowmelt(:,1) = Hourly_Temperature(:,1);

Final_East_Spreadsheet(:,1:4) = Hourly_Temperature(:,1:4);
Final_East_Spreadsheet(:,5) = Melt_Rate_East(:,2);
Final_East_Spreadsheet(:,6) = volume_east_snowmelt(:,3);
Final_East_Spreadsheet(:,7) = east_sublimation(:,2);
Final_East_Spreadsheet(:,8) = volume_sublimation_east(:,2);

Final_West_Spreadsheet(:,1:4) = Hourly_Temperature(:,1:4);
Final_West_Spreadsheet(:,5) = Melt_Rate_West(:,2);
Final_West_Spreadsheet(:,6) = volume_west_snowmelt(:,3);
Final_West_Spreadsheet(:,7) = west_sublimation(:,2);
Final_West_Spreadsheet(:,8) = volume_sublimation_west(:,2);

Final_South_Spreadsheet(:,1:4) = Hourly_Temperature(:,1:4);
Final_South_Spreadsheet(:,5) = Melt_Rate_South(:,2);
Final_South_Spreadsheet(:,6) = volume_South_snowmelt(:,3);
Final_South_Spreadsheet(:,7) = south_sublimation(:,2);
Final_South_Spreadsheet(:,8) = volume_sublimation_south(:,2);
```

C.3.3 2013

```
%this program imports snowpack data from excel in the format: relative X (m),
%relative Y (m), relative Z (m) and creates an interpolation of the
%snowpack - IT IS ***MAYBE**** NECESSARY TO IMPORT THE HEIGHTS OF THE SNOWPACK PLUS THE
%PILE, AND THEN SUBTRACT THE PILE HEIGHT FOR INTERPOLATION REASONS
%****SNOWPACK DATA MUST BE EXPRESSED IN SWE****

CMF = 0.016; %change to get full range %the CMF ranges from 0.016 to 0.024

%first import the xls file - all units in metres - snowpack plus pile height
ndata = xlsread('C:\Documents and
Settings\akrentz\Desktop\Thesis\Thesis\Work\Snowfall\Snow_survey\Surfer_SnowPacks\2013.xlsx','Snow_and_Pi
le_Above_Liner');

%now seperate out the X,Y and Z coordinates
x=ndata(:,1);
y=ndata(:,2);
z=ndata(:,3);

%Define the grid you want in the x (tix) and y (tiy) direction. Now there
%is a matrix Z1 that contains the interpolated height at 1m intervals
%within the domain specified
tix = -42:1:42;%defines the x domain and the discretization used
tiy = -29:1:29; %defines the y domain and the discretization used
[X1,Y1] = meshgrid(tix,tiy); %this defines the domain for the interpolated surface
Z1=griddata(x,y,z,X1,Y1);% this creates the interpolated surface

%check if the interpolation worked - you can only check one plot at a time,
%use % signs to block out the other plots
%mesh(X1,Y1,Z1), hold %this plots the surface that was previously created
%plot3(x,y,z,'o'), hold off %this plots the measurement points onto the surface

%Calculate the total volume of the snow and pile
total_volume_snow_and_pile=nansum(nansum(Z1));



%Now import the xls file for the pile only - all units in metres - pile only
pile_data = xlsread('C:\Documents and
Settings\akrentz\Desktop\Thesis\Thesis\Work\Snowfall\Snow_survey\Surfer_SnowPacks\2013.xlsx',
'Pile_Above_Liner');
x1=pile_data(:,1);
y1=pile_data(:,2);
z1=pile_data(:,3);

%Create interpolated surface
Z2=griddata(x1,y1,z1,X1,Y1);
%check if the interpolation worked - you can only check one plot at a time,
%use % signs to block out the other plots
%mesh(X1,Y1,Z2), hold; %this plots the surface that was previously created
%plot3(x,y,z,'o'), hold off; %this plots the measurement points onto the surface
```

```
%Calculate the total volume of the pile
total_volume_pile = nansum(nansum(Z2));

%calculate the volume of snow available - this should match the value in
%the write up +/- 3%
total_snow = total_volume_snow_and_pile - total_volume_pile;


%Now create a matrix that contains only the snow - to apply the snowmelt
%model too
Z3 = Z1-Z2;
Indices = (Z3<0.001); % find the elements showing less than 1/10cm snow (interpolation error)
Z3(Indices) = 0; % make these cells = zero
Z3(isnan(Z3))= 0; % make NaN cells = 0



%check that the total volume of snow has not been changed by removing the
%interpolation values
total_snow_check = nansum(nansum(Z3));%checks total snow volume.  Should = total_snow


% Plot this model to check if it worked
%mesh(X1,Y1,Z3), hold; %this plots the surface that was previously created

%Now divide the matrix into different aspects (east, south, west)
Z3_East = Z3(:,1:30);
Z3_South = Z3(:,31:57);
Z3_West = Z3(:,58:85);
%mesh(Z3_South);



%print a file showing the interpolated matrix. This is just a check. Skip
%this step once confident to avoid making too many excel files
%xlswrite('/Users/Andrew/Dropbox/Work/Snowfall/Snow_survey/Surfer_SnowPacks/Matlab_created_files/2010_
Snow_Meshgrid.xls',Z3);
%xlswrite('/Users/Andrew/Dropbox/Work/Snowfall/Snow_survey/Surfer_SnowPacks/Matlab_created_files/2010_
Snow_Meshgrid_East.xls',Z3_East);
%xlswrite('/Users/Andrew/Dropbox/Work/Snowfall/Snow_survey/Surfer_SnowPacks/Matlab_created_files/2010_
Snow_Meshgrid_South.xls',Z3_South);
%xlswrite('/Users/Andrew/Dropbox/Work/Snowfall/Snow_survey/Surfer_SnowPacks/Matlab_created_files/2010_
Snow_Meshgrid_West.xls',Z3_West);

%Now import the radiation data for the year of concern - the model must
%start the day after the survey was taken
Radiation = xlsread('C:\Documents and Settings\akrentz\Desktop\Thesis\Thesis\Work\Radiation
Calculations\Radiation_all_years_and_slopes_for_matlab.xlsx','2013');
East_Radiation = Radiation(:,4);
```

```
West_Radiation = Radiation(:,5);
South_Radiation = Radiation(:,6);


%Now caculate the volume of snow on each batter and check that all of the
%snow has been included
snow_east_batter_initial = nansum(nansum(Z3_East));
snow_west_batter_initial = nansum(nansum(Z3_West));
snow_south_batter_initial = nansum(nansum(Z3_South));
total_snow_check_1 = snow_east_batter_initial + snow_west_batter_initial + snow_south_batter_initial; % should
= total_snow_check


%Now import the hourly temperature and evaporation/sublimation data from excel
Hourly_Temperature = xlsread('C:\Documents and Settings\akrentz\Desktop\Thesis\Thesis\Work\Radiation
Calculations\Hourly_Temp_Evap\2013_Temperature_Hourly_For_Matlab.xlsx','2013');
east_sublimation(:,1) = Hourly_Temperature(:,1); % date and time
east_sublimation(:,2) = Hourly_Temperature(:,6); % sublimation rate
west_sublimation(:,1) = Hourly_Temperature(:,1);
west_sublimation(:,2) = Hourly_Temperature(:,7);
south_sublimation(:,1) = Hourly_Temperature(:,1);
south_sublimation(:,2) = Hourly_Temperature(:,8);

for i = 1:length(Hourly_Temperature)
      if Hourly_Temperature(i,4) <= -4
      east_sublimation(i,2) = 0;
      west_sublimation(i,2) = 0;
      south_sublimation(i,2) = 0;
      end
end



%now apply the melt model to the east batter, stepping through time in one
%hour increments

k = length(Hourly_Temperature); %counter that equals the total amount of hours considered
L = 1; %counter for days
time = Hourly_Temperature(:,2); % time counter, 100 to 2300 hours
Melt_Rate_East = zeros(k,2); % preallocate array for speed
night_radiation = min(East_Radiation); % this is the minimum energy value, which is used to describe nighttime
melting


for i = 1:k
   if time(i) < 0400 % modified equation to reflect short nights
      Melt_Rate_East(i,2) = CMF*night_radiation*Hourly_Temperature(i,4); % correct for low radiation at night -
need to alter this
      else if time(i) > 1800 % modified equation to reflect short nights
```

```
      Melt_Rate_East(i,2) = CMF*night_radiation*Hourly_Temperature(i,4); % correct for low radiation at night -
need to alter this
        else
      Melt_Rate_East(i,2) = CMF*East_Radiation(L) * Hourly_Temperature(i,4);
        end
   end

   if(Melt_Rate_East(i,2) < 0)
      Melt_Rate_East(i,2) = 0;
   end

   if time(i) == 2400
      L = L + 1;
   end
end
Melt_Rate_East(:,1) = Hourly_Temperature(:,1);

% Now calculate snow loss on the east batter - measure hourly
d = size(Z3_East);
Z3_East_Original = Z3_East;
k = length(Hourly_Temperature);



for i = 1:k
Z3_New_East = Z3_East_Original - Melt_Rate_East(i,2)/1000;
   for l = 1:d(1,1)
      for m = 1:d(1,2)
       if Z3_New_East(l,m) < 0
         Z3_New_East(l,m) = 0;
       end
      end
   end

  % mesh(Z3_New_East); %make a movie of snowmelt
   %axis([0 30 0 60 0 0.5]);%make a movie of snowmelt
   %M(k) = getframe;%make a movie of snowmelt
   %axis([0 10 0 10 0 1]);%make a movie of snowmelt

volume_east_snowmelt(i,3) = nansum(nansum(Z3_East_Original))-nansum(nansum(Z3_New_East));
Z3_East_Original = Z3_New_East;

%now apply sublimation
sublimation_matrix_east = Z3_East_Original - (east_sublimation(i,2)/1000);
for l = 1:d(1,1)
      for m = 1:d(1,2)
       if sublimation_matrix_east(l,m) < 0
         sublimation_matrix_east(l,m) = 0;
       end
      end
end
volume_sublimation_east(i,2) = nansum(nansum(Z3_East_Original))-nansum(nansum(sublimation_matrix_east));
```

```
Z3_East_Original = sublimation_matrix_east;
if i == 96
   Z3_East_Original = Z3_East_Original + 0.0015/2; % snowfall on April 14, 2013
end
if i == 312
   Z3_East_Original = Z3_East_Original + 0.0004/2; %snowfall on April 23, 2013
end
if i == 336
   Z3_East_Original = Z3_East_Original + 0.0006/2; %snowfall on April 24, 2013
end
if i == 360
   Z3_East_Original = Z3_East_Original + 0.0012/2; %snowfall on April 25, 2013
end
if i == 384
   Z3_East_Original = Z3_East_Original + 0.0008/2; %snowfall on April 26, 2013
end
if i == 408
   Z3_East_Original = Z3_East_Original + 0.0002/2; %snowfall on April 27, 2013
end
if i == 552
   Z3_East_Original = Z3_East_Original + 0.0002/2; %snowfall on May 3, 2013
end
if i == 600
   Z3_East_Original = Z3_East_Original + 0.006/2; %snowfall on May 5, 2013
end
if i == 624
   Z3_East_Original = Z3_East_Original + 0.0048/2; %snowfall on May 6, 2013
end
if i == 744
   Z3_East_Original = Z3_East_Original + 0.0002/2; %snowfall on May 11, 2013
end
if i == 768
   Z3_East_Original = Z3_East_Original + 0.0002/2; %snowfall on May 12, 2013
end
if i == 816
   Z3_East_Original = Z3_East_Original + 0.0004/2; %snowfall on May 14, 2013
end
if i == 840
   Z3_East_Original = Z3_East_Original + 0.0006/2; %snowfall on May 15, 2011
end
if i == 864
   Z3_East_Original = Z3_East_Original + 0.001/2; %snowfall on May 16, 2011
end
if i == 960
   Z3_East_Original = Z3_East_Original + 0.0014/2; %snowfall on May 20, 2011
end
end
volume_sublimation_east(:,1) = Hourly_Temperature(:,1);

%movie(M,1)%make a movie of snowmelt
volume_east_snowmelt(:,2) = Hourly_Temperature(:,4);
volume_east_snowmelt(:,1) = Hourly_Temperature(:,1);
```

```
%now apply the melt model to the west batter, stepping through time in one
%hour increments

k = length(Hourly_Temperature); %counter that equals the total amount of hours considered
L = 1; %counter for days
time = Hourly_Temperature(:,2); % time counter, 100 to 2300 hours
Melt_Rate_West = zeros(k,2); % preallocate array for speed
night_radiation = min(West_Radiation); % this is the minimum energy value, which is used to describe nighttime
melting



for i = 1:k
   if time(i) < 0400 % modified equation to reflect short nights
      Melt_Rate_West(i,2) = CMF*night_radiation*Hourly_Temperature(i,4); % correct for low radiation at night -
need to alter this
      else if time(i) > 1800 % modified equation to reflect short nights
       Melt_Rate_West(i,2) = CMF*night_radiation*Hourly_Temperature(i,4); % correct for low radiation at night -
need to alter this
         else
       Melt_Rate_West(i,2) = CMF*West_Radiation(L) * Hourly_Temperature(i,4);
         end
   end

   if(Melt_Rate_West(i,2) < 0)
      Melt_Rate_West(i,2) = 0;
   end

   if time(i) == 2400
      L = L + 1;
   end
end
Melt_Rate_West(:,1) = Hourly_Temperature(:,1);

% Now calculate snow loss on the west batter - measure hourly
d = size(Z3_West);

Z3_West_Original = Z3_West;
k = length(Hourly_Temperature);

for i = 1:k
Z3_New_West = Z3_West_Original - Melt_Rate_West(i,2)/1000;
   for l = 1:d(1,1)
      for m = 1:d(1,2)
       if Z3_New_West(l,m) < 0
         Z3_New_West(l,m) = 0;
       end
      end
   end

volume_west_snowmelt(i,3) = nansum(nansum(Z3_West_Original))-nansum(nansum(Z3_New_West));
```

```
Z3_West_Original = Z3_New_West;
%now apply sublimation
sublimation_matrix_west = Z3_West_Original - (west_sublimation(i,2)/1000);
for l = 1:d(1,1)
      for m = 1:d(1,2)
       if sublimation_matrix_west(l,m) < 0
         sublimation_matrix_west(l,m) = 0;
       end
      end
end
volume_sublimation_west(i,2) = nansum(nansum(Z3_West_Original))-
nansum(nansum(sublimation_matrix_west));
Z3_West_Original = sublimation_matrix_west;
if i == 96
   Z3_West_Original = Z3_West_Original + 0.0015/2; % snowfall on April 14, 2013
end
if i == 312
   Z3_West_Original = Z3_West_Original + 0.0004/2; %snowfall on April 23, 2013
end
if i == 336
   Z3_West_Original = Z3_West_Original + 0.0006/2; %snowfall on April 24, 2013
end
if i == 360
   Z3_West_Original = Z3_West_Original + 0.0012/2; %snowfall on April 25, 2013
end
if i == 384
   Z3_West_Original = Z3_West_Original + 0.0008/2; %snowfall on April 26, 2013
end
if i == 408
   Z3_West_Original = Z3_West_Original + 0.0002/2; %snowfall on April 27, 2013
end
if i == 552
   Z3_West_Original = Z3_West_Original + 0.0002/2; %snowfall on May 3, 2013
end
if i == 600
   Z3_West_Original = Z3_West_Original + 0.006/2; %snowfall on May 5, 2013
end
if i == 624
   Z3_West_Original = Z3_West_Original + 0.0048/2; %snowfall on May 6, 2013
end
if i == 744
   Z3_West_Original = Z3_West_Original + 0.0002/2; %snowfall on May 11, 2013
end
if i == 768
   Z3_West_Original = Z3_West_Original + 0.0002/2; %snowfall on May 12, 2013
end
if i == 816
   Z3_West_Original = Z3_West_Original + 0.0004/2; %snowfall on May 14, 2013
end
if i == 840
   Z3_West_Original = Z3_West_Original + 0.0006/2; %snowfall on May 15, 2011
```

```
end
if i == 864
   Z3_West_Original = Z3_West_Original + 0.001/2; %snowfall on May 16, 2011
end
if i == 960
   Z3_West_Original = Z3_West_Original + 0.0014/2; %snowfall on May 20, 2011
end
end
volume_sublimation_west(:,1) = Hourly_Temperature(:,1);
volume_west_snowmelt(:,2) = Hourly_Temperature(:,4);
volume_west_snowmelt(:,1) = Hourly_Temperature(:,1);

%now apply the melt model to the South batter, stepping through time in one
%hour increments

k = length(Hourly_Temperature); %counter that equals the total amount of hours considered
L = 1; %counter for days
time = Hourly_Temperature(:,2); % time counter, 100 to 2300 hours
Melt_Rate_South = zeros(k,2); % preallocate array for speed
night_radiation = min(South_Radiation); % this is the minimum energy value, which is used to describe nighttime
melting



for i = 1:k
   if time(i) < 0400 % modified equation to reflect short nights
      Melt_Rate_South(i,2) = CMF*night_radiation*Hourly_Temperature(i,4); % correct for low radiation at night -
need to alter this
      else if time(i) > 1800 % modified equation to reflect short nights
       Melt_Rate_South(i,2) = CMF*night_radiation*Hourly_Temperature(i,4); % correct for low radiation at night -
need to alter this
         else
       Melt_Rate_South(i,2) = CMF*South_Radiation(L) * Hourly_Temperature(i,4);
         end
   end

   if(Melt_Rate_South(i,2) < 0)
      Melt_Rate_South(i,2) = 0;
   end

   if time(i) == 2400
      L = L + 1;
   end
end
Melt_Rate_South(:,1) = Hourly_Temperature(:,1);

% Now calculate snow loss on the South batter - measure hourly
d = size(Z3_South);

Z3_South_Original = Z3_South;
k = length(Hourly_Temperature);
```

```
for i = 1:k
Z3_New_South = Z3_South_Original - Melt_Rate_South(i,2)/1000;
   for l = 1:d(1,1)
      for m = 1:d(1,2)
       if Z3_New_South(l,m) < 0
         Z3_New_South(l,m) = 0;
       end
      end
   end



volume_South_snowmelt(i,3) = nansum(nansum(Z3_South_Original))-nansum(nansum(Z3_New_South));
Z3_South_Original = Z3_New_South;

%now apply sublimation
sublimation_matrix_south = Z3_South_Original - (south_sublimation(i,2)/1000);
for l = 1:d(1,1)
      for m = 1:d(1,2)
       if sublimation_matrix_south(l,m) < 0
         sublimation_matrix_south(l,m) = 0;
       end
      end
end
volume_sublimation_south(i,2) = nansum(nansum(Z3_South_Original))-
nansum(nansum(sublimation_matrix_south));
Z3_South_Original = sublimation_matrix_south;
if i == 96
   Z3_South_Original = Z3_South_Original + 0.0015/2; % snowfall on April 14, 2013
end
if i == 312
   Z3_South_Original = Z3_South_Original + 0.0004/2; %snowfall on April 23, 2013
end
if i == 336
   Z3_South_Original = Z3_South_Original + 0.0006/2; %snowfall on April 24, 2013
end
if i == 360
   Z3_South_Original = Z3_South_Original + 0.0012/2; %snowfall on April 25, 2013
end
if i == 384
   Z3_South_Original = Z3_South_Original + 0.0008/2; %snowfall on April 26, 2013
end
if i == 408
   Z3_South_Original = Z3_South_Original + 0.0002/2; %snowfall on April 27, 2013
end
if i == 552
   Z3_South_Original = Z3_South_Original + 0.0002/2; %snowfall on May 3, 2013
end
if i == 600
   Z3_South_Original = Z3_South_Original + 0.006/2; %snowfall on May 5, 2013
end
if i == 624
```

```
   Z3_South_Original = Z3_South_Original + 0.0048/2; %snowfall on May 6, 2013
end
if i == 744
   Z3_South_Original = Z3_South_Original + 0.0002/2; %snowfall on May 11, 2013
end
if i == 768
   Z3_South_Original = Z3_South_Original + 0.0002/2; %snowfall on May 12, 2013
end
if i == 816
   Z3_South_Original = Z3_South_Original + 0.0004/2; %snowfall on May 14, 2013
end
if i == 840
   Z3_South_Original = Z3_South_Original + 0.0006/2; %snowfall on May 15, 2011
end
if i == 864
   Z3_South_Original = Z3_South_Original + 0.001/2; %snowfall on May 16, 2011
end
if i == 960
   Z3_South_Original = Z3_South_Original + 0.0014/2; %snowfall on May 20, 2011
end
end
volume_sublimation_south(:,1) = Hourly_Temperature(:,1);
volume_South_snowmelt(:,2) = Hourly_Temperature(:,4);
volume_South_snowmelt(:,1) = Hourly_Temperature(:,1);

Final_East_Spreadsheet(:,1:4) = Hourly_Temperature(:,1:4);
Final_East_Spreadsheet(:,5) = Melt_Rate_East(:,2);
Final_East_Spreadsheet(:,6) = volume_east_snowmelt(:,3);
Final_East_Spreadsheet(:,7) = east_sublimation(:,2);
Final_East_Spreadsheet(:,8) = volume_sublimation_east(:,2);

Final_West_Spreadsheet(:,1:4) = Hourly_Temperature(:,1:4);
Final_West_Spreadsheet(:,5) = Melt_Rate_West(:,2);
Final_West_Spreadsheet(:,6) = volume_west_snowmelt(:,3);
Final_West_Spreadsheet(:,7) = west_sublimation(:,2);
Final_West_Spreadsheet(:,8) = volume_sublimation_west(:,2);

Final_South_Spreadsheet(:,1:4) = Hourly_Temperature(:,1:4);
Final_South_Spreadsheet(:,5) = Melt_Rate_South(:,2);
Final_South_Spreadsheet(:,6) = volume_South_snowmelt(:,3);
Final_South_Spreadsheet(:,7) = south_sublimation(:,2);
Final_South_Spreadsheet(:,8) = volume_sublimation_south(:,2);
```